



University  
of Glasgow

Yang, Jingli (2015) *Nanotopography as a tool for the investigation of molecular mechanisms of osteogenesis of MSCs*. PhD thesis.

<http://theses.gla.ac.uk/6370/>

Copyright and moral rights for this thesis are retained by the author

A copy can be downloaded for personal non-commercial research or study, without prior permission or charge

This thesis cannot be reproduced or quoted extensively from without first obtaining permission in writing from the Author

The content must not be changed in any way or sold commercially in any format or medium without the formal permission of the Author

When referring to this work, full bibliographic details including the author, title, awarding institution and date of the thesis must be given

# Nanotopography as a Tool for the Investigation of Molecular Mechanisms of Osteogenesis of MSCs

A thesis submitted for the degree of Doctor of Philosophy (PhD) at  
the University of Glasgow

By

Jingli Yang



Centre for Cell Engineering  
College of Medical, Veterinary and Life Sciences  
Institute of Molecular, Cell and Systems Biology  
University of Glasgow  
Glasgow, G12 8QQ

September 2014

# Author's Declaration

The research reported within this thesis is my own work except where otherwise stated, and has not been submitted for any other degree.

Jingli Yang

## Abstract

Nanotopographical patterning of biomaterial substrates has great potential for biofunctionalisation of devices for clinical applications, such as in orthopaedics. Nanotopography comprising 120 nm diameter nanopits with a partially disordered arrangement of up to +/- 50 nm offset from a square lattice with 300 nm centre to centre spacing (NSQ50, fabricated by electron beam lithography) has been characterized as being osteogenic. Following the finding of osteogenesis of mesenchymal stromal cells derived from human bone marrow (MSCs) on the NSQ50 nanotopography, MSCs cultured on  $\epsilon$ -polycaprolactone (PCL) embossed with the NSQ50 pattern was used for this study on molecular mechanisms underlying NSQ50 induced MSC osteogenesis: the functional coupling of gene expression and osteogenesis, the molecular regulatory events driving gene expression and osteogenesis, and the possible link of metabolomics with molecular signalling of MSCs on the NSQ50 surface.

Temporal analysis of gene expression for MSCs on the NSQ50 surface revealed that MSC fate commitment and osteogenic differentiation was transcriptionally controlled. The cell cycle and growth regulating transcription factor C-MYC was found to be significantly repressed, whereas the osteogenic transcription factor RUNX2 was up-regulated at 5 days of cell culture, and this was followed up-regulation of the osteoblast specific transcription factor osterix (OSX) at days 11 and 13. Following this transcription factor activation, osteoblast specific marker genes were induced with increased alkaline phosphatase (ALP) observed at day 16, increased osteopontin (OPN) at day 20 and increased osteocalcin (OCN) at day 28. These data suggested that transcription factors regulated MSC osteogenic commitment at the early stage, and induced osteogenic specific marker gene expression at the late stages of cell culture on the NSQ50 surface, resulting in osteogenesis of the MSCs.

Signalling pathway analysis illustrated that bone morphogenetic protein 2 (BMP2) was the initial signalling molecule that triggered osteogenic differentiation of MSCs by inducing RUNX2 expression via the canonical SMAD pathway. BMP2 and its transmembrane receptor type 1A (BMPR1A) were stimulated by

nanotopographical cues by 3 days of cell culture on the NSQ50 surface, whereas the induction of other transmembrane receptors, including the low density lipoprotein-receptor related protein 5 (LRP5) and integrin subunits  $\alpha 3$ ,  $\alpha 4$ ,  $\beta 1$ , and  $\beta 3$  were not observed. Inhibition of BMP2 signalling by the BMP2 antagonist noggin resulted in down-regulation of RUNX2 and ALP. Further analysis of BMP2 signalling revealed that BMP2 also modulated expression of the microRNA (miR)-23b which targets RUNX2. The effect of BMP2 signalling on the expression of RUNX2 was enhanced by co-localizing with integrin  $\alpha\beta 5$  (the vitronectin (VN) receptor) which was found to be up-regulated after 5 days cell culture.

Metabolomics data for MSCs on the NSQ50 surface during early osteogenic differentiation was analysed. MSC cellular metabolite analysis revealed possible changes in bioenergetic balance with shifts towards more mitochondrial oxidative process, possibly indicating a switch in MSCs on the surface towards lineage-specific commitment. Further analysis of the metabolomics data illustrated PPAR $\gamma$  ligands from the polyunsaturated fatty acid family was down-regulated, suggesting the inhibition of adipocyte differentiation in MSCs on the surface. The down-regulation of unsaturated fatty acids could also be involved in the regulation of Ca<sup>2+</sup> channels which positively regulate BMP2 expression. The metabolomics data, together with gene expression and signalling pathway analysis demonstrated that MSCs on the NSQ50 surface initiated osteogenic commitment after 3 days of cell culture, with BMP2 initiating osteogenic transcription factor stimulation of mature and functional osteoblasts on the surface.

# Table of Contents

<b>AUTHOR'S DECLARATION .....</b>	<b>1</b>
<b>ABSTRACT .....</b>	<b>2</b>
<b>TABLE OF CONTENTS .....</b>	<b>4</b>
<b>LIST OF FIGURES .....</b>	<b>11</b>
<b>LIST OF TABLES .....</b>	<b>14</b>
<b>ABBREVIATIONS .....</b>	<b>15</b>
<b>ACKNOWLEDGEMENTS.....</b>	<b>18</b>
<b>CHAPTER 1. INTRODUCTION .....</b>	<b>19</b>
<b>SUMMARY .....</b>	<b>20</b>
<b>1.1 BONE TISSUE BIOLOGY.....</b>	<b>21</b>
1.1.1 BONE STRUCTURE AND FUNCTION .....	21
1.1.2 OSTEOLAST AND BONE MATRIX.....	22
1.1.3 OSTEOLAST AND BONE RESORPTION .....	25
1.1.4 MODELLING AND REMODELLING .....	25
<b>1.2 BONE TISSUE REGENERATION .....</b>	<b>27</b>
1.2.1 BONE TISSUE ENGINEERING.....	28
1.2.2 BIOMATERIALS FOR BONE TISSUE REGENERATION .....	31
1.2.3 STEM CELLS FOR BONE TISSUE REGENERATION .....	34
1.2.3.1 Embryonic stem cells.....	35
1.2.3.2 Induced pluripotent stem cells (iPSCs).....	36
1.2.3.3 Multipotent mesenchymal stromal cells (MSCs).....	37

<b>1.3 MSCS DIFFERENTIATION PROCESS.....</b>	<b>38</b>
1.3.1 MSCS SELF-RENEWAL AND REGULATION .....	38
1.3.2 MSCS DIFFERENTIATION .....	40
1.3.3 TRANSCRIPTIONAL CONTROL OF MSCS OSTEOGENIC DIFFERENTIATION.....	41
1.3.3.1 Runt-related transcription factor 2 (RUNX2).....	41
1.3.3.2 Osterix (OSX) .....	42
1.3.3.3 Homeobox proteins (DLX5 and MSX2) .....	43
<b>1.4 MOLECULAR SIGNALS AND PATHWAYS OF OSTEOGENIC DIFFERENTIATION .....</b>	<b>44</b>
1.4.1 BMP2 SIGNALLING .....	44
1.4.2 WNT SIGNALLING.....	46
<b>1.5. NANOTOPOGRAPHY .....</b>	<b>49</b>
1.5.1 EFFECTS OF NANOTOPOGRAPHY ON MSCS DIFFERENTIATION .....	49
1.5.2 BIOPHYSICAL AND BIOCHEMICAL EVENTS UNDERLYING THE EFFECTS OF NANOTOPOGRAPHY .....	51
1.5.2.1 Focal adhesions .....	51
1.5.3.2 Indirect mechanotransduction.....	53
1.5.3.3 Direct mechanotransduction .....	54
<b>1.6 AIMS OF THE PROJECT .....</b>	<b>57</b>
<b><u>CHAPTER 2. METHODS AND MATERIALS.....</u></b>	<b><u>59</u></b>
<b>SUMMARY .....</b>	<b>60</b>
<b>2.1 NSQ50 NANOTOPOGRAPHY.....</b>	<b>60</b>
<b>2.2 MESENCHYMAL STROMAL CELLS .....</b>	<b>61</b>
2.2.1 CELL ISOLATION FROM HUMAN BONE MARROW .....	61
2.2.2 CELL CULTURE AND HARVEST.....	62
<b>2.3 OLIGONUCLEOTIDES (PRIMERS) SYNTHESIS.....</b>	<b>63</b>
<b>2.4 TOTAL RNA EXTRACTION.....</b>	<b>65</b>
<b>2.5 COMPLEMENTARY DNA (cDNA) SYNTHESIS .....</b>	<b>65</b>

2.5.1	TOTAL RNA REVERSE TRANSCRIPTION .....	65
2.5.2	MICRORNA REVERSE TRANSCRIPTION .....	66
<b>2.6</b>	<b>NUCLEIC ACIDS QUANTIFICATION AND QUALITY CONTROL.....</b>	<b>66</b>
2.6.1	QUANTITATIVE REVERSE TRANSCRIPTION PCR (qRT-PCR).....	67
<b>2.7</b>	<b>PROTEIN ANALYSIS.....</b>	<b>70</b>
2.7.1	PROTEIN PREPARATION .....	70
2.7.1.1	Total protein preparation.....	70
2.7.1.2	Membrane protein preparation.....	71
2.7.2	PROTEIN QUANTIFICATION.....	71
2.7.3	PROTEIN SEPARATION (SDS-PAGE SEPARATION) .....	72
2.7.4	PROTEIN ANALYSIS (I) – IMMUNOPRECIPITATION.....	72
2.7.5	PROTEIN ANALYSIS (II) – WESTERN BLOTTING .....	72
<b>2.8</b>	<b>IMMUNOCYTOCHEMISTRY (ICC).....</b>	<b>73</b>
2.8.1	ICC FOR PROTEINS OF INTEREST.....	73
2.8.2	IMAGING .....	74
<b>2.9</b>	<b>BUFFERS AND ANTIBODIES IN PROTEIN WORK .....</b>	<b>74</b>
<b>2.10</b>	<b>ALIZARIN RED STAINING .....</b>	<b>75</b>
<b>2.11</b>	<b>METABOLOMICS .....</b>	<b>75</b>
<b>CHAPTER 3. TEMPORAL SEQUENCE GENE EXPRESSION OF MSCS ON NSQ50 SURFACE.....</b>		<b>77</b>
<b>SUMMARY .....</b>		<b>78</b>
<b>3.1</b>	<b>INTRODUCTION.....</b>	<b>78</b>
<b>3.2</b>	<b>METHODOLOGY AND EXPERIMENTAL DESIGN .....</b>	<b>80</b>
3.2.1	QUANTITATIVE REAL TIME PCR (qRT-PCR) .....	81
3.2.1.1	Taqman and SYBR Green qRT-PCR .....	81
3.2.1.2	Three modes of SYBR Green qRT-PCR.....	84
3.2.1.3	Endogenous control gene GAPDH.....	84

3.2.2	EXPERIMENTAL DESIGN .....	85
3.2.2.1	Assessment of bone marrow derived mesenchymal stromal cells .....	85
3.2.2.2	Work flow of gene expression measurement .....	86
3.2.2.3	Genes and time points chosen for temporal sequence gene expression .....	88
<b>3.3</b>	<b>RESULTS.....</b>	<b>90</b>
3.3.1	EFFECT OF NSQ50 TOPOGRAPHY ON C-MYC EXPRESSION .....	90
3.3.2	RUNX2 TEMPORAL SEQUENCE EXPRESSION PATTERN DURING NSQ 50 INDUCED MSC OSTEOGENIC DIFFERENTIATION .....	91
3.3.3	OSTERIX (OSX) TEMPORAL SEQUENCE EXPRESSION PATTERN DURING NSQ 50 INDUCED MSC OSTEOGENIC DIFFERENTIATION .....	92
3.3.4	ALP EXPRESSION PATTERN DURING NSQ50 INDUCED MSCS OSTEOGENIC DIFFERENTIATION .....	94
3.3.5	OPN EXPRESSION PATTERN DURING NSQ50 INDUCED MSC OSTEOGENIC DIFFERENTIATION.....	95
3.3.6	OCN EXPRESSION PATTERN DURING NSQ50 INDUCED MSC OSTEOGENIC DIFFERENTIATION.....	96
3.3.7	THE VALIDATION OF KEY GENES EXPRESSION .....	97
3.3.8	THE FORMATION OF BONE NODULES .....	99
<b>3.4</b>	<b>DISCUSSION AND CONCLUSION.....</b>	<b>101</b>
3.4.1	THE TRANSCRIPTIONAL CONTROL OF MSCS ON NSQ50 SURFACE.....	101
3.4.2	BONE MARKER GENES EXPRESSION ON NSQ50 SURFACE .....	103
3.4.3	TEMPORAL SEQUENCE GENE EXPRESSION COUPLES WITH MSC OSTEOGENIC DIFFERENTIATION ON NSQ50 SURFACE.....	103
3.4.4	THE EFFECT OF PLANAR CONTROL ON OSTEOGENIC GENE EXPRESSION.....	105
3.4.5	CONCLUSIONS .....	107
<b>CHAPTER 4. MOLECULAR MECHANISMS UNDERLYING OSTEOGENESIS OF MSCS ON NSQ50 SURFACE .....</b>		<b>108</b>
<b>SUMMARY .....</b>		<b>109</b>
<b>4.1</b>	<b>INTRODUCTION.....</b>	<b>109</b>
<b>4.2</b>	<b>METHODOLOGY.....</b>	<b>112</b>
<b>4.3</b>	<b>RESULTS.....</b>	<b>114</b>

4.3.1	TRANSMEMBRANE RECEPTOR RESPONSE TO THE NSQ50 SURFACE .....	114
4.3.1.1	Effect of the NSQ50 surface on integrins .....	114
4.3.1.2	Effect of NSQ50 surface on Wnt signalling.....	116
4.3.1.3	Effect of the NSQ50 surface on BMPs receptor expression .....	117
4.3.2	INDUCTION OF THE BMP2 – SMAD PATHWAY ON THE NSQ50 SURFACE .....	119
4.3.2.1	Activation of BMP2 (ligand of BMPR1A) signalling.....	119
4.3.2.2	Induction of SMADs - the mediators of canonical BMP2 signalling .....	121
4.3.2.3	Lack of change in the SMAD independent pathway of BMP2 signalling in MSCs on the NSQ50 surface.....	123
4.3.3	THE EFFECT OF BMP2 SIGNALLING IN MSCs ON NSQ50 SURFACE ON OSTEOGENIC DIFFERENTIATION .	124
4.3.3.1	The effect of BMP2 signalling on early bone marker RUNX2 expression.....	124
4.3.3.2	The effect of BMP2 signalling on the mature osteoblast marker gene OPN expression	126
4.3.3.3	The effect of low serum on RUNX2 expression in MSCs on the NSQ50 surface .....	129
4.3.4	THE EXPRESSION OF MIRNAS IN MSCs ON THE NSQ50 SURFACE .....	131
4.3.4.1	Prediction analysis of miRNAs targeting RUNX2 and OSX genes .....	131
4.3.4.2	The expression of miRNAs on NSQ50 surface.....	131
4.3.5	THE RELATION OF BMP2 SIGNALLING TO OTHER OSTEOGENIC REGULATORY EVENTS IN MSCs ON THE NSQ50 SURFACE.....	134
4.3.5.1	BMP2 signal and miRNAs .....	134
4.3.5.2	Crosstalk of BMP2 and integrin $\alpha\beta 5$ signalling.....	135
4.3.5.2.1	The effect of integrins $\alpha\beta 5$ on RUNX2 expression.....	135
4.3.5.2.2	The co-localization of the BMP2 receptor and integrins.....	138
4.3.5.2.3	The functional relation of BMP2 signalling and integrins on NSQ50 .....	140
4.3.5.2.4	The functional relation of integrins to BMP signalling .....	142
<b>4.4</b>	<b>DISCUSSION AND CONCLUSION.....</b>	<b>143</b>
4.4.1	BMP2 SIGNALLING .....	143
4.4.2	THE ROLE OF INTEGRINS IN OSTEOGENESIS OF MSCs ON NSQ50 SURFACE. ....	144

4.4.3	CROSS-TALK BETWEEN BMP2 SIGNALLING AND INTEGRINS. ....	146
4.4.4	MIRNAS. ....	146
4.4.5	CONCLUSIONS. ....	147
<b>CHAPTER 5. METABOLOMICS.....</b>		<b>149</b>
<b>RATIONALE .....</b>		<b>150</b>
<b>5.1 INTRODUCTION.....</b>		<b>150</b>
5.1.1	METABOLIC PROFILE OF PLURIPOTENT STEM CELLS (ESC AND IPSCs) .....	150
5.1.2	METABOLIC PROFILE OF MSCs .....	152
5.1.3	THE LINKS OF METABOLISM TO EPIGENETICS AND GENE EXPRESSION.....	153
<b>5.2 METHODOLOGY AND DATA ANALYSIS .....</b>		<b>154</b>
5.2.1	METHODOLOGY.....	154
5.2.2	DATA ANALYSIS .....	154
<b>5.3 RESULTS.....</b>		<b>156</b>
5.3.1	CLUSTERING ANALYSIS OF METABOLITES IN MSCs ON NSQ50.....	156
5.3.2	BIOENERGETICS OF MSCs ON THE NSQ50 SURFACE .....	161
5.3.3	THE LACK OF ANAEROBIC GLYCOLYTIC PHENOTYPE OF MSCs ON NSQ50 AT EARLY STAGE OSTEOGENESIS.....	161
5.3.4	THE INCREASED MITOCHONDRIAL ACTIVITY FOR BIOENERGETICS OF MSCs ON NSQ50 SURFACE.....	163
5.3.5	THE DOWN-REGULATION OF UNSATURATED FATTY ACIDS .....	166
5.3.6	THE RELATION OF UNSATURATED FATTY ACIDS TO SIGNALLING PATHWAYS.....	170
5.3.6.1	Unsaturated fatty acids induce Peroxisome proliferator-activated receptor gamma (PPARG) activity.....	170
5.3.6.2	The roles of fatty acids on Ca <sup>2+</sup> signalling.....	172
<b>5.4 DISCUSSION AND CONCLUSION.....</b>		<b>174</b>
5.4.1	DISCUSSION .....	174
5.4.2	CONCLUSION .....	176
<b>CHAPTER 6. CONCLUSIONS AND FUTURE WORK.....</b>		<b>178</b>

<b>SUMMARY .....</b>	<b>179</b>
<b>6.1 CONCLUSIONS .....</b>	<b>179</b>
6.1.1 FUNCTIONAL COUPLING OF GENE EXPRESSION AND OSTEOGENIC DIFFERENTIATION .....	179
6.1.2 TRANSCRIPTIONAL CONTROL OF MSC OSTEOGENIC DIFFERENTIATION .....	180
6.1.3 BMP2 SIGNALLING AND OSTEOGENESIS OF MSCS ON THE NSQ50 SURFACE .....	180
6.1.4 IMPLICATING INTEGRIN AVB5 IN OSTEOGENESIS OF MSCS ON THE NSQ50 SURFACE .....	181
6.1.5.1 SYNERGIC EFFECTS OF THE INTERPLAY OF BMP2 AND INTEGRIN AVB5 ON OSTEOGENESIS OF MSCS ON THE NSQ50 SURFACE .....	181
6.1.6 METABOLISM OF MSCS ON THE NSQ50 SURFACE .....	182
<b>6.2 FUTURE WORK .....</b>	<b>183</b>
<b><u>REFERENCES .....</u></b>	<b><u>185</u></b>

## List of Figures

Figure 1.1	Diagram of long bone anatomy and structure.....	22
Figure 1.2	Organization of bone tissue from its smallest components (right) to whole tissues (left).....	24
Figure 1.3	Bone remodelling cycle.....	27
Figure 1.4	Growth of research on bone tissue engineering reflected on the number of publications since 1985 on PubMed. ....	30
Figure 1.5	Schematic diagram describing MSCs self-renewal and differentiation.....	40
Figure 1.6	Diagram of indirect and direct mechanotransduction effectors.....	56
Figure 2.1	The feature of NSQ50 nanopits.....	61
Figure 2.2	Example of relative standard curve for the OPN gene.....	68
Figure 2.3	Example of SYBR green qRT-PCR melting curves generated during OPN gene amplification. ....	70
Figure 3.1	The selective mode of gene expression in MSC multilineage differentiation.	79
Figure 3.2	Fluorescent chemistries used in TaqMan and SYBR Green qRT-PCR. ....	83
Figure 3.3	Ct value of GAPDH measured for MSCs cultured on NSQ50 and planar surfaces at different time points.....	85
Figure 3.4	MSCs expanded in tissue culture flask negatively express tissue specific markers after two passaging.....	86
Figure 3.5	Diagram of parallel work flow for gene expression measurement.....	87
Figure 3.6	Gene expression analysis of C-MYC in MSCs on NSQ50 compared to those on planar control.....	90
Figure 3.7	Temporal sequence gene expression analysis of RUNX2 in MSCs on NSQ50.	92
Figure 3.8	Temporal gene expression analysis of OSX in MSCs on NSQ50. ....	93
Figure 3.9	Effects of NSQ50 surface on homeodomain factors MSX2 and DLX5. ....	94
Figure 3.10	Gene expression analysis of ALP in MSCs on NSQ50. ....	95
Figure 3.11	Gene expression analysis of OPN in MSCs on NSQ50. ....	96
Figure 3.12	Gene expression analysis of OCN in MSCs on NSQ50. ....	97

Figure 3.13	RUNX2 is abundant in cells cultured on the NSQ50 surface for 9 days. ....	98
Figure 3.14	OPN and OCN are abundant in cells cultured on NSQ50 surface for 28 days. ....	99
Figure 3.15	Calcium deposition by MSCs on NSQ50. ....	100
Figure 3.16	Temporal sequence genes expression pattern functionalized NSQ50 surface induced osteogenic differentiation. ....	105
Figure 4.1	The effect of NSQ50 surface on the expression of integrins in MSCs. ....	115
Figure 4.2	The effect of the NSQ50 surface on Wnt signalling at early stage MSCs osteogenic differentiation. ....	117
Figure 4.3	The effect of the NSQ50 surface on BMP receptor, BMPR1A at the early stages of MSCs osteogenic differentiation. ....	118
Figure 4.4	The effect of NSQ50 surface on BMP2 expression at the early stage of MSC osteogenic differentiation. ....	120
Figure 4.5	BMP2 protein expression in MSCs cultured on the NSQ50 and planar surfaces. ....	121
Figure 4.6	The induction of the BMP2 canonical pathway mediator SMAD on the NSQ50 surface. ....	122
Figure 4.7	Lack of activation of TGF-beta activated kinase 1 binding protein tab1 in the SMAD independent pathway of BMP2 signalling. ....	124
Figure 4.8	RUNX2 responses to the BMP2 antagonist noggin. ....	126
Figure 4.9	OPN responses to the BMP2 antagonist noggin. ....	128
Figure 4.10	RUNX2 expressions in low serum and normal medium. ....	130
Figure 4.11	The prediction of miRNAs targeting RUNX2 and OSX using TargetScan. ....	132
Figure 4.12	The expression of miRNAs targeting RUNX2 and OSX in MSCs on the NSQ50 surface. ....	133
Figure 4.13	The effects of BMP2 signalling on miRNAs. ....	135
Figure 4.14	The effect of integrins on RUNX2 expression. ....	137
Figure 4.15	Integrins co-localize with the BMP2 receptor when MSCs are cultured on the NSQ50 surface. ....	139
Figure 4.16	The effect of BMP2 signalling on integrin expression. ....	141
Figure 4.17	The effect of VN on integrin $\alpha\beta 5$ and BMPR1A expression. ....	143

Figure 5.1	The lipids profile of MSCs on the NSQ50 surface for cells cultured at 3, 5, and 7 days. ....	157
Figure 5.2	The amino acid profile of MSCs on the NSQ50 surface for cells cultured at 3, 5, and 7 days. ....	158
Figure 5.3	The nucleotides and other metabolites profile of MSCs on the NSQ50 surface for cells cultured at 3, 5, and 7 days. ....	159
Figure 5.4	The non-pathway mapping metabolites profile of MSCs on the NSQ50 surface for cells cultured at 3, 5, and 7 days. ....	160
Figure 5.5	Metabolites in MSCs on the NSQ50 surface involved in the glycolysis pathway. ....	162
Figure 5.6	The effect of the NSQ50 surface on the glycolytic bioenergetics pathway in MSCs. ....	163
Figure 5.7	NSQ50 surface shifting bioenergetics of MSCs to mitochondria. ....	165
Figure 5.8	Fatty acids involved in biosynthesis of unsaturated fatty acids in MSCs cultured on NSQ50 surface for 3, 5 and 7 days.....	167
Figure 5.9	Heatmap clustering of fatty acids in MSCs on the NSQ50 surface for cells cultured at 3, 5, and 7 days.....	168
Figure 5.10	Down-regulation of fatty acids involved in biosynthesis of unsaturated fatty acids in MSCs cultured on NSQ50 surface for 3, 5 and 7 days. ....	169
Figure 5.11	The down-regulation of PPARG ligands in MSCs on the NSQ50 surface.....	171
Figure 5.12	The expression of long chain saturated fatty acids involved in the regulation of Ca <sup>2+</sup> signalling in MSCs on the NSQ50 surface. ....	173

## List of Tables

Table 2.1	Components of transport medium for bone marrow. ....	62
Table 2.2	Components of modified basal medium for MSC culture.....	62
Table 2.3	Primers for genes encoding proteins. ....	64
Table 2.4	Primers for miRNAs. ....	65
Table 2.5	PCR cyclic parameters for SYBR Green qRT-PCR. ....	68
Table 2.6	The components of RIPA lysis buffer. ....	71
Table 2.7	Buffers used for protein work. ....	74
Table 2.8	Antibodies used for protein work. ....	75
Table 3.1	Genes associated with MSCs functional relationship between proliferation and osteogenic differentiation. ....	89
Table 4.1	Genes and/or proteins investigated for the analysis of osteogenic signalling pathway in MSCs on NSQ50 surface. ....	113

## Abbreviations

acetyl-CoA	acetyl coenzyme A
ACVR2A	activin A receptor II A
ALP	alkaline phosphatase
ANOVA	analysis of variance
ATP	adenosine triphosphate
BMP2	bone morphogenetic protein 2
MSCs	mesenchymal stromal cells
BMPR1A	BMP receptor type 1 A
BMU	basic multicellular unit
BRAM1	BMP receptor associated molecule 1
Ca <sup>2+</sup>	Calcium
CaP	calcium phosphate
CCD	cleidocranial dysplasia
CD markers	surface antigen markers
CDK	cyclin dependent kinase
cDNA	Complementary DNA
CFU-F	colony forming unit-fibroblast
CTNNBIP1	beta-catenin-interacting protein 1
DEX	dexamethasone
dsDNA	doubled strand DNA
EB	embryonic body
EBL	electron beam lithography
ECM	extracellular matrix
endosteum	inner membranous sheath
ERK	extracellular signal-regulated kinase
ERK1/2	extracellular signal-related kinase 1/2
ESCs	embryonic stem cells
ETC	Electron Transport Chain
FBS	fetal bovine serum
FGF2	fibroblast growth factor2
FGFs	fibroblast growth factors

FRET	fluorescence resonance energy transfer
GAPDH	Glyceraldehyde 3-phosphate dehydrogenase
Gla	3-gammacarboxy-glutamic acid residues
GLUT1/3	glucose transporter 1/3
GSK-3 $\beta$	glycogen synthase kinase 3 $\beta$
HA	hydroxyapatite
HACD4	histone deacetylase 4
HDs	homeodomain proteins
HIF-1	hypoxia-inducible factor 1
HILIC	hydrophilic interaction liquid chromatography
HK	hexokinase
IGFs	insulin-like growth factors
iPSCs	induced pluripotent stem cells
Jnk	c-jun-n-terminal kinase
LC-MS	liquid chromatography and mass spectrometry
LINC	linker of cytoskeleton and nucleoskeleton
LRP5/6	Low-density lipoprotein receptor-related protein 5 or 6
M-CSF	macrophase colony-stimulating factor
MAPKK1	mitogen-activated protein kinase kinase 1
MAR	matrix attachment region
miRNA	MicroRNA
mRNA	messenger RNA
MSCs	Multipotent mesenchymal stromal cells
NADH	Nicotinamide adenine dinucleotide
NF $\kappa$ B	nuclear factor kappa beta
NGS	next generation sequencing
NSQ50	near square50 surface
OCN	osteocalcin
OPN	osteopontin
OSE2	osteoblast specific <i>cis</i> -acting element
OSX	Osterix
OxPhos	Oxidative Phosphorylation

PI3K	phosphatidylinositol 3-kinase
p38 MAPK	include MAP kinase p38
PCL	polycarprolactone
periosteum	fibrous structure
PFK1	phosphofructokinase 1
PGA	polyglycolide
PGKs	glycolytic phosphoglycerate kinases
Pi	phosphate
PKs	pyruvate kinases
PLA	polylactide
PMMA	polymethylmethacrylate
PPARG	Peroxisome proliferator-activated receptor gamma
PPi	pyrophosphate
PPP	pentose phosphate pathway
rhBMP2	recombinant human BMP2
qRT-PCR	quantitative real time PCR
R-SMADs	receptor-regulated Smads
RANKL	receptor activator NF <sub>κ</sub> B of ligand
RGD	arg-gly-asp
ROS	Reactive Oxygen Species
RT-PCR	reverse transcription PCR
RUNX2	runt-related transcription factor 2
SAM	self-assembled monolayer
Smurf1	Smad-ubiquitination-regulatory factor 1
SQ	symmetries of square
TAK1	TGF-beta activated kinase 1
Tcf/Lef	T cell factor/Lymphoid enhancer binding factor
TGF-β	transforming growth factor-β
Tm	melting temperature
VN	vitronectin

## **Acknowledgements**

Firstly I would like to thank my supervision team, specifically professor Matthew Dalby, for his help, advice and support over the years. Next I would like to thank everyone in the laboratory for all their help.

My thanks and gratitude also goes to my wife and my son whose love and support was often the thing that kept me going.

## **Chapter 1. Introduction**

## Summary

This thesis aimed to address issues of fundamental understanding of how a nanotopography (NSQ50) which has been identified as osteoinductive (Dalby et al., 2007d) initiates osteogenesis. Mesenchymal stromal cells (MSCs) cultured on the NSQ50 nanotopography embossed polycaprolactone (PCL) were used for functional analysis of osteogenesis in MSCs. Cell growth modulators, transcription factors regulating MSC fate determination and osteogenic differentiation, signalling molecules modulating these transcription factors and osteogenic differentiation itself were explored. Metabolites likely influencing MSC early stage osteogenic differentiation on the NSQ50 surface were also investigated.

This chapter will introduce main themes for the thesis including bone tissue biology and stem cells, specifically MSCs as a major allogeneic cell resource for bone tissue regeneration. General background on biomaterial and tissue engineering are also described. Mechanisms underlying MSC osteogenic differentiation are introduced. More specific background is provided within each chapter. Chapter 2 contains the methods used during the course of this research. Chapter 3 describes quantitative real time PCR (qRT-PCR) experiments and verification of functionally coupling gene expression with osteogenic differentiation of MSCs on the NSQ50 surface. In chapter 4, molecular signalling and pathways stimulating MSC osteogenic differentiation on the NSQ50 surface, such as BMP2 signalling, are investigated. Furthermore, the role of BMP2 signalling interplay with integrins and regulating microRNAs (miRNA) are explored. Chapter 5 is concerned with metabolism and possible regulatory roles of metabolites in MSC osteogenic determination on the NSQ50 surface. Finally, chapter 6 presents the final conclusions of this thesis and the thinking for future work.

## **1.1 Bone tissue biology**

### **1.1.1 Bone structure and function**

In the adult human body, the skeleton is comprised of 213 bones and serves a variety of functions. The skeleton is the framework of the human body and it provides mechanical protection for vital internal organs. Skeletal bones offer the sites for muscle and tendon attachment, and thus support the body's movement and locomotion. Bone tissue contains 99% of the calcium and 85% of the phosphorus found within the whole body and maintains the body's mineral homeostasis. In addition, bone tissue provides the environment for bone marrow, which produces new blood cells and works as a vital part of the lymphatic system (Brandi, 2009; Taichman, 2005).

Macroscopically, there are two types of bones (Figure 1.1): one is the compact bones that constitute about 80% of the skeleton, and the other is spongy (trabecular) bones which make up the rest of the skeleton. Both compact bone and spongy bone are composed of osteons. Compact osteons are cylindrical in shape and form a branching network within the compact bone, which helps provide the strength of bone. Spongy osteons are a honeycomb-like network, and the spaces between trabecular plates and rods are filled with bone marrow cells. The compact bone has an outer fibrous structure (periosteum) which contains the blood vessels, nerve endings, osteoblasts and osteoclasts, and inner membranous sheath (endosteum) contacting the bone marrow space, spongy bone, and blood vessel canals. Like the periosteum, endosteum also contains blood vessels, and osteoblasts and osteoclasts (Brandi, 2009).

The periosteum of compact bone consists of an outer fibrous layer and inner osteogenic layer. The inner osteogenic layer contains osteoprogenitor cells that can develop into osteoblasts. Therefore, the activity of periosteum plays an important role for bone growth and fracture repair.

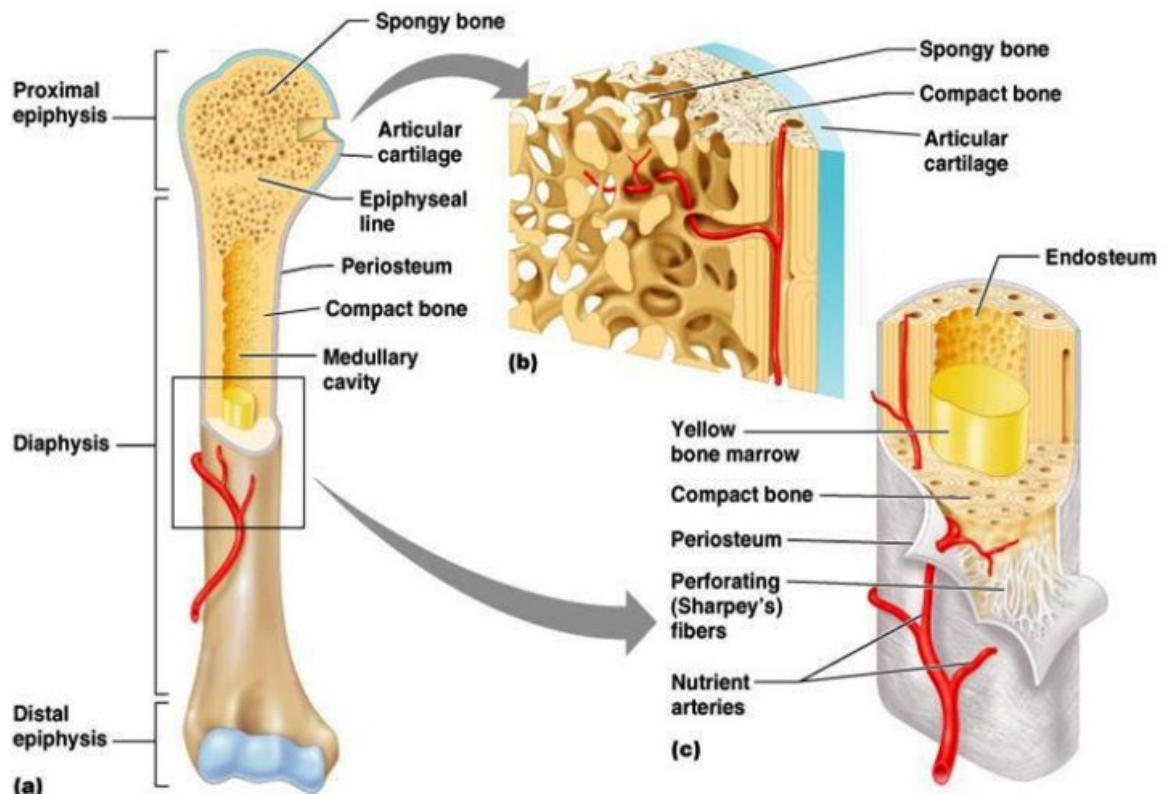


**Figure 1.1** Diagram of long bone anatomy and structure.

The long bone diagram shows: (a) long bone is composed of proximal epiphysis, diaphysis and distal epiphysis. (b) In the proximal epiphysis, most bone tissue is spongy bone arranged in a honeycomb-like network, and the spaces between trabecular plates and rods are filled with bone marrow. (c) Compact bone constitutes the diaphysis of the long bones. Compact bone contains branching networks surrounded by the outer fibrous structure (periosteum) which contains the blood vessels, nerve endings and osteoblasts and osteoclasts. The endosteum of compact bone contacts with bone marrow and contains blood vessels and osteoblasts and osteoclasts. (Cummings, 2004).

### 1.1.2 Osteoblast and bone matrix

Osteoblasts are bone forming cells which produce and secrete proteins forming the bone matrix (Benayahu et al., 1995). They are then responsible for subsequent matrix mineralization (Boskey, 1998).

Osteoblasts are derived from mesenchymal stem cells that give rise to osteoprogenitor cells. The fully differentiated (mature) osteoblasts produce type I collagen, the major component of bone matrix (Brodsky and Persikov, 2005). Type I collagen is a polymeric protein initially secreted by osteoblasts in the

form of a precursor that contains peptide extensions at both the amino-terminal and carboxyl ends. Further cellular processing results in the extra propeptides extensions being removed and the formation of mature type I collagen, which then assembles into a collagen fibril. Collagen molecules are interconnected by the formation of pyridinoline cross-links to form the primary matrix structure of bone (Viguet-Carrin et al., 2006).

Osteoblasts also synthesize a number of noncollagenous proteins which incorporate into the bone matrix, including osteocalcin (OCN), osteonectin, osteopontin (OPN), vitronectin, fibronectin and bone sialoprotein, alkaline phosphatase (ALP), etc. These proteins are produced in minor amounts compared to collagens, however they serve diverse functions in bone formation and turn over. ALP has been thought to play a role in bone mineralization by releasing phosphate and deficiency in ALP results in hypophosphatasia, a condition characterized by defective bone mineralization (Whyte, 1994). OCN is very specific marker for bone turn over and is an extracellular matrix (ECM) component the osteoblast use to capture calcium (Ducy et al., 1996). The others, such as OPN, vitronectin, fibronectin and bone sialoprotein serve as attachment factors interacting with integrins (OPN, as well as containing cell attachment peptide motifs is also involved in calcium acquisition (Kvansakul et al., 2004). Together these proteins serve to allow osteoblast adhesion and to sequester calcium and phosphate into the osteoblast environment - the recruitment of cells, calcium and phosphate leads to mineralization (Boskey, 1998; Buchet et al., 2013).

Mature bone matrix is a composite of polymeric collagen reinforced with nanocrystals made of hydroxyapatite mineral ( $\text{HCa}_5\text{O}_{13}\text{P}_3$ ). The nanocrystals provide mechanical stiffness and load-bearing strength to bone, while collagenous proteins make bone elastic and flexible. Bone matrix is highly ordered, well aligned structure over multiple size scales (Figure 1.2). Collagen proteins (~2 nm in diameter) self-assemble into fibrillar structures which then further accumulate into fibrils (~500 nm in diameter). Bone minerals (nanocrystals) deposit in 'hole' zones where are left at the ends of fibils when they stack into fibers (Landis, 1995).

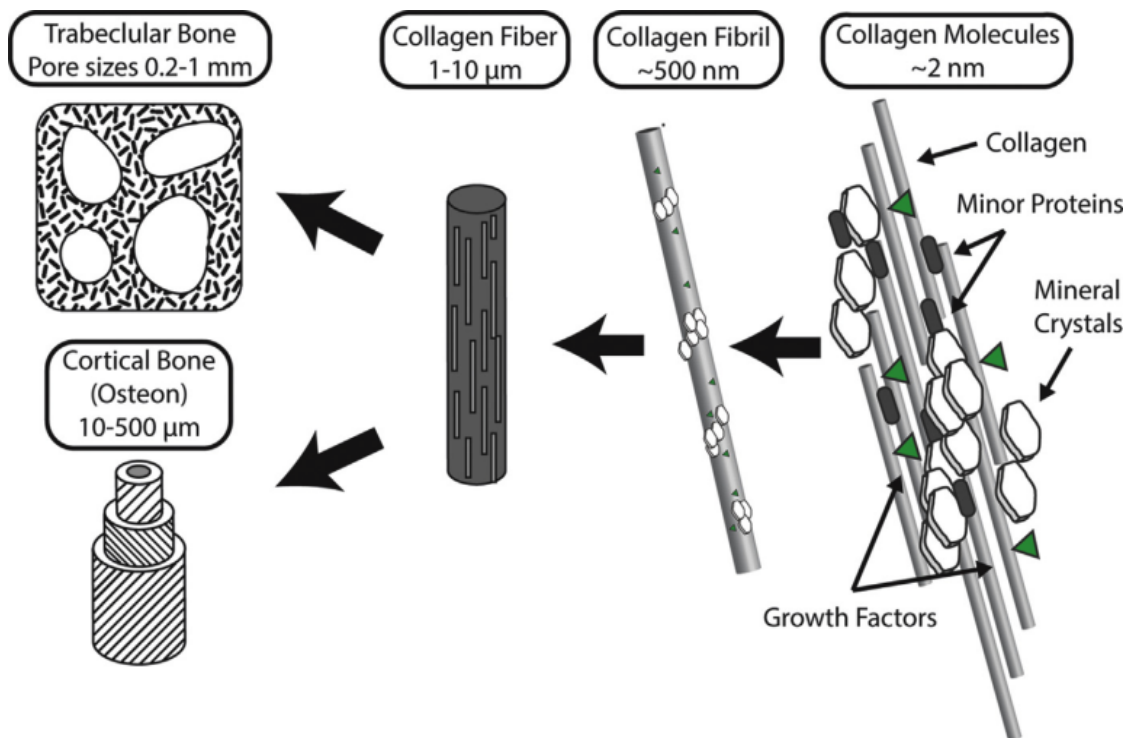


**Figure 1.2** Organization of bone tissue from its smallest components (right) to whole tissues (left).

Bone is a composite of collagen fibers reinforced with calcium phosphate nanocrystals arranged in a semi-regular pattern. Other components include minor proteins and growth factors. Mineralized collagen is aggregated into small fibrils, which further combine to form fibers a few microns in diameter and several mm long. In trabecular (spongy) bone the mineralized fibers are semi-randomly laid out in struts forming an open cell foam. Cortical bone is composed of circular osteons which feature aligned sheets of mineralized fibers wrapped around a central hollow core. (Picture taken from Kane et al, 2013).

Osteoblasts eventually terminally differentiate and are trapped in mineralized matrix forming osteocytes. Osteocytes are the most abundant cell type in bone, they are regularly spaced throughout the matrix and maintain connections with each other, with the cells on the bone surface and even with cells of the bone marrow through their multiple cytoplasmic extensions (Marotti, 1996). The communication networks through bone tissue make osteocytes ideal candidates for mechanosensory cells being able to detect and transduce stress signals into bone biological activity (Aarden et al., 1994; Rubin and Lanyon, 1987).

Buried osteoblasts on the top of unmineralized matrix that covers the quiescent bone (i.e., bone that is not undergoing remodeling), are termed bone lining cells

(Parfitt, 1994). Lining cells secrete collagenase to remove the unmineralized collagen layer, while producing 'homing' signals to guide osteoclast precursors to a specific location on bone for bone resorption (Parfitt et al., 1996).

### **1.1.3 Osteoclast and bone resorption**

Osteoclasts, unlike osteoblasts, are derived from the monocyte / macrophage haematopoietic lineage in bone marrow (Boyle et al., 2003). The formation of osteoclasts requires the presence of marrow stromal cells and osteoblasts which produce cytokines, such as receptor activator of NF $\kappa$ B ligand (RANKL) and macrophage colony-stimulating factor (M-CSF). RANKL is critical for osteoclast differentiation and formation, while M-CSF is required for proliferation, survival and cytoskeleton rearrangement of osteoclasts and their precursors (Cohen, 2006).

Mature osteoclasts are multinucleated cells with finger-shaped projections of the membrane (ruffled border) which mediate the resorption of the calcified bone matrix (Roodman, 1996). The ruffled border is surrounded by a specialized area (clear zone) which delineates and seals off the area of the attachment of osteoclast to the bone surface. Osteoclasts bind to bone matrix mainly through membrane receptor integrins  $\alpha_v\beta_3$ , which links to bone matrix noncollagenous protein, such as OPN (Ross and Teitelbaum, 2005). Hydrogen ions are released by an ATP-driven proton pump located in the ruffled border membrane to dissolve mineral components of bone matrix at the resorption site, and then the protein components, mainly collagen, are digested by matrix metalloproteinases and cathepsins K, B and L secreted by osteoclast. Through the process of endocytosis, some of the digested products of bone resorption are taken into the osteoclast (Wilson et al., 2009).

### **1.1.4 Modelling and remodelling**

Bone is highly specialized and dynamic organ that undergoes continuous regeneration. During development and growth, bones adapt their shape and size

in response to physiological and / or mechanical influences by a process known as modelling. In the modelling process, bones grow or reshape by removal or addition of bone to the appropriate surface through the independent action of osteoblasts and osteoclasts (Brandi, 2009; Yajima et al., 2008). Physiologically, bone modelling is less frequent than remodelling in adults. Modelling occurs with aging where bone normally widens in response to periosteal apposition of new bone and endosteal resorption of old bone. However, in the modelling process, bone formation and resorption are not coupled, which differ from bone remodelling (Kobayashi et al., 2003).

Bone remodelling is described as a process that involves the removal of old bone by osteoclasts followed by the deposition of new bone by osteoblasts at the same location. Bone tissue is renewed by remodelling throughout life to prevent bone microdamage, so as to maintain bone strength and mineral homeostasis (de Baat et al., 2005). Bone remodelling is achieved using a unique temporary structure, known as a basic multicellular unit (BMU) that contains a well-orchestrated spatial and temporal relationship of different cell types in four distinct phases (Figure 1.3). Removal of old bone is composed of quiescence and resorption phases in which monocyte-macrophage osteoclast precursors lift lining cells off the bone surface and fuse to form multinucleated pre-osteoclasts which bind to bone surface to resorb bone. Following bone resorption is the bone formation process which constitutes reversion and formation phases. In reversal, bone resorption is inhibited by mononuclear cells and pre-osteoblasts are recruited into the cavity to initiate the bone formation phase to form new bone. At the end of each remodelling cycle, a new osteon is created, and the remodeling process is equivalent in compact and spongy bone (Parfitt, 1994).

In bone remodelling, the transition of bone resorption to formation occurring in the reversal phase is crucial. Signals are required to couple the end of resorption with the recruiting of osteoblast precursors at the site of resorption hence inducing bone formation. It has been proposed that factors released from bone matrix during resorption involved in the coupling process, include transforming growth factor- $\beta$  (TGF- $\beta$ ), bone morphogenetic proteins (BMPs), insulin-like growth factors (IGFs) and fibroblast growth factors (FGFs) (Henriksen et al.,

2014; Henriksen et al., 2009). TGF- $\beta$  is an inducer of bone matrix protein synthesis in bone formation. It is released from bone matrix while bone is resorbed, and inhibits RANKL to decrease osteoclasts resorption (Bonewald and Mundy, 1990).

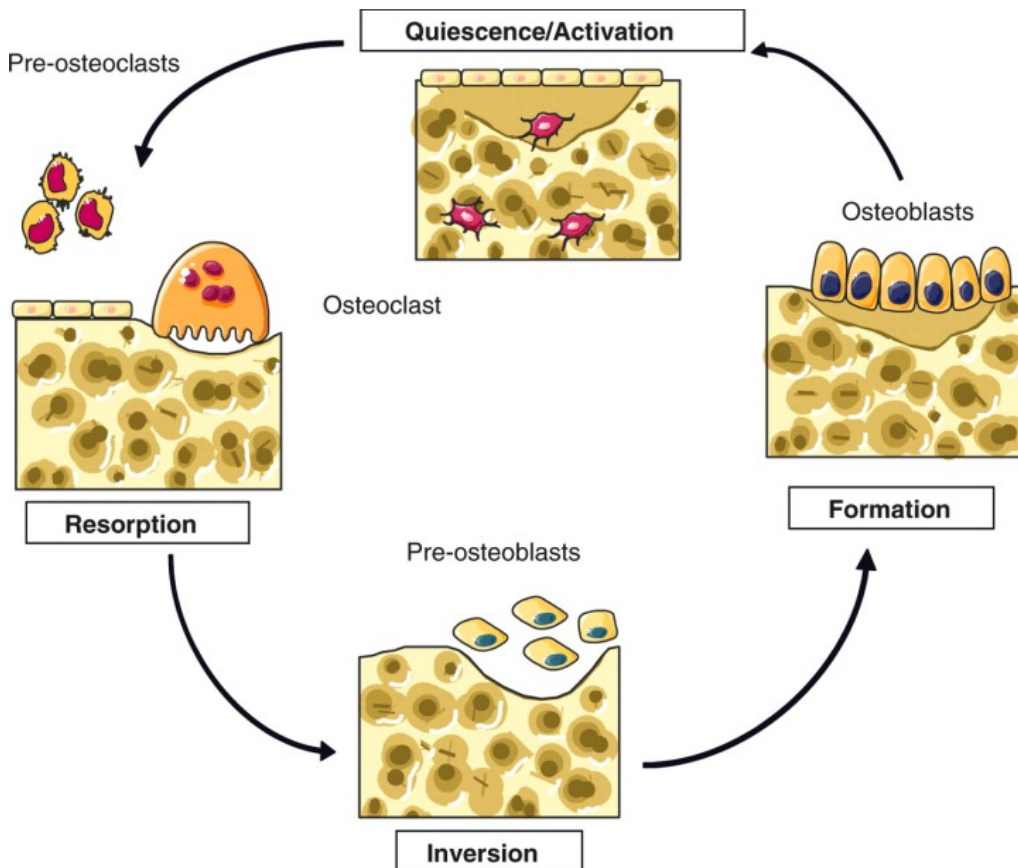


**Figure 1.3** Bone remodelling cycle.

The bone remodelling cycle contains four phases. In the quiescence phase, lining cells degrade unmineralized matrix and guide pre-osteoblasts bind to bone matrix noncollagenous proteins. In the resorption phase, osteoclasts release hydrogen ions and enzymes to digest minerals and collagenous components in matrix. In the reversal phase, at resorption cavities coupling signals are released to decrease osteoclasts activity and recruit pre-osteoblasts into the cavities. In the formation phase, osteoblasts synthesize new collagenous proteins and mineralize matrix by releasing calcium and phosphate. (Picture taken from Brandi, 2009).

## 1.2 Bone tissue regeneration

The aim of tissue regeneration is to restore, maintain or enhance damaged tissues and / or organs function. Nowadays, regenerative medicine has brought

high expectations for a number of intractable diseases, such as osteoporosis, Parkinson disease, Alzheimer's disease, spine injuries or cancer (Novikova et al., 2003; Oryan et al., 2014; Tataria et al., 2006). Like any other tissues/organs, bone tissue regeneration is a complex, fine-tuned physiological process. Although bone possesses the intrinsic capacity of self-regeneration in response to injury throughout adult life, it is either obviously impaired or simply insufficient if the injury is too great. In the common clinical setting, bone fracture healing often results in impaired bone formation owing to delayed union or fracture non-union (Audige et al., 2005), while in some other bone diseases, such as larger bone defects, avascular necrosis and osteoporosis, a large quantity of bone regeneration is required, which is beyond the normal potential of bone tissue self-regeneration. Many strategies have been evolved to augment bone tissue regeneration in clinical practice, including autologous bone grafts, allografts, xenografts and bone-graft substitutes, growth factors (Dinopoulos et al., 2012; Giannoudis et al., 2005), and distraction osteogenesis and bone transport (Aronson, 1997). Among those strategies, bone graft substitutes have attracted intensive investigation in the effort to overcome the drawbacks of autologous bone grafts and allografts, as bone graft substitutes combine scaffolds and bone cells and even osteoinductive proteins and growth factors to generate bone tissue constructs *in vitro* for subsequent transplantation (Dinopoulos et al., 2012).

### **1.2.1 Bone tissue engineering**

Bone tissue engineering, as an alternative solution for bone graft substitutes, first emerged in the 1980s and the technology evolved from principle of biomaterials used in bone tissue implantation (Vacanti, 2006). Nowadays, bone tissue engineering aims to produce new functional bone tissue *de novo*, by loading osteogenic cells on scaffolds (usually a biocompatible material), and with the applications of multidisciplinary techniques to promote cells proliferation and differentiation into bone tissue *in vitro* (Sachlos and Czernuszka, 2003).

Bone tissue engineering contains a few key components to achieve regenerative bone, including (Hardouin et al., 2000):

1. **Scaffolds:** In the context of bone tissue engineering, scaffolds are designed using biocompatible materials, such as polymers, ceramics to provide bone tissue specific environment and architecture for bone cell and tissue growth (Butler et al., 2000; Jones et al., 2009).
2. **Cells:** cells seeded on scaffold are essential factor of bone tissue engineering. They could be progenitor cells, such as MSCs or mature bone cells (e.g. osteoblasts). The ideal cell source should be easily isolated and expanded into high numbers, and after seeding on scaffold these cells can specifically proliferate and differentiate into bone tissue (Heath, 2000).
3. **Morphogenic signals:** Growth factors are secreted by many cell types and service as stimulus to induce morphogenic signals for cell adhesion, proliferation and differentiation. Thus, these molecules play important roles in tissue engineering. For example, growth factors such as BMP2, TGF- $\beta$ , have been used bone tissue engineering to enhance bone growth (Jadlowiec et al., 2003; Rose and Oreffo, 2002).
4. **Vascularization:** Both compact and spongy bones contains vascularized network, which is essential to supply nutrients, and clear metabolic by-products for bone growth. In the context of bone tissue engineering, it is vital to integrate a vascularization network into engineered bone constructs, which maintains the survival of large masses of cells and facilitates the integration of bone tissue constructs with host tissue (Das and Botchwey, 2011).

Although bone tissue engineering is an ideal strategy to eliminate the limitations of current clinically used treatments related to autografts, allografts and xenografts in bone diseases, only a few engineered bone grafts have been approved for clinical practice at the moment and their implementation as part of routine treatment for bone replacement in hospital is controversial (Hollister and Murphy, 2011). The main drawback of this approach is the involvement of

cell manipulation, which limits the widespread use in clinical practice. However, as a very promising strategy, research in this field has grown tremendously in the last decade. The numbers of publications in this field has increased year on year since 1985 (Figure 1.4A). The understanding and imitation of natural bone tissue developmental principles may be key to the future success of bone tissue engineering. Most researches have focused on scaffolds / biomaterials and stem cells in the last four years (Figure 1.4B). Properly designing scaffolds / biomaterials is important for mimicking bone tissue microenvironment's physical properties and initiating ectopic bone formation (Butler et al., 2000; Habibovic and de Groot, 2007), and the use of multipotent stem cells can support bone healing process at different stages of bone tissue development (Drosse et al., 2008).

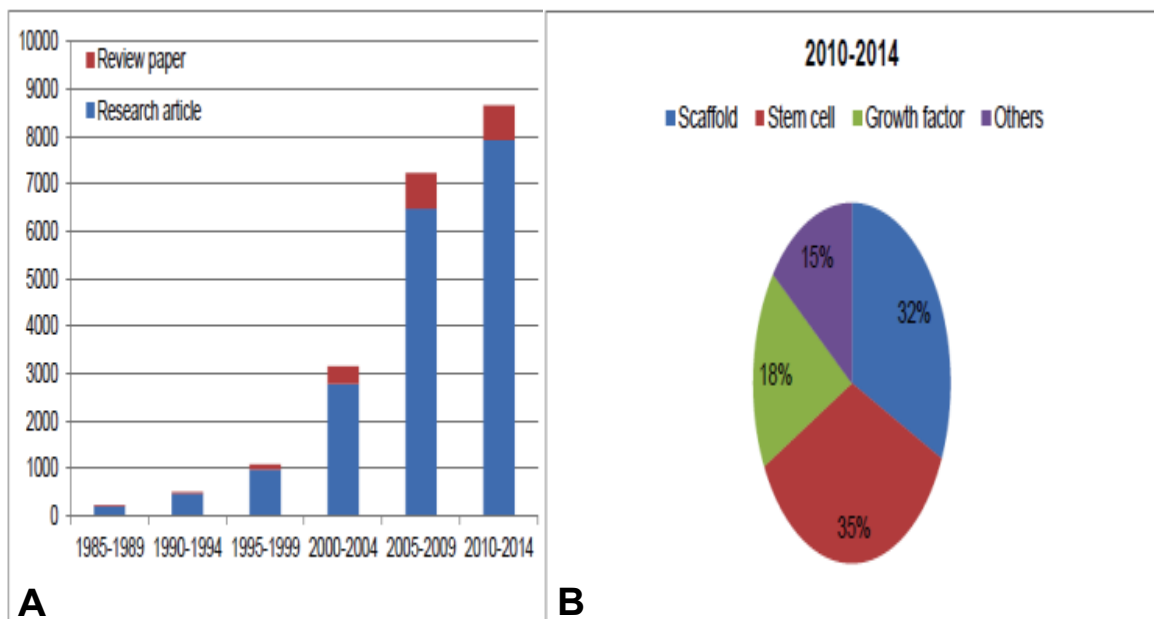


**Figure 1.4** Growth of research on bone tissue engineering reflected on the number of publications since 1985 on PubMed.

(A) Published research articles on bone tissue engineering (blue); published review articles on bone tissue engineering (red). (B) Break-down of articles published on bone tissue engineering focus since 2010. These publications are identified by a PubMed search using the terms: “bone tissue engineering research articles”, “bone tissue engineering review articles” “bone tissue engineering scaffolds”, “bone tissue engineering cells”, “bone tissue engineering growth factors” and “bone tissue engineering others”.

## 1.2.2 Biomaterials for bone tissue regeneration

Materials used in replacing human bone can be traced back to the prehistoric period. More recently, it is thought iron dental implants were used in Europe by 200 AD, and these implants integrated into bone after implantation (Artico et al., 2003). In the 1980s, biomaterials were defined as “non-viable materials used in a medical devices, intended to interact with biological systems” (Williams, 1999), and later on a comprehensive definition for the term of biomaterial was described as: “A biomaterial is a substance that has been engineered to take a form which, alone or as part of a complex system, is used to direct, by control of interactions with components of living systems, the course of any therapeutic or diagnostic procedure, in human or veterinary medicine” (Williams, 2009). These definitions echoed the evolution and progression of biomaterials as medical devices in the past half century, and biomaterials were further characterized to three generations according to materials properties and clinical applications (Hench, 1980; Hench and Polak, 2002).

### 1. The first generation biomaterials for bone tissue implantation.

The first generation of biomaterials are bioinert and thus are not rejected by the human body, while appropriate physical properties matches the requirements to support host tissues. This has resulted in a large set of implantable materials varying from metallic materials (Long and Rack, 1998), ceramic materials (Boutin, 1972; Christel et al., 1988) to polymers (Fisher and Dowson, 1991; Lewis, 1997) used in clinical applications. The main shortcoming of the first generation of biomaterials is the uncontrollable interface between implant material and living tissue. A layer of unspecific proteins is adsorbed onto the material surface after implantation, resulting in unspecific signalling to the cellular environment. Consequently, a layer of fibrous tissue grows on material surface, and with time such fibrous tissue encapsulates the implant, leading to the separation of implant from the host tissue (Hench, 1980).

### 2. The second generation biomaterials for bone tissue implantation.

To overcome the interfacial problems associated with first generation biomaterials, research within the field of biomaterials has focused on developing bioactive materials, which elicit specific biological responses from the host tissue (Hench and Polak, 2002). The key feature of the second generation biomaterials is the ability to interact with cells to stimulate specific cellular responses for appropriate tissue adherence and bonding (Hench, 1980).

Typical bioactive materials are ceramics which share similar structure and surface features with bone mineral phase, thus enabling binding to the bone without mediation of a fibrous interface (Schepers et al., 1991). The most commonly used ceramics are hydroxyapatite (HA), calcium phosphate (CaP) based materials and their combinations. These materials have been demonstrated to be biocompatible and osteoinductive (Pollick et al., 1995; Ripamonti, 1991; Yamasaki and Sakai, 1992; Yuan et al., 1998). Although the biological mechanisms of the osteoinduction from these materials are not fully understood, two hypotheses have been proposed. One is that the materials surface features absorb and present osteoinductive factors to the cells, the other is the releasing of calcium and phosphate ions exert osteoinductive effects on stem cell differentiation into bone cells (Barradas et al., 2011; Yuan et al., 2011).

Materials bioactivity can also be achieved for non-bioactive materials by either coating the surface of the implant with a bioactive ceramic or modifying the surface of the material to obtain the bioactivity. All metallic materials are non-specifically bioactive. Coating ceramics on metals can be achieved by electrophoretic deposition (Ducheyne et al., 1990), laser ablation (Serra, 2001), or plasma spraying (Ducheyne and Healy, 1988). However, these coating processes cannot generate covalent links with the materials, and are not cost-effective. A number of methods of chemical surface modification have been developed to produce apatite or CaPs layer chemically linked on metal surface, including thermochemical treatment (Kokubo, 1996), chemical etching (Ohtsuki et al., 1997), self-assembled monolayer (SAM) (Wheeler et al., 1997). These methods are mainly applied on titanium and its alloys.

Besides the above biomaterials, many polymers are characterized as the second generation of biomaterial in orthopaedics and bone regeneration, as they can bio-resorb. Polymers such as polyglycolide (PGA), polylactide (PLA) and polycaprolactone (PCL) can be degraded and resorbed by hydrolysis of their backbone chains due to enzymatic activities in living environment (Ciccone et al., 2001). The biodegradable property of polymers enables the interface between material and tissue to be controlled with time. The advantage of polymeric material over metallic implants is the potential reduction of the stress shielding effect, and their mechanical strength can be improved by self-reinforcing process through that polymer matrix is strengthened with oriented fibres or fibrils of the same material (Tormala, 1992; Vasenius et al., 1994).

### 3. The third generation biomaterials for bone tissue implantation.

The feature of third generation biomaterials is described as the materials ability to stimulate reproducible, specific cellular response at the molecular level resulting in regeneration of living tissue (Hench and Polak, 2002) . This requires materials possessing both increased, controllable bioactivity and biodegradable properties. The bioactivity of a material enables cells specifically to respond to the material at the molecular level and prompt cell invasion, attachment, proliferation and differentiation. Research and development of the third generation of biomaterials is ongoing, and the strategies to endow biodegradable and bio-absorbable materials with enhanced bioactivity have attracted particular attention. Although there are no conclusions as yet in the literature, these strategies show promising options for the third generation material in bone tissue engineering and bone regeneration:

- Composite polymers: Enhanced bioactivity of biodegradable polymeric materials can be achieved by combination of polymers with specific biomolecules that allow cell guidance and stimulation towards a particular response. The composite materials possess the advantages of each component (i.e., polymer biodegradability and biomolecule bioactivity), and demonstrate success in bone regeneration that exceeds the results when these materials are used separately. For example, addition of HA to various polymers, including PLA

(Wei and Ma, 2004), PLGA (Kim et al., 2006a), chitosan (Chesnutt et al., 2009) and collagen (Rodrigues et al., 2003; Wahl and Czernuszka, 2006) resulted in enhanced bone formation *in vitro* and *in vivo*.

- **Advanced hydrogels:** Hydrogels are water-swollen polymeric materials with a distinct three-dimensional structure, and have been used in clinical tissue repair and regeneration due to their capacity for mimicking ECM structure and delivering required bioactive agents that promote tissue regeneration (Lee and Mooney, 2001; Slaughter et al., 2009). Modification of hydrogels with growth factors and peptide sequences such as transforming growth factor  $\beta$ 3 (TGF $\beta$ 3), peptides RAD and RGD resulted in increases in production of ECM proteins and promoted cell-material interactions (Guarino et al., 2007; Na et al., 2007). Hydrogels fabricated by self-assembling peptides to form completely biological, biocompatible and biodegradable scaffolds for bone regeneration have gained attention recently (Semino, 2008). These hydrogels mimic the nature of ECM and demonstrate osteoinductivity, while the breaking down into amino acids results in safe and easily clearance *in vivo* (Kirkham et al., 2007; Kyle et al., 2010; Misawa et al., 2006).

Bioactivity for biodegradable polymers can also be elaborated by surface feature modification. Nano-featured materials / scaffolds have demonstrated significantly influence on osteoinductivity (Murugan and Ramakrishna, 2006). Specifically, nanotopographical materials stimulate bone formation and enhance bone-implant integration, leading to better tissue repair and regeneration (Dalby et al., 2007b; Dalby et al., 2007d). (described in more details in section 1.6).

### **1.2.3 Stem cells for bone tissue regeneration**

A variety of cell types have been investigated in terms of cell source for bone tissue engineering in the last decades with different advantages and restrictions. Ideally, cells need to be sufficient quantities after limit expansion *in vitro*, constant expression of specific bone markers and secreting bone matrix proteins. Autologous osteoblasts are the most obvious choice for bone tissue engineering. However, relatively few cells can be harvested from the isolation of the tissue,

and low expansion rate of osteoblasts *in vitro* limit the available cells seeded on scaffold. Moreover, osteoblasts dissociated from diseased states or elderly patients may not be appropriate for the cell source of tissue engineering (Heath, 2000). Alternatives include the use of allogous or xenologous osteoblastic cells. However, human allogous cells are in short supplies, and using xenologous cells have experienced serious immunogenicity and the possibilities of transmission of infectious agents (Platt, 1996). These limitations have restricted their applications on tissue engineering, and the xenologous cells are only suitable for *in vitro* studies.

Studies on stem cells have demonstrated that they are more promising cell sources for bone tissue engineering. Stem cells are characterized as unspecialized cells capable of renewing themselves by cell division and being able to differentiate into specialized cell types under certain physiological or experimental conditions. Stem cells, in general, are classified into three categories: embryonic stem cells (ESCs), induced pluripotent stem cells (iPSCs) and adult stem cells. Despite these three stem cell populations being obtained from different sources and having different advantages, they all hold great potential for regenerative medicine and have attracted significant attention in bone repair and regeneration (Gruenloh et al., 2011; Illich et al., 2011; Kuznetsov et al., 2011).

### **1.2.3.1 Embryonic stem cells**

Embryonic stem cells are derived from embryo following fertilization up until the ninth week of gestation and, can differentiate into any cell type. ESCs are highly proliferative and are pluripotent. Therefore they can be used as a single source for the derivation of multiple lineages present in bone tissue, including osteogenic cells, osteoclasts, vascular cells and nerve cells (Hoffman and Carpenter, 2005). To achieve osteogenesis from ESCs, two culture approaches have been developed. One is embryonic body (EB)-mediated osteogenic differentiation, from which osteogenesis is predominantly derived from the three dimensional cell spheroids, and then followed by addition of osteogenic reagents, such as ascorbic acid, dexamethasone (DEX), etc. (Buttery et al.,

2001; Karp et al., 2006). However, this approach is restricted to lineage specific differentiation of ESCs within EBs, which results in a limited number of osteoblasts. A new approach has been developed in which ESCs are directly differentiated into the osteogenic lineage bypassing EB formation. In this method, ESC colonies are immediately isolated into single cells and cultured in the presence of osteogenic supplements (Hwang et al., 2008; Karp et al., 2006). ESCs cultured on scaffolds have showed enhanced effectiveness compared to ESCs on culture dishes for the aim of bone tissue regeneration. For example, ESCs cultured on three-dimensional PLGA scaffolds demonstrated strong, abundant expression of ALP and OCN compared to the same cells cultured on culture dishes. Implantation of the ESCs-PLGA scaffold construct showed new bone formation within and around implanted scaffolds *in vivo* (Tian et al., 2008).

#### **1.2.3.2 Induced pluripotent stem cells (iPSCs)**

Induced pluripotent cells (iPSCs) are induced stem cells derived from adult cells that have been genetically reprogrammed to express defined ESCs transcription factors (i.e., Oct4, Sox2, Klf4 and Myc) (Takahashi et al., 2007a). Human iPSCs possess the primary properties of human ESCs in terms of morphology, gene expression, surface antigens, proliferation and differentiation into all cell types of the three germ layers (Takahashi et al., 2007b). Recent studies have demonstrated that iPSCs hold great potential as an alternative cell source for bone tissue regeneration. Transient transduction of the osteogenic transcription factor RUNX2 into iPSCs resulted in increases in ALP activity and calcium levels during osteoblast differentiation (Tashiro et al., 2009). Further study showed that culturing iPSCs in osteogenic medium along with resveratrol protects iPSCs derived osteocyte-like cells from DEX induced apoptosis, results in osteogenic differentiation and bone formation *in vivo* (Kao et al., 2010). Transplantation of human iPSCs - macrochanneled polycaprolactone constructs into mice demonstrated the induction of mineral deposition within the cell-scaffold implant, suggesting the utilization of iPSCs for bone tissue engineering (Jin et al., 2013).

### 1.2.3.3 Multipotent mesenchymal stromal cells (MSCs)

MSCs were first described as a minor subpopulation of bone marrow cells which are plastic-adherent, fibroblast-like, clonogenic cells (colony forming unit-fibroblast CFU-F), with high capacity for proliferation *in vitro* (Friedenstein et al., 1974; Friedenstein et al., 1968). Later on, the same group demonstrated that the CFU-F are a heterogeneous population of stem and progenitor cells with multipotent lineage potential being able to differentiate into skeletal tissues (i.e., osteoblasts, chondrocytes, adipocytes, and stroma) (Owen and Friedenstein, 1988). Further research has shown that MSCs exist in many adult tissues, including peripheral blood (Kuznetsov et al., 2001), dental pulp (Shi and Gronthos, 2003), and adipose (Zuk et al., 2002), etc. Apart from plastic-adherent and multipotent differentiation potential, MSCs are characterized by the presence of a set of surface antigen markers (CD markers) (Dominici et al., 2006). However, these CD markers are inconsistent and varying for MSCs derived from different tissues and expanded using different culture methods (P et al., 2011). It is a consensus view that the more primitive, most stem cell-like population of cells from the whole stromal compartment can be isolated using various can be isolated using various CD markers (i.e., positive for STRO-1, CD105, CD29, CD73, CD271, CD146 etc., and negative for CD34, CD45, CD14 etc.) (Arvidson et al., 2011). Many groups refer to unselected cells as mesenchymal stem cells, although mesenchymal stroma is perhaps more accurate.

Unlike ESCs and iPSCs, MSCs, specifically derived from bone marrow (BMSCs), have been recognized and studied for their potential in osteogenic differentiation and bone formation for many years (Tavassoli and Crosby, 1968). Using BMSCs as a cell source for bone repair and regeneration has been the focus of many studies in over the last two decades. This is, because BMSCs are easy to collect and expand *in vitro* to obtain sufficient cell numbers for tissue regeneration (Bianco et al., 2001). Moreover, MSCs possess immunosuppressive properties making them suitable for allogeneic transplantation (Arinze et al., 2003; Bartholomew et al., 2002). The incorporation of BMSCs into various biomaterials / scaffolds in animal models has demonstrated promising bone regeneration. Loading MSCs onto ceramic scaffolds and then transplanting the

construct into segmental defects in the femora of rats resulted in bone formation in the interface between the host and the construct, and across the defect (Bruder et al., 1998). Similar studies to incorporate MSCs into biopolymer scaffolds such as PLGA in rat (Ishaug-Riley et al., 1997), PCL, PEGT in mouse models (Mendes et al., 2003) also enhanced new bone formation. A study in humans using MSCs-macroporous HA constructs to recover large bone defects (up to 7 cm) in three patients revealed the potential reliability of MSC based constructs in bone tissue regeneration (Quarto et al., 2001).

## **1.3 MSCs differentiation process**

### **1.3.1 MSCs self-renewal and regulation**

Self-renew refers to stem cells maintaining their undifferentiated stem state by generating identical copies of themselves through mitotic division. Bone marrow derived MSCs (in the context of growth we refer to selected, primitive, stem cells rather than whole stroma where non-stem cells will have lost their self-renewal capacity) have been verified to possess a significant but variable self-renewal capacity upon expansion culture conditions. For instance, some reports indicate serial passage is not a problem with subcultivation of primary MSCs derived from human bone marrow growing up to 15 passages (MSCs in subcultivations exhibit exponential phase of growth until finally in the stationary phase) while retaining their osteogenic potency at every passage (Bruder et al., 1997). However, other researchers have reported that prolonged *in vitro* expansion results in reduction or losing the qualities of MSCs. For example, MSCs expanded *in vitro* over 5 passages significantly reduced their capacity of releasing vascular endothelial growth factor that protects ischemia injury (Crisostomo et al., 2006). It was proposed that extensive cell culture induced MSCs senescence due to growth arrest and apoptosis (Stenderup et al., 2003). Currently, specific in clinical studies, properties of MSCs *in vitro* expansion remain inconsistent due to different cell culture conditions, and the expansion passages used in most studies are less than five (Ikebe and Suzuki, 2014).

Multipotent MSC undergoes asymmetric division to give rise to two daughter cells: the identical copy of MSC and the less potent precursor, and then the precursor cells go through symmetric division to produce more precursor cells with less self-renewal potential and growing differentiation potential (transit amplification) (Figure 1.5) (Baksh et al., 2004).

The maintenance of MSCs self-renewal is not well understood. While we understand that ESCs remain pluripotent through expression of e.g. oct-4, sox2, nanog and rex-1, and there is some evidence that MSCs may use similar factors (possibly to regulate C-MYC involved in growth) (Boiani and Scholer, 2005; Boyer et al., 2006; Park et al., 2012; Ringrose and Paro, 2007). Perhaps more likely, some growth factors and cytokines are also implicated in the maintenance of MSCs stemness. For instance, fibroblast growth factor2 (FGF2) has shown capacity to enhance MSCs growth rate, and the effect of FGF2 is more noticeable in low density cultures than in high density cultures (Tsutsumi et al., 2001). Further study of FGF2 effect on MSCs self-renewal demonstrated that secreted FGF2 engages with its cell surface receptor directly without first being released into culture medium, suggesting a possible autocrine regulatory loop underlying FGF2 proliferation function (Zaragosi et al., 2006). In the same study, it was proposed that extracellular signal-related kinase 1/2 (ERK1/2) pathway is implicated in FGF2 mediated self-renewal, as inhibition of mitogen-activated protein kinase kinase 1 (MAPKK1) results in decrease in MSCs clonogenic potential, but without influencing differentiation potential.

Studies using biomaterials that can control MSC self-renewal have also implicated ERK1/2 as well as c-jun-n-terminal kinase (jnk), another MAPK (Dalby et al., 2014; McMurray et al., 2011). There is also a theory that MSCs undergoing self renewal pool unsaturated metabolites to increase redox plasticity (first observed in ESCs) (Yanes et al., 2010) while reducing metabolism involved in amino acid biosynthesis and energy demand (Dalby et al., 2014). There is also evidence that microRNAs may work to suppress expression of phenotypical mRNAs and hence proteins (McMurray et al., 2011).

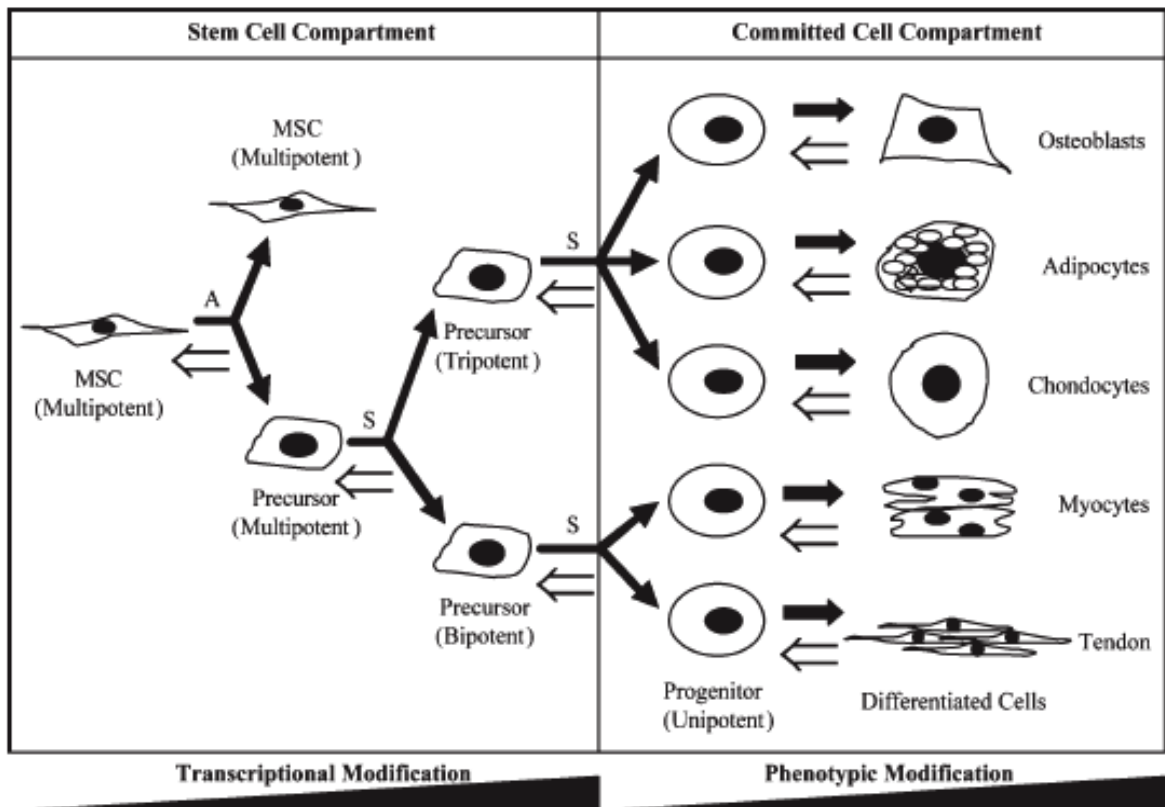


**Figure 1.5** Schematic diagram describing MSCs self-renewal and differentiation.

MSCs self-renewal occurs in the stem cell compartment, in which MSCs undergo asymmetric division (A) to produce two daughter cells: the copy of MSC and multipotent precursor, which then goes through symmetric division (S) to give rise to more precursors possessing less self-renewal and restricted differentiation capacity. In the committed compartment, the Tri- or Bi-potent precursors symmetrically divide into Unipotent precursors with pre-determined cell fate, which eventually give rise to multilineage specialized cells. Under specific inductive cues, dedifferentiation may occur (open arrow) from specialized cells to generate more potent cells. (Taken from Baksh et al, 2004).

### 1.3.2 MSCs differentiation

It has long been recognized that MSCs have multiple lineages differentiation capacity and can give rise to bone, cartilage, tendon, muscle, adipose tissue and hematopoietic-supporting stroma under defined environmental cues. Global gene expression analysis of three specific lineages derived from MSCs also demonstrated that osteoblasts and adipocytes shared more up-regulated genes during their terminally lineage specific differentiation (235 genes), compared to 3 genes shared between osteoblasts and chondrocytes and 10 genes shared

between chondrocytes and adipocytes (Song et al., 2006). These data perhaps, speculatively, indicate that osteoblast and adipocyte might share a common MSC precursor (i.e., the bi-potent precursor), and chondrocytes originate from a different precursor-this could further indicate the heterogeneous cell mixture we define as MSCs. Upon inductive cues, these multipotent precursors symmetrically divide into partially committed or pre-determined unipotent precursors (progenitor) which eventually develop into lineage specific cell types (Figure1.5).

### **1.3.3 Transcriptional control of MSCs osteogenic differentiation**

It is a putative view that MSCs fates are determined by transcriptional activities which are induced through major developmental pathways. Transcription factors including runt-related transcription factor 2 (RUNX2), osterix (OSX) and distal-less homeobox 5 (dls5) / msh homeobox 2 (MSX2), establish a regulatory network and molecular switches for bone development and osteoblast differentiation.

#### **1.3.3.1 Runt-related transcription factor 2 (RUNX2)**

RUNX2, one of the Runt-related transcription factors, has been characterized as the principal osteogenic master gene. RUNX2 controls osteoblast differentiation and bone formation by binding to the osteoblast specific *cis*-acting element (OSE2), which is located at the promoter of osteoblast marker genes, such as collagen type I, OPN, bone sialoprotein and OCN (Ducy et al., 1997).

The osteogenic regulatory function of RUNX2 has been demonstrated *in vivo* and *in vitro* in many studies in the last two decades (Harada and Rodan, 2003). RUNX2-deficiency in mice (RUNX2<sup>-/-</sup>) results in a lethal phenotype due to the complete lack of osteoblast activity and bone formation (Komori et al., 1997). The phenotype in mice lacking only one allele of RUNX2 is identical to human ossification disease cleidocranial dysplasia (CCD) and genetic analysis of CCD patients revealed that heterozygous mutations of RUNX2 is the cause of the disease (Otto et al., 1997). Enforced expression of RUNX2 in MSCs induce osteoblast specific gene expression, and increases matrix mineralization *in vitro*.

Transplantation of the MSCs with overexpressed RUNX2 into skull defect mice model results in an average of 85% osseous closure at four weeks, while controls with scaffold only and with nontransduced MSC-scaffold constructs showed no defect healing effect (Zheng et al., 2004). These data suggest RUNX2 expression is sufficient to promote osteogenic differentiation and osteogenesis. However, transgenic mice with overexpression of RUNX2 in osteoblasts showed osteopenia with multiple fractures which were enriched with OPN and invaded by osteoclasts, although there was an absence of enhanced osteoclastogenesis. Further examination of the transgenic mice revealed that mature osteoblasts were diminished greatly, despite pre-mature osteoblasts expressing OPN increasing in adult bone (Liu et al., 2001). These results indicate that the effect of RUNX2 on osteogenic differentiation and bone formation is developmental stage-dependent, RUNX2 accelerates osteogenic differentiation at early stage and inhibits terminal differentiation at late stage.

Recent studies suggest RUNX2 not only guides MSCs osteogenic differentiation but also plays regulatory roles in cell growth control. RUNX2 null cells exhibit a higher rate of proliferation than wild type, and *RUNX2* expression is regulated by the cell cycle with maximum expression in G1 phase. Forced elevation of *RUNX2* in preosteoblasts inhibits their proliferation suggesting *RUNX2* promotes cells to exit from cell cycle (Galindo et al., 2005; Pratap et al., 2005). Further evidence was observed that *RUNX2* targets at cyclin dependent kinase (CDK) inhibitors p21 and p27; overexpression of RUNX2 resulting in down-regulation of CDK, thus suppressing progression into S-phase and promoting cell cycle exit (Thomas et al., 2004; Westendorf et al., 2002).

#### **1.3.3.2 Osterix (OSX)**

OSX was recently identified as a zinc finger containing transcription factor expressed in all developing bones. OSX-null mice demonstrate similar phenotype to the RUNX2 knockout, indicating OSX is required for MSC differentiation into osteoblasts (Nakashima et al., 2002). Further investigation showed that RUNX2 expression in OSX-null mice is observed, while RUNX2-null mice do not express OSX, suggesting OSX acts downstream of RUNX2 (Nakashima and de

Crombrugge, 2003; Nakashima et al., 2002). Recent studies demonstrated the potent effects of OSX on osteogenesis. Some suggested that OSX alone is sufficient for osteogenesis and the expression of OSX is in a RUNX2 independent manner (Tai et al., 2004; Tu et al., 2006). Others indicated that the effect of OSX on terminal osteogenic differentiation relies on coordination of other transcription factors, such as RUNX2, DLX5 and MSX2, which recruit OSX to regulate osteogenesis at different stage (Kim et al., 2006b; Kurata et al., 2007; Matsubara et al., 2008). It has been recently suggested that OSX is induced by DLX5 or MSX2 when RUNX2 is absent (Liu et al., 2007a; Matsubara et al., 2008).

### **1.3.3.3 Homeobox proteins (DLX5 and MSX2)**

Distal-less homeobox protein 5 (DLX5) and Msh homeobox homologous 2 (MSX2) belonging to homeobox family, also play transcriptionally regulatory roles in osteoblast differentiation and skeletal development (Chen et al., 1996; Satokata et al., 2000). Studies on DLX5-null mutant mice demonstrated a delayed ossification of the skull and abnormal osteogenesis (Acampora et al., 1999; Depew et al., 1999). Targeted activation of both DLX5 and DLX6 in mice resulted in skeletal defects, and overexpression of DLX5 in the apical ectodermal ridge of *Dlx5/6* null mice can fully rescue limb development (Robledo et al., 2002). Cellular studies have also shown DLX5 is expressed at all stages of osteoblast differentiation, and acts as cofactor of RUNX2 to activate bone markers BSP and OCN (Hassan et al., 2004; Holleville et al., 2007; Ryoo et al., 1997).

In contrast to DLX5, MSX2 is stage-specifically expressed in osteoblast. MSX2 is mainly expressed in osteoprogenitors and is down-regulated in osteoblast differentiation (Hassan et al., 2004; Lynch et al., 1998). It is proposed that MSX2 represses RUNX2 activity and thus down-regulates osteoblast gene expression in mature osteoblasts (Newberry et al., 1998; Shirakabe et al., 2001). However, studies on MSCs osteogenic differentiation indicate MSX2 promote MSCs osteoblast proliferation and differentiation by inhibiting PPARG (Cheng et al., 2003; Ichida et al., 2004). Interestingly, both MSX2 and DLX5 can induce OSX activity in RUNX2 independent manner during BMP2 induced osteogenic differentiation (Lee et al., 2003; Matsubara et al., 2008).

## 1.4 Molecular signals and pathways of osteogenic differentiation

### 1.4.1 BMP2 signalling

Bone morphogenetic proteins (BMPs) constitute the largest subfamily of transforming growth factor  $\beta$  (TGF $\beta$ ) superfamily. To date, over 20 BMPs have been identified and characterised with varying functions. Among those, BMP2 plays an essential role in skeletal development and bone tissue regeneration (Tsuji et al., 2006). Temporal specific addition of BMP2 in MSC cultures significantly increases OCN expression (Huang et al., 2010b), and temporal expression of BMP2 is necessary and sufficient for bone formation (Noel et al., 2004). *In vivo* genetic analysis using mouse models also demonstrated that loss of BMP2 (rather than BMP4 or BMP7) results in severe osteogenic impairment (Bandyopadhyay et al., 2006). A similar study also indicated that the BMP2 signal is a necessary component for bone repair. BMP2-deficient mice have spontaneous limb fracture which cannot be repaired with time and other osteogenic stimuli (Tsuji et al., 2006).

The BMP2 signal exerts its effect to enhance osteogenic differentiation and bone formation in two signal transducing pathways. The canonical pathway (known as the SMAD-dependent pathway) is initiated when it binds with type I and type II BMP receptors to form ligand-receptors complexes. Within this complex, the type II receptor has the ability to phosphorylate and subsequently activate the type I receptor, leading to phosphorylation of receptor-regulated SMADs (R-SMADs). Once phosphorylated, bmp specific R-SMADs, including SMAD 1, 5 and 8, interact with common SMAD (SMAD4), which facilitates the translocation of R-SMADs and co-SMAD complex into the nucleus to integrate with RUNX2 to directly induce osteogenesis (Javed et al., 2009; Lee et al., 2000; Phimphilai et al., 2006). In parallel with the interaction with RUNX2, BMP2 induced SMAD proteins can up-regulate OSX (Matsubara et al., 2008).

Besides the canonical pathway, the BMP2 signal is able to trigger multiple downstream pathways through activation of the signalling molecules TGF-beta

activated kinase 1 (TAK1) and its binding protein TAB1. This signal transduction route is known as the non-canonical or SMAD-independent pathway and its downstream cascades include MAP kinase p38 (p38 MAPK) and ERK (Gallea et al., 2001; Lai and Cheng, 2002), and nuclear factor kappa beta (NFkB). The activation of the TAK1/TAB1 complex is achieved by the interaction of the BMP receptor associated molecule 1 (BRAM1) and the TAK1/TAB1 complex, in which BRAM1 directly associates with the cytoplasmic tail of the BMP receptor (Lu et al., 2007; Yu et al., 2002). Like the canonical pathway, the BMP non-canonical pathway is also important for osteogenic differentiation and bone formation (Hoffmann et al., 2005). *In vivo* study has shown that the p38 MAPK pathway is required for normal skeletogenesis in mice, and TAK1 is a crucial activator for p38 MAPK in osteoblasts. Further analysis revealed that the interaction of TAK1 with p38 MAPK phosphorylates RUNX2 resulting in regulation of osteoblast genetic programme (Greenblatt et al., 2010). The regulatory effect of the BMP2 induced non-canonical pathway was also observed in primary cultured calvaria derived osteoblastic cells (Guicheux et al., 2003). In this study, BMP2 induced p38 and Jnk activation resulting in osteogenic differentiation. Inhibition of p38 and Jnk led to down-regulation of alkaline phosphatase and OCN respectively. These data also suggested that p38 MAPK and Jnk have a distinct role in osteogenic differentiation.

BMP2 acting as a signal for osteogenic development is mediated by type I and type II serine/threonine transmembrane receptors, and is regulated at different molecular levels (Koenig et al., 1994). Active BMP2 contains 7 cysteines with 6 of them forming three intramolecular disulfide bonds and the seventh cysteine being used for dimerization with another monomer by forming a covalent disulfide bond. It has been observed that BMP2 dimerizes with other BMPs, such as BMP5, 6 or 7 to form heterodimers, leading to be more effective activator of the signalling pathway than its homodimer (Little and Mullins, 2009). In addition, the binding of BMP2 to different receptor complexes results in activation of distinct downstream pathways. BMP2 binds to its high affinity receptor type I, upon which receptor type II is recruited into the complex, leading to the activation of SMAD-independent pathways; while the SMAD-dependent pathway

is activated by BMP2 binding to a preformed complex of type Ia and type II (Hartung et al., 2006; Nohe et al., 2002). BMP2 signalling is regulated by BMP antagonists and co-receptors. Noggin, one of the best understood antagonists can bind to BMP2 and other BMPs to block their receptor epitopes on the ligands. Interestingly, noggin is induced by BMP2, 4 and 7 in osteoblasts, serving as a negative feedback loop attenuating BMP2 signalling (Gazzerro and Canalis, 2006). The downstream pathways of BMP2 signalling are also regulated by intracellular regulatory proteins. For example, in the SMAD-dependent pathway, smurf1 (SMAD-ubiquitination-regulatory factor 1) and smurf2 antagonize BMP2 signalling by interacting with R-SMADs and targeting them for degradation, and thus control the levels of R-SMADs of cells (Arora and Warrior, 2001).

The regulation of BMP2 signalling may occur also in non-transcriptional manner. MicroRNA (miRNA) functions at the posttranscriptional level by negatively regulating translation of its target gene. Recent study has shown that miR-210 inhibits activin type I receptor in a BMP4-dependent manner in ST2 cells and thus promotes differentiation of osteoblasts (Mizuno et al., 2009). Moreover, integrins are major transmembrane receptors for mechanosensing, integrin signals are transduced through the FAK-Ras-ERK pathway and cooperated with BMP pathway by enhancing SMAD1 expression (Miyazono et al., 2005). Therefore, mechanical stimuli may also play an important role in BMP2 signalling.

#### **1.4.2 Wnt signalling**

It has been long recognized that Wnt signalling is implicated in osteogenic differentiation and bone formation. The signal activates three pathways (i.e., canonical, non-canonical, and calcium ion channel related) to regulate cell growth, differentiation and function, however, the canonical pathway, also known as  $\beta$ -catenin pathway, appears more important for osteogenesis (Westendorf et al., 2004). The canonical pathway is initiated by the binding of Wnt proteins to frizzled receptor (Fz, a G protein-coupled receptor like protein) and a co-receptor LRP5/6 (low-density lipoprotein receptor-related protein 5 or 6), resulting in the inhibition of GSK-3 $\beta$  (glycogen synthase kinase 3 $\beta$ ) activity.

Consequently, the pathway mediator,  $\beta$ -catenin is stabilized and accumulated in cytosol, leading to its translocation to nucleus where  $\beta$ -catenin interacts with the Tcf/Lef (T cell factor/Lymphoid enhancer binding factor) to regulate the expression of canonical Wnt target genes (Hay et al., 2005; Levy et al., 2004).

The canonical Wnt signal positively regulates osteogenesis in multiple mechanisms. Loss-of-function mutation of LRP5, the co-receptor of Wnt signalling, was recently identified as the cause of osteoporosis-pseudoglioma, which is characterized low bone density and skeletal fragility (Gong et al., 2001; Little et al., 2002). In these studies, LRP5 expression was demonstrated by osteoblasts *in situ*. The bone formation marker, OCN was significantly increased in gain-of-function of LRP5 mutation, whereas levels of fibronectin, known as target of Wnt signalling were also markedly elevated (Gradl et al., 1999). *In vitro* experiments also demonstrated disruption of the endogenous LRP5 inhibitor dickkopf 1 (DKK1) enhances Wnt signalling and stimulates osteogenesis. Stimulation of canonical Wnt signalling can also be achieved by stabilizing  $\beta$ -catenin, the signalling mediator of canonical Wnt pathway. Studies using GSK-3 $\beta$  inhibitors which stimulate canonical Wnt signalling by stabilizing  $\beta$ -catenin demonstrated that Wnt signalling promotes mesenchymal precursors differentiation into osteoblasts (Jackson et al., 2005; Kulkarni et al., 2006). Moreover, activation of canonical Wnt signalling represses mesenchymal precursors differentiation into adipocytes, which in turn stimulates osteoblastogenesis, as these two cell types are given rise to from the same precursor (Bennett et al., 2005).

BMP2 and Wnt proteins are important signalling molecules in both tissue healing and development. They have profound effects in the control of bone tissue regeneration. The application of these signalling molecules and their signalling cascades within scaffolds represent powerful tool for controlling stem cell differentiation and function (Place et al., 2009; Rosen, 2011). Studies on modification of biomaterials surface demonstrated that surfaces feature alone, specifically nanotopography can promote MSCs osteogenic response by inducing cell-nanotopography interface reactions and a serial subsequent signalling cascades (Dalby et al., 2007b; Dalby et al., 2006b; Popat et al., 2007).

Nanotopography aids in revealing new discoveries in cell function, signalling molecules and cascades, which in turn contribute to the design of new generation scaffolds and the development of tissue engineering.

## 1.5. Nanotopography

Bone tissue matrix is composed of abundant proteins with nanoscale structures (described in section 1.2.2, figure 1.2) to be organized into varying micro- and submicro-scale topographical features to which cells respond in a manner known as contact guidance. The phenomenon of contact guidance was first observed in 1911 (Harrison, 1911), and then was described as topographical features on micrometer lead cells and tissue to alignment and migration (Curtis and Varde, 1964; Flemming et al., 1999; Friedl, 2004; Weiss and Garber, 1952). Recent developments in advanced nanofabrication techniques have enabled the fabrication of biomaterials with nanoscale features to mimic the nanostructures found in natural ECM. Cells respond to nanotopographies with diverse reactions depending on substrate chemistry, stiffness and topographical dimensions and conformation (i.e., grooves, pits and pillars etc.). It is noteworthy that the influence of nanotopography on cellular behaviors is more complex than that of micro-scale topography, as the nanofeatures are more compatible, sizewise, to precise structures at the cell surface. For example, epidermal growth factor receptors (EGFRs) in BHK cell were organized into receptor clusters with ranging from dimers to high order oligomers, and the average size of receptor clusters is less than 24 nm in radius (Ariotti et al., 2010). Also, the distance between integrin alpha and beta subunits is around 23 nm (Shattil and Newman, 2004). Therefore, nanofeatures have the distinct advantage of the possible to replicate features found in nature bone tissue and thus trigger osteogenic responses and bone formation *in vitro*.

### 1.5.1 Effects of nanotopography on MSCs differentiation

An easily observed cell response to nanotopography is the alteration of cell morphology. This response has been noted in many cell types on many different features (Bettinger et al., 2008; Choi et al., 2007; Yim et al., 2005). MSCs and other cell types have shown alignment and elongation on nanograting features in the direction of groove axis (Yim et al., 2007), and the responses couple with enhanced migration and reduction in adhesion size (Janson et al., 2014;

Kulangara et al., 2012). Other nano-features such as nanopillars and nanopits prompt more subtle effects on cell morphology. The growth of MSCs on nanopits results in increased formation of filopodia and modification of focal adhesion morphology, leading to changes in cell spreading and organisation of the cytoskeleton (Dalby et al., 2006a; Dalby et al., 2006b). The effects of nanofeatures on MSCs morphology might rely on the dimension of feature. MSCs seeded on titanium (Ti) surfaces with pillar structures of either 15, 55, or 100 nm heights demonstrated that the smallest feature (15 nm of height) prompted well-spread MSCs with highly organized cytoskeleton and larger focal adhesion formation, and these responses decreased with increase in feature size (i.e., the 100 nm height showed poorly defined cytoskeleton organization and few, smallest focal adhesions) (Sjostrom et al., 2009). The smallest feature size cells have been seen to respond to, again on Ti, were 8 nm high islands with 25 nm diameters - remarkably close to the size of an integrin adhesion site (5 nm high and 23 nm wide). At this size cells used nanopodia rather than full filopodia (McNamara et al., 2014).

A notable effect of nanotopography on MSCs is the control of MSCs fate commitment. A study by Matthew Dalby in 2007 (Dalby et al., 2007d) demonstrated that MSCs fate was determined by nanopit symmetry and order. In this study, nanopit with 120 nm diameter and 100 nm in depth were patterned on substrates of polymethylmethacrylate (PMMA) by electron beam lithography (EBL), and arranged in ordered pattern with symmetries of square (SQ) and hexagonal, in partly disordered pattern with pits placed randomly by up to  $\pm 50$  nm (NSQ50) and  $\pm 20$  nm (NSQ20) on both x and y axes from their position in a true square array, and in a random pattern with pits placed within a repeating random  $1 \text{ mm}^2$  tile to fill  $1 \text{ cm}^2$ . MSCs cultured on these nanopit features, planar substrates in the presence of DEX (positive control), a soluble factor capable of inducing osteogenesis, and planar substrates without DEX (negative control) were analysed for the effects of nanopit geometries on MSCs osteogenic fates. MSCs cultured on NSQ50 surface demonstrated osteoblast genotype (up-regulation of OPN and OCN) and subsequent formation of bone nodules after 28 days. Moreover, mineral was produced by MSC on the NSQ50 surface in the

absence of osteogenic supplements similarly to that of MSCs cultured on the planar control with osteogenic supplement. MSCs cultured on other nanopit patterns did not show significant osteogenic phenotype compared to MSCs cultured on planar surface. A follow up study (McMurray et al., 2011), demonstrated that the same size of nanopit described above arranged in square symmetry maintained MSCs stemness and growth up to eight weeks. These complementary findings suggest the potential for selective, controllable determination of MSC fate and terminal differentiation based only on the symmetry of nanopography.

## **1.5.2 Biophysical and biochemical events underlying the effects of nanotopography**

### **1.5.2.1 Focal adhesions**

Interactions of cells with their surrounding ECM play an essential role in cell shape, attachment, migration and other cellular functions. Cells interact with ECM by the formation of specialized structures, termed focal adhesions, where transmembrane receptors assemble and bind to ligand components of the ECM. At these sites, numerous cytoplasmic proteins, including structural and signalling proteins, assemble at the cytoplasmic face through transmembrane receptors clustering to provide both physical and regulatory links between the ECM and cellular microfilament system (Geiger et al., 2009).

Integrins are the main transmembrane receptors constituting focal adhesions. Integrins are a large family of 24  $\alpha/\beta$  heterodimeric transmembrane glycoprotein receptors resulting from different pairings among eighteen  $\alpha$  and eight  $\beta$  subunits in humans. The large extracellular domains of both  $\alpha$  and  $\beta$  subunits bind to ECM proteins, whereas their short cytoplasmic tails interact directly or indirectly with cytoskeleton-signalling networks. On the extraplasmic face, the diversity of the integrin family enables them to recognize and bind a wide variety of soluble and surface-bound components of the ECM, including collagens, fibronectin, VN and laminin. In general, integrins bind to ligands by recognizing the motifs on ligands such as RGD, LDV and GFOGER (Humphries et

al., 2006) and this is mediated by divalent cations. Integrin binding to ligands on rigid surfaces results in force generation at focal adhesions which is the key element in the assembly and remodeling of ECM.

Upon interaction with components and surface structures of ECM or following physical or chemical stimulations, the formation of focal adhesions is complex and regulated by both intracellular and extracellular events. The cytoplasmic domain of integrins plays a critical role in the processes. The  $\beta$  chain of the cytoplasmic region contains information to direct integrins to focal adhesions, and removal of the cytoplasmic  $\beta$  domain results in failure to localize to focal adhesions (Hayashi et al., 1990). The major biochemical grouping regulating formation of focal adhesions is the Rho GTPase family which stimulates actin-myosin contraction and contributes to the assembly of stress fibres and focal adhesions (Chrzanowska-Wodnicka and Burridge, 1996). Other extracellular events which control integrin clustering and focal adhesion formation include the chemical nature of ECM (Greenwood and Murphy-Ullrich, 1998), the density and organization of the specific ligands (Cavalcanti-Adam et al., 2007), and the topography of ECM (Le Saux et al., 2011).

Specific to nanotopography, a study, using well-defined gold nanodots on a rigid template coated with cyclic RGDfK peptide demonstrated that, in many cell types, the universal length scale for integrin clustering and activation is 58 to 73 nm. Spacing the adhesive nanodots over 73 nm resulted in limited cell attachment, spreading, and reducing focal adhesions formation and actin stress fibres (Arnold et al., 2004). Focal adhesion formation regulated by other nanotopographies, such as pits or islands was also observed, and it was evidenced that over 50-60 nm of space between nanofeatures impaired cell adhesion and response (Cavalcanti-Adam et al., 2006; Dalby et al., 2003). Further studies demonstrated that stem cell differentiation is linked to focal adhesion formation which is modulated by nanotopography (Biggs et al., 2008; Park et al., 2007).

### 1.5.3.2 Indirect mechanotransduction

Focal adhesions are mechanosensitive and protein-rich structures (Figure 1.6A)(Campbell, 2008). The cytoplasmic domains of integrins bind to various proteins which are important for the regulation of integrin affinity to its extracellular ligands and cytoskeletal interaction. Some proteins, such as chaperon, tyrosine kinase FAK, directly bind to  $\alpha$  chain of cytoplasmic integrins, while most cytoskeletal proteins (talin,  $\alpha$ -actinin) and regulatory proteins can directly bind to the  $\beta$  tail domain of integrins. These biochemical properties and physical structures make integrins a suitable candidate for bidirectional signalling transmission across plasma membranes despite having no enzymatic activity themselves (Calderwood et al., 2000; Evans and Calderwood, 2007). Integrins transmit mechanical signals into the cell, providing information on cell location, local environment, adhesive state, and surrounding matrix. These signals determine cellular responses such as survival, migration, proliferation and differentiation (Calderwood, 2004; Hynes, 2002).

Nanotopography regulated cellular functions via focal adhesions/integrins may thus involve indirect, biochemical, mechanotransduction. A study on nanoimprinting using nanocolloidal substrates demonstrated that inhibiting integrin  $\beta 1$  subunits increased the ability of fibroblasts to nanoimprint (develop the shape of the topographies they are cultured on within the cytoskeleton-topographical mirroring), while blocking  $\beta 3$  subunits resulted in a decrease in nanoimprinting of the topography into the cell cytoskeleton (Wood et al., 2008). Osteoprogenitor cells derived from bone marrow cultured on nanogrooved surfaces with dimensions of 240 nm or 540 nm deep and 12.5  $\mu$ m width (25  $\mu$ m pitch) demonstrated more focal adhesion formation with lower proportions of mature adhesions relative to that on planar surface. Osteogenic markers were assessed and showed down-regulation on nanogrooves compared to the planar control. The authors proposed that the correlation of the down-regulation of osteogenic markers to less focal adhesion maturation indicated the implication of ERK 1/2 negative feedback pathways following integrin-mediated FAK activation (Cassidy et al., 2014). Another study demonstrated that if the groove

width was increased to 50  $\mu\text{m}$  (100  $\mu\text{m}$  pitch) and so the cells perceived steps rather than alignment cues, the focal adhesion size increased and osteogenesis was observed (Biggs et al., 2009; Biggs et al., 2008). In fact, it appears that for osteogenesis, the formation of very large, super-mature adhesions (adhesion > 5  $\mu\text{m}$  long), is a pre-requisite (Biggs et al., 2009). A number of reports have indicated the importance of cytoskeletal tension in driving osteogenesis and such increases in intracellular tension would need to be stabilised through large adhesions (Dalby et al., 2014; Kilian et al., 2010).

### **1.5.3.3 Direct mechanotransduction**

In direct mechanotransduction, cells are described as being able to have 'tensegrity architecture' to allow long distance force transfer relying on force balance in the cytoskeletal network in which different structural elements, such as microtubules bearing most of the compressive and contractile microfilaments and ECM molecules bearing most of the tension, are interconnected. Moreover, cytoskeletal networks link to nuclear scaffolds, chromatin and DNA inside nucleus through LINC (linker of cytoskeleton and nucleoskeleton) complexes linking the nucleus to the cytoskeleton and MAR (matrix attachment regions) that link telemetric DNA to the nucleoskeletal lamins (Kilian et al., 2010; McBeath et al., 2004). Therefore, from ECM receptors to nuclear scaffolds, the 'hard-wired' tensegrity network may allow and transfer of mechanical forces in such way that not only activate membrane signalling events (indirect mechanotransduction), but also result in structures rearrangement in the cytoplasm and nucleus (Figure 1.6B) (Ingber, 2003; Maniotis et al., 1997).

Direct mechanotransduction is supported by some key experimental findings in recent years. Stress mapping technologies enable visualization force of transmission in the cytoplasm and confirm that transmembrane receptor deformation by small forces could propagate to long distance sites from the force application, even to the sites at near the nucleus and at the opposite pole of the cell (Hu et al., 2003; Hu et al., 2004). Mechanical signals transmission is rapid and faster than diffusion-based chemical signals (Na et al., 2008). More importantly, a nuclear anchoring complex that links the cytoskeleton and

nucleocytoskeleton was identified, containing nesprins, suns and lamins - the LINC complex (Crisp et al., 2006; Haque et al., 2006).

In general, nesprins are rod-like proteins and locate at the outer nuclear membrane, which connects microfilaments to suns on the inner nuclear membrane; and this complex further binds to lamin A in the nuclear scaffolds. Lamins might connect to the genetic machinery and to DNA both directly and by binding to other nuclear proteins, including lamin B receptor and emerin that associated with many regulatory proteins stimulating downstream chromatin modification, transcriptional regulation and mRNA processing (Wang et al., 2009). Consequently, physical connections between cytoskeletal filaments and the nuclear anchoring complex enable 'tugging' of the cytoskeleton on the nucleus to effect changes in gene expression by chromatin modification. Nanotopographies have been shown to have effects on the nucleus. Fibroblasts cultured on nanocolumns showed repositioning of the chromosome 3 in the interphase nuclei (Dalby et al., 2007a). The authors suggested that the repositioning of the chromosome is due to a decrease in cell spreading and nuclear area. Fibroblasts cultured on hexagonally arrayed nanopits, also demonstrated that the inter-centromeric distance was reduced for both chromosomes 3 and 11, and the cells were markedly less spread than controls (Dalby et al., 2007c). Similar has also been seen in MSCs (Tsimbouri et al., 2013). Chromosome repositioning may affect gene expression, for example from hetero- to euchromatin would de-repress silenced chromosomes resulting in the relaxation of condensed chromatins and subsequently enhance gene expression (Lanctot et al., 2007).

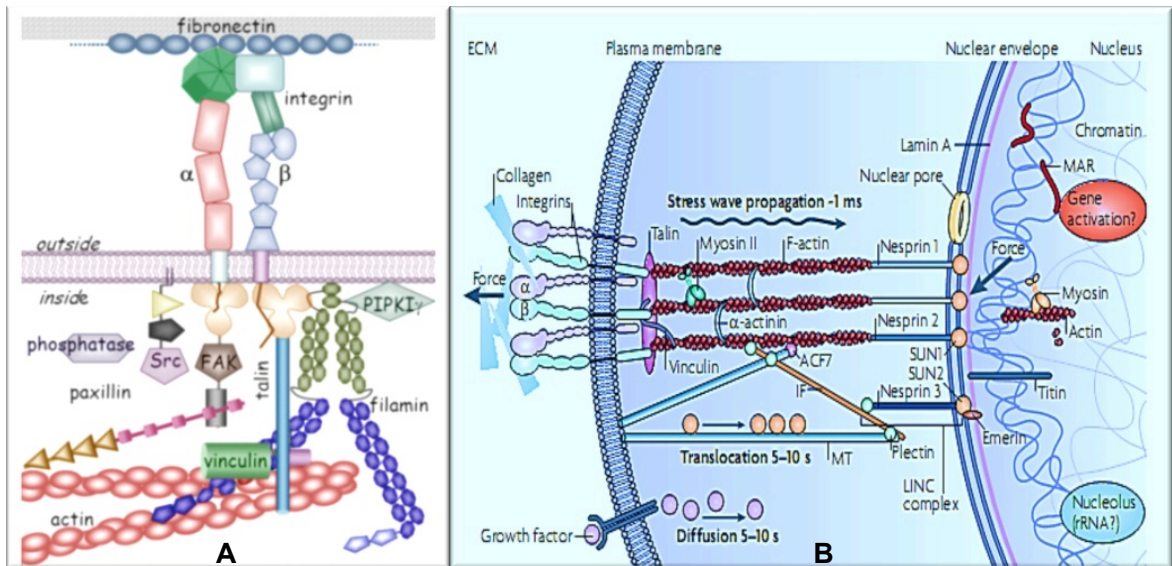


**Figure 1.6** Diagram of indirect and direct mechanotransduction effectors.

Box A (Taken from Campbell, 2008) shows the structure of integrin mediated focal adhesion complexes which enable physical cues outside of membrane to be transmitted into the cytoplasm. The ECM at the top of the diagram is made up of molecules such as fibronectin. Integrins, membrane-crossing  $\alpha\beta$  heterodimers, bind to ECM components using their extracellular regions. The short flexible intracellular tail regions of integrins are linked to the actin cytoskeleton by talin. Filamin A which has an actin-binding domain and 24 Ig-like domains, cross-links actin filaments as well as binding to integrin tails. Other important associated molecules include kinases Src, PIPKI, FAK and phosphatases. Paxillin and vinculin facilitate the formation of the dynamic complexes by cross-linking several different proteins. Box B (Taken from Wang, *et. al.* 2009) shows a local force outside the membrane directly transmits into the nucleus through focal adhesions. A local force applied to integrins through the ECM is concentrated at focal adhesions and channeled to filamentous (F)-actin, which is bundled by  $\alpha$ -actinin and made tense by myosin II, which generates prestress. F-actins are connected to microtubules (MTs) through actin-crosslinking factor 7 (ACF7), and to intermediate filaments (IFs) through plectin 1. Plectin 1 also connects IFs with MTs and IFs with nesprin 3 on the outer nuclear membrane. Nesprin 1 and nesprin 2 connect F-actin to the inner nuclear membrane protein SUN1; nesprin 3 connects plectin 1 to SUN1 and SUN2. Owing to cytoplasmic viscoelasticity, force propagation from the ECM to the nucleus might take up to ~1 ms. The sun proteins connect to the lamins that form the lamina and nuclear scaffold, which attaches to chromatin and DNA (for example, through matrix attachment regions (MARs)). Nuclear actin and myosin102 (and nuclear titin) might help to form the nuclear scaffold, control gene positioning and regulate nuclear prestress.

## 1.6 Aims of the project

Recent advances in nanofabrication techniques enable fabrication of biomaterials with nanoscale features. Studies in the present group and others have demonstrated nanotopography alone can control MSCs proliferation and differentiation. As non-invasive physical cues, nanotopography is a powerful tool for studies in stem cells function and in turn the discoveries can be used as guidances for stem cell therapy and the design of new scaffolds in terms of bone tissue engineering.

A nanotopography, namely NSQ50 was identified by Matthew Dalby in the present group (Dalby et al., 2007b) as osteoinductive, which specifically promotes MSC osteogenic differentiation. MSCs fate determination and specific lineage differentiation are controlled by selective gene expression. An osteogenic differentiation model was established by Lian and Stein (Lian and Stein, 1992), in which osteoblastic phenotype is functionally coupled with a sequential expression of cell cycle and growth genes and bone marker genes. We hypothesize the NSQ50 nanotopography induced MSCs osteogenesis would obey Lian's model and MSCs osteogenic commitment and bone marker genes expression on the surface would be controlled by transcription factors. Thus the primary aim of this project is to look into the functional coupling of sequential gene expression and MSCs phenotype development so that the major transit point of MSCs osteoblast phenotype development on the nanotopography would be established.

The genotype alteration of MSCs on the nanotopography is governed by nanotopographical cues. Cells sense the extrinsic signals mainly through transmembrane receptors. The major theories for the mechanisms of cells responding to nanotopography include: 1) Spatial biasing of focal adhesions formation and the subsequent signalling connection with cytoskeleton proteins. 2) Dynamic actin polymerization rearranges cytoskeleton to guide cell migration and morphological alterations. However, major biochemical signalings, which have been well studied for osteogenic differentiation and bone formation *in vivo*

and *in vitro*, have yet been well defined at the instance of nanotopography. Thus, the second aim of the project is to identify signalling and other regulatory molecules (i.e., miRNAs) and the pathways that drive transcription factors alteration to determine MSCs fate and osteogenic differentiation on the surface.

It has been emerged that a great different energy production between stem cells and their terminal differentiation. The NSQ50 nanotopography mimicking the structure of bone tissue ECM and non-invasively inducing osteogenesis of MSCs provides an ideal tool for the investigation of metabolic alteration during MSCs osteogenic commitment and differentiation. Thus, the third aim of this project is to characterize bioenergetics process of MSCs on the NSQ50 surface, and to probe the intricacy of metabolic and biochemical regulation in MSCs osteogenic commitment and differentiation.

It is hope that this project would extend the understanding of nanotopography induced MSCs osteogenic differentiation, and in turn, the findings would provide guidance for future application in terms of bone tissue engineering.

## **Chapter 2. Methods and materials**

## Summary

This chapter describes the experimental methods used in this thesis. The methods are described in sequence of application, from MSCs cultured on NSQ50 nanotopography to functional analysis of the effects of the NSQ50 surface on MSC osteogenic differentiation. Thus, it begins with embossing the NSQ50 surface into PCL and MSC cell culture, describing the NSQ50 nanotopography features, MSC isolation and cell culture methods. Next, oligonucleotides, protein analysis methods are described. Immunostaining, qRT-PCR and Western blotting are then introduced as techniques for the functional analysis of the NSQ50 surface on MSC osteogenesis, and finally methods for metabolites measurement are introduced.

### 2.1 NSQ50 nanotopography

A 'near square' arrangement of nanopillars with 120 nm in diameter, 100 nm height and with an average 300 nm centre-to-centre spacing with up to  $\pm 50$  nm offset from a square lattice (NSQ50) were fabricated by electron beam lithography on a silicon master with topography area of  $1 \times 1\text{cm}^2$ . This was used as a shim to allow replication of nanopits into polycaprolactone (PCL) (cut from sheets of the polymer  $\epsilon$ -polycaprolactone) by embossing on a hotplate at  $70^\circ\text{C}$ , and then the PCL sheets with embossed NSQ50 surface was used as substrates for MSC cell culture. Planer PCL sheets used as control substrates for MSCs culture were embossed against a microscope cover slip with surface roughness less than 0.5 nm.

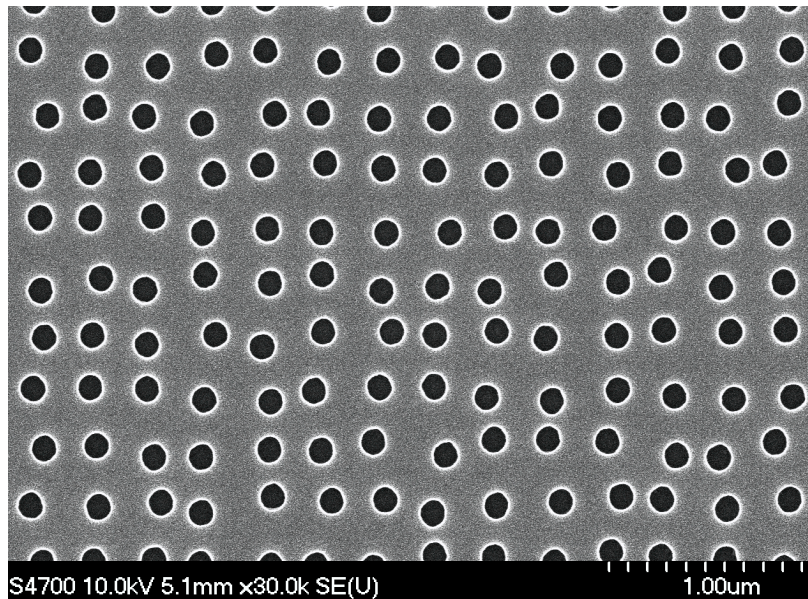


**Figure 2.1** The feature of NSQ50 nanopits

The NSQ50 nanopit is 120 nm in diameter, 100 nm depth with partially disordered arrangement of up to  $\pm 50$  nm offset from a square lattice and 300 nm center-to-center spacing (taken from Matthew Dalby, 2007).

## **2.2 Mesenchymal stromal cells**

### **2.2.1 Cell isolation from human bone marrow**

The original MSCs were isolated from bone marrow obtained from patients undergoing routine arthroplasty, with ethical approval. Bone marrow was stored in transport media (Table 2.1) after arthroplasty. For MSC isolation, the aspirates were diluted 1:2 with 10 ml modified basal medium (Table 2.2), removing as many residues as possible and then centrifuged at 1400 rpm for 10 minutes. After centrifugation, media was discarded and the pellet resuspend in 10 ml of fresh media. The above washing process was repeated until the cell pellet changed to a white color (i.e. most of the blood cells were removed from the bone marrow). The cell pellet was resuspended in 10 ml modified media (table 2.2) and overlaid on 7.5 ml Ficoll gradient media, followed by centrifugation at 1513 rpm for 45 minutes. The mononucleated cells were collected at the interphase. Cells were gently washed with 10 ml medium and medium was removed by centrifugation at 1400 rpm for 10 minutes. Following three washes, cells were collected and seeded into TC75 vented flasks for culture.

## 2.2.2 Cell culture and harvest

MSCs were maintained in modified basal media at 37°C until 90% confluence was reached (medium was changed every 5 days). Cells were passaged with a dilution ratio 1:3, and cells of passage 1 or 2 were used in this work.

For seeding cells on to the substrates, cells were seeded onto NSQ50 PCL and planar PCL sheets with density of  $1 \times 10^4$  cells/cm<sup>2</sup> and then cultured in medium for different time points. Cells on PCL sheets were harvested using trypsin for downstream nucleotide assays, or using cell scrapers for downstream protein assays or were fixed for microscopy. Harvested cells were immediately stored at -80°C for further use.

**Table 2.1 Components of transport medium for bone marrow.**

Components	Volume/Amount
1xPBS	200 ml
EDTA	0.6 g
Penicillin	1 mg
pH: 7.2, Filter before use.	

**Table 2.2 Components of modified basal medium for MSC culture.**

Components	Volume
DMEM	430 ml
FBS	50 ml
Penicillin (Conc. 0.1mg/ml)	10 ml
100mM sodium pyruvate (1mM/ml)	5 ml
Non-Essential amino acids (100x)	5 ml
Filter before use	

## 2.3 Oligonucleotides (primers) synthesis

Oligonucleotide primers were designed using primer3 or other online resources (NCBI; Oligodesign, invitrogen UK). The sequences were then sent to eurofins mwg|operon for synthesis on a scale of 30 nmol. Primers were purified using high purity salt-free (HPSF) technology (MWG) based on reverse phased chromatography and the quality of primers was assessed by matrix assisted laser desorption ionisation - time of flight (MALDI-TOF) analysis. Primer stock concentrations at 100  $\mu\text{M}$  were obtained for each primer by resuspending the lyophilised powder in ddH<sub>2</sub>O and a working concentration of 6.6  $\mu\text{M}$  was prepared from the stocks. Primers were stored at -20°C until further use. Primers for genes encoding proteins and primers for miRNA genes used in this thesis are listed in table 2.3 and 2.4 respectively.

**Table 2.3 Primers for genes encoding proteins.**

Gene name (ID number)	Primer sequence	PCR product size	Efficiency (%)
GAPDH (ID: 2597)	Forward: TCAAGGCTGAGAACGGGAA Reverse: TGGGTGGCAGTGATGGCA	376bp	94
RUNX (ID: 860)	Forward: CAGACCAGCAGCACTCCATA Reverse: CAGCGTCAACACCATCATTC	178bp	92
OSX (ID:121340)	Forward: CAAAGCAGGCACAAAGAAGC Reverse: CCAGGAGCCATAGGGGTG	295bp	86
C-MYC (ID: 4609)	Forward: TTTCTACTGCGACGAGGAGG Reverse: GGCAGCAGCTCGAATTTCTT	105bp	89
OPN (ID: 6696)	Forward: ACAGCCGTGGGAAGGACAGT Reverse: GACTGCTTGTGGCTGTGGGT	76bp	98
OCN (ID: 632)	Forward: GCCCTCACACTCCTCGCC Reverse: CTACCTCGCTGCCCTCCTG	130bp	85
ALP (ID: 250)	Forward: ACAACTACCAGGCGCAGTCT Reverse: TCAGAACAGGACGCTCAGG	260bp	92
BMP2 (ID: 650)	Forward: GTCCTGAGCGAGTTCGAGT Reverse: ACCTGAGTGCCTGCGATAC	120bp	96
BMPR1A (ID: 657)	Forward: TATGGATGGGCAAATGGC Reverse: GCTTTCCTTGGGTGCCATAA	324bp	94
Integrin $\alpha$ v (ID: 3685)	Forward: ACTCGCCAGGTGGTATGTG Reverse: GTTCTCCTTGTGCTCCAGT	270bp	97
Integrin $\alpha$ 3 (ID: 3675)	Forward: CTGCCGACCACCTGGAGAC Reverse: CAGCAGCCAGAGTGACAGGT	143bp	91
Integrin $\alpha$ 4 (ID: 3676)	Forward: AGCAACAGGTTTTCCAGAGC Reverse: ACAATAAGTCCAAGTAGCAAGC	156bp	92
Integrin $\beta$ 1 (ID: 3688)	Forward: GTGCAATGAAGGGCGTGTT Reverse: GTTGCACCTCACACACGACA	277bp	98
Integrin $\beta$ 3 (ID: 3690)	Forward: CCCAGAGGGTGGCTTTGAT Reverse: AACTGCCCGTCATTAGGCT	166bp	99
Integrin $\beta$ 5 (ID: 3693)	Forward: GGAACCCAACAGTGCCAGG Reverse: CGGCACAGGTTCTGGTACA	135bp	96
SMAD1 (ID: 4086)	Forward: TTTCCAGCAACCCAACAG Reverse: TCAGGAGGCAGGTAAGCA	168bp	91
SMAD5 (ID: 4090)	Forward: TGTCAAGGGTTGGGGAGC Reverse: TATGGGGTTCAGAGGGGAG	136bp	89
LRP5 (ID: 4041)	Forward: CGTGTGTGACAGCGACTACA Reverse: GCGGGAAGAGATGGAAGTAG	179bp	91
DLX5 (ID: 1749)	Forward: GACCCAATGGCGTGTA Reverse: GCTGCACTTGTGTACCAGGA	161bp	93
MSX2 (ID: 4488)	Forward: GACGAGGAGGGCCCAGCAGT Reverse: GCCTCCACGCTGAAGGGCAG	113bp	95
Tab1 (ID: 10454)	Forward: TCCACCAACACGCACACGCA Reverse: CGCCATGGTCCACGCTCCAG	157bp	94

**Table 2.4 Primers for miRNAs.**

Gene name	Primer sequence	PCR product size	Efficiency (%)
MiR-23a (ID: 4070100)	Forward: CTGGGGTTCCTGGGGAT Reverse: TGGTAATCCCTGGCAATGTG	60bp	89
MiR-23b (ID: 407011)	Forward: AAGCCCAGTGTGTGCAGAC Reverse: ACCACGGTTTCTGGAGGA	75bp	92
MiR-96 (ID: 407053)	Forward: AGAGAGCCCGCACCAGT Reverse: CTTGAGGAGGAGCAGGCT	75bp	95
MiR-93 (ID: 407050)	Forward: GGGCTCCAAAGTGCTGTT Reverse: GGGCTCGGGAAGTGCTA	72bp	87
MiR-143 (ID: 406935)	Forward: TCCAGCCTGAGGTGC Reverse: CCCAACTGACCAGAGATGC	41bp	94
MiR-203 (ID: 406986)	Forward: TCCAGTGGTTCTTAACAGTTCA Reverse: GGTCTAGTGGTCCTAAACATTTTC	66bp	96
U6 snRNA (ID: 26827)	Forward: CTCGCTTCGGCAGCACA Reverse: AACGCTTCACGAATTTGCGT	94bp	95

## 2.4 Total RNA extraction

RNA extraction was carried out in a nuclease-free environment using RNeasy Mini columns according to the manufacturer's protocol (Qiagen UK). The cell pellet was washed with 1xPBS and then lysed in RLT buffer vortexing for 1 minute. The lysates were homogenized using ultrasonic cell disruptor (Misonix, Inc., USA). The rest of the procedures of total RNA extraction were according to the Qiagen kit, including the on column DNA digestion step to reduce genomic DNA contamination. RNA was eluted using 16 µl of nuclease-free water from the column and it was stored at -80°C until further use.

## 2.5 Complementary DNA (cDNA) synthesis

### 2.5.1 Total RNA reverse transcription

cDNAs for qRT-PCR were synthesised using 5-50 ng of total RNA. Recombinant reverse transcriptase (SuperScript® II; Invitrogen UK) was used to reverse transcribe the RNA in a total of 20 µl of reaction volume. 50 ng of random primers, 5 to 50 ng of total RNA and 1 µl of dNTP (10 mM each of dCTP, dGTP,

dATP and dTTP) and sterile distilled water to make up to 12 µl total volume were combined in a nuclease-free PCR tube. The mixture was heated at 65°C for 5 minutes and quickly chilled on ice. The contents were collected by brief centrifugation and mixed with 4 µl of 5x first strand buffer, 2 µl of 0.1 M DTT and 1 µl (40units) of RNaseOUT. The reaction mixture was then incubated at 25°C for 2 minutes. After incubation, 1 µl (200 units) of SuperScript® II RT was added and mixed by pipetting gently up and down. Then incubated at 42°C for 50 minutes and the reaction terminated by heating to 70°C for 15 minutes. The reaction was briefly centrifuged to collect the cDNA contents and stored at -20°C for further use.

### **2.5.2 MicroRNA reverse transcription**

cDNAs for microRNA qRT-PCR were synthesised using 5-50 ng of total RNA. ThermoScript reverse transcriptase (ThermoScript®; Invitrogen UK) was used to reverse transcribe the RNA in a total of 20 µl of reaction volume. 20 pmol of gene specific primer, 5 to 50ng of total RNA, 1 µl of dNTP (10 mM each of dCTP, dGTP, dATP and dTTP) and sterile distilled water to make up to 12 µl total volume were assembled in a nuclease-free PCR tube. The mixture was heated at 65°C for 5 minutes and chilled on ice immediately. Contents of the tube were collected by brief centrifugation and mixed with 4 µl of 5x first strand buffer, 1 µl of 0.1 M DTT and 1 µl (40units) of RNaseOUT, 1 µl of sterile H<sub>2</sub>O and 1 µl of ThermoScript™ RT (15 unites). The reaction mixture was incubated at 65°C for 1 hour, and then the reaction was terminated by heating to 85°C for 15 minutes. cDNAs were collected to the bottom of the tube by brief centrifugation and stored at -20°C.

## **2.6 Nucleic acids quantification and quality control**

Quantification of DNA and RNA was carried out using a Nanodrop 1000 spectrophotometer (Thermo UK). The Nanodrop 1000 uses 1.0 mm and 0.2 mm paths that have capacity to measure samples as small as 1 µl and 50 times higher concentrated samples than the standard cuvette spectrophotometer. For nucleic

acid quantification, the Nanodrop 1000 spectrophotometer was blanked by reading the absorbance of water, then background absorbance was read using the reference (water or the buffer in which the nucleic acid was diluted) and zeroed for background. Sample absorbance was read at two wavelengths  $A_{260}$  and  $A_{280}$  nm. The reading at  $A_{260}$  was used for quantification and the ratio of  $A_{260}/A_{280}$  was used for nucleic acid purity assessment. A ratio of ~1.8 for DNA and ~2.0 for RNA were used as a guide for sample purity.

Further quality assessment for RNA samples was carried out using an Agilent 2100 Bioanalyzer (Agilent UK). This is a computer assisted nanogel electrophoresis tool for total RNA. The integrity of an RNA sample can be measured using the ratio of 28s integrity/18s integrity, which is called the RIN number. Lower RIN numbers indicate degraded RNA, and the threshold setting for intactness of RNA is 8.0.

### **2.6.1 Quantitative reverse transcription PCR (qRT-PCR)**

qRT-PCR was performed on an ABi7500 thermal cycler using the SYBR Green relative standard method (Larionov et al., 2005). SYBR Green master mix was purchased from Applied Biosystems, which contained SYBR Green I dye, AmpliTaq® DNA polymerase, dNTPs with dUTP, and PCR reaction buffer. The SYBR Green I dye detects the double-stranded DNA, AmpliTaq® DNA polymerase minimizes nonspecific product formation, and the dUTP reduces carryover contamination. The starting materials for qRT-PCR were cDNAs, each sample was scaled down to its corresponding RNA concentration of 5ng/ $\mu$ l. 2  $\mu$ l of SYBR Green master mix, 2  $\mu$ l of primer pair (forward and reverse primer) and 1  $\mu$ l of cDNA sample were mixed up to 20  $\mu$ l of final reaction volume for each well. Negative controls (samples without reverse transcriptase) and blanks (reactions without cDNA samples) were set for each experiment to monitor genomic DNA contamination and substrate fluorescence background respectively. Three technical and biological replicates were applied for each experiment. The qRT-PCR cycling parameters used are presented in the table 2.5.

**Table 2.5 PCR cyclic parameters for SYBR Green qRT-PCR.**

	Number of cycle	Temperature	Time
Holding stage	1	50°C	2 minutes
	1	95°C	10 minutes
Cycling Stage	40	95°C	15 seconds
		60°C	30 seconds
		75°C	10 seconds
Melting curve stage	Melting curve was recorded for each cycle.	95°C	15 seconds
		60°C	1 minute
		95°C	30 seconds
		65°C	15 seconds

Standards were made by serial dilution of cDNA with dilution factor of 2. Figure 2.1, as an example, showed the standard curve generated for the osteopontin (OPN) gene, which gave slope of -3.3124, Y-inter of 21.192 and correlation coefficient  $R^2 = 0.984$ .

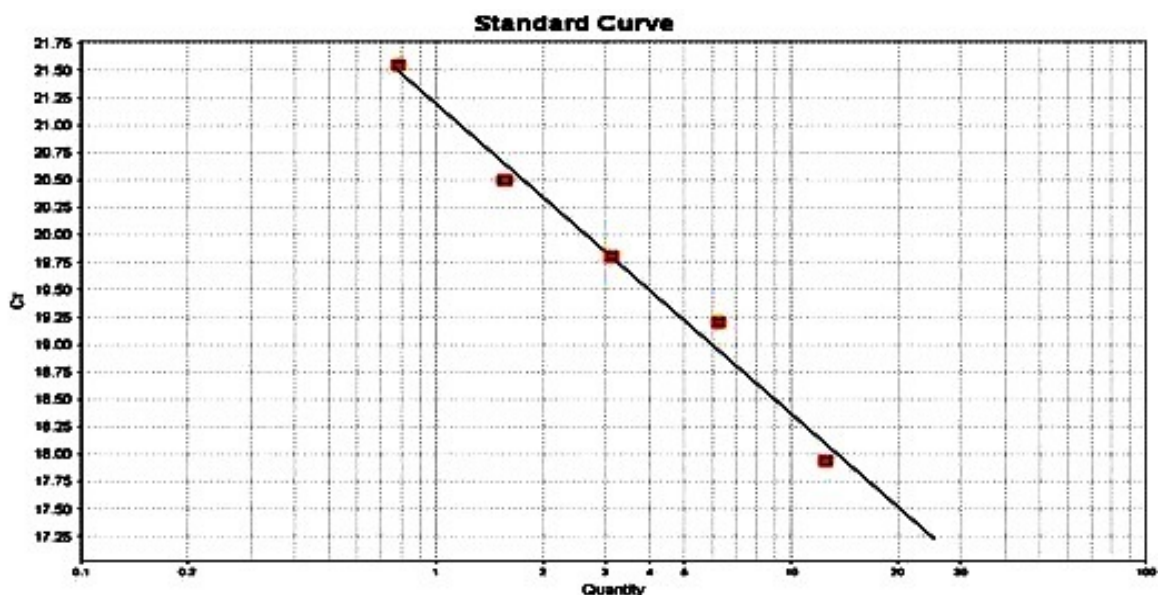


**Figure 2.2 Example of relative standard curve for the OPN gene.**

cDNA was diluted with dilution factor of 2. qRT-PCR for the OPN gene was carried out and a relative standard curve was generated for the OPN gene quantification (standard curve: slope, -3.3124, Y-inter, 21.192 and correlation coefficient  $R^2 = 0.984$ ).

To further control the qRT-PCR reaction quality, a melting curve step was used to monitor if primers amplified one specific PCR product. If a primer pair generates one specific PCR product, the melting curve from the reactions will be

a single homogeneous melt peak for all sample reactions, and the data from these reactions can be considered reliable and meaningful for gene expression analysis. Figure 2.2, as an example, shows the melting curve of the osteopontin gene (OPN) primers used in this work, which present a single melt peak at the expected melting temperature of 81.5°C predicted for its PCR product.

The GAPDH gene and small nuclear RNA U6 were used as reference controls for protein coding RNA and microRNA respectively to normalize the data. Gene differential expression was then expressed as fold change after comparison to control samples. The standard deviation (SD) and p-value for statistical significance were analyzed using GraphPad Prism software.

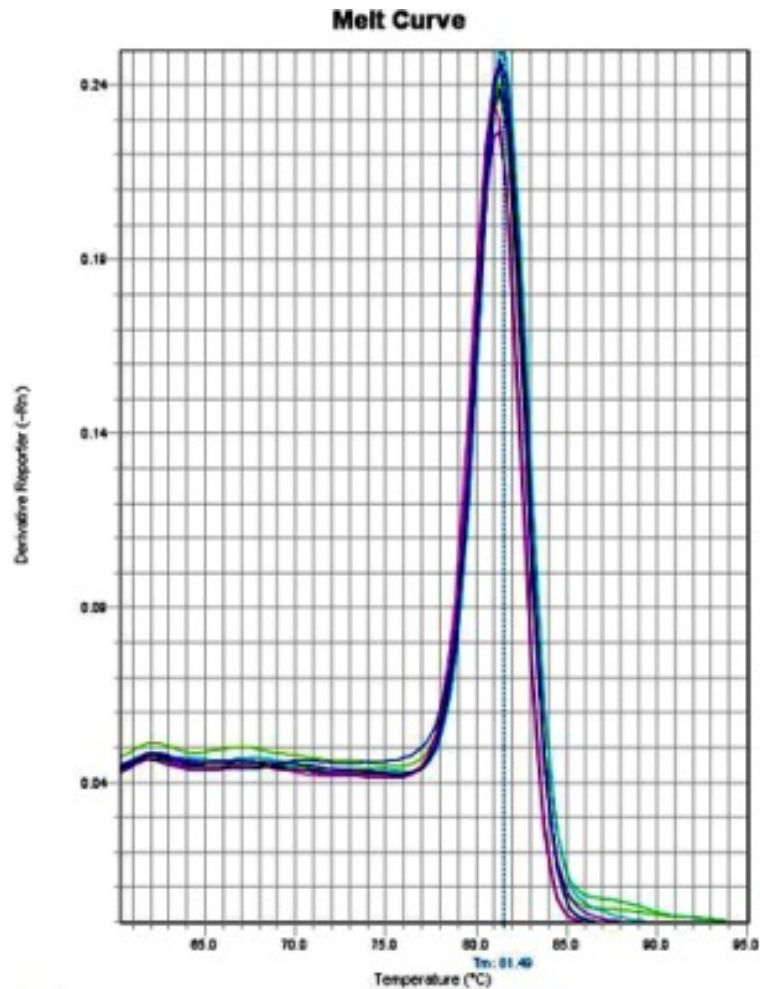


**Figure 2.3** Example of SYBR green qRT-PCR melting curves generated during OPN gene amplification.

Melting curves of OPN in different cDNA samples were generated using SYBR green qRT-PCR, demonstrating OPN was specifically amplified by the primers used.

## 2.7 Protein analysis

### 2.7.1 Protein preparation

#### 2.7.1.1 Total protein preparation

Cells frozen at  $-80^{\circ}\text{C}$  were taken out of the freezer and thawed on ice. 100  $\mu\text{l}$  of RIPA buffer (Table 2.7) was added to the cells and kept on ice for 15 minutes. The lysates were homogenized on ice using ultrasonic cell disruptor (Misonix, Inc., USA) and then were clarified by centrifugation at 13000 rpm for 5 minutes

at room temperature. The supernatant was transferred to a fresh eppendorf tube and the pellet was discarded. Protein concentration was assessed and stored at -80°C until required.

**Table 2.6 The components of RIPA lysis buffer.**

Component	Volume (10 ml)
100 mM Tris/HCl, 300 mM NaCl	5 ml
10% Triton X100	1 ml
10% Na deoxycholate	1 ml
10% SDS	100 $\mu$ l
200 mM PMSF	50 $\mu$ l
0.01 M EDTA (pH 7.4)	100 $\mu$ l
Protease and phosphatase inhibitor	1 tablet
H <sub>2</sub> O	2.75 ml

### **2.7.1.2 Membrane protein preparation**

Pellets of cells were thawed on ice and resuspended in ice-cold TE buffer (10 mM Tris/HCl, pH 7.4, and 0.1 mM EDTA) supplemented with protease inhibitor cocktail, and homogenized on ice using ultrasonic cell disruptor, followed by centrifugation at 600xg for 10 minutes at 4°C to remove unbroken cells and nuclei. The supernatant was transferred to a new vial and subjected to centrifugation at 10000 X g for 30 minutes at 4°C. The pellet was collected and resuspended in ice-cold TE buffer. Protein concentration was assessed and stored at -80°C until required.

### **2.7.2 Protein quantification**

Proteins were quantified using a Bio-Rad Protein Assay Kit (BIO-RAD, 500-0006). The Bradford dye reagent was diluted at a ratio of 1:5 with distilled water. Appropriate standard concentrations (Quick Start™ Bovine Serum Albumin Standard Set (BIO\_RAD, 500-0207)) were used to obtain sample concentration; typically eight BSA standards of 0 - 3.0 mg/ml were set up. 10  $\mu$ l of standards and protein samples were pipetted in respective wells of microtiter plate. 200  $\mu$ l of diluted Bradford dye was added to each well and mixed by pipetting. The plate was then incubated at room temperature for 10 minutes. The absorbance at 595 nm was read using plate reader and standard absorbance was plotted

against the known concentration to interpolate the unknown protein sample absorbance to calculate their concentration.

### **2.7.3 Protein separation (SDS-PAGE separation)**

Proteins were separated using Novex NuPAGE™ electrophoresis system. Protein samples were diluted with 4X NuPAGE LDS loading buffer and denatured at 95°C for 5 minutes. The denatured protein samples and prestained protein marker were loaded on 12-well of 4-12% Bis-Tris-HCl polyacrylamide gel and run in 1xNuPAGE™ MOPS SDS running buffer at 200V constant for 50 minutes.

### **2.7.4 Protein analysis (I) – Immunoprecipitation**

Proteins were isolated using lysis buffer and then centrifuged at 13000 rpm for 15 minutes at 4°C. The supernatant was transferred to a fresh tube with protein A agarose beads (Sigma) to preclean the samples. After 1 hour incubation at 4°C, samples were recentrifuged and collected into new tubes. Protein A agarose beads were incubated with primary antibody at 4°C for 1 hour and centrifuged at 4°C for 2 minutes and discarded the supernatant. The mixture of primary antibody and agarose beads was washed with lysis buffer and then centrifuged, repeated this for three times. Equal amount of protein samples were added into mixture of primary antibody and agarose beads and incubated under rotation at 4°C overnight. Samples were subsequently washed four times with lysis buffer and then proteins were eluted with SDS buffer for western blot analysis.

### **2.7.5 Protein analysis (II) – Western blotting**

Proteins separated on SDS-PAGE were transferred on to Hybond-N+ membrane (Amersham Bioscience). Membrane was dried and then dipped in methanol for 30 seconds, and then blocked in blocking buffer (table 2.7) overnight at 4°C. The overnight blocked membrane was washed three times (10 minutes for each) with PBST buffer and then the membrane was incubated with primary antibody (table 2.8) against the protein of interest (diluted 1:1000 in blocking buffer) at room temperature for 2 hours followed by three times washes (each for 10 minutes)

with PBST buffer. Membrane was then incubated with secondary antibody (table 2.8) linked to a reporter enzyme horseradish peroxidase (HRP) (dilution 1:10000 or 1:15000 in blocking buffer) at room temperature for 1 hour followed by three times washes (each for 10 minutes) with PBST buffer. The dried membrane was then covered by detection reagents (Amersham Bioscience) for 30 seconds and then dried on soft tissue for X-ray developing.

## **2.8 Immunocytochemistry (ICC)**

### **2.8.1 ICC for proteins of interest**

Cells cultured on substrates were washed once with 1XPBS, then PBS removed and added fixative solution (table 2.7) to cover cell surface. Cells were then incubated at 37°C for 15 minutes. After incubation, fixative was removed and the cells washed with 1XPBS once. Cells were then permeabilized by adding perm buffer (table 2.7) and incubated at 4°C for 5 minutes. Excess solution was removed and cells were blocked in blocking buffer (table 2.7) at 37°C for 5 minutes. Cells were washed with 1XPBS twice and then incubated with primary antibody (table 2.8) at 37°C for one hour followed by washing three times with PBST buffer (table 2.7) (each for 5 minutes). Biotinylated secondary antibody (table 2.8) was added and incubated at 37°C for one hour followed by another three times PBST buffer wash (each for 5 minutes). Cells were then incubated at 4°C for 30 minutes with streptavidin-FITC. Excess streptavidin-FITC was removed and cells were washed three times with PBST buffer (each for 5 minutes). For nucleus visualization, a small drop of vectrosshield-DAPI was placed and sealed with microscope coverslip for imaging. Note that for actin counterstain, rhodamine-phalloidin at 1:500 in blocking buffer was added at the same time as the primary antibody.

## 2.8.2 Imaging

Immunostained cells were imaged using a Zeiss immunofluorescence microscope. Images were processed using imageJ or LMS imaging software, and images that were to be compared against one another were taken with the same exposure.

## 2.9 Buffers and antibodies in protein work

Buffers used in immunostaining and Western blotting are listed in table 2.8. Antibodies used in immunostaining, Western blotting and immunoprecipitation are presented in table 2.9.

**Table 2.7 Buffers used for protein work.**

Buffer Name	Concentration	Components
Fixative	10% (v/v)	10 ml formaldehyde and 2 g sucrose in 90 ml 1XPBS
Blocking buffer	1% (w/v)	1 g BSA in 100 ml 1XPBS.
PBST	0.5% (v/v)	0.5 ml Tween 20 in 99.5 ml 1XPBS.
Perm buffer	0.5% (v/v)	10.3 g sucrose, 0.292 g NaCl, 0.06 g MgCl.6H <sub>2</sub> O and 0.476 g Hepes in 99.5 ml 1XPBS with pH 7.2, then adding 0.5 ml Triton X-100.

**Table 2.8 Antibodies used for protein work.**

Antibody and Source	Dilution and Use
Anti-Integrin $\beta 5$ (Rabbit monoclonal)	1:250 ICC 1:50 blocking
Anti-GAPDH (Rabbit polyclonal)	1:2000 Western
Anti-BMP2 (Mouse monoclonal)	1:250 ICC 1:1500 Western
Anti-Integrin $\alpha\beta 5$ (Mouse monoclonal)	1:250 ICC 1:1500 Western 1:1000 Immunoprecipitation
Anti-BMPR1A (Mouse monoclonal)	1:250 ICC 1:1500 Western
Anti-RUNX2 (Mouse monoclonal)	1:250 ICC 1:1500 Western
Anti-OPN (Mouse monoclonal)	1:250 ICC
Anti-OCN (Mouse monoclonal)	1:250 ICC
Anti-mouse IgG-HRP	1:10000 Western
Anti-rabbit IgG-HRP	1:10000 Western
Anti-goat IgG-HRP	1:10000 Western
Biotinylated anti-mouse IgG	1:250 ICC
Biotinylated anti-rabbit IgG	1:250 ICC
Biotinylated anti-goat IgG	1:250 ICC

## 2.10 Alizarin Red Staining

Cells cultured on NSQ50 surface embossed PCL and planar PCL were washed with 1xPBS and fixed with 10% formaldehyde at room temperature for 15 minutes. Fixative was then removed and cells were rinsed three times (5 minutes each) with distilled water. The plates were then left at an angle for couples of minutes to remove excess water. 1 ml/well Alizarin Red Stain Solution was then added and incubated at room temperature for 30 minutes. Excess dye was removed and cells were carefully washed five times with deionized water (5 minutes each). Calcium ( $\text{Ca}^{2+}$ ) mineralization was visualized using an inverted microscope (Nikon).

## 2.11 Metabolomics

Metabolites from cells cultured on NSQ50 surfaces and control samples for 3, 5 and 7 days were extracted using ice cold chloroform:methanol:water (1:3:1,v/v)

on a shaker for 1 hour and maintained at 4°C. Samples were centrifuged and 10 µl of the supernatant was injected in to the LC-MS system.

The LC separation was carried out using hydrophilic interaction chromatography with a ZIC-pHILIC 150 mm x 4.6 mm, 5 µm column (Merck Sequant), operated by an UltiMate liquid chromatography system (Dionex, Camberley, Surrey). Mass spectrometric detection was performed using an Orbitrap Exactive (Thermo Fisher Scientific, Hemel Hempstead, U.K.) within the mass range  $m/z$  70 - 1400 in polarity switching mode (Creek et al., 2011).

Chromatographic peak selection and metabolite identification were done using XCMS/Ideom/MzMatch analysis pipeline (Creek et al., 2011; Creek et al., 2012; Scheltema et al., 2011), and peak intensities were normalized by protein content as measured using the Bradford assay (Compton and Jones, 1985).

## **Chapter 3. Temporal sequence gene expression of MSCs on NSQ50 surface**

## Summary

It has been previously established that the NSQ50 surface is osteogenic inducing MSCs commitment to osteoblast differentiation (Dalby et al., 2007d). This chapter introduces the functional relationship of temporal gene expression patterns and MSC fate determination on the NSQ50 surface. In the methodology and the experiment design, I will discuss the fitness of SYBR Green quantitative real time PCR (qRT-PCR) for quantifying gene expression, and genes assessed according to their functions demonstrated in previous research (Boskey, 1998; Denhardt et al., 2001; Wan et al., 2010). The results presented include the temporal expression pattern of osteoblast marker genes (ALP, OPN and OCN) encoding bone cell ECM components for hMSCs on the NSQ50 surface compared to control. Experimental data demonstrates hMSC osteogenic commitment on the NSQ50 surface is transcriptionally controlled. Protein expression of key genes to confirm the gene expression pattern is also shown and bone nodule formation is observed at longer time points. Finally, a discussion of the roles of transcription factors, the functions of osteoblast marker genes and the possible transition points of hMSC osteogenic commitment is presented and conclusions drawn.

### 3.1 Introduction

The fate of MSC populations is determined by their intrinsic characteristics and microenvironmental factors which govern MSC populations' gene expression at very early stage and through their differentiation toward a specific lineage. Global gene expression profile of MSC populations shows that MSCs multilineage differentiation involves selective gene expression (Baksh et al., 2004). To keep multipotentiality, promiscuous genes are expressed in uncommitted MSCs, which characterize diverse lineages actively expressed. Upon extrinsic stimulation, certain groups of genes are selectively suppressed and those responsible for a lineage specific phenotype are activated, resulting in tissue specific differentiation (Figure 3.1)(Song et al., 2006).

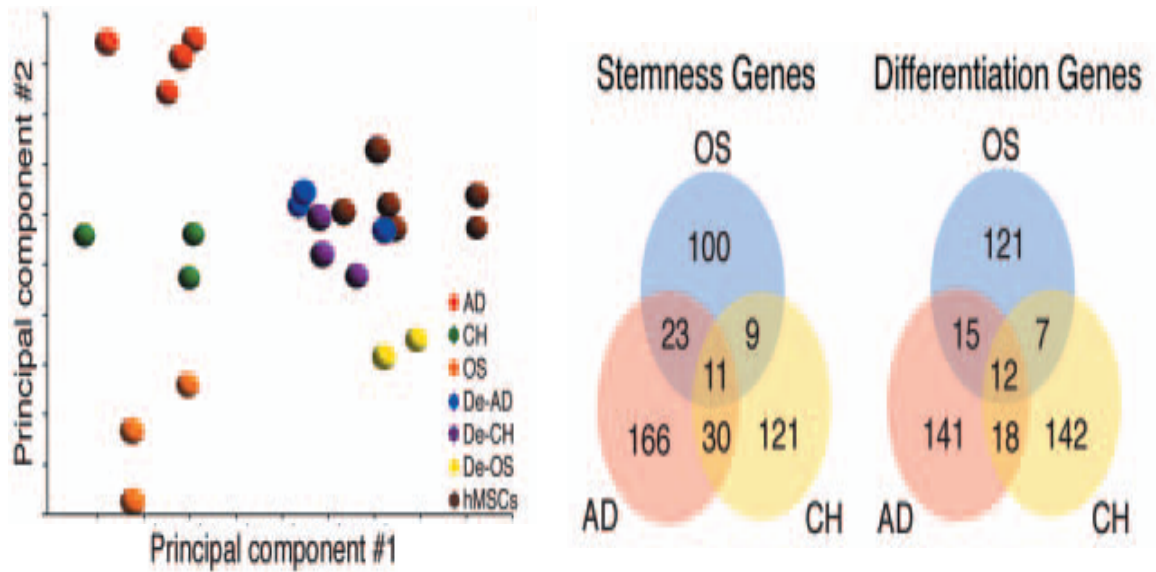


**Figure 3.1 The selective mode of gene expression in MSC multilineage differentiation.**

(A) Principal component analysis of global gene expression. Differentiated cells (AD: Adipocytes, CH: Chondrocytes, OS: Osteoblasts) exhibited a significantly different global gene expression profile compared with undifferentiated MSCs and dedifferentiated cells (De-AD, De-CH, and De-OS). (B) Venn diagrams showing the genes that changed their expression levels during differentiation and dedifferentiation processes by at least twofold ( $p < 0.05$ ). (Picture taken from Song et al., 2006).

The study on MSC commitment development shows that multipotent MSC undergo asymmetric division to give rise to multipotent precursors and these precursors are under transcriptional control to symmetrically divide into unipotent precursors that eventually differentiate into tissue specific lineage (Baksh et al., 2004).

For the osteoblast differentiation, a classic model was established by Lian and Stein (Lian and Stein, 1992). In this model it was proposed that the development of the osteogenic phenotype couples with a sequence of gene regulations and expressions. These genes were identified as cell cycle and growth genes c-fos and/or C-MYC, genes encoding ECM proteins, (i.e. ALP, OPN and OCN). The temporal sequence expression of these genes defined three principal periods of osteoblastic phenotype development (i.e. proliferation, ECM maturation and mineralization). Two transition points are pivotal elements of this osteoblast

developmental process to support cell proliferation and differentiation. The first transition point occurs at the end of proliferation where cell cycle and growth genes are down-regulated, and genes encoding ECM proteins start to become up-regulated. The second transition point is marked as ECM mineralization occurred. This osteoblast growth and differentiation model combined with other research implies the existence of temporal sequence gene expression and / or regulation controls for MSCs functional capabilities, (i.e. self-renew, osteogenic differentiation and osteoblast maturation) (Lian and Stein, 1992; Lian et al., 2006; McMurray et al., 2011).

Modification of biomaterial surfaces with well-defined nanoscale features, which mimic the structure of ECM can guide MSC lineage specific commitment in terms of tissue engineering (Stevens and George, 2005). As described in section 1.6.1, previous work from our group demonstrates that the near square 50 surface (NSQ50) which has an offset of up to +/- 50 nm in X and Y from a perfect square lattice arrangement of 120 nm diameter, 100 nm deep pits with 300 nm centre-centre spacing can specifically promote MSC osteogenesis. The NSQ50 surface printed on biocompatible and biodegradable PCL is a noninvasive stimulator for MSC osteogenesis, hence providing an ideal tool to get insight into the underlying mechanisms of the MSC differentiation process *in vitro*. Thus, in this chapter the NSQ50 nanotopography is used to modulate the expression of genes directing and going through MSCs osteogenic differentiation over a time course. Aims were to:

1. Assess temporal sequence of gene expression pattern during MSCs osteogenic differentiation on the NSQ50 surface.
2. Identify key points at which MSC turn from stemness into the osteogenic lineage-specific commitment and differentiation.

## **3.2 Methodology and experimental design**

To date, there are several methods that can be used for semi-quantitative and quantitative measurement of gene expression, from northern blot (Streit et al., 2009), reverse transcription PCR (RT-PCR) (Riedy et al., 1995), quantitative real

time PCR (qRT-PCR) (Arya et al., 2005) to gene expression microarray (Schulze and Downward, 2000) and the new development of next generation sequencing (NGS) (Mardis, 2008). Northern blot uses DNA or RNA hybridization probe complementary to part of or entire of gene sequence of interest. The probe is labelled either with radioactive isotopes or with chemiluminescent substrates to produce detectable signals. This method has been broadly used for gene detection, gene expression, function and localization in tissues, organs and their developmental stages due to its high sensitivity (Streit et al., 2009). However, compared to RT-PCR and / or qRT-PCR, this method has low sensitivity, suffers RNA sample degradation, and uses potentially more risky chemicals for the users. Compared to northern blotting and qRT-PCR, RT-PCR (or semi-quantitative PCR, as described in section 2.6.1) provides low accuracy data quantification. Thus, this method is only suitable for rapid, primary screening of bulk of samples or 'on/off' genes (Ferre, 1992). Gene expression microarray and NGS are powerful tools for global genes analysis, but are high cost. Due to the number of genes being investigated, the RT-PCR was used for primary screening and qRT-PCR was applied for accurate gene expression detection and comparison in this work.

### **3.2.1 Quantitative real time PCR (qRT-PCR)**

#### **3.2.1.1 Taqman and SYBR Green qRT-PCR**

QRT-PCR is, nowadays, widely applied in research and clinical diagnosis for gene detection, mutation and gene expression comparison as it is a powerful, sensitive and accurate method for quantification of RNA expression. This method allows for the direct measurement of PCR products during the exponential phase of a PCR reaction and combines the amplification and detection in one single step. This technology is a fluorescence - based reverse transcription PCR system, and many methods have been developed in the last couple of decades.

The fluorescence - based qRT-PCR reporter system can be classified into two principal groups based on fluorescent agent used and the specificity of PCR product detection: DNA binding dyes and Fluorophore-labelled oligonucleotides.

There are a variety of commercial available DNA binding dyes for PCR product detection, including SYBR Green I (Ririe et al., 1997), SYBR Green Gold (Tuma et al., 1999), SYTO (Monis et al., 2005), and EvaGreen (Wang et al., 2006). These dyes bind to double-stranded DNA (dsDNA) resulting in increase in fluorescent signal that can be measured in the extension phase of each PCR cycle (Wittwer et al., 1997). Among these, the SYBR Green I is the most commonly used in qRT-PCR. SYBR Green I is undetectable fluorescence when it is in its free form. In the PCR process, the fluorescence emission is propagated with the increase of PCR product as SYBR green dye binds to dsDNA (Figure. 3.2A and B). The major drawback of SYBR Green qRT-PCR is that SYBR Green qRT-PCR has less specificity as SYBR Green dye can bind to any dsDNA including nonspecific PCR products, primer-dimers, at the same time it binds to specific PCR product in amplification process. However, this problem can be handled in a couple of ways: (1) carefully designing primers and optimizing reaction conditions that can minimize the formation of primer dimers. (2) Nonspecific PCR products and / or primer dimers can be distinguished from specific PCR product by analyzing the melting curve. Once melting curves are set up, the fluorescence signal can be acquired above the dimer melting temperature ( $T_m$ ) and below specific PCR product  $T_m$ .

The fluorophore-labelled oligonucleotides are small fluorophore molecules attached to oligonucleotides servicing as probes for the detection of PCR product. In general, these probes use two types of fluorophore molecules, the reporter and quencher which are within specific distance (10 to 100 Å), through fluorescence resonance energy transfer (FRET). The emitted fluorescence from reporter fluorophore transfers to the quencher fluorophore. There are many these probes in commercial market (Navarro et al., 2015), the Taqman probe is a typical and commonly used in qRT-PCR. Taqman probe is a dual-labeled probe flanked by a fluorescence reporter dye at the 5' end and a quencher dye at the 3' end. As long as the probe is in its free form, or annealed on its complementary sequence on target template, the reporter dye and quencher dye are intact and the fluorescence signal emission from the reporter dye is absorbed by the quenching dye through FRET (Clegg, 1992). In the Taqman PCR extension phase, *Taq* DNA polymerase, which possesses the 5' → 3' exonuclease

activity, cleaves the 5' end nucleotides of the Taqman dual-labeled probe and separates reporter and quencher dyes, resulting in an increase of reporter fluorescence emission. This process occurs in every cycle and does not interfere with the exponential accumulation of PCR products (Wong and Medrano, 2005) (Figure. 3.2C and D).

SYBR Green qRT-PCR can be used with any pair of primers for any target of interest, this makes it less expensive than Taqman probes. Currently, the market price of one SYBR Green qRT-PCR assay is only 1/5 of a Taqman assay. Moreover, SYBR Green qRT-PCR provides high comparable results in gene expression measurement to data gained with Taqman qRT-PCR, as long as specific primers are designed and primer-dimers are minimized (Arikawa et al., 2008).

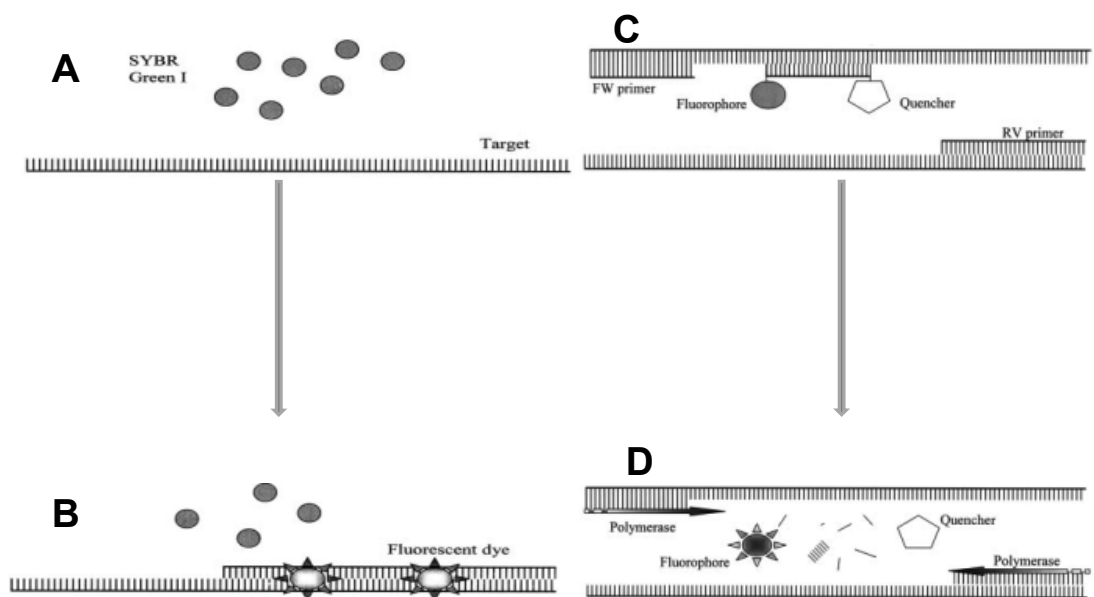


**Figure 3.2** Fluorescent chemistries used in TaqMan and SYBR Green qRT-PCR.

(A) SYBR Green I dyes that are free in the PCR reaction do not emit a fluorescent signal. (B) Once SYBR Green I dyes bind to the dsDNA, target fluorescent signal occurs. (C) In Taqman, primers and probe anneal to the target but fluorescent signal does not occur due to the proximity between fluorophore and quencher. (D) During the PCR extension phase, the probe is cleaved by Taq Polymerase. Thereby, fluorophore and quencher are separated, allowing fluorescence emission from the report dye (Picture modified from (Giulietti et al., 2001).

### **3.2.1.2 Three modes of SYBR Green qRT-PCR**

To quantify the results obtained from real time qRT-PCR, three modes of quantification are commonly used which are; the absolute standard curve method, the relative standard curve method and the comparative method. The absolute standard curve method is used for quantifying absolute RNA copy numbers in a sample. It needs more RNA sample to amplify the genes of interest, which are then used for making standard curves. The main drawback of this method is time and material consuming, especially for multiple gene quantification. The comparative method is the simplest way to quantify amount of RNA. However, this mode needs the same PCR reaction efficiency (or a difference of less than 10%) of sample RNA as of endogenous control gene for accurate measurement. In practice, it is almost impossible for multiple genes of interest to have the same PCR efficiency as the endogenous control gene. Relative standard curve method was used in this work to compromise for the drawbacks of the absolute and comparative methods (Larionov et al., 2005). The relative standard curve method uses a set of relative standards derived from any stock cDNA containing appropriate target genes. The target gene quantity is determined by interpolating from standard curve.

### **3.2.1.3 Endogenous control gene GAPDH**

Quantitative gene expression data are often normalized to the expression levels of endogenous control genes whose expression remains constant in the cells or tissues under investigation. GAPDH is one of the most commonly used endogenous control gene in comparisons of gene expression (Gorzelnik et al., 2001) and it is widely used for bone marrow derived stem cells research (Ponte et al., 2007) (Raaijmakers et al., 2002). To investigate whether GAPDH as endogenous control suits this work, the expression of GAPDH mRNA was measured in a course for MSCs cultured on the NSQ50 and planar surfaces. The expression of GAPDH was constant during MSC osteogenic lineage specific commitment. Significant differences of GAPDH expression in different time points and samples were not observed (Figure 3.3).

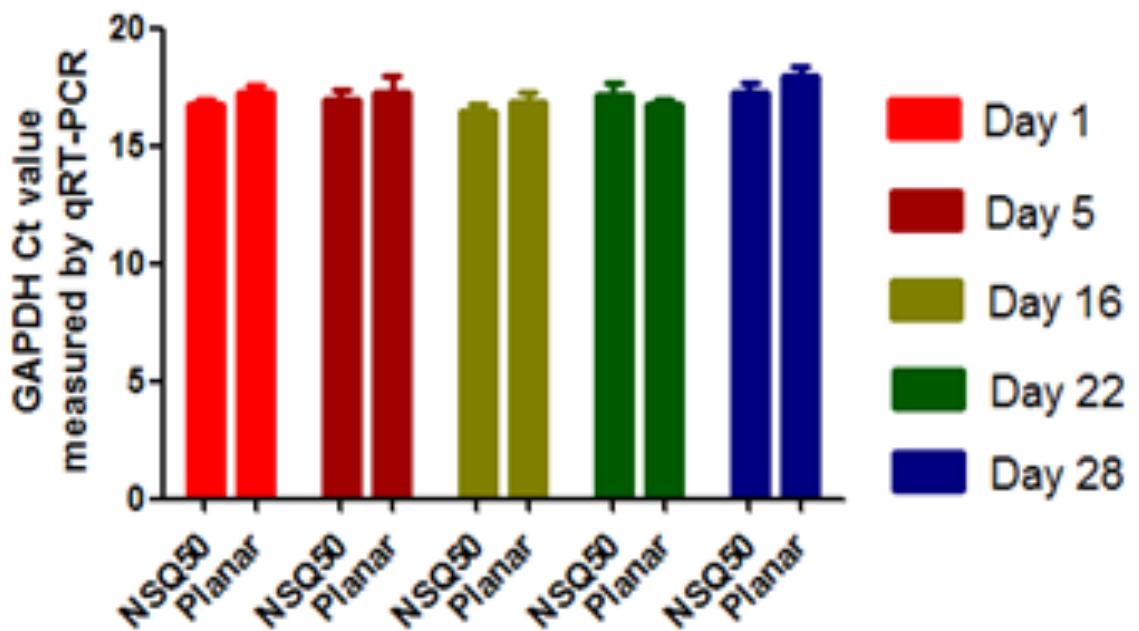


**Figure 3.3** Ct value of GAPDH measured for MSCs cultured on NSQ50 and planar surfaces at different time points.

GAPDH expression levels are constant during NSQ50 surface induced osteogenic process. The graph illustrates that there is no significant change in the expression of GAPDH on NSQ50 and planar surfaces at different time point.

### 3.2.2 Experimental design

#### 3.2.2.1 Assessment of bone marrow derived mesenchymal stromal cells

Bone marrow derived MSCs without surface antigen markers selection are a heterogeneous cells population that contains stem cells, multipotent precursors and uncommitment precursors as well as mature cells. Therefore, these cells must first be assessed to confirm that they were not in a lineage specific commitment state before using them as cell resources to investigate the temporal sequence of gene expression for osteo specific differentiation on the NSQ50 surface.

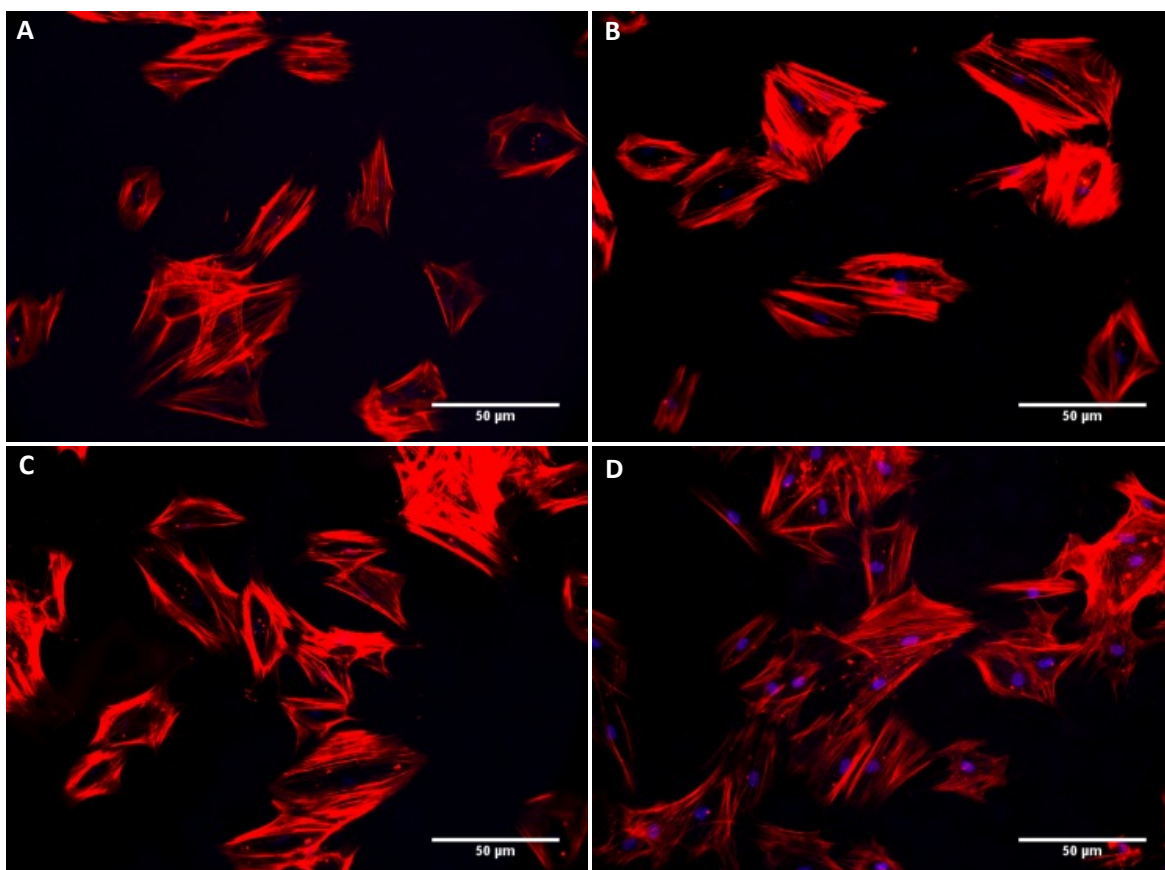


**Figure 3.4** MSCs expanded in tissue culture flask negatively express tissue specific markers after two passaging.

Immunostaining for (A) myod (muscle), (B) sox9 (cartilage), (C) pparg (fat) and (D) RUNX2 (bone) (red: actin, blue: nuclear, green: tissue specific markers).

The assessments were carried out by immunostaining using tissue specific transcription factors which putatively are the earliest markers of tissue specific commitments (i.e., myod for myogenesis, RUNX2 for osteogenesis, pparg for adipogenesis and SOX9 for chondrogenesis) before they seeded on the test surface. The negative expression of these markers indicated that MSCs maintain their uncommitted state after expansion, and can be used for the follow-up experiments (Figure 3.4).

### 3.2.2.2 Work flow of gene expression measurement

To investigate the temporal sequence of gene expression pattern for NSQ50 induced MSCs osteogenic differentiation, the experiment was designed to produce gene expression comparison for MSCs on the NSQ50 surface to those on

planar control surface.  $1 \times 10^4$  MSCs were seeded on NSQ50 modified PCL and planar PCL (at given surface roughness 0.5 nm) separately, and follow-up experiments were carried out in parallel (Figure 3.5). Three biological replicates were carried out for all experiments (i.e., N=3, N refers to MSCs from different donors bone marrow). Data was analyzed by analysis of variance (ANOVA) using GraphPad 5 software, and the final gene expression results are presented in fold change after compared to planar control.

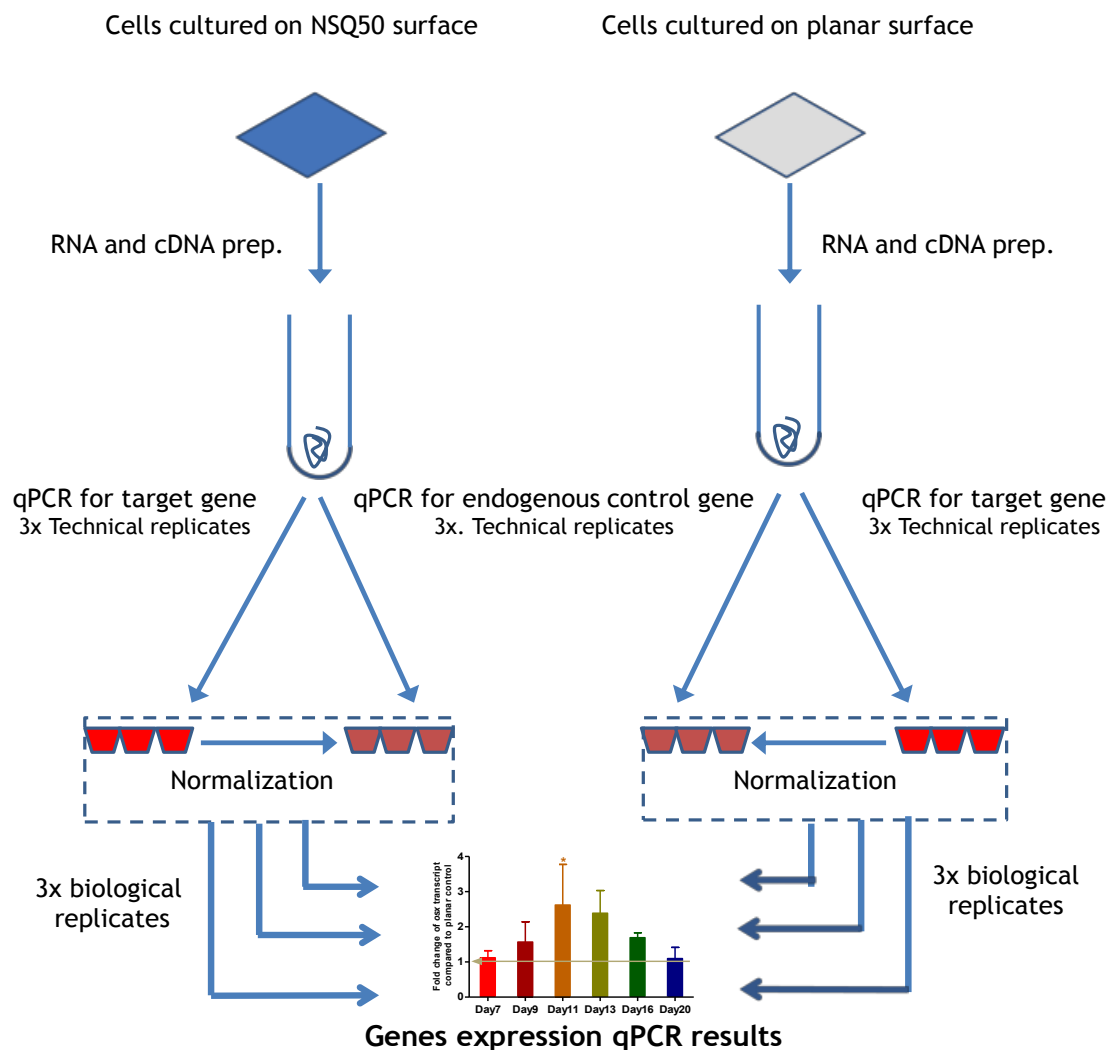


**Figure 3.5** Diagram of parallel work flow for gene expression measurement.

### **3.2.2.3 Genes and time points chosen for temporal sequence gene expression**

MSCs isolated from human bone marrow maintain their multipotent property after one or two passages culture and to maintain a highly proliferative phenotype. Therefore, seeded onto osteogenic materials, we may characterize expression of cell growth and proliferation genes at the earliest stages of the culture on the NSQ50 surface with osteogenic marker genes expression expected to follow the down-regulation of such proliferative genes. However, osteogenic marker genes are regulated by specific transcription factors. Thus, the order of genes being examined was designed to capture proliferation genes, osteogenic transcription factors and finally osteogenic markers (table 3.1).

Gene expression was then validated at protein level. In this work, key proteins expression including RUNX2, OPN and OCN was assessed by western blot and / or immunostaining using their specific antibodies.

To confirm mature osteoblast phenotype occurred on NSQ50 after the osteogenic markers were observed, bone nodule formation was assessed using Alizarin red staining (described in section 2.10).

**Table 3.1 Genes associated with MSCs functional relationship between proliferation and osteogenic differentiation.**

Gene name	Gene function	References
C-MYC	Cell growth and proliferation regulation.	(Park et al., 2012), (Sawada et al., 2006).
RUNX2	Osteogenic transcription factor regulating osteogenic marker genes for pre-osteoblast commitment.	(Ducy et al., 1997), (Komori et al., 1997), (Zheng et al., 2004).
OSX	Osteogenic transcription factor regulating osteogenic marker genes for mature osteoblast commitment.	(Nakashima et al., 2002), (Nakashima and de Crombrughe, 2003), (Tu et al., 2006).
ALP	An ectoenzyme involved in the formation of hydroxyapatite of bone matrix.	(Whyte, 1994), (Boskey, 1998), (Buchet et al., 2013).
OPN	Non-collagenous protein secreted by osteoblast cells, expressed during bone matrix formation and mineralization. Also contains an RGD group and is involved in cell adhesion.	(Pedraza et al., 2008), (Giachelli, 2001), (Denhardt et al., 2001)
OCN	An osteoblast specific protein, binding to hydroxyapatite in mature osteogenesis.	(Ducy et al., 1996), (Wang et al., 2007), (Wan et al., 2010).

### 3.3 Results

#### 3.3.1 Effect of NSQ50 topography on C-MYC expression

C-MYC is a proto-oncogene encoding transcription factor that supports cell growth and proliferation in many cell types, including MSCs derived from human bone marrow and hematopoietic stem cell (Sawada et al., 2006). C-MYC expression is switched on and increased when cells are in growth and proliferation stage, and switched off while cells start to differentiation (Deng et al., 2008).

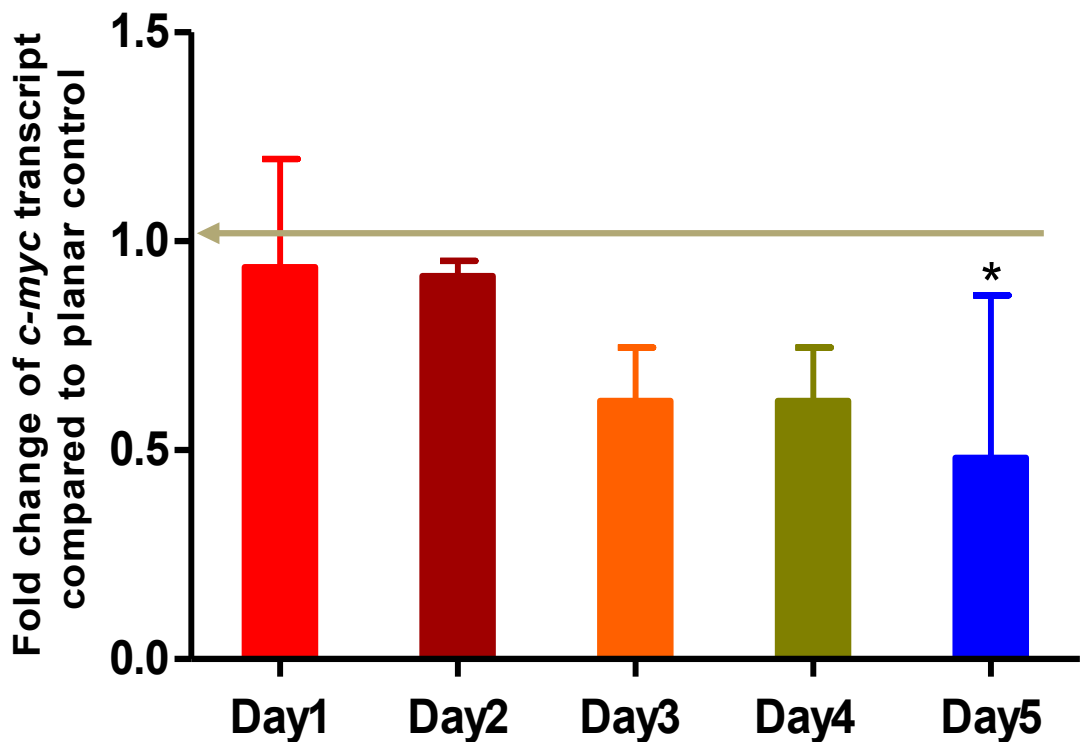


Figure 3.6 Gene expression analysis of C-MYC in MSCs on NSQ50 compared to those on planar control.

Relative qRT-PCR shows C-MYC expression on NSQ50 is almost unchanged compared to those on planar control before day 5. Significant down-regulation of C-MYC on NSQ50 was observed by day 5. (N=3,  $\pm$  SD) ANOVA analysis, \* p value < 0.05.

The expression of C-MYC in cells on NSQ50 was measured using qRT-PCR after MSCs had been cultured on the NSQ50 and planar control from 1 day to 5 days.

The relative expression of C-MYC on the NSQ50 surface compared to on planar surface is shown in Figure 3.6. At day 1 and day 2, expression of C-MYC on NSQ50 was roughly the same as for cells on the planar surface. After day 3, expression of C-MYC on the NSQ50 surface was decreased and significantly suppressed relative to planar surface was observed at day 5.

### **3.3.2 RUNX2 temporal sequence expression pattern during NSQ 50 induced MSC osteogenic differentiation**

RUNX2 is a master osteogenic transcription factor regulating osteoblast commitment and osteogenic differentiation of mesenchymal stromal cells (Deng et al., 2008; Ducy et al., 1997). RUNX2 temporal sequence expression pattern in MSCs cultured on NSQ 50 surface was examined by qRT-PCR (Figure. 3.7).

The expression of RUNX2 in nanotopographically induced MSCs was only slightly modulated after 3 days of culture relative to planar controls. However, the results showed that RUNX2 was about 2 to 3 fold enriched in MSCs on the NSQ50 surface compared to those on planar surface at days 5 and 7, and peaked at day 5. RUNX2 then gradually decreased and showed no difference to the planar control at day 13. The up-regulation of RUNX2 indicated that the NSQ50 surface induced MSCs lineage specific commitment and was osteogenic. However, the data also demonstrated that the master osteogenic transcription factor was induced by NSQ50 in a transient manner and the up-regulation only occurred at the early stage of MSC osteogenic lineage commitment.

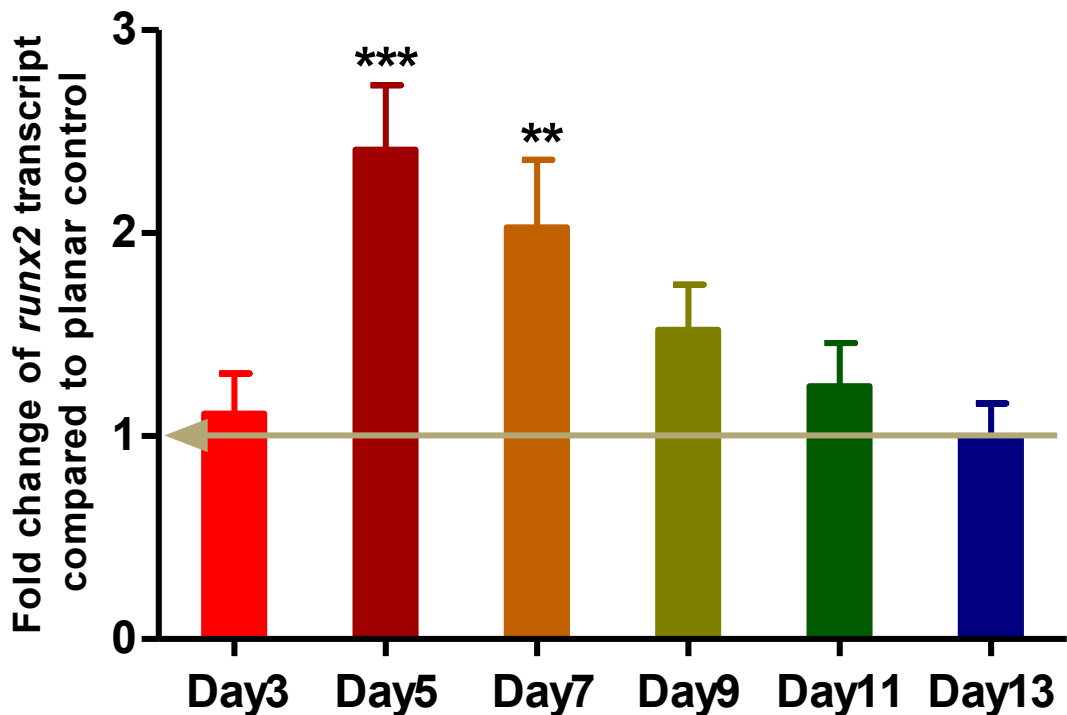


**Figure 3.7** Temporal sequence gene expression analysis of RUNX2 in MSCs on NSQ50.

The fold change of RUNX2 in MSCs on NSQ50 compared to those on planar controls were assessed by qRT-PCR for cells cultured from 3 to 13 days. The expression of RUNX2 was significantly up-regulated at day 5 and day 7, with the peak at day 5. After 7 days cell culture, RUNX2 gradually decreased to an equal level to that on planar control at day 13. (N=3,  $\pm$  SD) ANOVA analysis, \*\*  $p < 0.01$ , \*\*\*  $p < 0.001$ .

### 3.3.3 Osterix (OSX) temporal sequence expression pattern during NSQ 50 induced MSC osteogenic differentiation

NSQ50 induced MSC osteogenesis showed RUNX2 was significantly up-regulated at the early stages of MSC osteoblast lineage commitment (day 5 and 7). To test whether OSX expression is required in NSQ50 surface induced MSC osteogenesis, the temporal expression pattern of OSX was assessed by qRT-PCR from time points 7 to 20 days (Figure 3.8). The data showed that OSX expression was gradually up-regulated before day 11, and was significantly abundance at days 11 and 13 with about three fold enrichment compared to cells on planar control. Then reduced until it was statistically the same as the planar control at day 20. The temporal expression pattern of OSX was similar to that of RUNX2 with time

course shifted on, suggesting the NSQ50 induced MSC osteogenesis requires both osteogenic transcription factors, RUNX2 and OSX, and potentially demonstrating that MSC osteogenic differentiation on the NSQ50 surface shares the same transcriptional control of bone development *in vivo*.

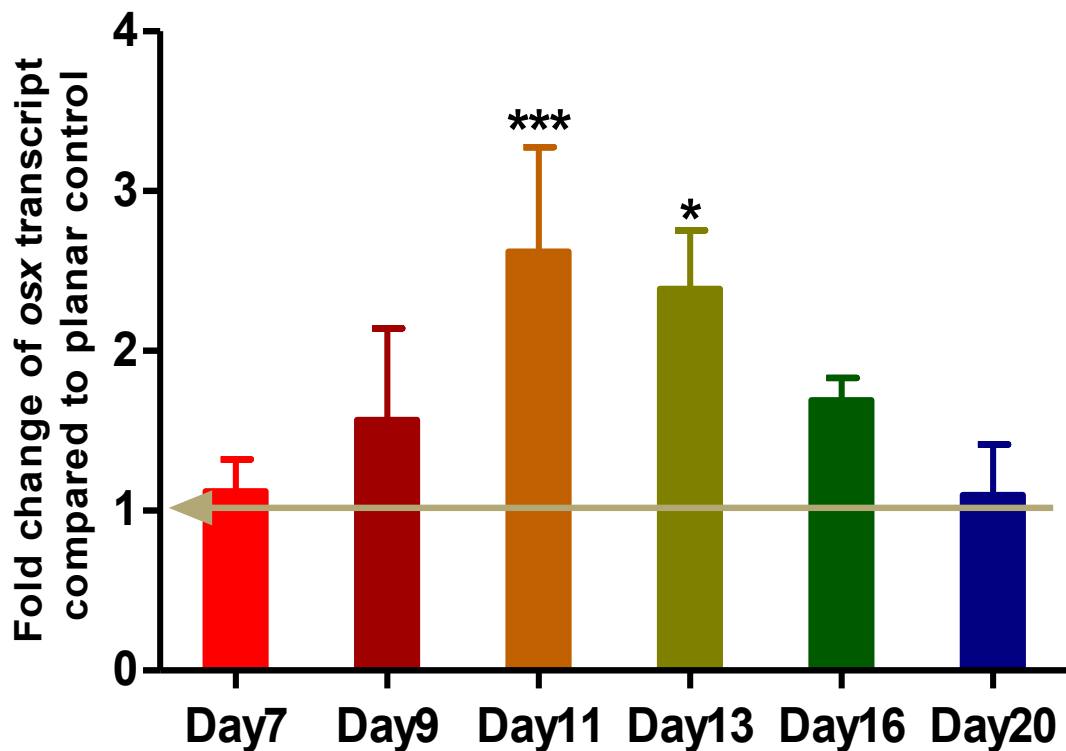


**Figure 3.8** Temporal gene expression analysis of OSX in MSCs on NSQ50.

The fold change of OSX in MSCs on NSQ50 compared to those on planar control were assessed by qRT-PCR for cells cultured 7 days to 20 days. The expression of OSX shows a wave pattern in which OSX gradually increased and peaked at day 11 and then gradually decreased to an equal level of that on planar control at day 20. Significant increases of OSX on NSQ 50 was observed at day 11 and day 13. (N=3,  $\pm$  SD) ANOVA analysis, \*  $p < 0.05$ , \*\*\*  $p < 0.001$ .

MSC differentiation into mature osteoblasts is a multistage process which is controlled at transcriptional level by a number of regulatory factors. Besides RUNX2 and OSX, some homeodomain proteins (HDs), such as MSX2 and DLX5 regulate osteoblast differentiation by interacting with RUNX2 and / or OSX. Moreover, OSX expression is either dependent on or independent of RUNX2. The RUNX2-independent expression of OSX is mediated by either MSX2 or DLX5 (Liu

et al., 2007a; Matsubara et al., 2008). To test whether OSX was controlled by RUNX2 or not, gene expression of MSX2 and DLX5 was assessed using qRT-PCR for cells cultured on the NSQ50 surface and planar control for 9 days immediately prior to OSX up-regulation (Figure 3.9). The data, after comparing to planar control showed that the expression of MSX2 and DLX5 were not significantly changed, indicating these two HD factors were not involved in the transcriptional regulatory network induced by the NSQ50 surface and indicating that OSX expression was RUNX2-dependent controlled.

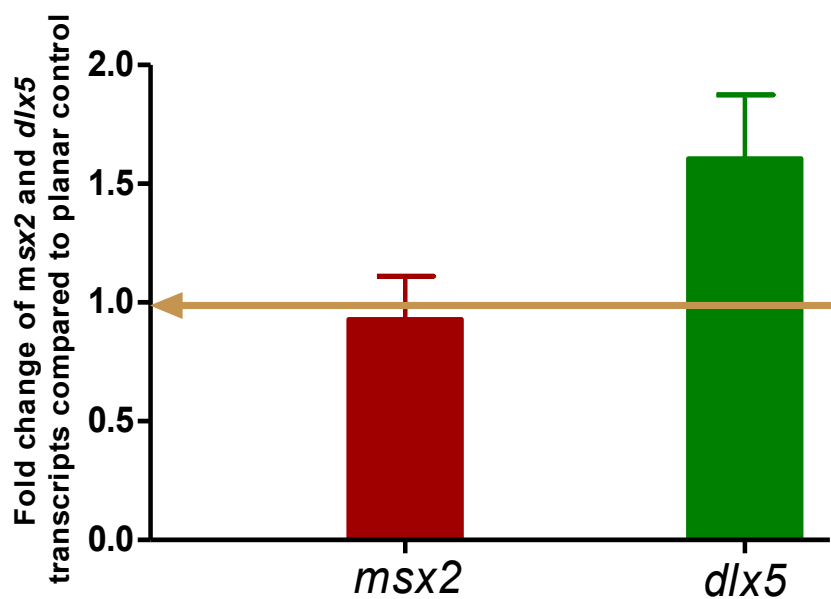


**Figure 3.9** Effects of NSQ50 surface on homeodomain factors MSX2 and DLX5.

MSCs were cultured on NSQ50 and planar surfaces for 9 days before expression of *MSX2* and *DLX5* on NSQ50 surface were assessed by qRT-PCR and compared to those on planar surface. *MSX2* and *DLX5* were unchanged relative to planar control. (N=3,  $\pm$  SD) ANOVA analysis,  $p > 0.05$ .

### 3.3.4 ALP expression pattern during NSQ50 induced MSCs osteogenic differentiation

ALP is an ectoenzyme secreted by osteoblast, which hydrolyzes extracellular pyrophosphate (PPi) to phosphate (Pi) leading to the formation of hydroxyapatite (HA) (Orimo, 2010). To examine whether NSQ50 surface induces MSC osteogenesis into mature osteoblasts, the expression of ALP assessed using qRT-

PCR after the induction of osteogenic transcription factors RUNX2 and OSX. The expression of ALP was measured at days 11, 16 and 28. ALP expression on the NSQ50 surface showed significant increase at day 16 and continuously increased upto day 28 with a fold change up to about 40, compared to MSCs on planar control (Figure 3.10).

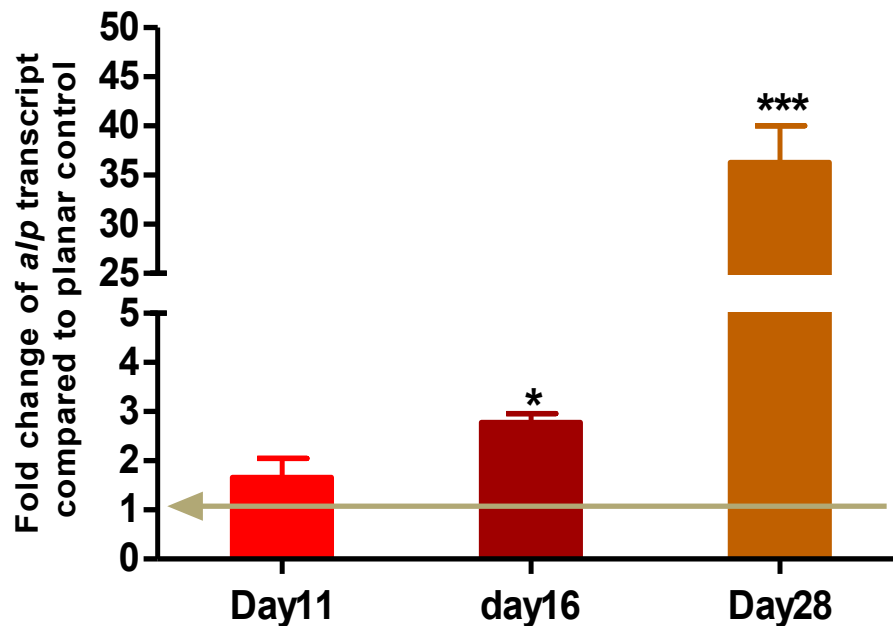


**Figure 3.10** Gene expression analysis of ALP in MSCs on NSQ50.

The fold change of ALP in MSCs on NSQ50 compared to those on planar control was assessed by qRT-PCR for cells cultured for 11, 16 and 28 days. ALP on NSQ 50 was significantly up-regulated at day 16 and about 40 fold change was observed at day 28. (N=3,  $\pm$  SD) ANOVA analysis, \*  $p < 0.05$ , \*\*\*  $p < 0.001$ .

### 3.3.5 OPN expression pattern during NSQ50 induced MSC osteogenic differentiation

Unlike *ALP*, which is expressed at the matrix maturation stage of osteoblast development, *OPN*, a phosphorylated sialic acid-rich non-collagenous protein secreted by osteoblast cells, expresses at both matrix maturation stage and at the onset of mineralization (Lian and Stein, 1992). *OPN* bridges osteoblast cells to their matrix minerals, as its amino acid sequence contains arg-gly-asp (RGD) which mediates cell attachment (Bautista et al., 1994). The expression of *OPN* in MSCs cultured on the NSQ50 surface was measured and compared to those on

planar control at days 11, 16, 20 and 28 (Figure 3.12). ALP on NSQ50 showed significant increase at day 20 and continuously increased upto day 28 with fold change up to  $\geq 100$ .

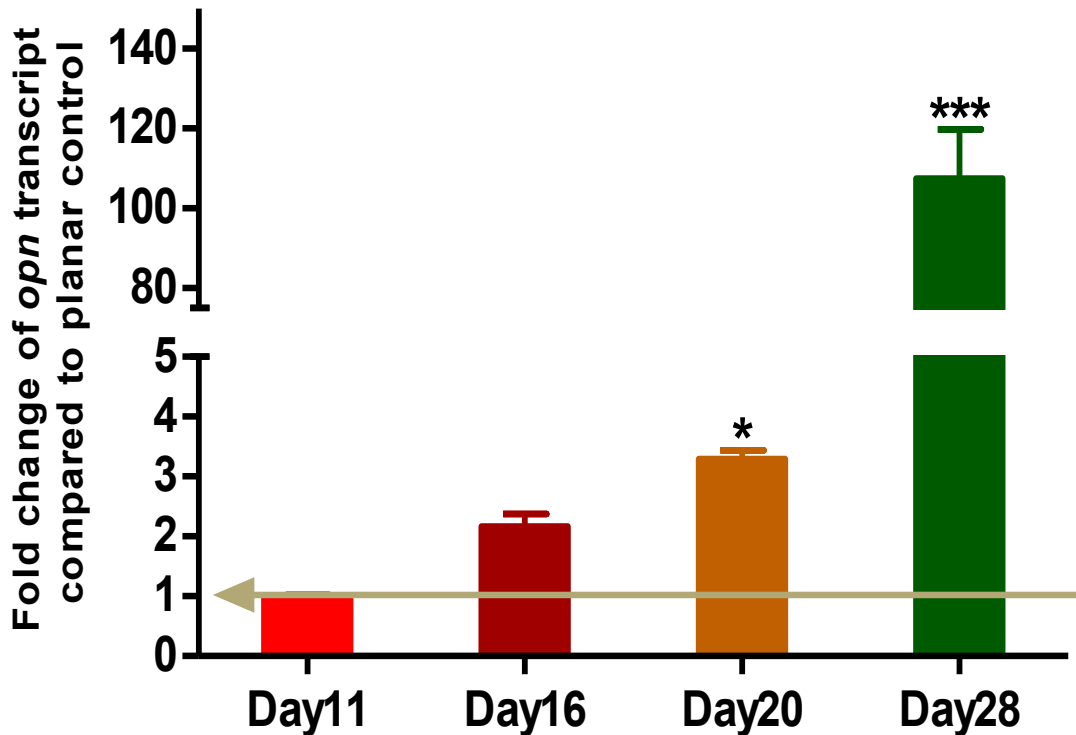


Figure 3.11 Gene expression analysis of OPN in MSCs on NSQ50.

The fold change of OPN in MSCs on the NSQ50 surface compared to those on planar control was assessed by qRT-PCR for cells cultured from 11 to 28 days. OPN on NSQ50 was significantly up-regulated at day 20, and a  $\geq 100$  fold change was observed at day 28. (N=3,  $\pm$  SD) ANOVA analysis, \*  $p < 0.05$ , \*\*\*  $p < 0.001$ .

### 3.3.6 OCN expression pattern during NSQ50 induced MSC osteogenic differentiation

OCN is an osteoblast specific protein containing 3-gammarcarboxy-glutamic acid residues (Gla). The gammarcarboxylated form of OCN binds hydroxyapatite and is abundant in bone ECM (Kapustin and Shanahan, 2011). The expression of OCN in MSCs cultured on the NSQ50 surface was measured and compared to those of planar control through day 11 to day 28 (Figure 3.12). OCN showed no significant up-regulation until day 28 on the NSQ50 surface compared to control.

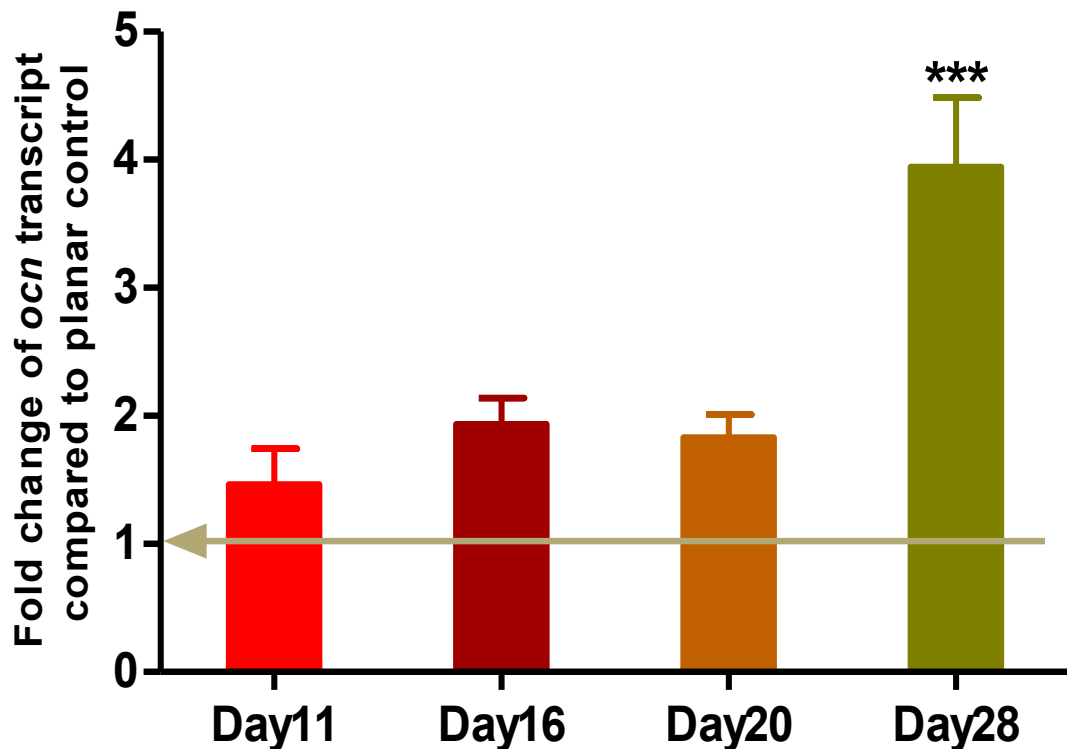


Figure 3.12 Gene expression analysis of OCN in MSCs on NSQ50.

The fold changes of OCN in MSCs on NSQ50 compared to those on planar control was assessed by qRT-PCR for cells cultured 11 days to 28 days. OCN on NSQ50 was significantly up-regulated at day 28 with a fold change about 5. (N=3,  $\pm$  SD) ANOVA analysis, \*\*\*  $p < 0.001$ .

### 3.3.7 The validation of key genes expression

Protein expression of master osteogenic transcription factor RUNX2 and ECM components of OPN and OCN in MSCs cultured on NSQ50 were assessed. The abundance of RUNX2 on NSQ50 was detected by both western blotting and immunostaining when cells cultured for 9 days (Figure 3.13). Immunostaining of RUNX2, using RUNX2 specific antibody, showed RUNX2 was abundant on NSQ50 surface (Figure 3.13A) and the expression of RUNX2 on planar surface (Figure 3.13B) was almost null after 9 days cell culture. The enrichment of RUNX2 on the NSQ50 surface compared to that on planar surface was also observed using Western blotting. The same amount of total proteins (10  $\mu$ g) from cells on NSQ 50 surface and planar surface were separated on a SDS-PAGE gel. RUNX2 was detected using its specific antibody for cells cultured on the NSQ50 surface

(Figure 3.13C) and the same amount of total protein loaded into wells of SDS-PAGE gel was controlled by GAPDH (Figure 3.13D). Both immunostaining and Western blotting showed the same result with RUNX2 being most abundant on the NSQ50 surface and negligible on the planar surface after cells were cultured for 9 days, which confirmed the gene expression of RUNX2 assessed in section 3.4.2.

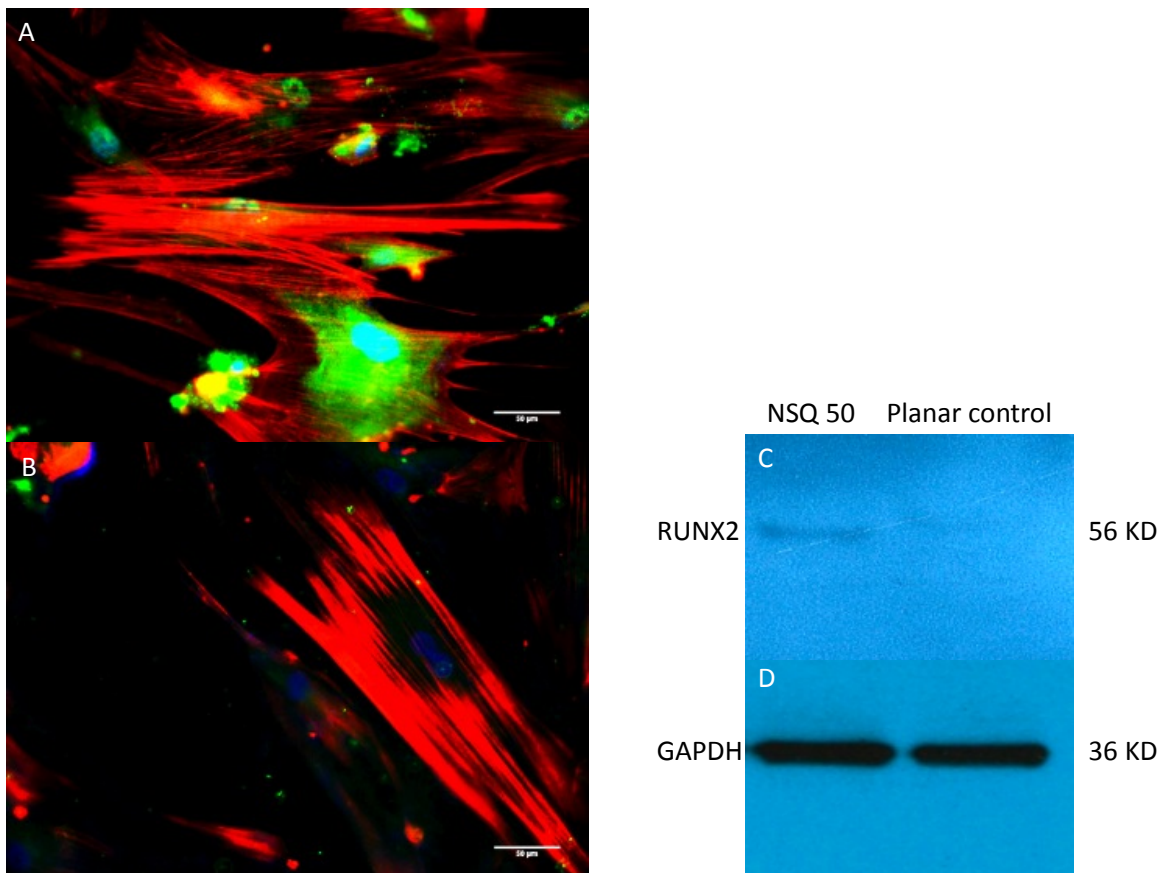


**Figure 3.13** RUNX2 is abundant in cells cultured on the NSQ50 surface for 9 days.

MSCs cultured on NSQ50 and planar surface for 9 days. Immunostaining using anti-RUNX2 showed RUNX2 was abundant in cells cultured on NSQ50 surface (A) compared to cells on planar surface (B). (Green: RUNX2, Red: actin, Blue: DAPI). The overall expression of RUNX2 was also detected using Western blot. (C), again illustrating greater expression on NSQ50 while GAPDH levels remained the same (D).

The abundance of OPN and OCN on NSQ50 surface compared to that on planar control was observed using immunostaining after 28 days of culture (Figure

3.14). OPN (Figure 3.14A, green) and OCN (Figure 3.14C, green) expression on the NSQ50 surface are observed while expression remained negligible on the planar control (Figure 3.14B: OPN and D: OCN). The protein expression of OPN and OCN were therefore in agreement with their gene expression, which is described in section 3.3.5 and section 3.3.6 respectively.

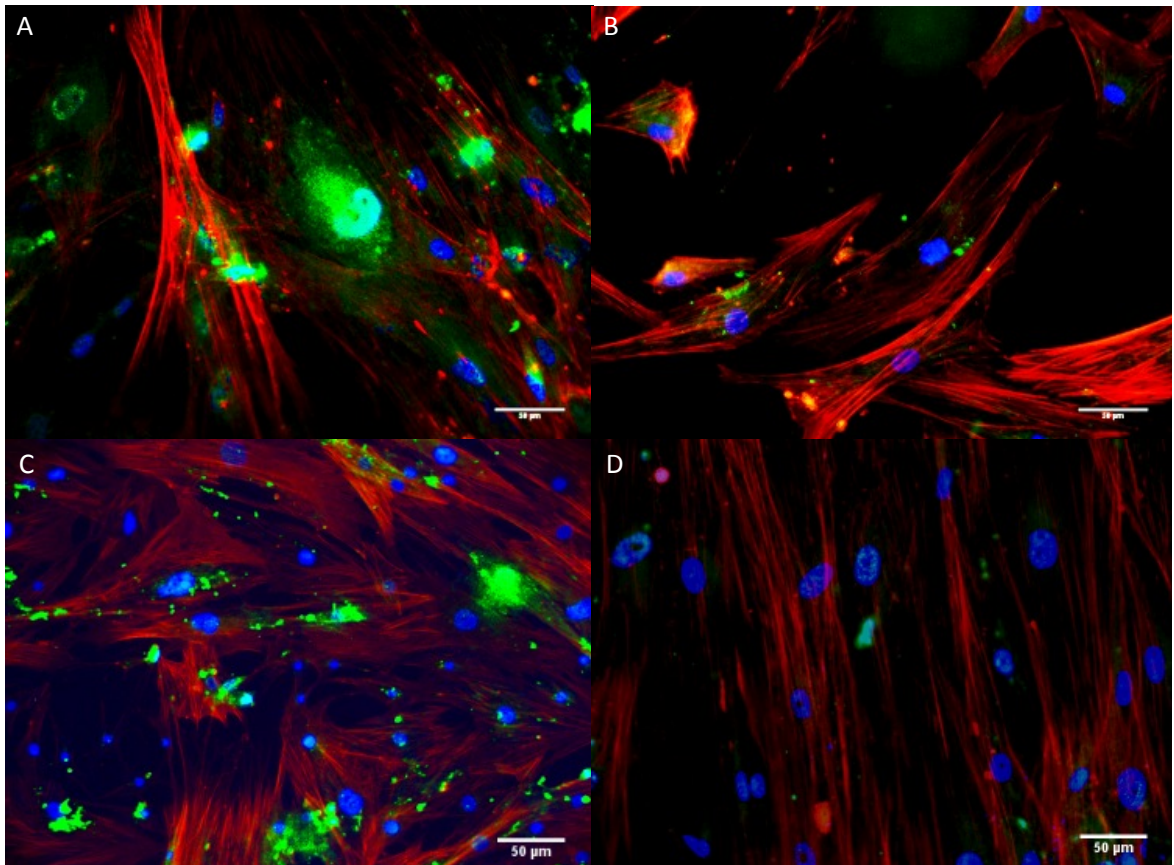


**Figure 3.14** OPN and OCN are abundant in cells cultured on NSQ50 surface for 28 days.

MSCs cultured on NSQ50 and planar surface for 28 days. Immunostaining using anti-OPN showed OPN was abundant in cells cultured on the NSQ50 surface (A) compared to cells on planar control (B) (Green: OPN, Red: actin, Blue: DAPI). The over-expression OCN was also detected on NSQ50 surface (C) compared to that on planar control (D) using anti-OCN (Green: OCN, Red: actin, Blue: DAPI).

### **3.3.8 The formation of bone nodules**

The formation of bone nodules characterized by calcium deposition in the ECM of osteoblast cell, indicates the presence of mature osteoblasts at the

mineralization stage (Lian and Stein, 1992). Calcium deposition of MSCs cultured on the NSQ50 surface after 32 days was observed using Alizarin red staining (Figure 3.15). After 32 days of cell culture, cells on the NSQ50 surface exhibited calcium deposition.

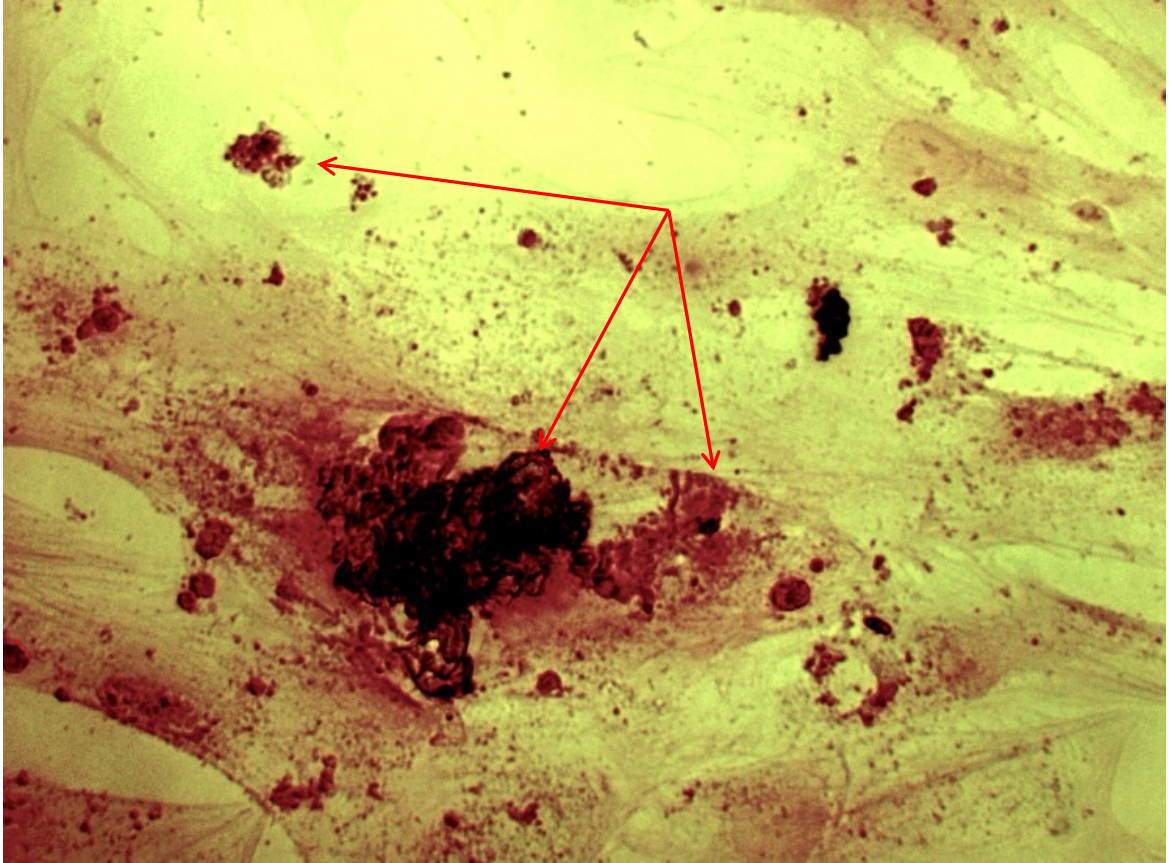


**Figure 3.15** Calcium deposition by MSCs on NSQ50.

MSCs cultured on the NSQ50 surface for 32 days were stained with Alizarin red. Bone nodule formation could be seen *in vitro* on the NSQ50 surface.

## **3.4 Discussion and conclusion**

### **3.4.1 The transcriptional control of MSCs on NSQ50 surface.**

In this chapter, the effects of the NSQ50 surface on expression of transcription factor C-MYC, RUNX2, OSX, MSX2 and DLX5 were investigated and it was seen that C-MYC expression was down-regulated at the early stage of cells cultured on NSQ50, while up-regulation of RUNX2 and OSX in a sequential manner was observed before osteoblast marker genes were induced. These data indicated that NSQ50 surface induced MSCs osteogenic differentiation and that this osteogenesis was transcriptionally controlled.

C-MYC is a key regulator of cell growth and proliferation in many cell types. Over-expression of C-MYC drives cell proliferation and growth, inhibits cell differentiation and reduces cell adhesion. In contrast, down-regulation of C-MYC results in the inhibition of cell proliferation and growth, enhancement of cell differentiation and enlargement of cell adhesion (Aizawa et al., 1999). Previous studies have also demonstrated that C-MYC exerts regulatory effects on MSC proliferation and growth. For example, C-MYC was down-regulated by the up-regulation of TGFs and their receptors via SMAD protein, resulting in MSC proliferation being arrested (Sawada et al., 2006). C-MYC was also characterized as a marker gene for osteoblast proliferation in osteogenic culture system (Lian and Stein, 1992). The expression of C-MYC in MSCs cultured on the NSQ50 surface rapidly decreased after day 3 of culture compared to MSCs on planar surfaces, and was reduced to about half of those on planar control at day 5. Statistical analysis using ANOVA showed the reduction at day 5 was significant ( $p < 0.05$ ). This data suggested that proliferation activity of MSCs on NSQ 50 was repressed.

The down-regulation of C-MYC on NSQ50 was coupled with the up-regulation of the osteogenic master transcription factor RUNX2 and subsequently OSX. RUNX2 expression was in a wave pattern in the time frame of day 3 to day 13, significant enrichment of RUNX2 on NSQ50 compared to planar surface was

observed at days 5 and 7. The significant up-regulation of RUNX2 was coincident with down-regulation of C-MYC on NSQ50 at day 5 suggesting that MSCs on the NSQ50 surface had initiated osteoblast commitment. However, the up-regulation of RUNX2 was not persistent and gradually decreased to the same level as that of MSCs on the planar surface. The temporal wave expression pattern of RUNX2 suggested that the effect of RUNX2 on its osteogenic transcriptional control is stage-dependent. Previous studies on RUNX2-overexpression in mice demonstrated that enriched expression of RUNX2 at late stage osteoblastic development in fact abrogated bone formation and enhanced bone resorption (Liu et al., 2001). Therefore, the up-regulation of RUNX2 at an early stage (rather than late stage) promised the initiation of osteogenic lineage specific commitment of MSCs on NSQ50 surface but without disruption of bone formation at later stages. Furthermore the observation of enriched expression of RUNX2 coincident with down-regulation of C-MYC at day 5 also supported the role of RUNX2 in NSQ50 surface induced osteogenic differentiation. RUNX2 null cells have been shown to exhibit higher proliferation rates than wild type cells (Galindo et al., 2005). Also, RUNX2 has been demonstrated to target CDK inhibitors p21 and p27 in order to promote cell cycle exit (Galindo et al., 2005; Thomas et al., 2004). Therefore, RUNX2 was the earliest switch molecule to turn MSCs towards osteogenic differentiation on the NSQ50 surface.

RUNX2 expression is necessary for the initiation of osteoblast differentiation. However, RUNX2 alone is not sufficient for mature osteoblast development. Previous studies have demonstrated that OSX was required for osteoblast differentiation, and acted downstream of RUNX2 (Matsubara et al., 2008; Nakashima et al., 2002). RUNX2 and OSX may play different roles in the regulation of osteogenic differentiation and bone formation. Unlike RUNX2-deficient lethal phenotype, OSX-deficient mice showed perinatal lethal phenotype due to nonmineralized bone formation, suggesting OSX functionalizes mature osteoblast development (Zhang, 2010). In NSQ50 surface induced osteogenic differentiation, up-regulation of OSX was observed downstream of RUNX2, which filled in the temporal gap between RUNX2 expression (at day 5 and 7) and induction of osteoblasts marker genes (ALP, OPN and OCN, initiated

at day 16). Further analysis indicated that OSX expression was RUNX2 dependent, as the induction of MSX2 and DLX5 on the NSQ50 surface was not observed. These data suggested that NSQ50 surface induced osteogenic differentiation required regulation from both RUNX2 and OSX, and these two transcription factors acted at temporal, sequential manner.

### **3.4.2 Bone marker genes expression on NSQ50 surface**

Bone tissue specific marker genes (ALP, OPN, and OCN) are downstream of, and regulated by osteogenic transcription factors. These bone markers are secreted by osteoblasts in osteogenesis. Expression of ALP and OPN on the NSQ50 surface was significantly enhanced at day 16 and were highly expressed at day 28 (about a 40 fold change for ALP and over 100 fold change for OPN). OCN was also significantly induced at day 28, however its expression level (about 4 fold change) was lower than those of ALP and OPN. MSCs are known to form super-mature adhesions (>5  $\mu\text{m}$  long) on the NSQ50 surface (Biggs et al., 2009). This could perhaps explain the use of OPN rather than OCN as OPN contains the RGD motif required for integrin ligation and hence would aid focal adhesion formation.

### **3.4.3 Temporal sequence gene expression couples with MSC osteogenic differentiation on NSQ50 surface**

MSCs cultured on the NSQ50 surface showed repressed expression of C-MYC by day 5, concomitant with up-regulation of RUNX2, indicating MSCs growth and proliferation were being arrested and the cells orientated towards osteogenic lineage specific commitment. The up-regulation of RUNX2 alone in a transient manner on the NSQ50 surface could lead MSCs to form other cell phenotypes, such as chondrocyte (Takeda et al., 2001). However, the subsequent induction of OSX by RUNX2 helps assure the osteoblastic lineage direction on the surface, because OSX is a more specific transcription factor in directing pre-osteoblast to mature osteoblast differentiation (Nakashima et al., 2002). Therefore, it is logical to interpret the temporal genes expression pattern on the NSQ50 surface as the different stages of MSCs osteogenic differentiation (Figure 3.16). It is thus

likely that the NSQ50 surface induces MSCs into a pre-osteoblast phase after cells have been cultured on the surface for about a week. The pre-osteoblasts were governed by the RUNX2 recruited OSX which led pre- and immature osteoblasts into mature osteoblasts and eventually a mineralization phase. The transit point (around a cell culture period on NSQ50 of 21 days) could be viewed as the immature osteoblast marker ALP had been significantly increased and OCN had started to be up-regulated.

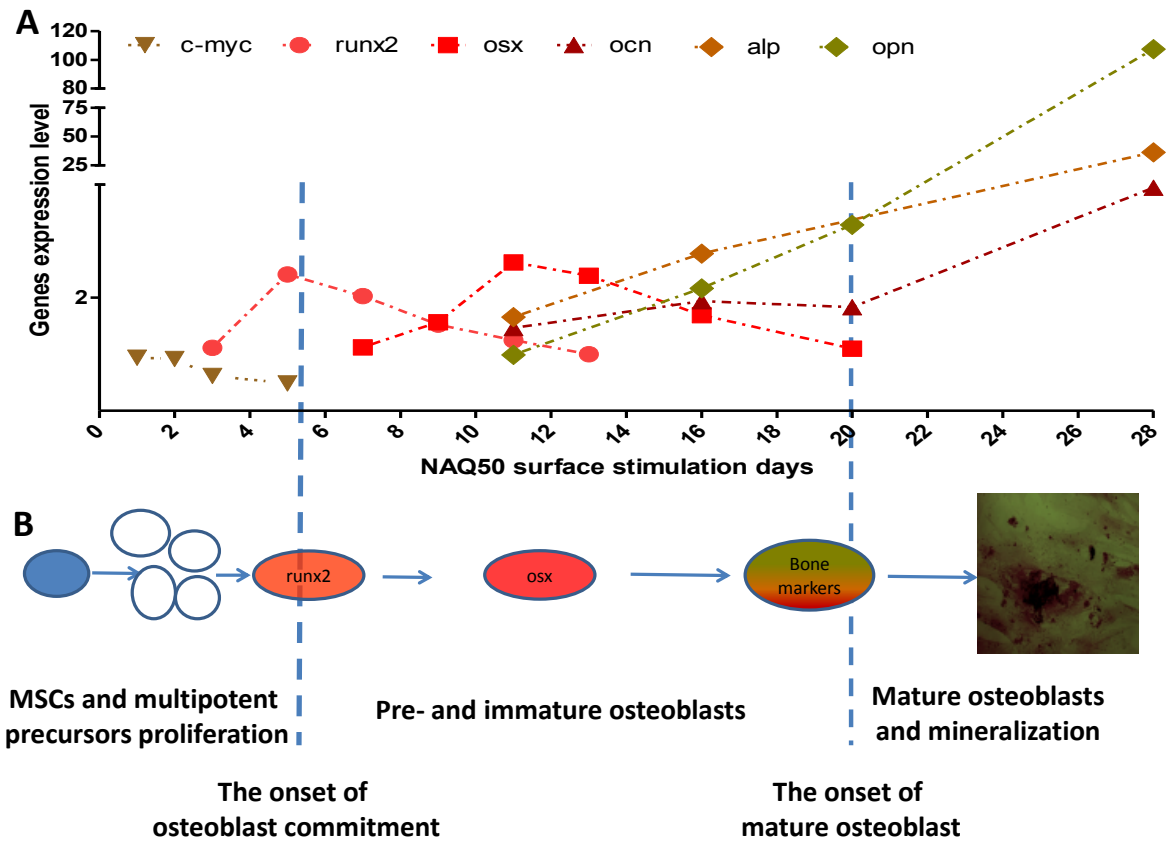


**Figure 3.16** Temporal sequence genes expression pattern functionalized NSQ50 surface induced osteogenic differentiation.

(A): The summation of temporal gene profile expression as reported individually in section 3.4.1 to 3.4.7. (B): According to gene expression pattern, the NSQ50 surface induced MSC osteogenic differentiation process can be viewed as three phases, the MSCs and multipotent precursors proliferation stage, the pre- and immature osteoblasts stage and the mature and mineralization stage. In general, MSCs were under transcriptional control before their progression into the mature osteoblasts phase. The transit point between proliferation and the pre-osteoblasts phase can be viewed as the onset of osteoblast commitment at which point RUNX2 was significantly up-regulated and C-MYC down-regulated. The transit point from pre-osteoblasts to mature osteoblasts occurred around 21 days after cells cultured on the surface, at which time the immature osteoblast marker ALP had been significantly up-re-regulated and the mature osteoblast markers OCN and OPN were starting to increase.

### 3.4.4 The effect of planar control on osteogenic gene expression

The biocompatible and biodegradable characterization of PCL rise the question that whether the up-regulation of osteogenic genes on the NSQ50

nanotopography was owing to the down-regulation of these genes on the planar surface or the alteration of the NSQ50 nanotopography by degradation of PCL, especially the gene fold change format used for the presentation of genes expression in this work.

Study on transcriptome of MSCs on PCL by Sabine Neuss (Neuss et al., 2011) demonstrated PCL is osteoinductive polymer compared to tissue culture polystyrene. PCL moderately induces broader osteogenic genes expression and lead to osteogenic differentiation, indicating osteogenic genes in MSCs cultured on PCL planar surface would not be down-regulated. Furthermore, protein expression of the osteogenic genes on PCL planar surface and nanofeatures in this work and others (Mavis et al., 2009; Porter et al., 2009) also demonstrated that it is unlikely that the increased fold changes comparing genes expression level on nanofeature to those on planar surface were resulted from the down-regulation of these genes by PCL substrate.

PCL is one of the most slowly degradation polymer with a degradation time of the order of two years (Middleton and Tipton, 2000). Study on PCL degradation rate and its effect on 2D and 3D structures by Sung et al (Sung et al., 2004) demonstrated that the significant degradation of PCL was occurred after 28 days cell culture. Cell viabilities on the PCL scaffolds were not significantly decreased after 28 days compared to those on cell culture flask (TCPS). Moreover, PCL scaffolds morphology was relatively little change at 14 days, and appeared less affected at 28 days.

The time period of gene expression investigation in this work was within 28 days, and most of work was in early response of MSCs to the NSQ50 nanotopography. Thus, the impact of PCL degradation to gene expression could be negligible. However, it should be notice here, for accurate demonstration of differential of the genes expression on the NSQ50 and planar surfaces, it would be better to present the gene expression level in MSCs on both NSQ50 and planar surfaces.

### **3.4.5 Conclusions**

The results presented here indicate that NSQ50 surface induced osteogenic differentiation is transcriptionally controlled in which RUNX2 plays a central role to switch on osteoblast commitment and recruit OSX. The temporal gene expression pattern also suggests that OSX is a pivotal element for mature osteoblast formation. Results from the expression of bone tissue marker genes indicate that NSQ50 surface induced osteogenic differentiation requires OPN expression more than OCN as OPN protein contains RGD motif. This would aid super-mature adhesion formation and buildup of intracellular cytoskeletal tension required in osteogenesis (Engler et al., 2006; Kilian et al., 2010; McBeath et al., 2004). Generally, MSCs on the NSQ50 surface demonstrate a similar osteogenic differentiation pattern described by Lian and Stein (Lian and Stein, 1992), but I add more detailed information on transcription factors in this study.

**Chapter 4. Molecular mechanisms underlying osteogenesis of MSCs on NSQ50 surface**

## Summary

In Chapter 3, the temporal sequence of genes expression pattern and their relationship to MSCs osteoblast differentiation on the NSQ50 surface was established. This chapter describes the molecular mechanisms that regulate the cascade of events leading to MSC osteogenic differentiation on the surface. This chapter begins by introducing known osteogenic signalling pathways which have been attributed to the osteogenesis of MSCs. Interactions between osteogenic signalling pathways and the regulatory effects of miRNAs on osteogenesis of MSCs are explored. The results presented include the findings of the roles of BMP2 signalling in NSQ50 induced osteogenic differentiation of MSCs. Further analysis indicates BMP2 signalling exerts the effect on osteogenesis of MSCs on NSQ50 surface via a SMAD dependent pathway. The effects of BMP2 signalling on other regulatory events are explored, including the physical and functional co-localization with integrins, and the regulation on miR-23b which targets RUNX2.

### 4.1 Introduction

MSCs fate determination and subsequent lineage specific differentiation are transcriptionally controlled. Multiple signalling molecules and pathways have been identified to modulate osteogenic transcription factors and their regulatory network in osteogenesis of MSCs. Studies have demonstrated the instrumental role of BMP2 signalling pathway in regulation of MSC osteogenic differentiation, in which the canonical pathway regulates the osteogenic transcription factor RUNX2 via SMAD proteins (Javed et al., 2009; Phimphilai et al., 2006), whereas the BMP non-canonical pathway triggers interaction of TAK1 and p38 MAPK to phosphorylate RUNX2 (Greenblatt et al., 2010) resulting in osteogenic differentiation (pathway details described in section 1.5.1). Studies have also evidenced that Wnt signalling can be involved in the transcriptional regulatory process of osteogenic differentiation and bone formation. The canonical Wnt pathway regulates RUNX2 by the interaction of the  $\beta$ -catenin/LEF/TCF complex with the RUNX2 promoter (Gaur et al., 2005). Wnt signalling is initiated by the

binding of Wnt proteins to the Fz receptor and its co-receptor LRP5 (Hay et al., 2005). Interestingly, LRP5 itself has been identified as crucial player in osteogenic differentiation and bone formation, and disruption of LRP5 activation results in suppression of Wnt signalling (Ai et al., 2005; Boyden et al., 2002).

Studies on signalling pathways involved in MSC osteogenesis and bone formation have demonstrated the interplay of BMP signalling with other osteogenic pathways at different regulatory levels. BMP2 induces Wnt signalling activity in osteoblast differentiation of C2C12 cells via the interaction of the SMAD1/4 and  $\beta$ -catenin/LEF complexes (Nakashima et al., 2005). Fibroblast growth factor (FGF) signalling was reported to increase BMP2 and TGF $\beta$ 1 expression in bone formation through modulation of RUNX2 activation (Choi et al., 2005; Naganawa et al., 2008). BMP signalling and the notch pathway have synergistic effects on bone formation: activation of notch signalling enhances BMP2-induced ALP activation (Nobta et al., 2005; Tezuka et al., 2002), whereas BMP2 and TGF $\beta$  regulated notch signalling induce genes related to signal transduction, including *hey1* and *hes1* in osteoblast differentiation (de Jong et al., 2004). Similar synergy is found between BMP2 and integrins in human osteoblasts. BMP2 stimulates the levels of  $\alpha$ v-containing ( $\alpha$ v $\beta$ ) integrins on osteoblast surface and enhances cell adhesion to the ECM, and blocking of integrins reduces BMP2-induced SMAD signalling and subsequent osteogenic phenotype (Lai and Cheng, 2005).

Non-transcriptional regulation of osteogenesis of MSCs has been recently emerged with findings of microRNA (miRNA) regulatory functions in diverse pathways (Ambros, 2004; Hassan et al., 2010; Huang et al., 2010a). MiRNAs are endogenous, ~22 nucleotide non-coding RNAs. These small RNAs bind to the 3'-untranslated region (3'-UTR) of their target messenger RNAs (mRNAs), including transcription factors, receptors, and kinases to negatively regulate the targets mRNA stability and/or translation (Sun et al., 2010). MiRNAs complementarily bind to their targets at highly conserved seed regions. These regions are miRNA segment sequences exactly matching the complementary sequences within the 3'UTR of the targets, and are usually located at around the nucleotide 2-8

position. With this shorter sequence, one miRNA may target different genes, and one gene may be regulated by different miRNAs.

The regulation of miRNAs on osteogenic differentiation of MSCs has been found to occur for different osteogenic genes in different pathways. MiR-204/211 and -133 target RUNX2 in MSCs resulting in adipocyte differentiation and inhibition of osteoblast differentiation (Huang et al., 2010a; Li et al., 2008). MiR-26 and miR-135 repress SMAD1 and SMAD5 translation, blocking the BMP-SMAD pathway and subsequently inhibiting osteogenic differentiation in adipose tissue derived MSCs (Luzi et al., 2008) and the C2C12 cell line (Li et al., 2008). MiR-141 and -200a were found to be involved in the regulation of preosteoblast differentiation by targeting their common gene DLX5 (Itoh et al., 2009). These findings demonstrate the negative regulatory effects of miRNAs on osteogenic differentiation of MSCs. However, some miRNAs target inhibitors of osteoblastogenesis and thus exert positive effects on osteogenic differentiation of MSCs. A typical example is miR-29b that targets multiple inhibitors of osteoblast differentiation, including histone deacetylase 4 (HACD4), activin A receptor II A (ACVR2A) and beta-catenin-interacting protein 1 (CTNNBIP1), and thereby enhances osteoblast differentiation (Li et al., 2009).

MSCs growth on the NSQ50 surface results in an osteogenic phenotype. Studies to understand the process by which cells interpret the nanotopographical cues have been focused on focal adhesion interactions and the resulting changes in intracellular tension. It has been proposed that nanotopography can modulate integrin clustering and focal adhesion formation and that this, in turn, regulates MSC differentiation (Arnold et al., 2004; McMurray et al., 2011; Schwartzman et al., 2011; Tsimbouri et al., 2012). Such alterations may result in the modulation of interfacial forces to guide cytoskeletal organization and the organization of transmembrane receptors, and thus may subsequently regulate the intrinsic signalling of the cells (Ingber, 2006). This may occur through, for example, FAK and G-proteins feeding into signalling cascades such as the ERK 1/2 pathway (Kilian et al., 2010). However, other key pathways and regulatory events which involved in osteogenesis of MSCs have been less well studied in relation to nanotopography-driven osteogenesis. Thus, this chapter aims to:

1. Identify major signalling molecules and pathways which regulate osteogenesis of MSCs on NSQ50 surface.
2. Dissect the relations of these molecules and pathways.

## 4.2 Methodology

Adhesive cells perceive extrinsic signals (biochemical and/or biophysical) in the ECM via their transmembrane receptors (Stevens and George, 2005). To examine the molecular mechanisms of MSC response to the NSQ50 surface, transmembrane receptors of MSCs, as the transducer of nanotopographical cues to transmit the extrinsic signals into intracellular and subsequently guide MSCs to response, should be first explored.

Signalling pathways will be examined in three ways:

1. Signalling molecules or ligands expression: for example BMP2 for BMP signalling, vinculin for integrin signalling.
2. Pathway mediator expression: for example SMADs, tab1 for BMP pathway,  $\beta$ -catenin for Wnt pathway.
3. Manipulating signalling pathways to see the response of RUNX2, which has been identified as the earliest osteogenic transcription factor in osteogenesis of MSCs in this project (chapter3) and others (Lian et al., 2006).

The genes and/or proteins that were assessed in this chapter for the analysis of osteogenic signalling pathways related to the NSQ50 surface are listed in table 4.1. Methods for the assessments are briefly introduced in each experiment, and further details are described in chapter 2.

**Table 4.1 Genes and/or proteins investigated for the analysis of osteogenic signalling pathway in MSCs on NSQ50 surface.**

Gene/Molecule Name	Functions	Reference
BMPR1A	BMP signalling receptor	(Kua et al., 2012)
BMP2	BMP signalling ligand	(Javed et al., 2009)
SMAD1 and 5	BMP-SMAD pathway signalling mediators	(Javed et al., 2009)
Tab1	BMP non-SMAD pathway mediator	(Greenblatt et al., 2010)
LRP5	Wnt signalling co-receptor	(Gong et al., 2001)
B-catenin	Wnt signalling mediator	(Moon et al., 2004)
Integrin $\alpha$ 3, $\alpha$ 4, $\alpha$ v, $\beta$ 1, $\beta$ 3, $\beta$ 5	Membrane receptors for cell adhesion.	(Kanchanawong et al., 2010)
vinculin	Focal adhesion molecule	(Ziegler et al., 2006)
RUNX2	Osteogenic transcription factor	(Ducy et al., 1997)
OPN	Osteoblast marker	(Manolagas, 2000)
miR-23a, -23b, -93, -203	MiRNAs targeting RUNX2	<a href="http://www.targetscan.org">www.targetscan.org</a>
miR-96, -143	MiRNAs targeting OSX	<a href="http://www.targetscan.org">www.targetscan.org</a>

## 4.3 Results

### 4.3.1 Transmembrane receptor response to the NSQ50 surface

#### 4.3.1.1 Effect of the NSQ50 surface on integrins

Integrins are the main transmembrane receptors which primarily link adherent cells to the ECM and modulate multiple intracellular signalling pathways to regulate cell adhesion, spreading, migration and other cellular functions in many cell types (Arnaout et al., 2005). Integrin binding with ECM components depends on the pairing of  $\alpha$  and  $\beta$  subunits and it is widely accepted that the pairing of  $\alpha_v$  with  $\beta_1/\beta_3/\beta_5$  binds to the RGD motif in osteopontin and with  $\beta_3/\beta_5$  binds to VN (Kilian et al., 2010),  $\alpha_3$  with  $\beta_1$  binds to laminin (Hynes, 2002), and  $\alpha_4$  with  $\beta_1$  binds to VCAM and fibronectin in the ECM (Goessler et al., 2008). To test whether integrins are directly involved in the initiation of MSC osteogenic differentiation on the NSQ50 surface, the expression of integrins  $\beta_1$ ,  $\beta_3$ ,  $\beta_5$ ,  $\alpha_3$ ,  $\alpha_4$ ,  $\alpha_v$  on NSQ50 and planar surfaces at early stages of culture were investigated using qRT-PCR. Cells cultured on the NSQ50 and planar surface for 3, 5 and 7 days were assessed (Figure 4.1). The relative amounts integrins transcripts on NSQ50 and planar surfaces were normalized to endogenous control gene GAPDH, and then comparisons were made and analysed using ANOVA to obtain the fold change of integrin transcripts on NSQ50 relative to those on planar surface.

The integrin subunits  $\beta_1$ ,  $\beta_3$  and  $\alpha_3$  were not induced by the NSQ50 surface when MSCs cultured on the surface for 3, 5, and 7 days compared to planar controls, indicating these integrins were not differentially expressed in MSCs osteoblast commitment on the surface. However, the up-regulation of integrins  $\beta_5$ ,  $\alpha_4$ ,  $\alpha_v$  was noted at day 5. The up-regulation of both  $\alpha_v$  and  $\beta_5$  in MSCs on NSQ50 surface suggested a key role for VN in adhesion to the surface. Although the enrichment of  $\alpha_4$ ,  $\alpha_v$  was observed, the  $\beta_1$  and  $\beta_3$  were not stimulated significantly by the surface up to 7 days, indicating MSCs on NSQ50 initially used VN for adhesion rather than fibronectin. The expression of  $\alpha_v\beta_5$  pair also could

possibly implicate a rationale for the strong expression of osteopontin at the late stage of MSCs osteogenic differentiation observed in section 3.3.5

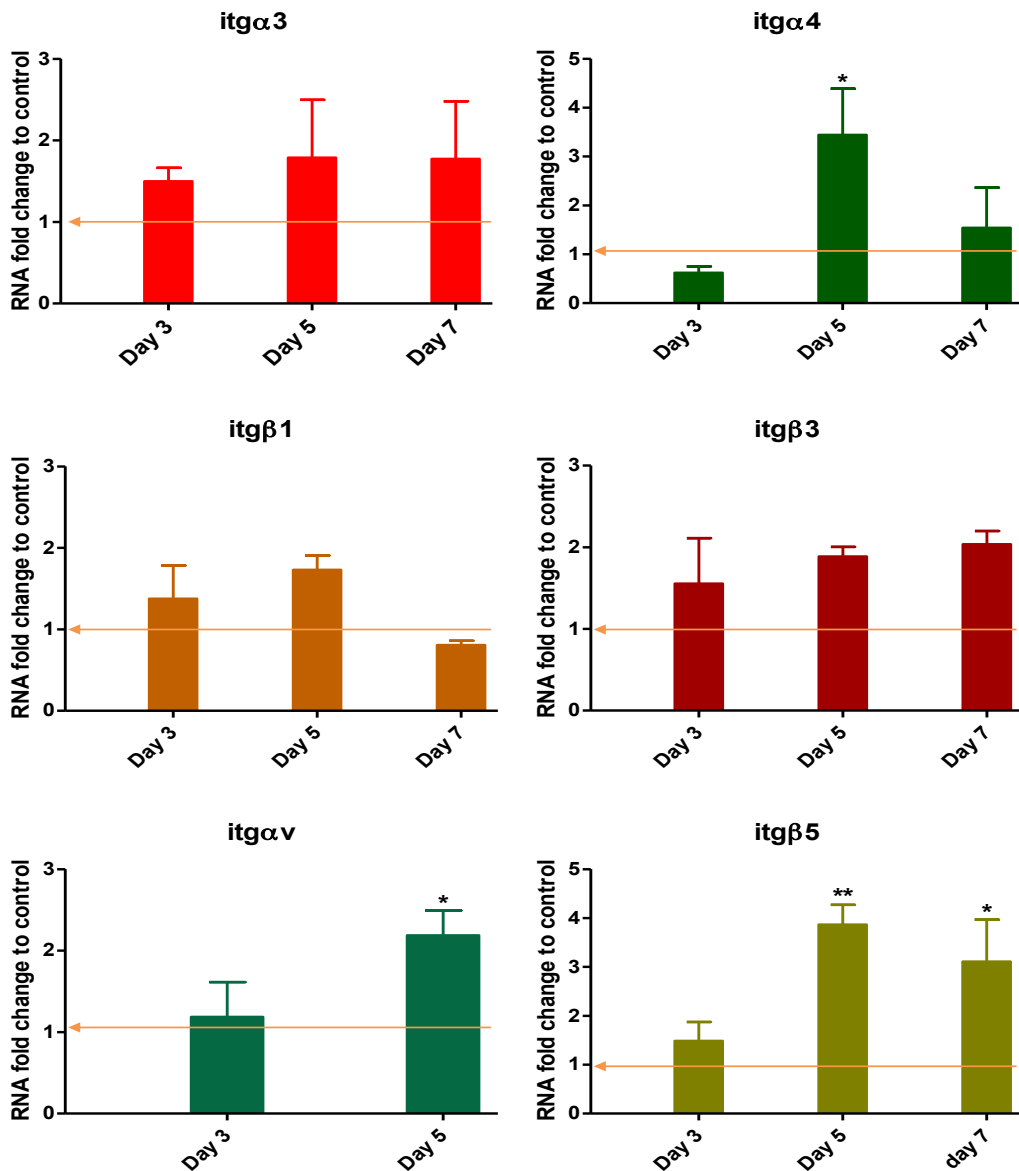


**Figure 4.1** The effect of NSQ50 surface on the expression of integrins in MSCs.

mRNA fold change of integrins (itgs) B1, B3, B5,  $\alpha$ 3,  $\alpha$ 4,  $\alpha$ v in MSCs on NSQ50 surface compared to those on planar surface was assessed by qRT-PCR for cells cultured at 3, 5 and 7 days. ItgB5,  $\alpha$ 4, and  $\alpha$ v on NSQ50 were significantly up-regulated, and about 4, 4, 2.5 fold changes were observed respectively at day 5. The expression of itg $\beta$ 1, B3 and  $\alpha$ 3 was not affected by the surface. (N=3,  $\pm$  SD) ANOVA analysis, \* p < 0.05, \*\* p < 0.01. Arrows on graphs show the control level.

#### **4.3.1.2 Effect of NSQ50 surface on Wnt signalling**

Recent findings have clearly established the causal link between LRP5, a co-receptor for Wnt proteins, and bone mass in human and mice (Boyden et al., 2002; Gong et al., 2001). LRP5 regulates bone mass by determining MSC osteoblast commitment and / or osteoblast differentiation through the canonical Wnt pathway (described in section 1.5.2). To test whether Wnt signalling is implicated in the early events that initiate MSCs osteogenic differentiation on the NSQ50 surface, the expression of LRP5 and beta-catenin were examined at 3, 5 and 7 days using qRT-PCR. The relative amounts LRP5 and beta-catenin transcripts on NSQ50 and planar surfaces were normalized to endogenous control gene GAPDH, and then comparisons were made and analysed using ANOVA to obtain the fold changes of LRP5 and beta-catenin transcripts on NSQ50 relative to those of planar surface (Figure 4.2A). The expression of LRP5 on the NSQ50 surface did not show a significant difference from those on planar surface, indicating Wnt signalling receptor did not change in response to the NSQ50 surface at the early stage of osteoblastogenesis. Moreover, the canonical Wnt pathway mediator, beta-catenin, did not change in response to NSQ50 at day 3 and day 5 (Figure 4.2B). This helps to confirm that Wnt signalling did not influence the early events that initiate MSC osteogenic commitment and differentiation on the NSQ50 surface.

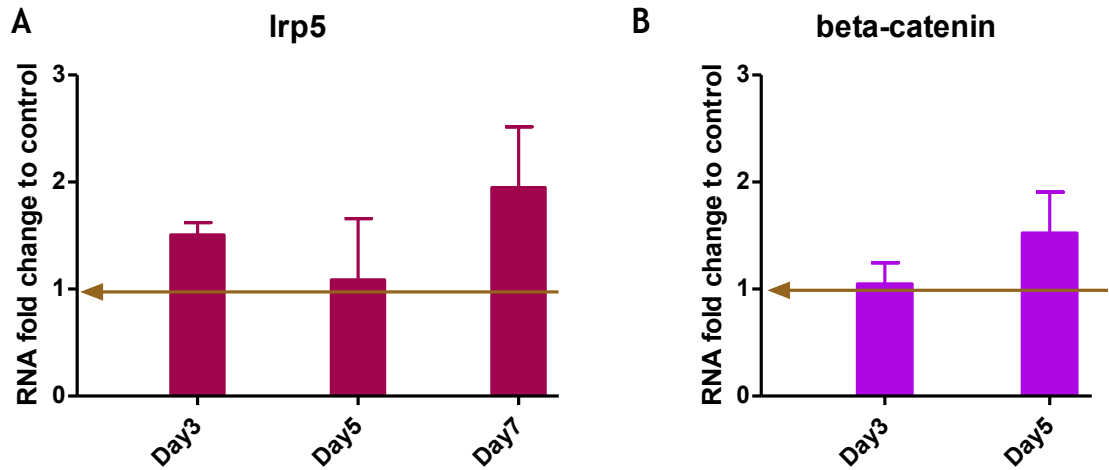


**Figure 4.2** The effect of the NSQ50 surface on Wnt signalling at early stage MSCs osteogenic differentiation.

Wnt protein co-receptor LRP5 and Wnt pathway mediator beta-catenin were not affected by NSQ50 surface. (A): qRT-PCR targeted at mRNA of LRP5 at 3, 5, and 7 days showed insignificant fold change compared to those planar surfaces. (B): qRT-PCR targeted at mRNA of beta-catenin at 3 and 5 days showed insignificant fold change compared to those planar surfaces. (N=3,  $\pm$  SD) ANOVA analysis, \*  $p < 0.05$ , \*\*  $p < 0.01$ , \*\*\*  $p < 0.001$ . Arrows on graphs show the control level.

#### 4.3.1.3 Effect of the NSQ50 surface on BMPs receptor expression

The essential role of BMP2 signalling for osteoblastic differentiation of MSCs and subsequent bone formation has been established. BMP2 triggers intracellular pathways through binding to its type I and type II transmembrane serine/threonine kinases receptors to form a ligand-receptor complex (Nohe et al., 2004). BMPR1A receptor possesses high binding affinity to BMPs, including BMP2, and recent studies indicate the BMPR1A receptor plays important roles for osteogenic differentiation of MSCs (Kaps et al., 2004; Kua et al., 2012).

In this thesis, the effect of the NSQ50 surface on BMPR1A expression was assessed at different time points, starting from the first 24 hours to day 11 using qRT-PCR. The relative amounts BMPR1A transcripts on NSQ50 and planar surfaces were normalized to endogenous control gene GAPDH, and then comparison was made and analysed using ANOVA to obtain the fold change of BMPR1A transcripts on NSQ50 relative to those of planar surface (Figure 4.3).

BMPR1A expression in MSCs on the NSQ50 surface showed no significant difference from those on planar at first 2 days. Significant up-regulation was, however, observed at day 3 and day 5. Then, the expression levels of BMPR1A at day 7 and day 9 dropped back towards control levels. At day 11, BMPR1A expression on the NSQ50 surface was back to the same level as that on planar surface. It appears that BMPR1A expression on the NSQ50 surface shared the same pattern as RUNX2 (Figure 3.7), but the time course was shifted to be slightly earlier, i.e. just ahead of RUNX2 expression. This data indicates that the transmembrane serine/threonine kinases receptor was stimulated by NSQ50 surface at an early stage of MSC osteogenic differentiation.

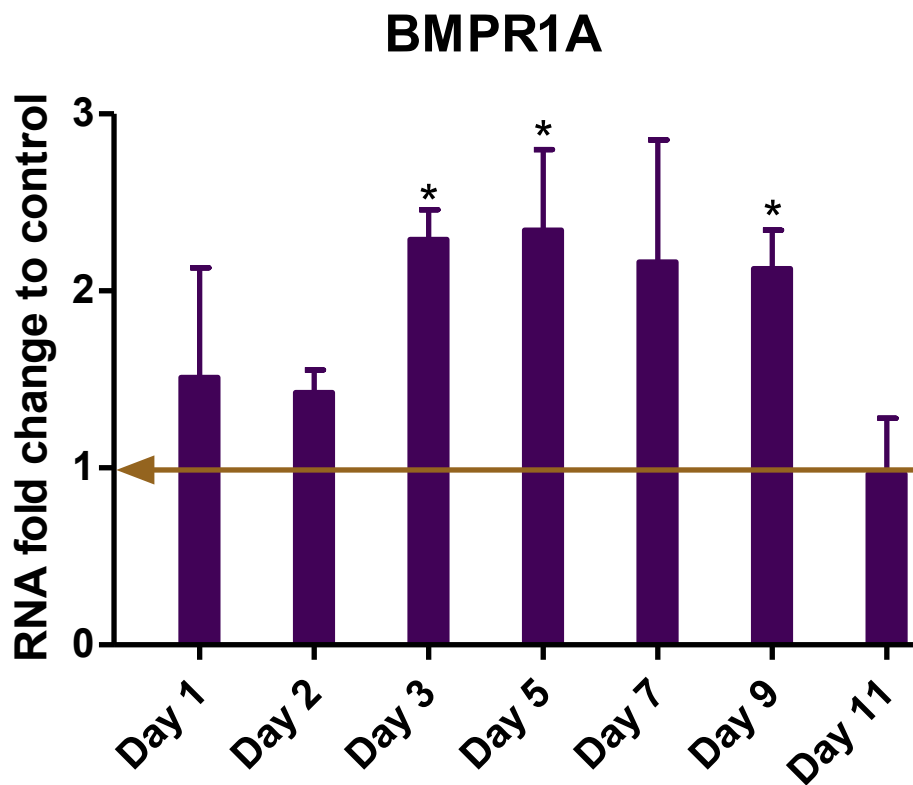


**Figure 4.3** The effect of the NSQ50 surface on BMP receptor, BMPR1A at the early stages of MSCs osteogenic differentiation.

Bone morphogenic proteins receptor, BMPR1A was measured by qRT-PCR to MSCs cultured on NSQ50 and planar surfaces for time course up to 11 days. MSCs response to NSQ50 surface with about 2.5 folds change of BMPR1A mRNA compared to on planar surface at day3 and day5. (N=3,  $\pm$  SD) ANOVA analysis,\*  $p < 0.05$ . Arrow on graph shows the control level.

## **4.3.2 Induction of the BMP2 – SMAD pathway on the NSQ50 surface**

### **4.3.2.1 Activation of BMP2 (ligand of BMPR1A) signalling**

The temporal gene expression analysis in section 4.4.1 has demonstrated that BMPR1A, one of the osteoblast related transmembrane receptors, responds very quickly to the NSQ50 surface, suggesting that BMP2 signalling is involved in the early events of MSCs osteoblast commitment and differentiation. To confirm the activation of the signal, the expression of BMP2, one of the BMPR1A ligands, was assessed from the first 24 hours of culture to day 11 by qRT-PCR. The relative amounts BMP2 transcripts on the NSQ50 and planar surfaces were normalized to endogenous control gene GAPDH, and then comparison was made and analysed using ANOVA to obtain the fold change of BMP2 transcripts for cells on NSQ50 relative to those on the planar surface (Figure 4.4). The significant up-regulation of BMP2 on NSQ50 surface was noted from day 3 to day 7. The temporal expression pattern of BMP2 was similar to that of its receptor, BMPR1A, following the same time course.

BMP2 protein expression was also examined by Western blot and immunostaining. Total proteins were extracted from MSCs cultured on NSQ50 and planar surfaces at 7 days respectively, and isolated on a SDS-PAGE gel. By using an anti-BMP2 antibody, it was found that expression of BMP2 by MSCs on the NSQ50 surface was substantially increased when compared to that on the planar surface (top row in figure 4.5A, BMP2 approximately 45 KDa). Equal amounts of total protein (10 µg) were loaded on the gel and demonstrated by anti-GAPDH immuno-reactivity (bottom row in figure 4.5A, GAPDH approximately 36 KDa).

BMP2 expression in MSCs was also observed by immunostaining. MSCs cultured on NSQ50 and planar surfaces for 5 days were washed by 1xPBS and fixed on the surfaces. By using a monoclonal anti-BMP2 antibody, it was found that BMP2 on NSQ50 surface (green in figure 4.5B) was substantially enriched when compared to that on planar surface (green in figure 4.5C). BMP2 staining was apparent in

the cytoplasm and out towards the membrane, indicating endogenous BMP2 was up-regulated by the NSQ50 surface.

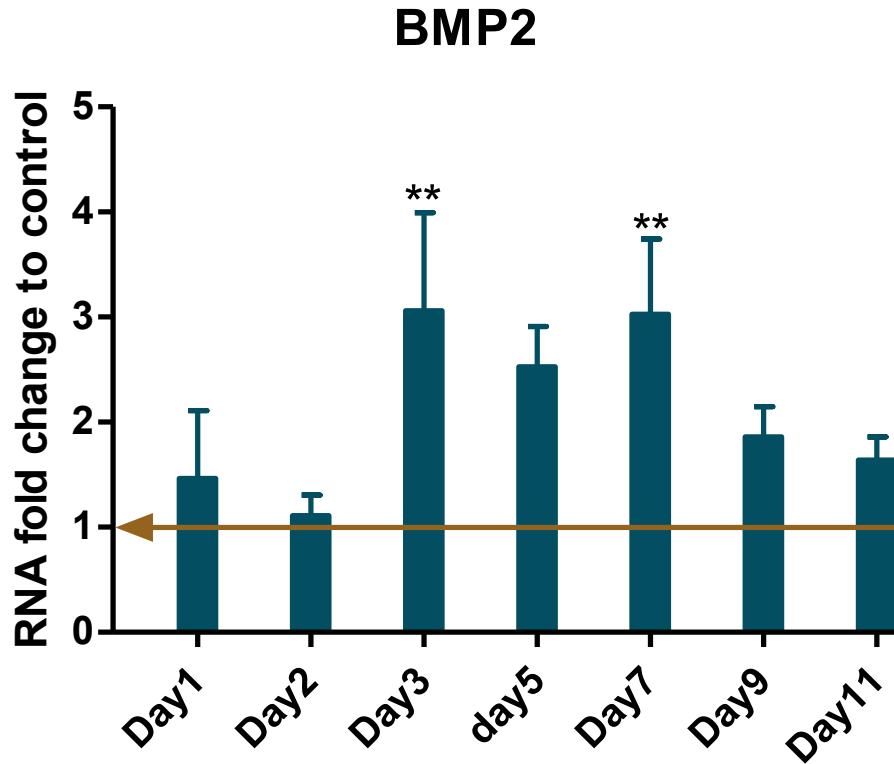


**Figure 4.4** The effect of NSQ50 surface on BMP2 expression at the early stage of MSC osteogenic differentiation.

BMP2 was measured by qRT-PCR to MSCs cultured on NSQ50 and planar surfaces for time course up to 11 days. MSCs responded to the NSQ50 surface with about a 3 fold change in BMP2 mRNA compared to on planar surface through day 3 to day 7. (N=3,  $\pm$  SD) ANOVA analysis, \*  $p < 0.05$ , \*\*  $p < 0.01$ . Arrow on graph shows the control level.

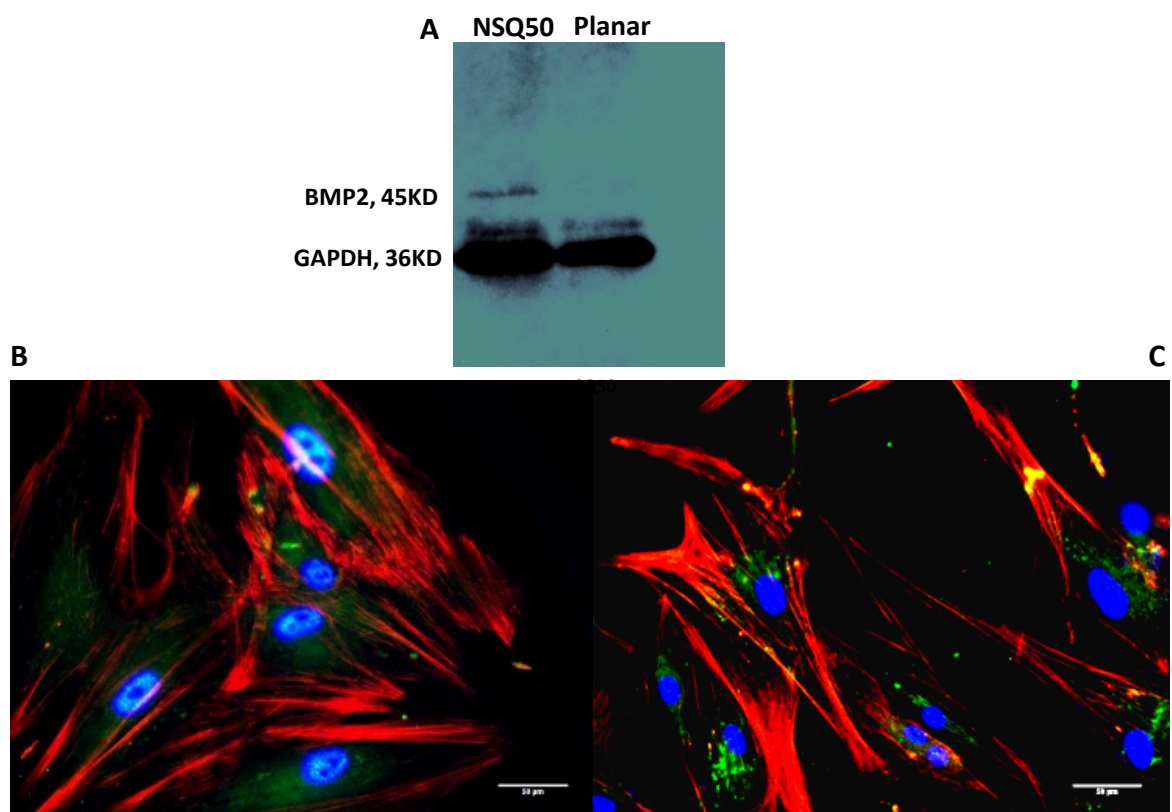


**Figure 4.5** BMP2 protein expression in MSCs cultured on the NSQ50 and planar surfaces.

Total protein was extracted from MSCs cultured on NSQ50 and planar surfaces at day 7, and Western blot performed using an anti-BMP2 antibody (Millipore, catalog number: ABN303). BMP2 was detected on the NSQ50 surface at the size of 45 KDa. GAPDH, as control for equal amounts of loaded protein, was detected on both NSQ50 and planar surfaces at the size of 36 KDa (A). MSCs cultured on NSQ50 (B) and planar surfaces (C) were stained for F-actin (red) using phalloidin, for cell nucleus (blue) using DAPI and for BMP2 (green) using monoclonal anti-BMP2 antibody (R&D system, Catalog number: MAB3551). BMP2 was expressed in cytoplasm and spread towards the membrane on the NSQ50 surface.

#### 4.3.2.2 Induction of SMADs - the mediators of canonical BMP2 signalling

BMP2 binds with its receptors to form ligand-receptor complexes, hence evoking the BMP2 signal. The signal may transduce through the canonical pathway in which SMAD proteins are required to be phosphorylated and subsequently translocate into the nucleus to regulate gene expression (described in detail in section 1.5.1). To test whether NSQ50 induces the BMP2 canonical pathway, receptor-regulated SMAD transcripts SMAD1 and SMAD5 were measured by qRT-

PCR when MSCs were cultured on NSQ50 and planar surfaces for 3 and 5 days. The relative amounts SMAD1 and SMAD5 transcripts on NSQ50 and planar surfaces were normalized to endogenous control gene GAPDH, and then comparison were made and analysed using ANOVA to obtain the fold changes of SMAD1 and SMAD5 transcripts on NSQ50 relative to those on planar surface (Figure 4.6).

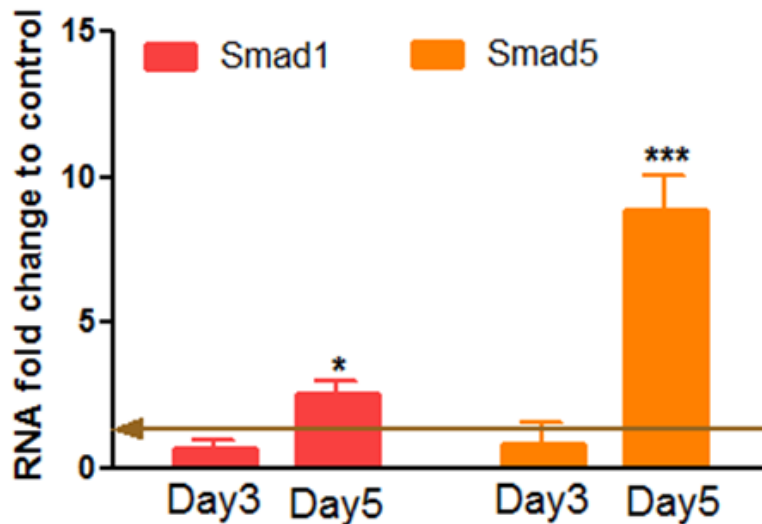


**Figure 4.6** The induction of the BMP2 canonical pathway mediator SMAD on the NSQ50 surface.

The expression of the BMP2 receptor-regulated SMAD1 and SMAD5 transcripts were examined by qRT-PCR. SMAD1 and SMAD5 were significantly up-regulated by the NSQ50 surface at day 5 when compared to those on planar surface with their mRNA fold changes of about 2.5 and 9 respectively. Expression of SMAD5 on the NSQ50 surface was about 4 times enriched compared to SMAD1 at day5, indicating SMAD5 maybe the predominant mediator of the BMP2 canonical pathway in this case. (N=3,  $\pm$  SD) ANOVA analysis, \*  $p < 0.05$ , \*\*  $p < 0.01$ , \*\*\*  $p < 0.001$ . Arrow on graph shows the control level.

SMAD1 and SMAD5 did not exhibit up-regulation on the NSQ50 surface at day 3. However, the significant up-regulation of both SMADs occurred at day 5. The same temporal genes expression of BMP2, BMPR1A and SMADs indicated the induction of BMP2 canonical pathway on NSQ50 surface. Furthermore, SMAD5 demonstrated about 4 times higher expression than SMAD1 at day5, suggesting smad5 is perhaps the predominant mediator of BMP2 canonical pathway for

nanotopography. However, it should notice that up-regulation of the SMAD genes expression is inadequate for affirmation of the BMP2 canonical pathway activation; phosphorylation SMAD proteins should be assessed for the samples.

#### **4.3.2.3 Lack of change in the SMAD independent pathway of BMP2 signalling in MSCs on the NSQ50 surface**

The SMAD independent pathway, also known as non-canonical pathway of BMP2 signalling, can trigger multiple downstream cascades, including p38 MAPK, ERK, and NFκB which are supposed to regulate MSCs differentiation and bone formation. The BMP2 SMAD independent pathway is achieved by the activation of tak1 and tab1 (described in details in section 1.5.1). Tab1 is the binding protein of tak1, thus BMP2 signalling will not transduce through the SMAD independent pathway without the induction of tab1. Expression of the tab1 on NSQ50 and planar surfaces was investigated by qRT-PCR after 5 days cell culture. The relative amounts of tab1 transcripts on NSQ50 and planar surfaces were normalized to the endogenous control gene GAPDH, and then comparison was made and analysed using ANOVA to obtain the fold change of tab1 on NSQ50 relative to that on planar surface (Figure 4.7). The data showed that no effect of NSQ50 surface on tab1 expression in MSCs, indicating that NSQ50 surface induced BMP2 signalling was not transduced through the SMAD independent pathway.

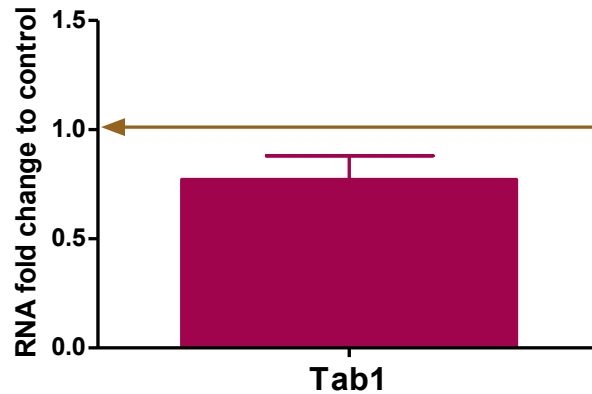


**Figure 4.7** Lack of activation of TGF-beta activated kinase 1 binding protein tab1 in the SMAD independent pathway of BMP2 signalling.

Tab1 was not affected by NSQ50 surface. qRT-PCR targeted at the mRNA of tab1 at 5days showed insignificant fold change compared to that planar surface. (N=3,  $\pm$  SD) ANOVA analysis, \*  $p < 0.05$ , \*\*  $p < 0.01$ , \*\*\*  $p < 0.001$ . Arrow on graph shows the control level.

### 4.3.3 The effect of BMP2 signalling in MSCs on NSQ50 surface on osteogenic differentiation

#### 4.3.3.1 The effect of BMP2 signalling on early bone marker RUNX2 expression

Since BMP2-SMAD signalling is induced by the NSQ50 surface, and previous studies have demonstrated that this signal directly functionalise MSCs osteogenic differentiation and bone formation both *in vivo* and *in vitro*, this was investigated here. The relation of the BMP2 signal to the induction of MSC osteogenic differentiation on NSQ50 surface was investigated using noggin, the antagonist of BMP2. MSCs were seeded on NSQ50 and planar surfaces in culture medium and after allowing cells to settle down on the surfaces; 10  $\mu$ l noggin solution with concentration of 5 ng/ $\mu$ l was added on to make up 50 ng/ml of final noggin concentration in culture medium. Cells were treated with and without noggin on NSQ50 and planar surfaces for 5 days. RUNX2 expression was examined by qRT-PCR. The RUNX2 fold change on NSQ50 surface compared to that on planar surface without noggin treatment was about 2.2 (Figure 4.8A noggin(-)), after normalization to endogenous control of GAPDH respectively, whereas RUNX2 fold change on NSQ50 surface compared to that on planar

surface with noggin treatment was less than 1.0 (Figure 4.8A noggin(+)), after normalization to endogenous control of GAPDH respectively. Statistical analysis with ANOVA showed that noggin significantly down-regulated RUNX2 expression in MSCs on the NSQ50 surface.

The down-regulation of the RUNX2 protein in MSCs on the NSQ50 surface by noggin was also observed by Western blot analysis when MSCs were cultured on the NSQ50 surface for 7 days with and without noggin treatment (Figure 4.8B). These data demonstrated that the NSQ50 surface induced RUNX2 expression was through the activation of BMP2 signalling.

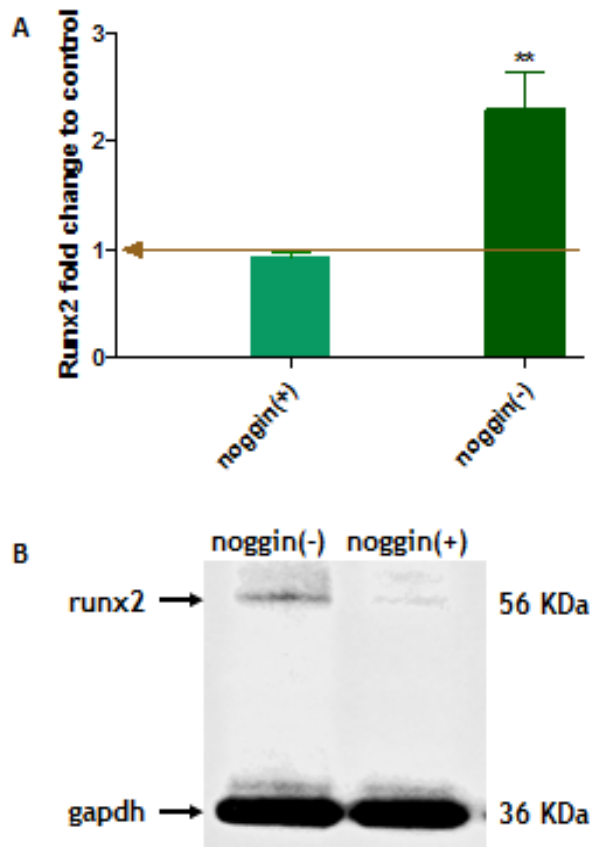


**Figure 4.8** RUNX2 responses to the BMP2 antagonist noggin.

Noggin down-regulates RUNX2 expression on the NSQ50 surface. MSCs cultured on the NSQ50 and planar surfaces were treated with and without noggin for 5 days (noggin treatment at 50ng/ml final concentration in cell culture medium). (A): qRT-PCR results show the fold change of RUNX2 when compared of MSCs on NSQ50 to planar surfaces in the present of noggin (noggin(+)) and in the absent of noggin (noggin(-)). (N=3,  $\pm$  SD) ANOVA analysis, \*\*  $p < 0.01$ . Arrow on graph shows the control level. (B): Western blot shows RUNX2 protein expression on NSQ50 surface with noggin treatment (noggin(+)) and without noggin treatment (noggin(-)).

#### 4.3.3.2 The effect of BMP2 signalling on the mature osteoblast marker gene OPN expression

BMP2 signalling induced osteogenic differentiation on the NSQ50 surface was further confirmed by examining expression of the mature osteoblast marker OPN. MSCs on NSQ50 and planar surfaces were cultured in the presence of noggin for the first 7 days, and then the medium was replaced with normal medium without noggin for the rest of the culture period, up to 28 days. OPN expression was examined by qRT-PCR. OPN was significantly up-regulated with a fold change

about 125 on the NSQ50 surface compared to that on the planar surface without noggin treatment (Figure 4.9A noggin(-)), after normalization to endogenous control of GAPDH respectively. However, OPN expression was unchanged on the NSQ50 surface compared to that on planar surfaces with noggin treatment (Figure 4.9A noggin(+)), after normalization to endogenous control of GAPDH respectively. Statistical analysis with ANOVA showed that noggin significantly down-regulated OPN expression on NSQ50 surface. The down-regulation of the OPN protein on the NSQ50 surface by noggin was also observed by immunostaining when MSCs were cultured on the NSQ50 surface for 28 days with noggin treatment (Figure 4.9B). These data again demonstrated that osteogenesis on NSQ50 surface was regulated by BMP2 signalling.

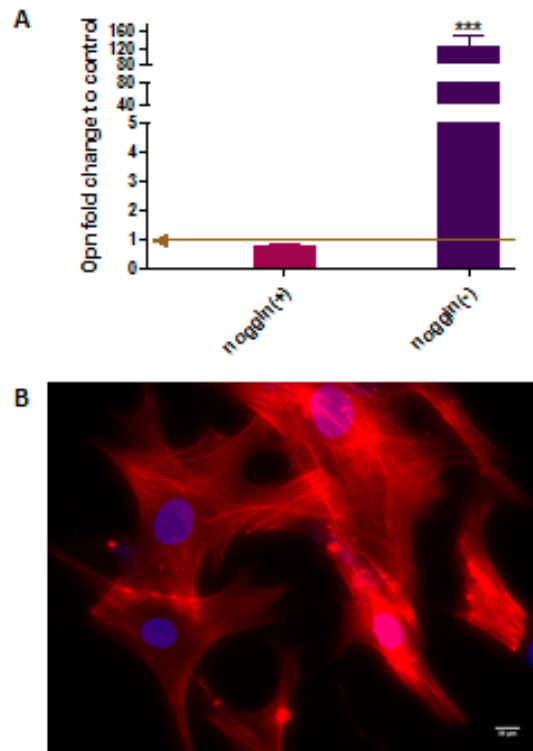


**Figure 4.9** OPN responses to the BMP2 antagonist noggin.

Noggin down-regulated osteopontin expression on the NSQ50 surface. MSCs cultured on NSQ50 and planar surfaces were treated with and without noggin for the first 7 days of culture (noggin treatment at 50ng/ml final concentration in cell culture medium), and then the medium was replaced with normal medium without noggin for the rest of the culture period, up to 28 days (A): qRT-PCR results show the fold change of OPN when compared of MSCs on NSQ50 to planar surfaces in the presence of noggin (noggin(+)) and in the absent of noggin (noggin(-)). (N=3,  $\pm$  SD) ANOVA analysis, \*\*\*  $p < 0.001$ . Arrow on graph shows the control level. Immunostaining using anti-OPN shows lack of OPN protein expression on NSQ50 surface with noggin treatment (B)(red: actin, blue: DAPI).

#### **4.3.3.3 The effect of low serum on RUNX2 expression in MSCs on the NSQ50 surface**

The above data demonstrated osteogenic genes were induced by BMP2 signalling on the NSQ50 surface. BMP2 belongs to the largest subfamily of the transforming growth factor  $\beta$  (TGF $\beta$ ) superfamily. It is noted that the typical components of fetal bovine serum (FBS), making up 10% of cell culture medium in this work, contains hormones, adhesion molecules and growth factors, including TGF $\beta$ . These proteins in FBS, specifically TGF $\beta$  having the similar regulatory effect to BMP2 might influence MSCs fate determination and subsequent differentiation on the NSQ50 surface.

To test whether serum components influence the osteogenic effect of the NSQ50 surface on MSCs, RUNX2 expression was examined using both low serum cell culture medium (containing 1% FBS) and normal culture medium (containing 10% FBS). It should note that complete serum free medium resulted in MSCs apoptosis in 24 hours. MSCs seeded on NSQ50 surfaces were cultured in low serum and normal medium for three days, then the medium were replaced by fresh normal medium for cell culture up to five days. RUNX2 expression in both serum free and normal medium was examined by immunostaining using a monoclonal anti-RUNX2 antibody (Figure 4.10). The NSQ50 surface induced RUNX2 expression was apparently slightly affected by the low serum culture medium. It appeared that there was a reduced intensity and expression pattern (predominantly localised in nucleus) of RUNX2 in low serum conditions compared to normal medium. This indicates that the protein components of FBS in the cell culture medium used in this work play a part in NSQ50 surface induced osteogenesis, but that the cells are stimulated by endogenously induced BMP2 on the NSQ pattern.

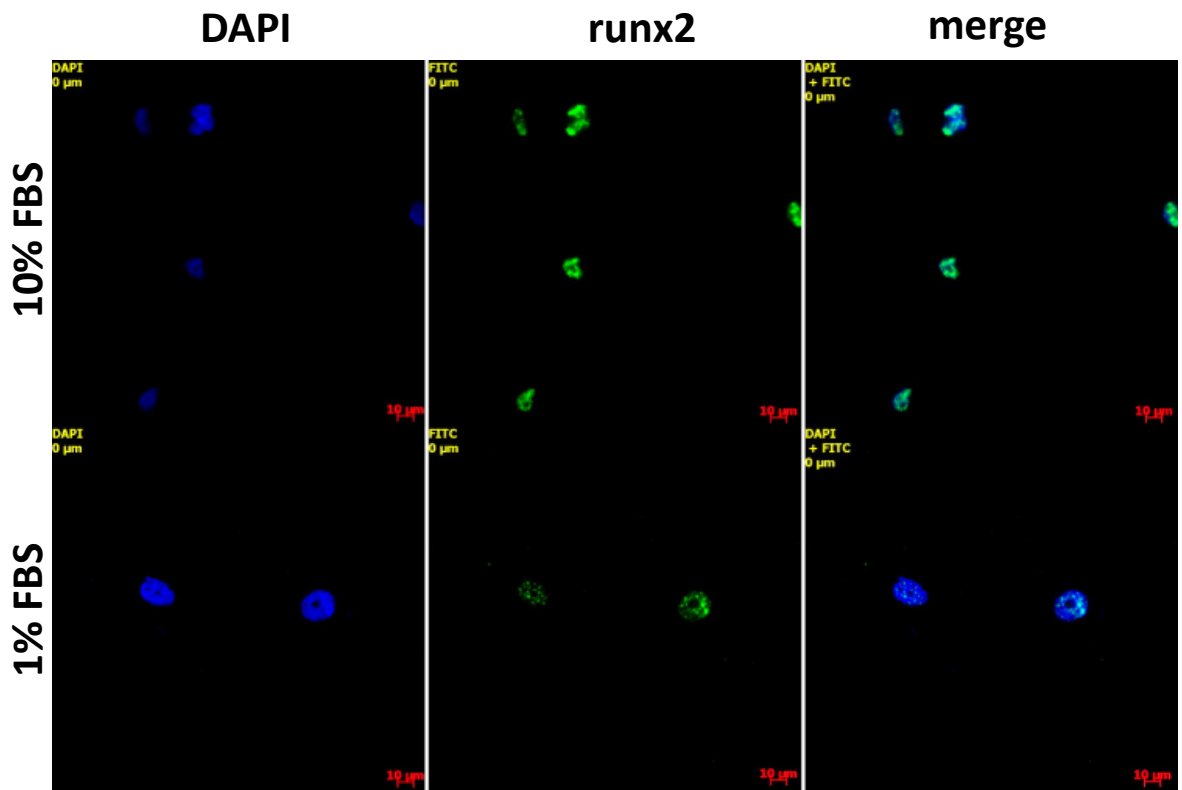


**Figure 4.10** RUNX2 expressions in low serum and normal medium.

The expression of RUNX2 was slightly reduced in terms of both staining intensity and expression pattern in the culture medium containing 1% of FBS (low serum) and 10% of FBS (normal). MSCs seeded on NSQ50 surfaces were cultured in low serum and normal medium for three days respectively, and then media was replaced by fresh normal media for cell culture up to 5 days. Immunostaining for RUNX2 using monoclonal anti-RUNX2 (Millipore, Cat. No 05-1478) and DAPI for cell nuclei were carried out and results were viewed by Zeiss microscope (green: RUNX2, blue: DAPI).

#### **4.3.4 The expression of miRNAs in MSCs on the NSQ50 surface**

##### **4.3.4.1 Prediction analysis of miRNAs targeting RUNX2 and OSX genes**

MicroRNAs (miRNAs) have recently been recognised as key regulators of diverse biological processes by imperfect binding to their target mRNA 3' UTRs to negatively regulating translations of the target genes. The impact of miRNAs on osteoblastic differentiation of various cell types have been investigated recently (Hu et al., 2010), and miRNAs targeting RUNX2 in MSCs have shown inhibition of osteogenic differentiation and stimulation of adipocyte phenotype (Huang et al., 2010a). To gain further insight into the molecular mechanisms underlying BMP2-induced osteogenic differentiation on the NSQ50 surface, miRNAs targeting osteogenic transcription factors RUNX2 and OSX were focused on here. A search for miRNAs that predictably target RUNX2 and OSX was performed using the bioinformatics program TargetScan, and the extent of sequence conservation was examined using University of California Santa Cruze genome browser. MiRNAs targeting RUNX2 and OSX were selected with sequence positions 2 to 8 (seed sequences) exactly complementary to the targets 3' UTR and highly conserved among vertebrates and/or mammals (Figure 4.11). The search results predicted miR-23a, -23b, -93 and -203 as potentially targeting RUNX2, and miR-96, -143 as targeting OSX.

##### **4.3.4.2 The expression of miRNAs on NSQ50 surface**

Expression of the miRNAs selected using targetScan on the NSQ50 surface were examined using qRT-PCR. Since RUNX2 and OSX were up-regulated on the NSQ50 surface at day 5 and day 11 respectively, miRNAs targeting RUNX2 were assessed at day 5 and day 7, and miRNAs targeting OSX were measured at day 9 and day 11. The relative amounts of miRNAs in MSCs on NSQ50 and planar surfaces were normalized to the endogenous control gene, small nuclear RNA U6, and the fold change of the miRNA on NSQ50 was obtained by comparison to its planar control. Data was analysed using ANOVA in GraphicalPrism software.

MiR-23b (targeting RUNX2) was significantly down-regulated at day 5 and 7 with 0.34 and 0.53 fold changes respectively (Figure 4.12b), whereas other miRNAs predicted to target RUNX2 remained unchanged compared to their planar controls (Figure 4.12a, c, d), indicating miR-23b contributes to the activation of RUNX2 in MSCs on the NSQ50 surface. However, miRNAs targeting OSX (miR-96, and -143) showed significant up-regulation at day 11 with fold changes of 3.2 and 4.2 when compared to their planar control respectively (Figure 4.12e and f). The up-regulation of miR-96 and -143 to their controls at day 11 compared to those at day 9, specifically for miR-143 correlated to the significant increase of OSX expression at day 11, indicating miR-96 and -143 are involved in OSX expression on NSQ50 surface. However, unlike miR-23b that negatively targets RUNX2, miR-96 and 143 potentially target OSX in a positively regulatory way.

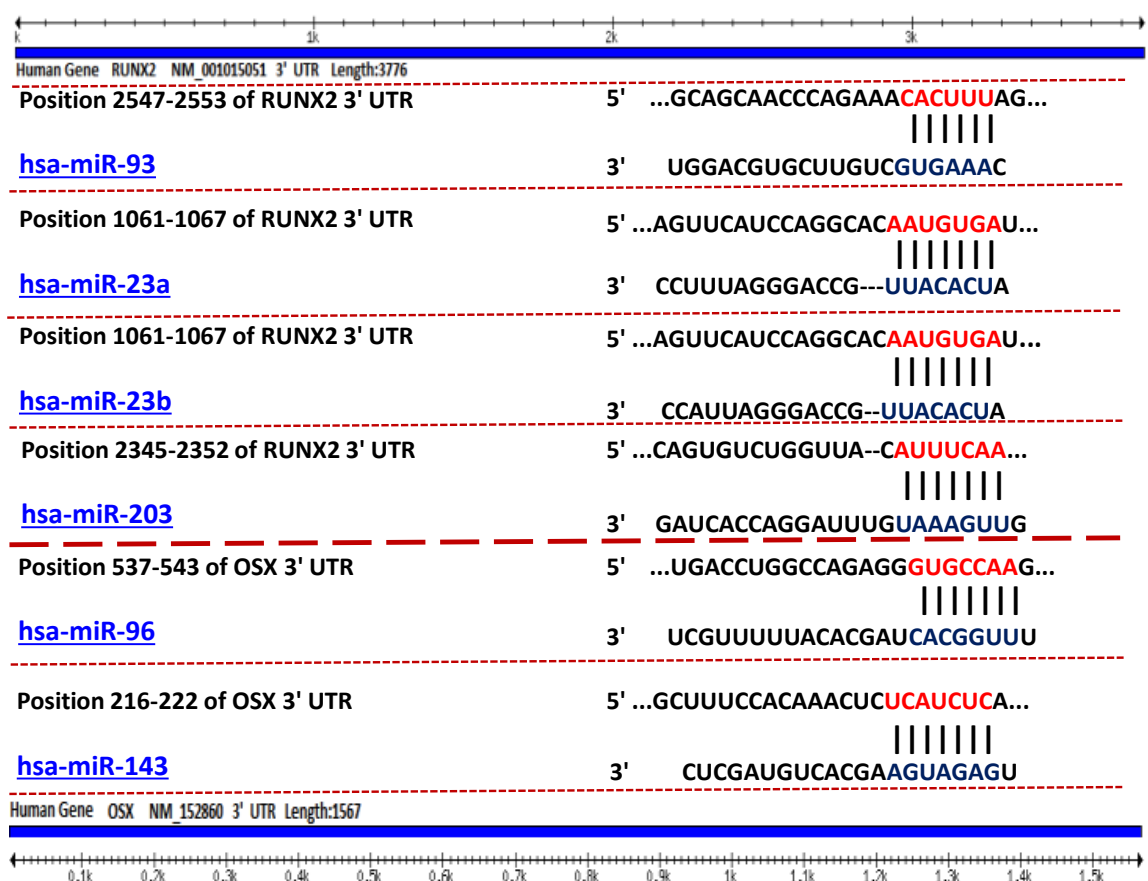
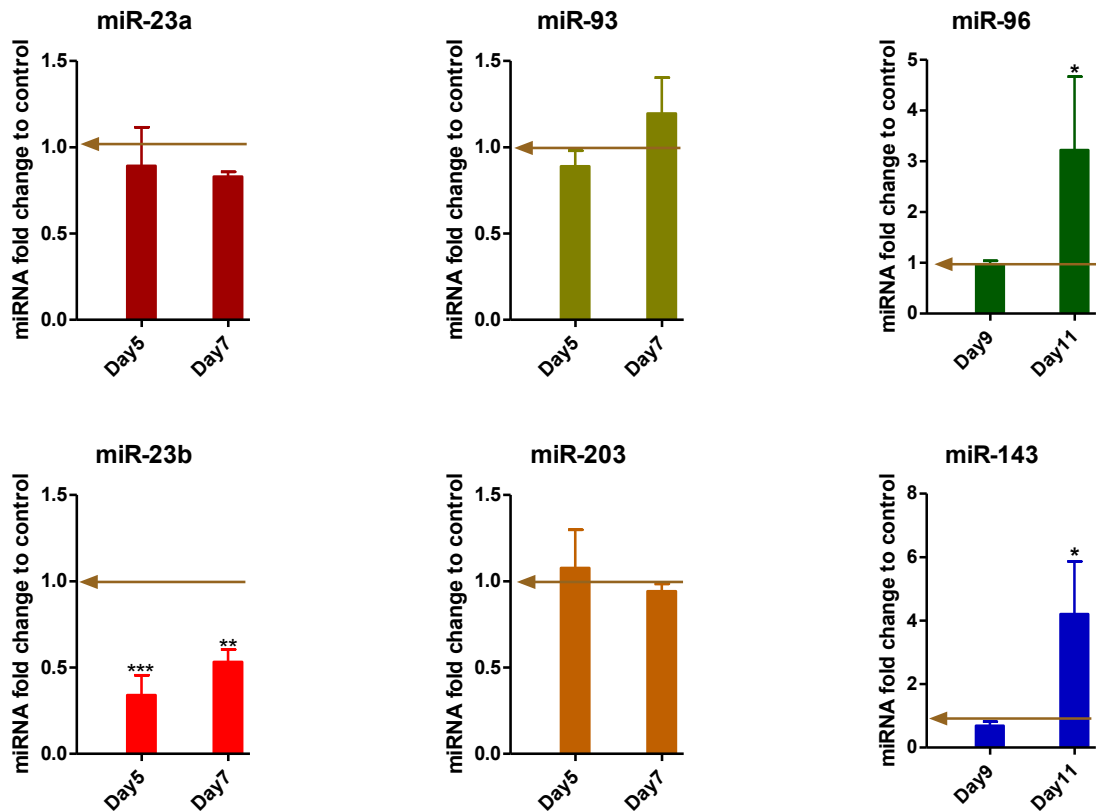


Figure 4.11 The prediction of miRNAs targeting RUNX2 and OSX using TargetScan.

Computational analysis shows the complementarities of miR-23a, -23b, -93 and -203 seed sequences (blue) to the 3' UTR (red) of RUNX2, and of miR-96, -143 (blue) to the 3' UTR (red) of OSX.



**Figure 4.12** The expression of miRNAs targeting RUNX2 and OSX in MSCs on the NSQ50 surface.

Expression of the miRNAs targeting RUNX2 in MSCs cultured on NSQ50 and planar surfaces for 5, and 7 days at which time RUNX2 was induced in MSCs on the NSQ50 surface, were assessed by qRT-PCR. MiR-23b on NSQ50 showed significant down-regulation compared to that on the planar surface (b), whereas miR-23a (a), -93 (c) and -203 (d) remained unchanged when compared to their controls. MiRNAs targeting OSX were measured at day 9 and 11 at which time OSX was over-expressed in MSCs on the NSQ50 surface. Both miR-96 (e) and -143 (f) showed significant increase in MSCs on the NSQ50 surface when compared to their planar controls at day 11, whereas the increase of miR-143 on NSQ50 at day 11 was substantially higher than that at day 9. All data was normalized to the endogenous control gene, small nuclear RNA U6. (N=3,  $\pm$  SD) ANOVA analysis, \*  $p < 0.05$ , \*\*  $p < 0.01$ , \*\*\*  $p < 0.001$ . Arrows on graphs show the control level.

### **4.3.5 The relation of BMP2 signalling to other osteogenic regulatory events in MSCs on the NSQ50 surface**

#### **4.3.5.1 BMP2 signal and miRNAs**

The effects of miRNAs targeting the osteogenic transcription factors RUNX2 and OSX in MSCs on NSQ50 surface was described in the above sections. To investigate the relation of BMP2 signal to the miRNAs, MSCs cultured on NSQ50 and planar surfaces were exposed to noggin (50ng/ml of final concentration in medium) for 5 and 11 days. The expression of miR-23b was assessed at day 5, and miR-96, -143 were measured at day 11 by qRT-PCR (in line with RUNX2 and OSX expression profiles). MiR-23b expression returned to the basal levels observed in cells cultured on planar surface (Figure 4.13a), indicating miR-23b targeting RUNX2 in MSCs on the NSQ50 surface was regulated by the BMP2 signal. However, the expression of miR-96 (Figure 4.13b) and -203 (Figure 4.13c) were not affected by the present of noggin, suggesting the over-expression of miR-96 and -143 were independent of the BMP2 signal.

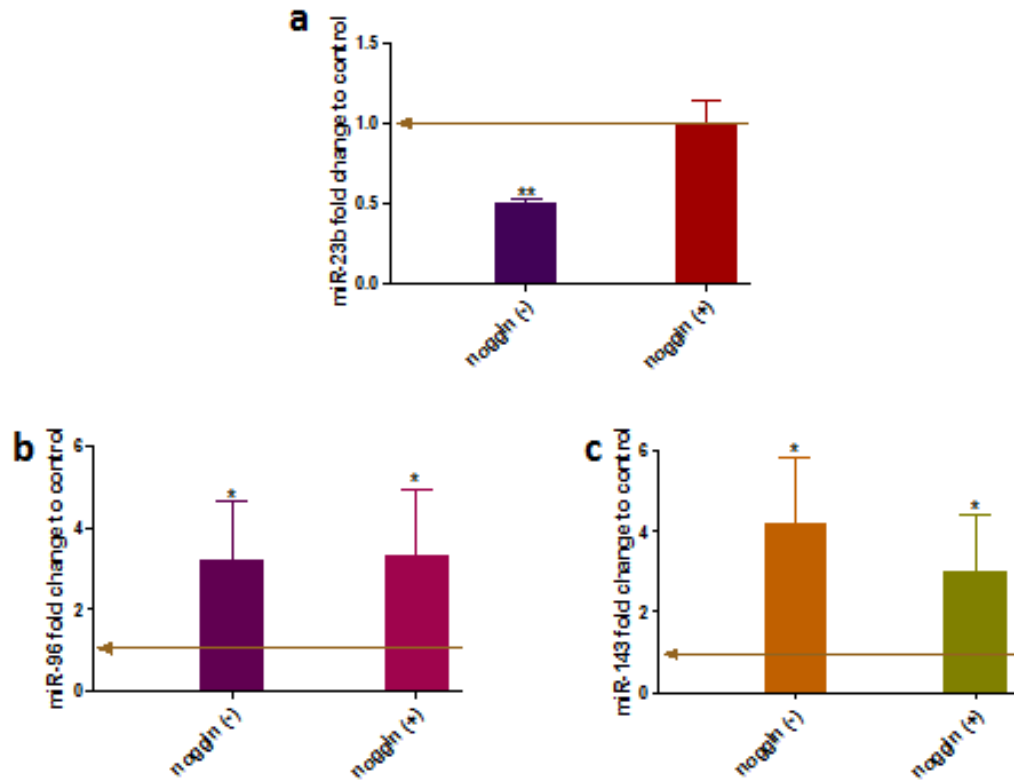


**Figure 4.13 The effects of BMP2 signalling on miRNAs.**

Expression of miRNAs was assessed for MSCs cultured on NSQ50 and treated with the BMP2 signal inhibitor noggin (noggin (+)) compared to cells in normal culture medium (noggin (-)). (a) MiR-23b targeting RUNX2 was up-regulated by noggin, indicating miR-23b targeting RUNX2 is BMP2 dependent. MiR-96 (b) and -143 (c) targeting OSX was unaffected by noggin, suggesting their expression on NSQ50 surface is BMP2 independent. (N=3,  $\pm$  SD) ANOVA analysis, \*  $p < 0.05$ , \*\*  $p < 0.01$ .

#### 4.3.5.2 Crosstalk of BMP2 and integrin $\alpha\beta 5$ signalling

##### 4.3.5.2.1 The effect of integrins $\alpha\beta 5$ on RUNX2 expression

It has been evident that integrin binding exerts effects on osteogenic differentiation of MSCs (Biggs et al., 2009; Kilian et al., 2010), and the current study also demonstrated that the pairing of integrins  $\alpha\beta 5$  was up-regulated on NSQ50 surface at early stage of MSCs osteogenesis (section 4.3.1.1). The effect of  $\alpha\beta 5$  on the early osteogenic marker RUNX2 was investigated using qRT-PCR. MSCs were seeded onto the NSQ50 and planar surfaces, and an integrin  $\beta 5$  antibody was added to the cell media with the ratio of 1:50 in volume of

antibody to medium. Cells were cultured for 5 days on the surfaces and RUNX2 expression was examined. It appeared RUNX2 expression was not significantly reduced after integrin  $\beta$ 5 blocking when compared to cells in normal cultured medium (Figure 4.14A).

To further investigate the effect of the pair of integrin  $\alpha\beta$ 5 on osteogenesis of MSCs on NSQ50 surface, the NSQ50 surface was coated with VN which is the ligand of integrin  $\alpha\beta$ 5. The PCL template embossed with the NSQ50 pattern was incubated with medium containing  $5\mu\text{g/ml}$  of VN at  $4^{\circ}\text{C}$  for 24 hours. The surface (NSQ50+VN) was washed with 1xPBS and pre-warmed at  $37^{\circ}\text{C}$  before MSCs were seeded on to it. Immunostaining using anti-RUNX2 was carried out for cells cultured on NSQ50 and NSQ50+VN surfaces after 5 days cell culture, and enhanced RUNX2 expression on NSQ+VN surface was observed (Figure 4.14B), indicating the activation of integrin  $\alpha\beta$ 5 does stimulate RUNX2 expression.

This is in line with the hypothesis that expression of the VN receptor,  $\alpha\beta$ 5, is important, but goes against results that blocking  $\beta$ 5 does not impact on RUNX2 expression (Figure 4.14A). However, looking at expression of  $\beta$ 3 while  $\beta$ 5 is blocked indicates up-regulation of this other beta subunit (Figure 4.14C). It is important to note that  $\beta$ 3 can be used by cells instead of  $\beta$ 5 for VN ligation.

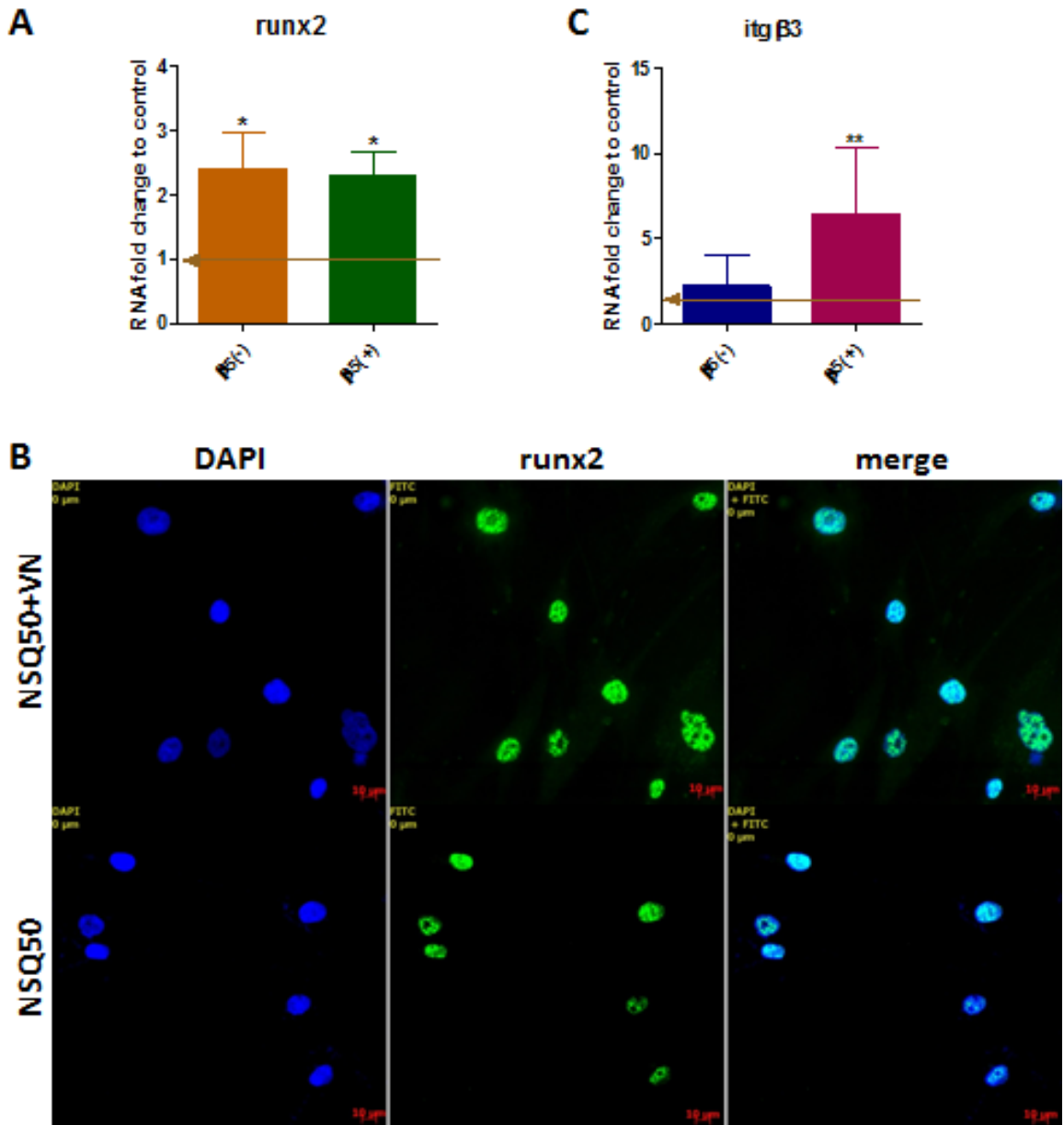


**Figure 4.14** The effect of integrins on RUNX2 expression.

RUNX2 expression (A) was assessed for MSCs cultured on NSQ50 and treated with the blocking antibody of integrin B5 (B5 (+)) compared to cells in normal culture medium (B5 (-)). The data shows unaffected RUNX2 expression after blocking integrin B5. Immunostaining for RUNX2 (B) demonstrated that enhanced expression of RUNX2 was observed on NSQ50 surface coated with vitronectin (NSQ50+VN) compared to cells on uncoated surface (NSQ50) (RUNX2: green, DAPI: blue). Integrin B3 (itgB3) expression (C) was assessed while B5 was blocked by its antibody on NSQ50 surface. The data shows significant up-regulation of B3 when B5 was inhibited, suggesting a possible switch of B5 to B3 which paired with  $\alpha v$  to bind to VN on the NSQ50 surface. For qPCR assay: (N=3,  $\pm$  SD) ANOVA analysis, \*  $p < 0.05$ , \*\*  $p < 0.01$ .

#### 4.3.5.2.2 The co-localization of the BMP2 receptor and integrins

Since both BMP2 and integrin  $\alpha\beta 5$  signalling occurred in the early stages of MSC osteogenesis on the NSQ50 surface, the relation of these two signals was investigated. Previous studies suggest the interplay between TGF receptors and integrins (Ivaska and Heino, 2010), and the crosstalk between BMP2 receptors and integrins ( $\alpha\beta$ ) pairing in osteoblastic functionalization (Lai and Cheng, 2005). To investigate the spatial relation of BMPR1A and integrin  $\beta 5$  on the NSQ50 surface, immunostaining using antibodies specific to BMPR1A and integrin  $\beta 5$  was carried out for MSCs cultured on NSQ50 and planar surfaces for 5 days (Figure 4.15A). On the NSQ50 surface, MSCs expressed  $\beta 5$  at focal adhesion sites and BMPR1A was expressed at the same site as the  $\beta 5$  subunits - i.e. close to adhesions.  $\beta 5$  subunits as part of adhesions were clear on the planar control surfaces, but no co-localisation with BMPR1A was seen (Figure 4.15A). The data demonstrated that the physical co-localization of the two receptors occurred on the osteogenic NSQ50 surface alone.

To further demonstrate co-localization of BMPR1A and integrin  $\beta 5$  on the NSQ50 surface, co-immunoprecipitation was performed using integrin  $\alpha\beta 5$  pairing antibody and protein A agarose beads to pull-down  $\alpha\beta 5$ . The subsequent western analysis using anti-BMPR1A and anti- $\alpha\beta 5$  demonstrated these two receptors were co-localised in MSCs on the NSQ50 surface only (Figure 4.15B). The integrin subunit  $\alpha\beta$  was detected on NSQ50 and planar surfaces, but with more abundance on planar surface than on NSQ50. This is perhaps due to  $\alpha\beta$  paired with other  $\beta$  subunits. The western blot of the immunoprecipitation also showed that the co-localization of BMPR1A and  $\alpha\beta 5$  was enriched at day 5 more than at day 3 on the NSQ50 surface.

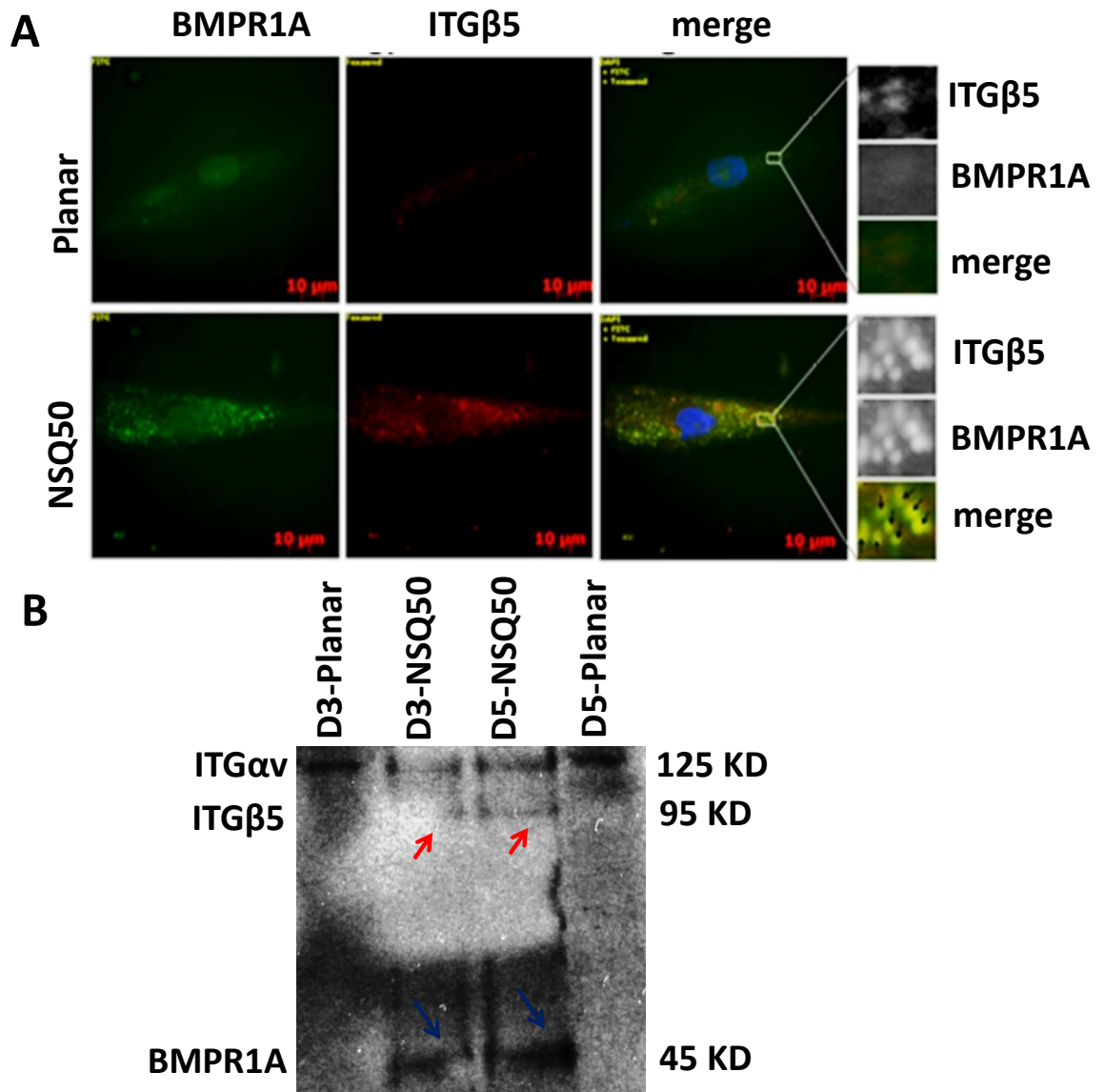


**Figure 4.15** Integrins co-localize with the BMP2 receptor when MSCs are cultured on the NSQ50 surface.

Double immunostaining after 5 days cell culture of MSCs on the NSQ50 and planar surface (A) using integrin (ITG) β5 (red) and BMPR1A (green) specific antibodies. MSCs cultured on the NSQ50 surface demonstrated co-localization of these two receptors (yellow and arrows in the outset merge), whereas the co-localization was not observed in cells on the planar surface. (B) The co-localization of ITG αβ5 and BMPR1A on the NSQ50 surface was confirmed by co-immunoprecipitation using αβ5 antibody (β5: red arrows) and BMPR1A (blue arrows) specific antibodies.

#### 4.3.5.2.3 The functional relation of BMP2 signalling and integrins on NSQ50

The BMP2 receptor and integrin  $\alpha\beta 5$  have been shown to co-localize on the NSQ50 surface. The interplay of these two receptors was investigated to see if the co-localization affects osteogenesis of MSCs on the NSQ50 surface.

MSCs were cultured on the NSQ50 surface and treated with noggin for 5 days to block BMP2 signalling on the surface. Expression of integrins  $\alpha v$  and  $\beta 5$  was measured and compared to their expression in normal culture. Both  $\alpha v$  and  $\beta 5$  showed significant down-regulation on the NSQ50 surface after blocking the BMP2 signal, indicating BMP2 signalling enhances integrins  $\alpha v$  and  $\beta 5$  expression on the surface (Figure 4.16a and b).

Furthermore, expression of the focal adhesion molecule vinculin, a cell adhesion protein used as marker for cell-ECM adhesions (i.e. focal adhesions) (Ziegler et al., 2006) was investigated. Immunostaining for vinculin using an anti-vinculin antibody in MSCs cultured on the NSQ50 and planar surfaces for 5 days was used after noggin treatment. This demonstrated that BMP2 signalling modulates integrin expression in MSCs on the NSQ50 surface (Figure 4.16). MSCs cultured on the NSQ50 surface in normal culture medium showed larger focal adhesion formation (Figure 4.16c), whereas MSCs treated with noggin, which blocks BMP2 signalling, showed a reduction in vinculin expression (Figure 4.16d). Expression of vinculin in MSCs cultured on planar surfaces with and without noggin remained almost unchanged (Figure 4.16e and f). This data, together with the gene expression of integrin  $\alpha\beta 5$  demonstrated that BMP2 signalling regulates integrin expression on the NSQ50 surface.

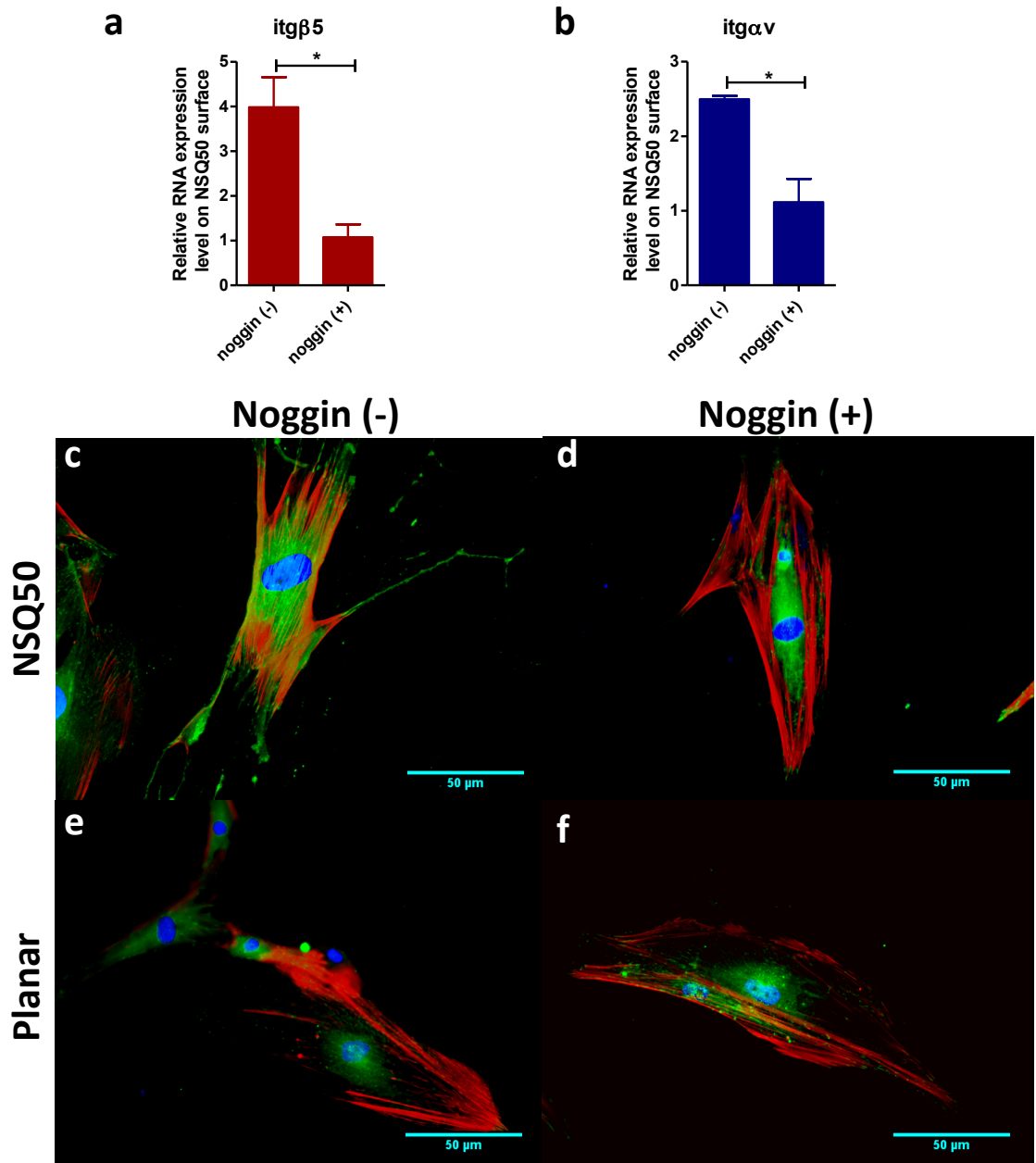


**Figure 4.16** The effect of BMP2 signalling on integrin expression.

MSCs were cultured on the NSQ50 and planar surfaces for 5 days and treated with/without the BMP2 antagonist noggin. Gene expression of B5 and  $\alpha v$  in MSCs on the NSQ50 surface was assessed by qRT-PCR, and B5 and  $\alpha v$  were down-regulated by blocking BMP2 signalling (a and b). Immunostaining for vinculin in MSCs cultured in normal medium on NSQ50 showed larger focal adhesion formation (c), whereas the cells treated with noggin on the surface demonstrated a reduction in vinculin expression (d). Vinculin in MSCs cultured on planar surfaces with and without noggin remained almost unchanged (e and f). For qPCR assay: (N=3,  $\pm$  SD) ANOVA analysis, \*  $p < 0.05$ . Immunostaining, red: actin, blue: DAPI, green: vinculin.

#### 4.3.5.2.4 The functional relation of integrins to BMP signalling

The effects of integrins on BMP2 signalling and subsequent osteogenic differentiation of MSCs on the NSQ50 surface was further investigated by functionalising the surface with the  $\alpha\beta 5$  ligand, VN. This resulted in enhanced expression of RUNX2 on the surface (Figure 4.14B). To see whether the increased RUNX2 expression induced by the activation of integrin  $\alpha\beta 5$  resulted from the co-localization of BMP2 receptors and integrin  $\alpha\beta 5$ , expression of these two receptors was examined by immunostaining.

MSCs cultured on VN coated and standard NSQ50 surfaces were stained with anti-BMPR1A and anti- $\alpha\beta 5$  antibodies (Figure 4.17). Expression of BMPR1A and  $\alpha\beta 5$  on the VN coated NSQ50 surface was enhanced when compared to expression on the uncoated surface. This data indicates that activation of  $\alpha\beta 5$  stimulates BMPR1A expression and augments the interplay of BMP2 and integrin signalling. This data together with figure 4.14B demonstrates that integrins regulate BMP2 signalling via receptors co-localising and subsequently modulate osteogenesis of MSCs on the NSQ50 surface.

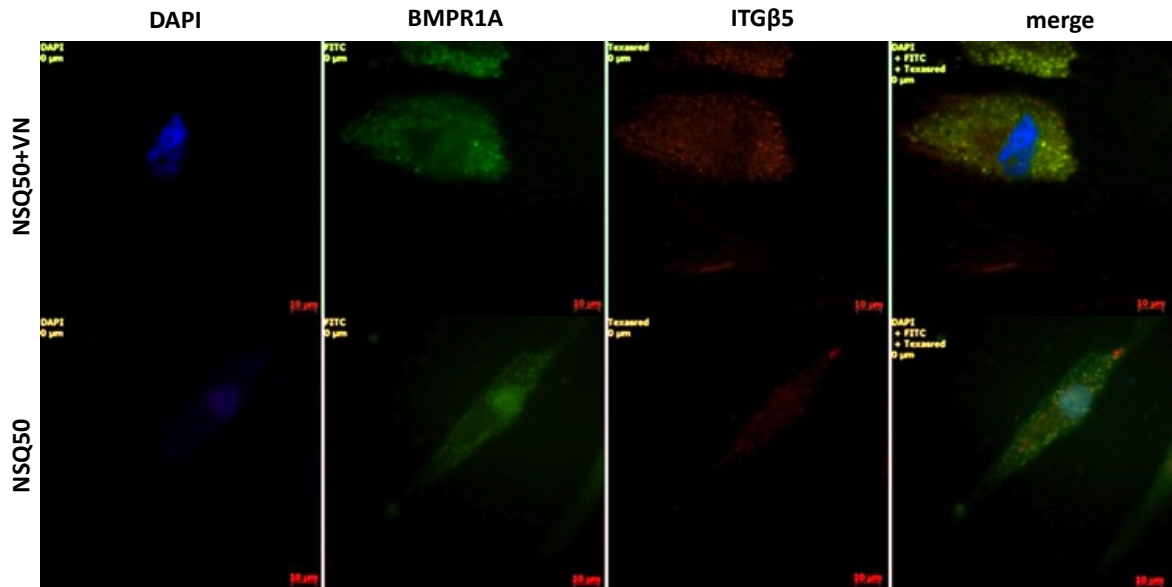


**Figure 4.17** The effect of VN on integrin  $\alpha\text{v}\beta\text{5}$  and BMPR1A expression.

Immunostaining for BMPR1A and integrin  $\alpha\text{v}\beta\text{5}$  in MSCs on VN coated and standard NSQ50 surfaces using anti-BMPR1A and anti-  $\alpha\text{v}\beta\text{5}$  antibodies. Enhanced expression of these two receptors and enhanced co-localisation was observe on the vitronectin coated surface (NSQ50+VN). (blue: DAPI, green: BMPR1A, red:  $\alpha\text{v}\beta\text{5}$ , yellow: co-localization).

## 4.4 Discussion and conclusion

### 4.4.1 BMP2 signalling

BMP2 has been characterised as osteoinductive, inducing bone formation *in vivo* and *in vitro* (Bandyopadhyay et al., 2006; Javed et al., 2009). In the context of bone tissue engineering, biomaterials combining BMP2 represent a powerful strategy for enhancing MSCs osteogenic differentiation and bone formation (Kim et al., 2014). Furthermore, recombinant human BMP2 (rhBMP2) has been used for spinal fusion and open fracture treatment in clinic (Gautschi et al., 2007). The results presented in this chapter add a new finding to the field by showing that nanotopography induces BMP2 expression and enhances BMP2 signalling, and subsequently contributes to osteogenesis of MSCs.

Both BMP2 and its receptor BMPR1A in MSCs on NSQ50 surface were found to be up-regulated at the time (day 3) where C-MYC was starting to become decreased

and the increase of osteogenic transcription factor RUNX2 was not yet observed (section 3.4.1 and 3.4.2). The downstream signalling molecules of BMP2, SMAD1 and SMAD5 were highly expressed at day 5, indicating BMP2 signalling was activated in MSCs on the NSQ50 surface. Thus, it is rational to expect BMP2 as an early stage event in NSQ50 induced osteogenesis. The effect of BMP2 signalling on osteogenesis of MSCs was demonstrated by manipulating the signal: when BMP2 signalling was blocked by noggin, the up-regulation of RUNX2 on NSQ50 was inhibited, and furthermore, the osteoblast marker OPN expression was abrogated on the surface. These data indicated that osteogenesis of MSCs on NSQ50 surface was induced by BMP2 via RUNX2.

BMP2 signalling may go through the SMAD-independent pathway in which the downstream pathways of BMP2, including ERK, p38MAPK, and JNK are initiated (Guicheux et al., 2003; Nohe et al., 2004). It is thought that this pathway is transduced by the interaction of BRAM1 and TAK1/TAB1 complex (Shim et al., 2009). However, the TAK1 binding protein TAB1 showed no significant difference between MSCs on the NSQ50 and planar surfaces. This suggests that the NSQ50 induced osteogenesis is not reliant on SMAD-independent BMP2 signalling.

Recent studies demonstrate that MSCs can secrete growth factors and BMP2 (Huang et al., 2007; Kim et al., 2010; Kim and Ma, 2013) during proliferation and differentiation. Immunostaining BMP2 in MSCs on the NSQ50 surface after 7 days of cell culture demonstrated that BMP2 is localised in the cytoplasm. Furthermore, when MSCs were cultured on the NSQ50 surface in low serum conditions, expression of RUNX2 was only slightly reduced comparing to that in normal medium cell culture. These data suggests NSQ50 surface induces endogenous BMP2 expression and may sequester BMP2 to guide osteogenesis of MSCs (Hudalla et al., 2011; Impellitteri et al., 2012).

#### **4.4.2 The role of integrins in osteogenesis of MSCs on NSQ50 surface.**

Integrins play an essential role in nanotopographical cue-induced osteogenesis of MSCs - while they themselves have no enzymatic activity, they scaffold for

signalling proteins like FAK and Src. It has been proposed that nanotopography can modulate integrins clustering and focal adhesion formation, and in turn regulate cell function and differentiation (Arnold et al., 2004; McMurray et al., 2011; Schwartzman et al., 2011). Expression of the integrins  $\alpha\beta 5$  and the effect on up-regulation of the RUNX2 were observed in MSCs on the NSQ50 surface. This data together with previous studies (McMurray et al., 2011; Tsimbouri et al., 2012) indicate integrins are involved in the regulation of osteogenesis of MSCs. Integrins exert effects by binding with components of ECM through pairing of  $\alpha$  and  $\beta$  subunits. It is widely accepted that the pairing of  $\alpha\upsilon$  with  $\beta 1/\beta 3/\beta 5$  and  $\alpha 5$  with  $\beta 1$  binds to the RGD motif in OPN, and fibronectin (mainly  $\alpha\upsilon\beta 3$ ) and VN (mainly  $\alpha\upsilon\beta 5$  but also  $\alpha\upsilon\beta 3$ ) in ECM (Hynes et al., 2002). The up-regulation of  $\alpha\upsilon\beta 5$  in MSCs on the NSQ50 surface, and immobilising VN on NSQ50 surface, resulted in the up-regulation of RUNX2, suggesting a key role for VN in adhesion to the surface of osteo-differentiating cells. Blocking of the subunit  $\beta 5$  resulted in up-regulation of  $\beta 3$ , whereas RUNX2 remained unchanged compared to the those in normal culture medium on MSCs, suggesting MSCs recruit  $\beta 3$  instead of  $\beta 5$  for VN binding, and thus demonstrate the indisputable role of integrins for osteogenesis of MSCs on NSQ50 surface.

### **4.4.3 Cross-talk between BMP2 signalling and integrins.**

The roles of BMP2 signalling and integrins ( $\alpha\text{v}\beta\text{5}$ ) for the osteogenesis of MSCs on the NSQ50 surface presents interesting questions about how and where these two signals function in MSCs osteogenesis on the surface. This interest was further encouraged by the finding that BMP2 signalling modulates focal adhesion formation on the surface. Vinculin expression was down-regulated by inhibition of the BMP2 signalling by adding noggin to the culture on the NSQ50 surface when compared to those on the surface without noggin, and on planar surfaces with and without noggin. This result supports the evidence that BMP2 promotes cell adhesion and stimulates osteoblast differentiation (M et al., 1996; Nissinen et al., 1997; Shah et al., 1999).

The co-localization of the BMP2 receptor BMPR1A and integrins  $\alpha\text{v}\beta\text{5}$  was found on the surface when double immunostaining was applied using specific antibodies for these two receptors, and the result was further confirmed by immunoprecipitation. The physical co-localisation of the two receptors results in synergic effects stimulating osteogenesis on NSQ50. Enhancing activation of the  $\alpha\text{v}\beta\text{5}$  by immobilising NSQ50 surface with VN stimulated both BMPR1A and  $\alpha\text{v}\beta\text{5}$  expressions and the co-localization of these two augmented RUNX2 expression on the surface compared to the standard NSQ50 surface. Inhibition of BMP2 signalling reduced  $\alpha\text{v}$  and  $\beta\text{5}$  gene expression and focal adhesion formation, as well as the subsequent reduction of RUNX2 and OPN on the surface.

### **4.4.4 MiRNAs.**

Studies have shown miRNAs play important roles in the regulation of skeletal differentiation (Chen et al., 2006; Mizuno et al., 2009; Mizuno et al., 2008), and are involved in the osteogenic differentiation via targeting of RUNX2 (Huang et al., 2010a) and OSX (Shi et al., 2013). MiRNAs targeting RUNX2 and OSX were predicted using the targets can programme which is the first computing tool to use the concept of seed-region matches to predict highly conserved miRNA sequences that are perfectly complementary to the small segment sequence

(usually 7 nt) in 3'-UTR of mRNA. MiR-23a, -23b, -93 and -203 were predicted to target RUNX2, and miR-96 and -143 to target OSX.

Expression of the miRNAs targeting RUNX2 showed that miR-23b was down-regulated, whereas others tested remained similar to those on the planar surface when RUNX2 was stimulated in MSCs on the NSQ50 surface. Further examining by addition of noggin indicates that the down-regulation of miR-23b on the surface is regulated by BMP2. Thus, miR-23b is involved in osteogenesis of MSCs as a negative regulator in BMP2-dependent manner. However, miR-96 and -143 targeting OSX were shown to have positive correlation to their target. This could be that miR-96, and -143 target inhibitors of OSX as well, because one miRNA can target different genes, and one gene can be targeted by different miRNAs (Kim, 2005), and indeed further search in TargetScan found miR-96 can target parathyroid hormone (PTH) which is an inhibitor of OSX (Barbuto and Mitchell, 2013). Furthermore, noggin showed no effect on the expression of miR-96, and -143, thus miR-96 and -143 are positive regulators to OSX and also BMP2-independent on NSQ50 surface.

#### **4.4.5 Conclusions.**

MSCs differentiation is a highly regulated process. Nanoscale materials possess the potential capacity for dissecting stem cell mechanisms without recourse to the use of soluble factors to drive differentiation. Membrane receptor signalling plays essential roles in osteogenic differentiation of MSCs on the NSQ50 surface, in which BMP2 and integrin  $\alpha\beta 5$  are important, but Wnt appears not to be.

BMP2 signalling appears an initial regulatory event required to stimulate osteogenesis on the NSQ50 surface.

RUNX2 which controls the osteogenic fate of MSCs is directly associated with BMP2 signalling, either by BMP2-SMAD pathway or BMP2-miR-23b, or both. BMP2 signalling induced RUNX2 is sufficient for the induction of its downstream transcription factor OSX. Thus, MSC osteogenesis on the NSQ50 surface starts

with increased BMP2 sensitivity and then enters a well-orchestrated cascade of growth, transcriptional and ECM-modulating events.

## **Chapter 5. Metabolomics**

## Rationale

NSQ50 nanotopographies ability to activate BMP2 and other signalling molecules resulting in MSCs osteogenic differentiation was established in chapter 4. To extend the understandings of mechanisms of nanotopography induced MSC differentiation, a systematic approach-metabolomic investigation was employed. In this chapter, previously characterized metabolic features of undifferentiated MSCs and differentiated MSCs are introduced, and this is followed by a description of metabolomics experiments and data analysis procedures. The results presented in this chapter include shifting the balance of bioenergetics from anaerobic to aerobic when MSCs on the NSQ50 surface switch stemness to differentiation. Specific metabolic pathways identified by the KEGG database are also presented. The findings of significant down-regulation of unsaturated fatty acids lead me to discuss their roles in MSC osteogenic lineage commitment and differentiation on the NSQ50 surface. Finally, a discussion of metabolic features, the possible roles of metabolites involved in the regulation of MSC osteogenesis on the surface is presented and conclusions made.

### 5.1 Introduction

Recent advances of metabolomics and computing analysis have implicated the pivotal role of metabolism in determining whether stem cells proliferate, differentiate or remain quiescent. Metabolism regulates stem cell function and fate by alteration of cell specific metabolic pathways (Pattappa et al., 2011), and subsequent integration with epigenetic and genetic programmes (Shyh-Chang et al., 2013b). The metabolic regulatory mechanisms underlying stem cell fate may vary in different stem cell types.

#### 5.1.1 Metabolic profile of pluripotent stem cells (ESC and iPSCs)

Pluripotent stem cells (PSCs) are characterized by a short G1 phase of cell cycle to limit cell growth and differentiation potential (Singh and Dalton, 2009). In the proliferative state, PSCs have to balance the bioenergetic and biosynthetic

activities to support the rapid cell duplication. In the proliferating process, cells uptake nutrients to achieve a high rate of glucose flux resulting in an increase in glucose transporter 1/3 (GLUT1/3) expression, and the activation of hexokinase (HK) and phosphofructokinase 1 (PFK1), which activate glycolytic pathways. As a result, adenosine triphosphate (ATP) is generated by glycolytic phosphoglycerate kinases (PGKs) and pyruvate kinases (PKs), and decoupled from oxygen consumption by the mitochondrial Electron Transport Chain (ETC). Although rate of ATP synthesis is low in the glycolytic pathway (2 mol ATP per mol glucose), it is sufficient for nucleotide, amino acid and lipid biosynthesis to maintain PSC pluripotency and proliferation (Locasale and Cantley, 2011; Manganelli et al., 2012).

It is thought that proliferating cells under anaerobic glycolysis (inefficient ATP synthesis) prefer to shunt glycolytic intermediates into nucleotide, amino acid and lipid synthesis (Vander Heiden et al., 2009), and indeed the increased activity of the pentose phosphate pathway (PPP) which allows rapid nucleotide synthesis observed in undifferentiated mouse ESCs (Manganelli et al., 2012; Varum et al., 2011). The low efficiency of ATP synthesis in proliferating PSCs is also in favour of consuming oxygen through the ETC to oxidize Nicotinamide adenine dinucleotide (NADH) into  $\text{NAD}^+$  and maintain the Krebs cycle flux, which is a cyclic series of chemical reactions to generate energy, as well as providing precursors for generating certain amino acids in the mitochondria. This allows PSCs to maintain an optimal redox potential for lipid synthesis from citrate and for amino acid synthesis from  $\alpha$ -ketoglutarate (Shyh-Chang et al., 2011; Zhang et al., 2011). Thus, anaerobic glycolysis is a common feature of metabolism in proliferating PSCs.

However, glycolytic flux dramatically decreases and mitochondria activities increase in differentiating PSCs. This indicates that energy production shifts to the mitochondrion resulting in a decrease in the PPP pathway and an increase in oxygen consumption as ECT recouples to ATP synthesis to fulfil the requirements from cell differentiation (Cho et al., 2006; Chung et al., 2007; Prigione et al., 2010). In mitochondria, ATP is generated by increased Oxidative Phosphorylation (OxPhos) activity which oxidizes nutrients, such as pyruvate via proton gradients

at the mitochondrial membrane. The increased ECT activity results in increase in Reactive Oxygen Species (ROS) which oxidizes highly unsaturated structures such as unsaturated lipids to form eicosanoids which promote differentiation (Yanes et al., 2010).

### **5.1.2 Metabolic profile of MSCs**

MSCs share the same metabolic profile of PSCs when the cells are in a quiescent state in which MSCs express higher levels of glycolytic enzymes and increase lactate production rate, and lower levels of OxPhos proteins, suggesting MSCs are reliant on glycolysis (Chen et al., 2008). However, MSCs expanded under normoxia which increase in OxPhos and ROS, result in three to four fold increase in senescence. This indicates that glycolysis maybe an environmental adaptation (Pattappa et al., 2011; Pattappa et al., 2013). *In vivo*, MSCs reside in more hypoxic environments, thus hypoxia-induced glycolysis helps maintain MSC long term self-renewal (Chen et al., 2008; Pattappa et al., 2013).

Metabolic profiles of MSCs differentiation rely on lineage-specific commitment. During adipogenesis, a lipogenic programme involving in ATP citrate lyase is activated, which converts glucose-derived citrate into acetyl coenzyme A (acetyl-CoA) to increase glucose metabolism and synthesize lipids for fat storage (Wellen et al., 2009). This suggests that the increased mitochondrial activity in OxPhos and ROS is necessary for adipogenesis (Tormos et al., 2011). Similarly, the bioenergetics and biosynthesis in osteogenesis of MSCs leads to an increase in mitochondrial biogenesis and oxygen consumption resulting in a rise of OxPhos in osteoblasts. However, the increase in OxPhos is accompanied by up-regulated expression of antioxidant enzymes (oxidoreductases) such as catalase and superoxide dismutase, leading to cellular ROS decrease in osteogenesis of MSCs (Chen et al., 2008; Lonergan et al., 2006).

### **5.1.3 The links of metabolism to epigenetics and gene expression**

The integration of metabolism with epigenetic and genetic programs in coordinated regulation of stem cell function and fate has emerged. Recent studies have demonstrated that metabolite flux can be controlled by enzymes regulated by cellular mediators of signalling transduction and gene expression, including transcription factors such as C-MYC and hypoxia-inducible factor 1 (HIF-1), and signalling network molecules such as phosphatidylinositol 3-kinase (PI3K) (DeBerardinis et al., 2008), whereas intermediate metabolites can be used as substrates or cofactors for enzymes to regulate chromatin structure and gene expression. Examples include acetyl-CoA generated by catabolism in mitochondria can be transported into the cytosol and enter into the nucleus and promote the acetylation of histones specifically at growth genes (Cai et al., 2011), and that the metabolites in the S-adenosyl methionine cycle contain methyl groups which are the most common substrate for DNA methylation and are highly present in iPSCs (Panopoulos et al., 2012). Therefore, metabolites integrate into the epigenome, and thereafter may influence chromatin structure, gene expression, miRNAs, non-coding elements, and posttranslational modification of histone (Katada et al., 2012) to determine stem cell fate.

NSQ50 nanotopography, as a non-invasive osteoinduction tool for MSCs, has demonstrated the capacity for systematic investigation of mechanisms that determine stem cell fate and lineage-specific differentiation (Dalby et al., 2007b; McMurray et al., 2011). The emergence of metabolomics like other 'omics' (e.g. transcriptomics, proteomics) provides a new systematic approach to extend our understanding of NSQ50 induced osteogenesis of MSCs. Thus, in this chapter, metabolites changed in MSCs on the NSQ50 surface at early stage commitment, which has been characterized in this thesis as a crucial time period for MSC osteogenic differentiation, were investigated with the aims of:

1. Characterize the bioenergetics and biosynthesis of MSCs on NSQ50 surface.

2. Attempt to probe the relations of specific metabolites to the regulatory mechanisms of osteogenesis of MSCs on the NSQ50 surface.
3. Help validate the time point at which MSCs switch to osteogenic differentiation.

## **5.2 Methodology and data analysis**

### **5.2.1 Methodology**

The gene expression and signalling analysis have illustrated that MSCs shift from stem cell state towards osteogenic phenotype at around 5 to 7 days on the NSQ50 surface. Thus, the roles of metabolism for osteogenic differentiation of MSCs on the surface should be investigated around this time period.

Untargeted metabolic analysis was used with the aim of measuring (ideally) all metabolites in MSCs on the NSQ50 surface, and comparing different time point samples (biological groups) to identify potential metabolites of interest, and find the differences among those samples. Thus, MSCs cultured on the NSQ50 and planar surfaces for 3, 5 and 7 days had metabolites extracted, and liquid chromatography and mass spectrometry (LC-MS) performed in the Glasgow Polyomics Centre. The LC-MS platform (UltiMate 3000 RSLC (Thermo Fisher)) consists of hydrophilic interaction liquid chromatography (HILIC) (Thermo Fisher) using a 150 x 4.6mm ZIC-column to separate polar compounds like sugars, amino sugars, amino acids, vitamins, carboxylic acids, and nucleotides etc., and Exactive Orbitrap mass analyser (Thermo Fisher) for metabolite identification and quantification.

### **5.2.2 Data analysis**

The raw MS data from three biological samples (MSCs cultured on NSQ50 surfaces) and three control samples (MSCs cultured on planar surfaces) at each time point was pre-processed using analysis pipeline generated in Glasgow Polyomics Centre. The pipeline consists of XCMS (Smith et al., 2006) for peak

picking, MzMatch (Scheltema et al., 2011) for filtering and grouping, and IDEOM (Creek et al., 2012) for further filtering and identification. Metabolite identifications were validated against a panel of unambiguous standards by mass and retention time. Additional putative identifications were assigned by mass and predicated retention time (Creek et al., 2011).

Further data analysis was performed manually, including:

1. Data merging: merging all tables from all datasets in IDEOM (i.e. identification, rejected, allBasePeaks, alldata) for consistency checks, identical value checks and redundancies. This resulted in a peak-list of 1697 peaks, of which 617 have been associated with metabolite names.
2. Data associations: About 400 known metabolites were associated with KEGG accession identifiers (KEGG ID#).
3. Fold changes and p-values were calculated by comparing three biological samples on NSQ50 to three biological samples on planar surfaces at each time point.
4. The profile of metabolite changes at different time points was mapped using log-transformed fold change to generate heatmaps in R.
5. Pathway mapping: all KEGG accession numbers were submitted to the KEGG database ([http://www.genome.jp/kegg/tool/map\\_pathway1.html](http://www.genome.jp/kegg/tool/map_pathway1.html)) and potentially relevant pathways were noted. Pathways associated with bioenergetics, biosynthesis and mitochondrial activities were paid particular attention, and associated metabolite changes among three time points were further analyzed using ANOVA.

## 5.3 Results

### 5.3.1 Clustering analysis of metabolites in MSCs on NSQ50

The metabolic profile of MSCs on the NSQ50 surface at the early stage of nanotopography induced osteogenesis was analysed by clustering in a heatmap matrix (Figure 5.1). Metabolic data generated from LC-MS and then the IDEOM pipeline was further checked for consistency, identical value and redundancies, which resulted in about 400 metabolites with KEGG accession numbers. Metabolite fold changes in MSCs on the NSQ50 surface at 3, 5 and 7 days obtained by comparing to those on planar surfaces respectively, and were subjected to heatmap analysis. For better visualization, the total metabolites were cataloged into four groups namely lipids (Figure 5.1), amino acids (Figure 5.2), nucleotides and others (Figure 5.3), and non-pathway mapping metabolites (Figure 5.4) according to metabolite properties. All lipids and amino acids were classified into lipid and amino acid groups respectively. Nucleotides, carbohydrates, cofactors etc., were all included in the nucleotides and others group. Metabolites with KEGG identification and accession number but without pathway mapping were classified into non-pathway mapping metabolites group. The clustering analysis showed that metabolites in MSCs on the NSQ50 surface were clustered for cells cultured for 5 and 7 days and differed from those for cells cultured for 3 days, indicating metabolic profile changed during the 3 to 5 day time progression on the NSQ50 surface. The main difference in the lipid group occurred in the fatty acyls sub-group (Figure 5.1), and about all of amino acids were showing difference between 3 and 5 to 7 days cell culture (Figure 5.2). About 60% of metabolites changed in the nucleotide group (Figure 5.3), and about 30% of metabolites without KEGG pathway mapping were changed (Figure 5.4).

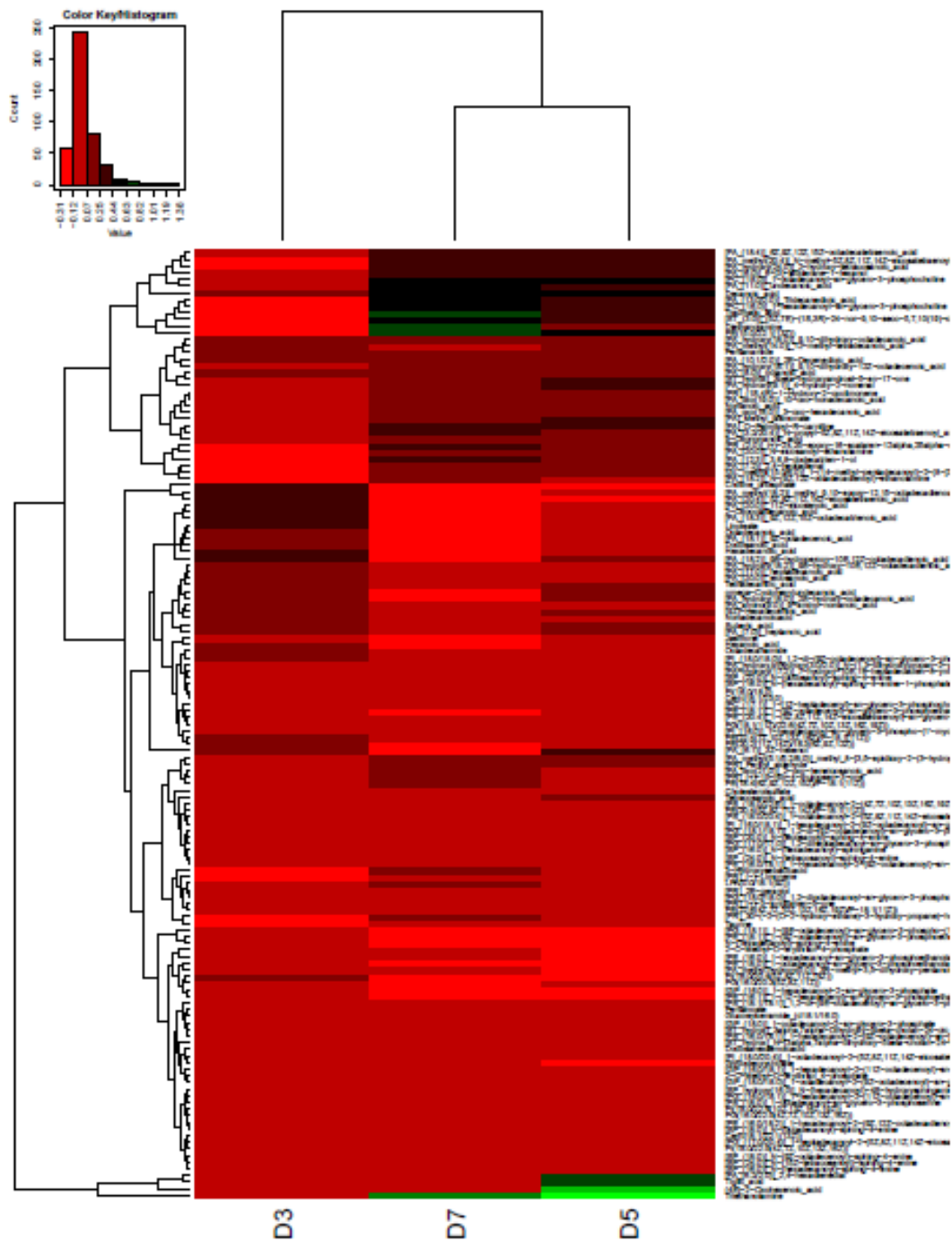


**Figure 5.1** The lipids profile of MSCs on the NSQ50 surface for cells cultured at 3, 5, and 7 days.

Heatmap clustering shows lipids fold change in MSCs cultured for 3 days (D3), 5 days (D5) and 7 days (D7), (biological replicates: N=3). The color range (top left corner) indicates the log-transformed fold change from down-regulation (red) to up-regulation (green). Lipids in MSCs at 5 and 7 days show co-clustering and differ from those at 3 days.



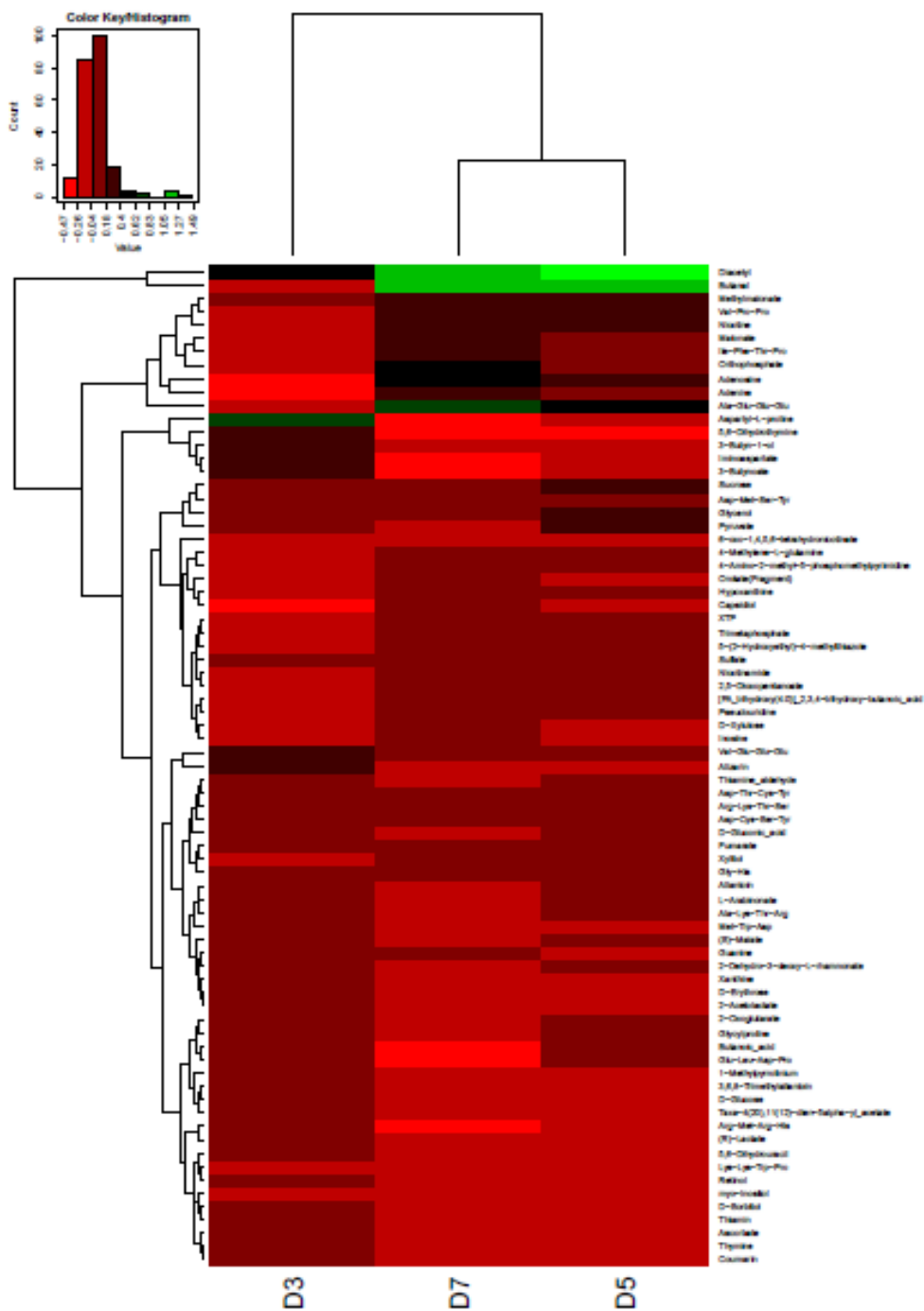


**Figure 5.3** The nucleotides and other metabolites profile of MSCs on the NSQ50 surface for cells cultured at 3, 5, and 7 days.

Heatmap clustering shows nucleotides and other metabolites fold change in MSCs cultured for 3 days (D3), 5 days (D5) and 7 days (D7), (biological replicates: N=3). The color range (top left corner) indicates the log-transformed fold change from down-regulation (red) to up-regulation (green). Nucleotides and others in MSCs at 5 and 7 days show co-clustering and differ from those at 3 days.

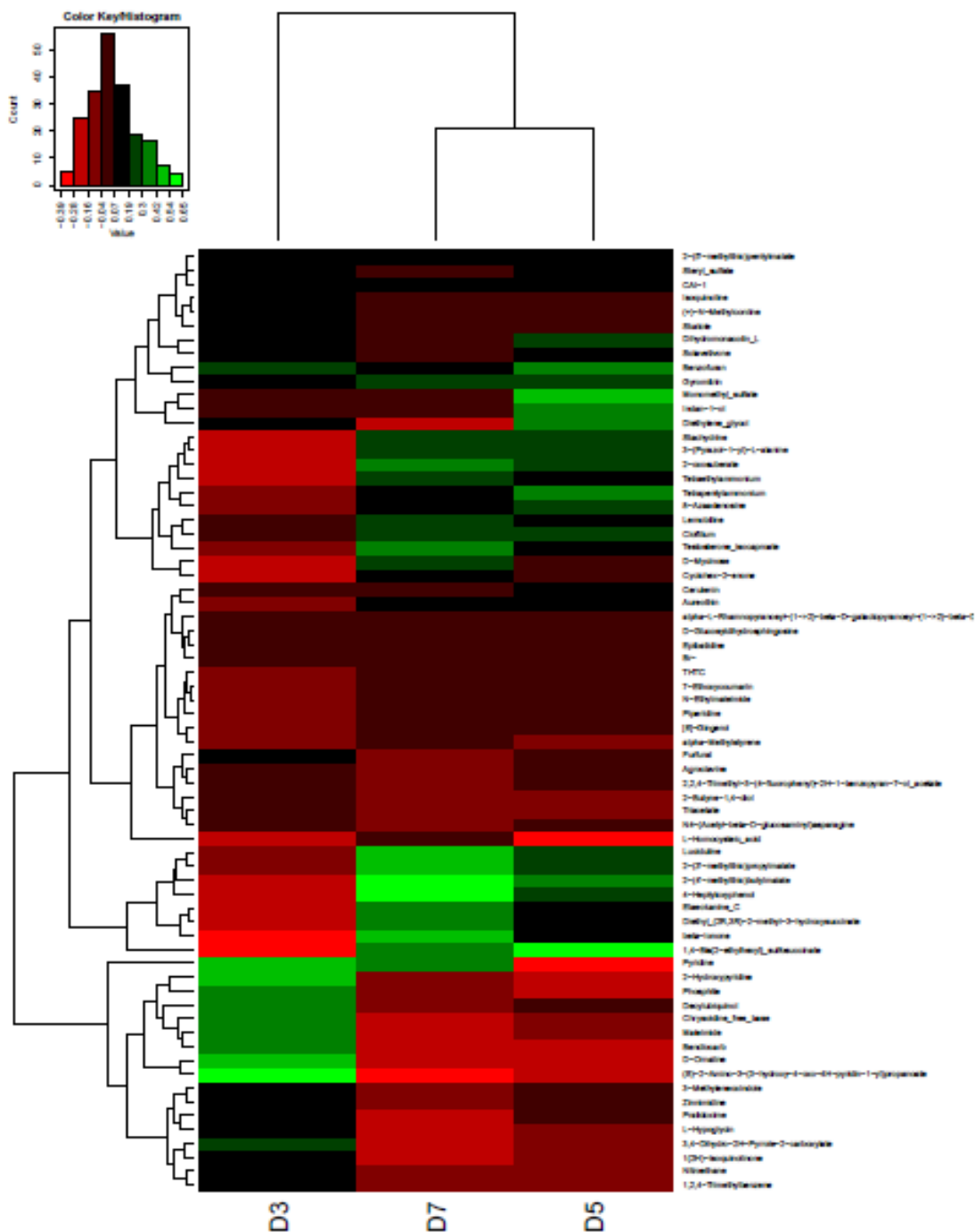


**Figure 5.4** The non-pathway mapping metabolites profile of MSCs on the NSQ50 surface for cells cultured at 3, 5, and 7 days.

Heatmap clustering shows non-pathway mapping metabolites fold change in MSCs cultured for 3 days (D3), 5 days (D5) and 7 days (D7), (biological replicates: N=3). The color range (top left corner) indicates the log-transformed fold change from down-regulation (red) to up-regulation (green). Non-pathway mapping metabolites in MSCs at 5 and 7 days also show co-clustering and differ from those at 3 days.

### **5.3.2 Bioenergetics of MSCs on the NSQ50 surface**

Metabolic profiles changed in MSCs on NSQ50 surface between 3 days to 5 and 7 days cell culture, and previous studies have demonstrated that the bioenergetics of proliferating stem cells differ from that of differentiating stem cell (Cho et al., 2006; Pattappa et al., 2011). This led to further analysis of bioenergetics in MSCs on the NSQ surface.

### **5.3.3 The lack of anaerobic glycolytic phenotype of MSCs on NSQ50 at early stage osteogenesis**

Stem cells utilize glycolysis for ATP generation to support proliferation and other cell activities. The anaerobic glycolysis pathway starts with glucose flux and goes through serial enzymatic reactions to the final product of lactate (Shyh-Chang et al., 2013a). In this pathway, glucose may flux into PPP for nucleotide synthesis. To see whether the glycolytic bioenergetics altered in MSC on the NSQ50 surface, carbohydrate metabolites with KEGG accession identification numbers were submitted to the KEGG database. The output of KEGG pathway searches showed that D-glucose and pyruvate, the two major components of the glycolysis pathway, were observed in MSCs on NSQ50 surface (Figure 5.5A, red arrow), and that three metabolites including D-glucose and pyruvate were observed in PPP (Figure 5.5B, red arrow). Further quantitative analysis for those components being made by comparing these metabolites in MSCs on the NSQ50 to those on planar surfaces for 3, 5 and 7 days cell culture, and the fold changes were statistically analysed by ANOVA (Figure 5.6). The data showed that D-glucose was significantly decreased at day 5 relative to day 3 (Figure 5.6a). However, pyruvate (a key intermediate metabolite of the pathway) and lactate (the final product of the pathway) (Figure 5.6b, d) remained almost unchanged during 3, 5 and 7 days of cell culture. Furthermore, the insignificant change of D-gluconic acid, which is involved in the PPP pathway, was also observed (Figure 5.6c). These data indicate that glycolysis was not affected by the increased consumption of D-glucose at day 5, and suggests shifts in cell energetics to other pathways at day 5.



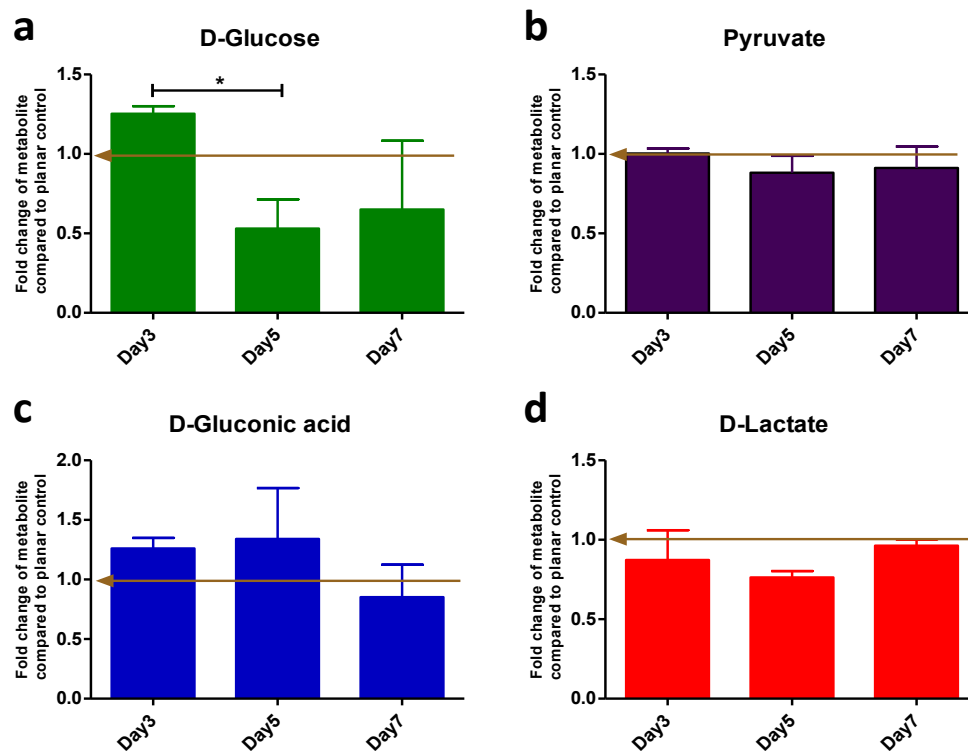


**Figure 5.6** The effect of the NSQ50 surface on the glycolytic bioenergetics pathway in MSCs.

Metabolites in MSCs on the NSQ50 surface were compared to those on the planar surface. D-glucose was significantly decreased on the NSQ50 surface at day5 relative to day3 (a). Pyruvate (b), D-gluconic acid (c) and D-lactate (d) remained almost unchanged from day 3 to day 5 and 7. (biological replicates: N=3,  $\pm$  SD) ANOVA analysis, \*  $p < 0.05$ . Arrows on graphs show the control level.

### 5.3.4 The increased mitochondrial activity for bioenergetics of MSCs on NSQ50 surface

The significant decrease of D-glucose was not followed by an increase in glycolytic level in MSCs on the NSQ50 surface, suggesting cells exploit other pathways in bioenergetics. Mitochondria have been long recognised as playing important roles for the production of ATP and synthesizing lipids. Recent studies have demonstrated the regulatory roles for a variety of cellular processes such as proliferation and differentiation in many cell types (McBride et al., 2006), including MSC (Chen et al., 2008).

The Krebs cycle (TCA cycle) occurs in the mitochondria, in which carbohydrates and fatty acids are oxidized and OxPhos level is increased for ATP generation. Pathway analysis for metabolites of MSCs on the NSQ50 surface showed that

changes in fumarate (produced by mitochondria complex II and also an intermediate metabolite of TCA) and orthophosphate were noted (Figure 5.7A). Further analysis demonstrated fumarate and orthophosphate were significantly increased at day 5 and day 7 when compared to planar control (Figure 5.7B). Fumarate is the product of OxPhos by mitochondrial complex II, and orthophosphate is involved in mitochondrial complex V for the final step of ATP generation. Thus, these data indicates mitochondrial OxPhos level is significantly increased and the bioenergetics process shift to mitochondrial OxPhos when MSCs are cultured on the NSQ50 surface for 5 days.

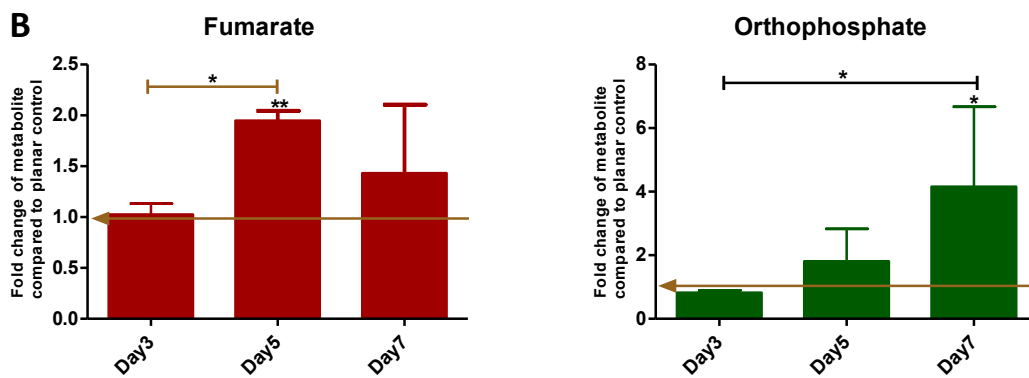
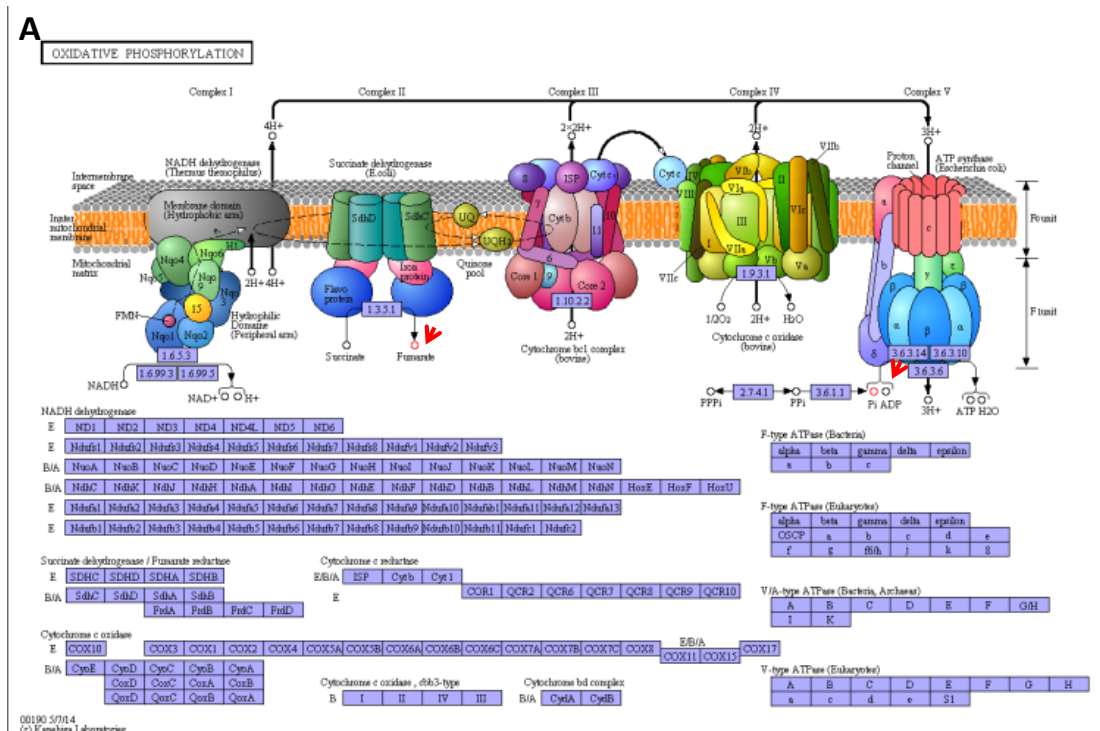


**Figure 5.7** NSQ50 surface shifting bioenergetics of MSCs to mitochondria.

Fumarate and orthophosphate are marked in the TCA pathway by KEGG pathway search (A, red arrows)). Both fumarate and orthophosphate were significantly increased after 5 days cell culture on the NSQ50 surface (B). (biological replicates: N=3,  $\pm$  SD), ANOVA analysis, \*  $p < 0.05$ , \*\*  $p < 0.01$ . Arrows on graphs show the control level. Panel A: Oxidative phosphorylation pathway (KEGG map: oo190). The top panel shows the electron transport chain in the inner membrane of mitochondrion, which consists of five enzymatic complexes (through complex I to complex V) to oxidase NADH. The blue rectangles at the bottom panel of A show the genes encoding the enzymatic complexes and enzymes involved in the oxidative phosphorylation.

### 5.3.5 The down-regulation of unsaturated fatty acids

Recent study has found stem cells possess different unsaturated fatty acid profiles from differentiated cells, which demonstrated unsaturated fatty acids are decreased in stem cell differentiation (Yanes et al., 2010). To get insight into the profile of unsaturated fatty acids in MSCs on the NSQ50 surface, fatty acid metabolites noted by identification in IDEOM were submitted to the KEGG database, and 12 metabolites involved in KEGG biosynthesis of unsaturated fatty acids were returned, which represent the features of unsaturated fatty acids in MSCs on the NSQ50 surface (Figure 5.8). Among those, 7 metabolites are unsaturated fatty acids and 5 are saturated fatty acids. Heatmap clustering analysis of fatty acids also demonstrated that most of fatty acids were down-regulated on the NSQ50 surface after 3 days cell culture and the fatty acids involved in KEGG biosynthesis of unsaturated fatty acids were noticed in the heatmap clustering (Figure 5.9).

Statistical analysis of these 12 fatty acids show that 3 out of 5 saturated fatty acids were significantly down-regulated from 3 days to 7 days cell cultured on NSQ50 surface when compared to their planar controls (Figure 5.10a, c, e), and one showed a clear downwards trend without statistically significant difference (Figure 5.10d) and the other appeared no different to control during the 7 day cell culture on the NSQ50 surface (Figure 5.10b). For the 7 unsaturated fatty acids, 6 of them were significantly down-regulated from 3 days to 7 days in cells cultured on NSQ50 surface when compared to their planar controls (Figure 5.10f, g, i, j, k, l), and one showed no difference at 7 days (Figure 5.10h). These data indicate that the profile of unsaturated fatty acids has changed and been characterized as down-regulation from MSCs cultured on the NSQ50 surface for 3 days.

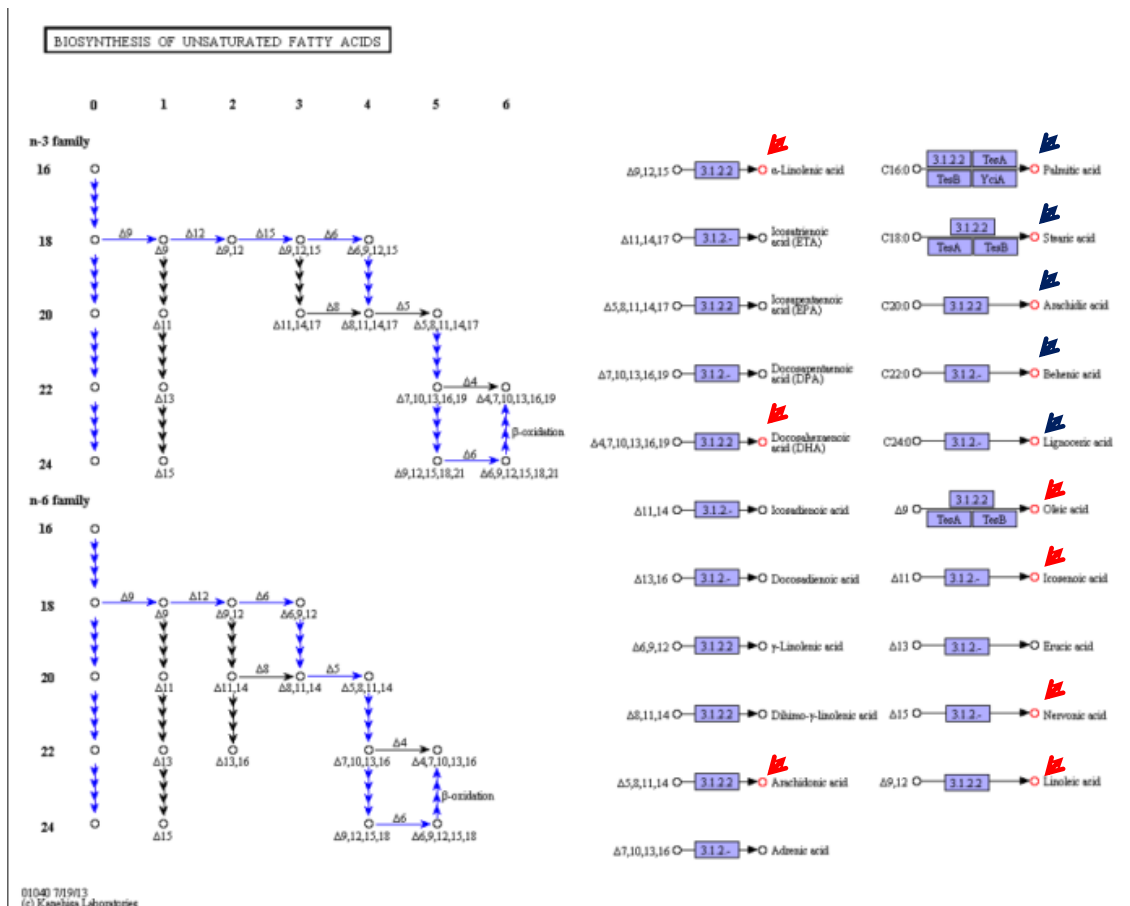


**Figure 5.8** Fatty acids involved in biosynthesis of unsaturated fatty acids in MSCs cultured on NSQ50 surface for 3, 5 and 7 days.

12 fatty acids were noted by KEGG pathway search which were involved in biosynthesis of unsaturated fatty acids in MSCs on the NSQ50 surface. Among those, 5 were saturated fatty acids (blue arrow) and 7 were unsaturated fatty acids (red arrow). Left panel:  $\Delta$  number: desaturase, blue arrows: enzymatic reaction steps. Right panel: blue rectangle: enzyme with KEGG accession number.

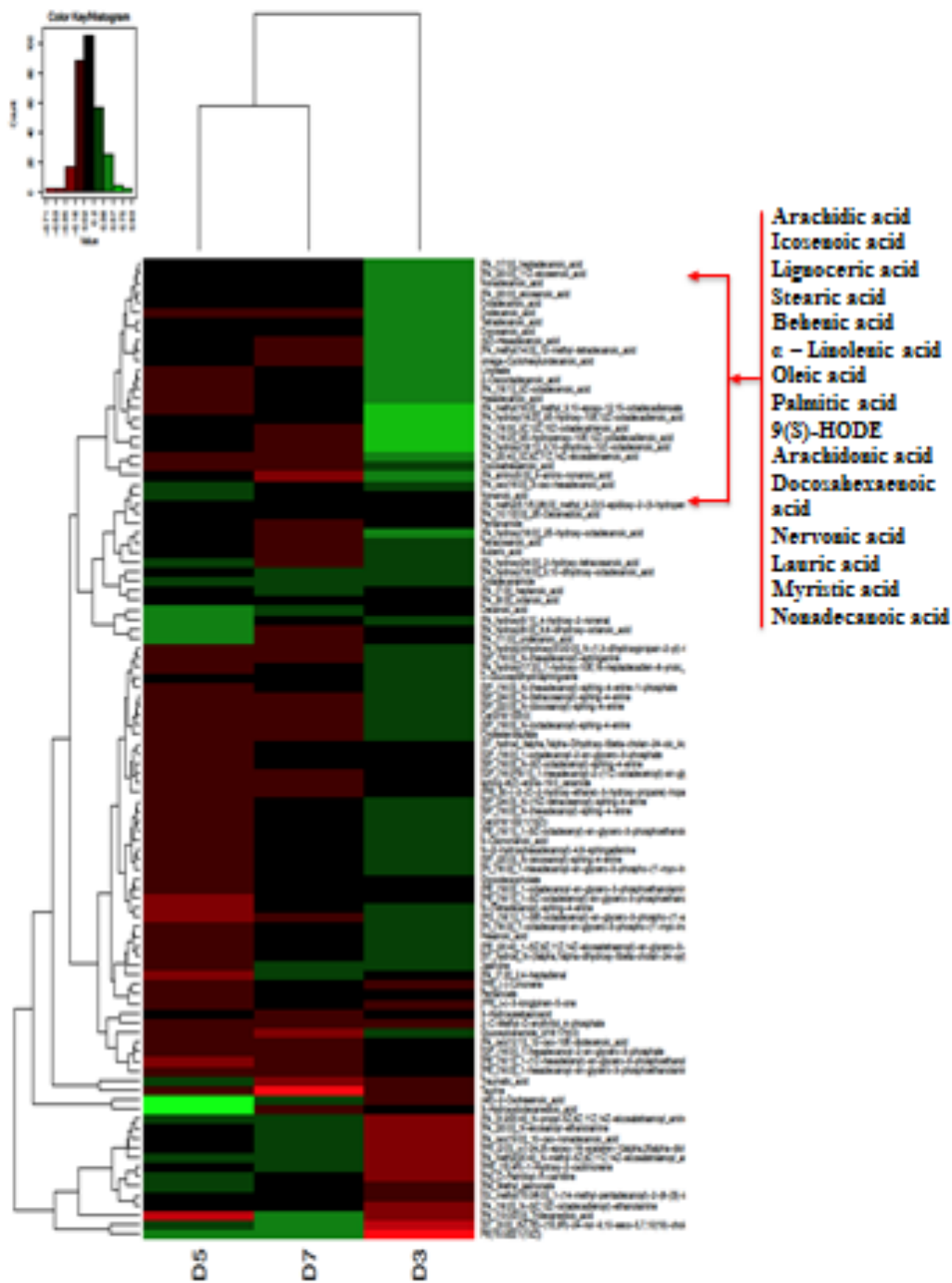


**Figure 5.9** Heatmap clustering of fatty acids in MSCs on the NSQ50 surface for cells cultured at 3, 5, and 7 days.

Heatmap clustering shows fatty acids fold change in MSCs cultured for 3 days (D3), 5 days (D5) and 7 days (D7), (biological replicates: N=3). The color range (top left corner) indicates the log-transformed fold change from down-regulation (red) to up-regulation (green). Fatty acids involved in KEGG biosynthesis of unsaturated fatty acids were noticed at the right corner.

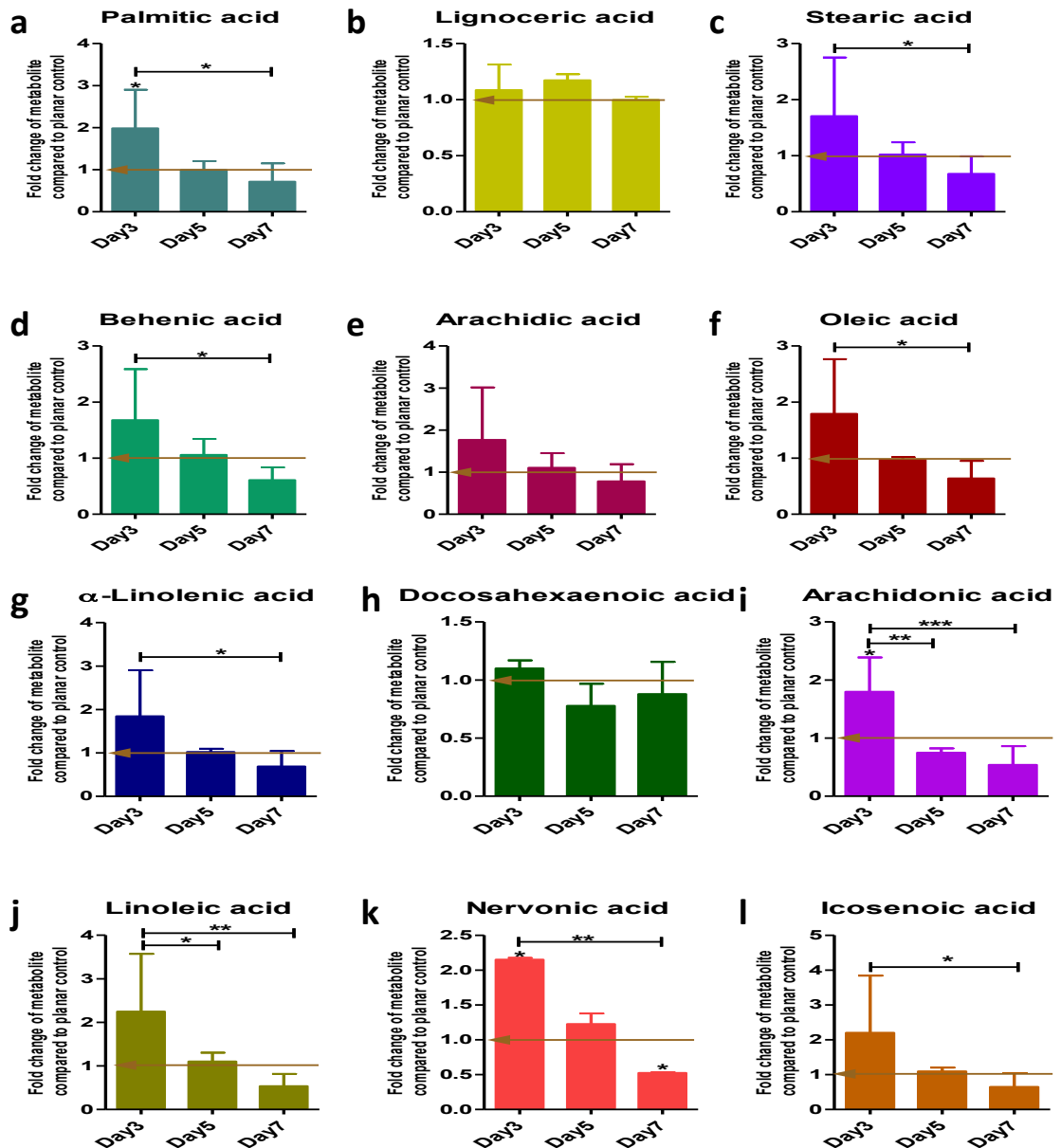


**Figure 5.10** Down-regulation of fatty acids involved in biosynthesis of unsaturated fatty acids in MSCs cultured on NSQ50 surface for 3, 5 and 7 days.

Seven unsaturated fatty acids were found in MSCs cultured on NSQ50 surface that were involved in biosynthesis of unsaturated fatty acids. Among them, six unsaturated fatty acids showed significant down-regulation (f, g, i, j, k and l), and one had no change (h) after 3 days cell culture. Five saturated fatty acids noted as being involved in the biosynthesis of unsaturated fatty acids were also highlighted. Three of them showed significant down-regulation (a, c and d) and one showed no change (b) after 5 days cell culture. The other one showed a clear downwards trend but no statistical significant difference was observed (e). (biological replicates: N=3,  $\pm$  SD) ANOVA analysis: \*  $p < 0.05$ , \*\*  $p < 0.01$ , \*\*\*  $p < 0.001$ . Arrows on graphs show the control level.

### **5.3.6 The relation of unsaturated fatty acids to signalling pathways**

#### **5.3.6.1 Unsaturated fatty acids induce Peroxisome proliferator-activated receptor gamma (PPARG) activity**

KEGG pathway search of the differentially regulated fatty acids showed eicosanoids have direct links to PPARG (Figure 5.11A). Eicosanoids are a group of compounds derived from polyunsaturated fatty acids, predominantly from arachidonic acid (Smith, 1989). 9(S)-HODE derived from linoleic acid metabolism is one of the eicosanoids noted by KEGG. Statistical analysis showed 9(S)-HODE was significantly down-regulated in MSCs on the NSQ50 surface after 3 days of cell culture (Figure 5.11B).

PPARG is nuclear receptor involved in transcriptional network to induce adipocyte commitment (Takada et al., 2009). Eicosanoids activate PPARG transcriptional cascades by binding to the receptor and subsequently result in MSC adipocyte differentiation (Tontonoz et al., 1994a; Tontonoz et al., 1994b). Thus, the significant down-regulation of 9(S)-HODE may reduce the activation of PPARG and inhibit adipocyte differentiation for MSCs on the NSQ50 surface. However, PPARG transcriptional activation is not only instigated by binding to eicosanoids, but also by binding to unsaturated fatty acids, such as linoleic acid, oleic acid and arachidonic acid (Kliwer et al., 1997; Kuniyasu, 2008). These unsaturated fatty acids showed significant down-regulation in MSCs on the NSQ50 surface in section 5.3.5 (Figure 5.10f, g, I and j). The down-regulation of these PPARG ligands indicates NSQ50 surface inhibits PPARG activity and thus inhibits adipocyte differentiation on the surface.

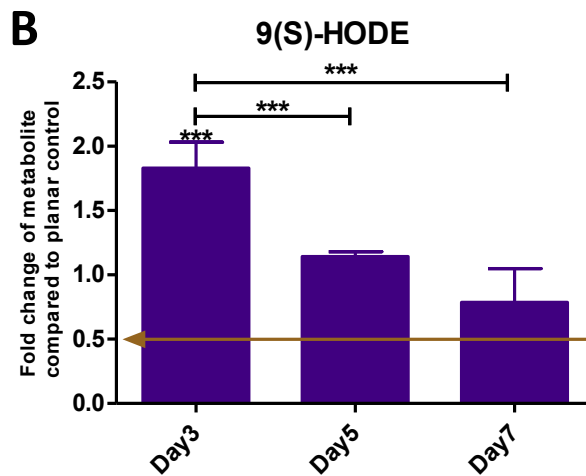
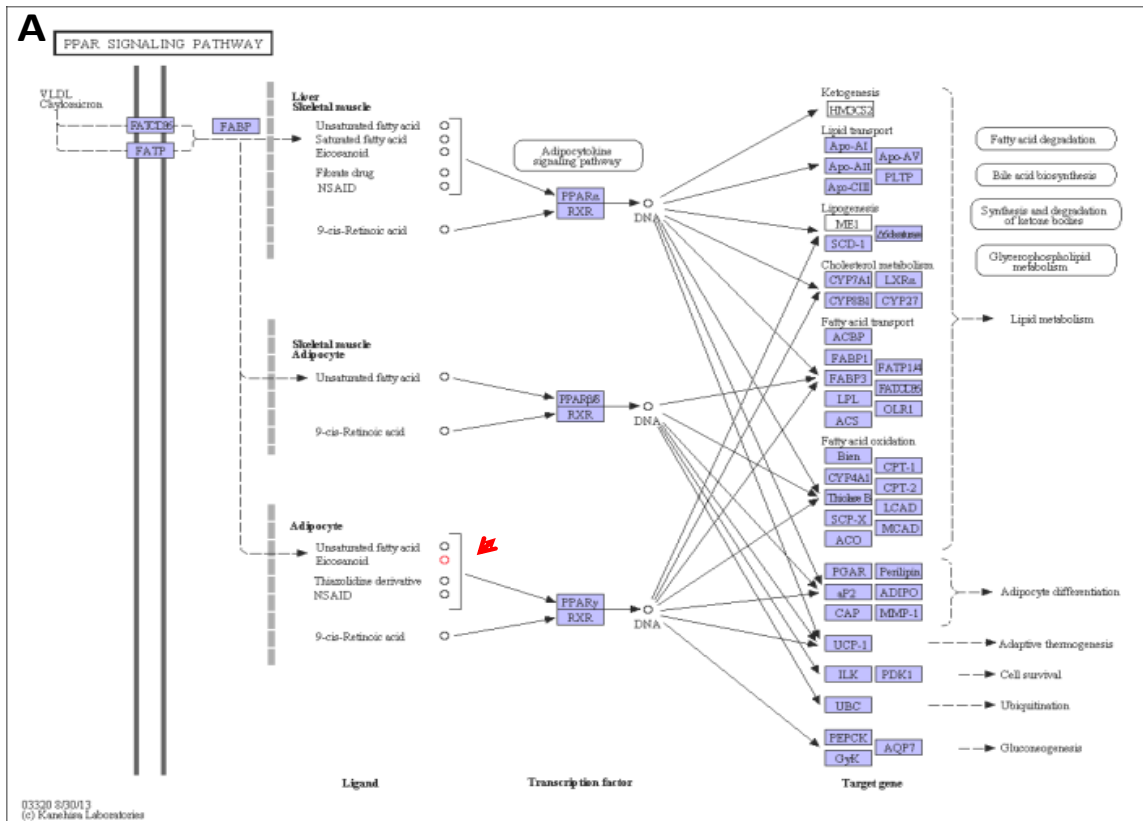


**Figure 5.11** The down-regulation of PPARG ligands in MSCs on the NSQ50 surface.

PPARG ligands, the eicosanoids, are noted in the PPAR signalling pathway by KEGG pathway searching for MSCs cultured on the NSQ50 surface for 3, 5 and 7 days, which directly link to PPARG signalling (A, red arrow). 9(S)-HODE, one of eicosanoids, showed significant down-regulation after MSCs were cultured on the NSQ surface. (biological replicates: N=3,  $\pm$  SD) ANOVA analysis: \*\*\*  $p < 0.001$ . Arrow on graph shows the control level. Panel A: PPAR signaling pathway (KEGG map 03320). The adipocyte differentiation pathway (bottom panel in A) shows PPARG ligands binding with PPARG and PRX which interact to DNA to regulate down-stream adipocyte genes (the blue rectangle with gene symbol).

### 5.3.6.2 The roles of fatty acids on Ca<sup>2+</sup> signalling

Fatty acids regulating Ca<sup>2+</sup> signalling have been characterized by modulation of voltage-gated L-type Ca<sup>2+</sup> current and long-chain fatty acids and polyunsaturated fatty acids appeared having different effects on the current (Xiao et al., 1997). It has been reported that polyunsaturated fatty acids inhibit this signalling, whereas long-chain fatty acids, such as lauric acid, can enhance Ca<sup>2+</sup> signalling (Shimada and Somlyo, 1992; Xiao et al., 1997). Polyunsaturated fatty acids, such as oleic acid and arachidonic acid were found to be significantly down-regulated in MSCs on the NSQ50 surface after 3 days of cell culture (section 5.3.5, Figure 5.10f, I). Three long chain saturated fatty acids associated with Ca<sup>2+</sup> signalling were changed in MSCs on the NSQ50 surface (lauric acid, myristic acid and nonadecanoic acid) and statistical analysis illustrated downwards trends for lauric and myristic acids in MSCs on NSQ50 surface after 3 days cell culture, and upwards trends were noted in nonadecanoic acid but no statistical significance was found (Figure 5.12).

Ca<sup>2+</sup> signalling has been recently found to enhance BMP2 expression and hence augment osteogenesis (Zayzafoon, 2006). Moreover, another recent study found Ca<sup>2+</sup> signalling exerts effects on BMP2 expression by the voltage-gated L-type Ca<sup>2+</sup> channel (Barradas et al., 2012). Thus, the significant down-regulation of unsaturated fatty acids in MSCs on the NSQ50 surface after 3 days cell culture may activate Ca<sup>2+</sup> signalling and subsequently contribute to BMP2 signalling as has been described in chapter 4.

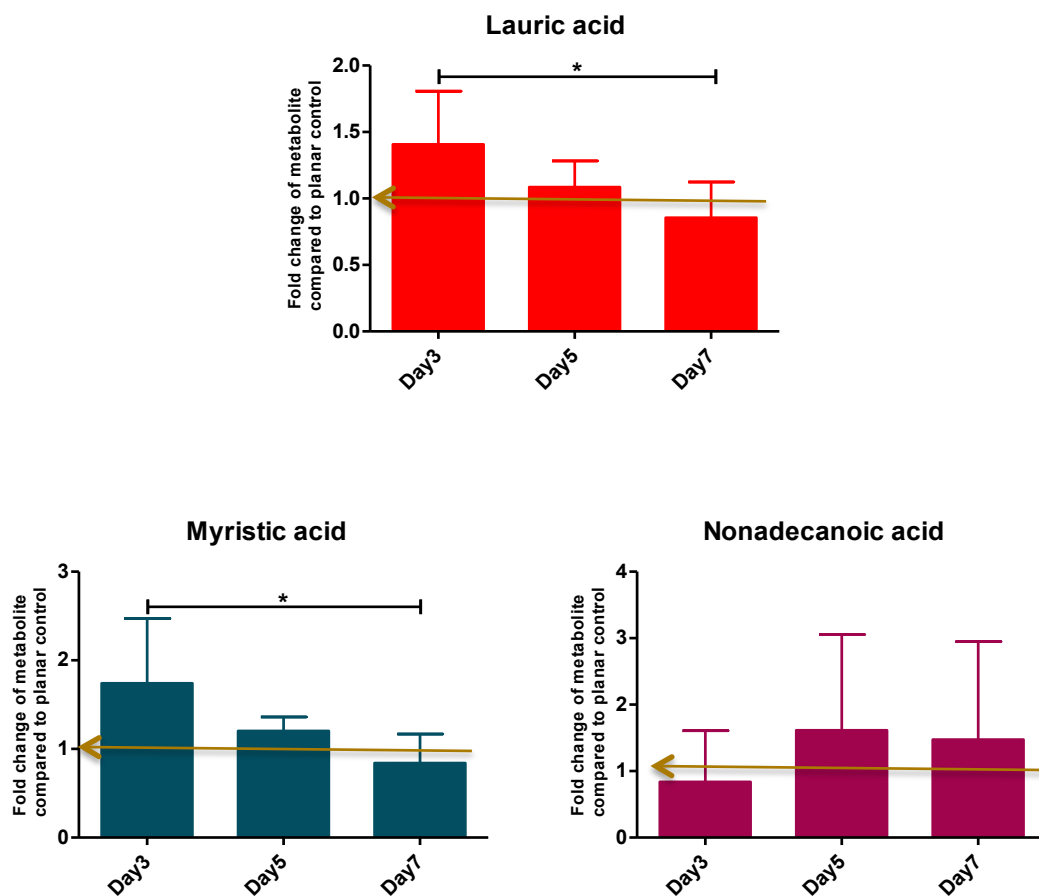


**Figure 5.12** The expression of long chain saturated fatty acids involved in the regulation of  $\text{Ca}^{2+}$  signalling in MSCs on the NSQ50 surface.

Lauric and myristic acids in MSCs on the NSQ50 surface showed downtrends after initial up-regulation at 3 days of cell culture, and nonadecanoic acid was up-regulated but not in a statistically significance manner. (biological replicates:  $N=3$ ,  $\pm$  SD) ANOVA analysis: \*  $p < 0.05$ . Arrows on graphs show the control level.

## 5.4 Discussion and conclusion

### 5.4.1 Discussion

Numerous studies on identifying stem cell self-renewal and lineage specific differentiation have been conducted on cell cycle regulators, transcription factors and their associated downstream pathways (Singh and Dalton, 2009). Recent advances in metabolomics have provided a systematic approach to get insight into stem cell metabolite features, their regulatory functions on stem cell fate determination and lineage specific differentiation, and potentially linking to transcriptional regulation and signalling pathways (Baumann, 2013; Ramm Sander et al., 2013).

Metabolites in MSCs cultured on the osteoinductive NSQ50 surface at early stage of lineage commitment (i.e., after 3 to 7 days exposed to the surface) were detected and measured by LC-MS. It is possible due to the the cells being in a lag phase in this early stage of culture on the surface that a restricted number of 400 metabolites were authentically or putatively identified. Clustering analysis of the metabolites in MSCs on the NSQ50 surface for the all-time points (3, 5 and 7 days cell culture) showed all categories of metabolites in MSCs for 5 and 7 days cell culture clustered together and differed from those at 3 days of cell culture. These data demonstrate that the metabolome had started to undergo large changes on the NSQ surface after this time point compared to control. Interestingly, the timing of this general pattern change is concurrent with the down-regulation of cell cycle regulator C-MYC and up-regulation of osteogenic transcription factor RUNX2, and the activation of BMP2 signalling which was identified in previous chapters, suggesting metabolites may be involved in the MSCs fate determination and osteogenic lineage specific differentiation, and thus may help provide detailed insight into the roles of metabolites for early stages of MSCs growth on the NSQ50 surface.

Stem cells switching from stemness to lineage specific commitment and subsequent differentiation is accompanied by a shift in the balance of anaerobic and aerobic bioenergetics to meet biosynthetic demands (Chung et al., 2007;

Varum et al., 2011). In MSCs cultured on the NSQ50 surface for 5 days, D-glucose, the main resources of cell bioenergetics was significantly decreased compared to 3 days cell culture, indicating MSCs consumed more glycolytic flux. However, the output of glycolysis remained almost the same as that of day 3, suggesting the glycolytic flux was alternatively utilized by mitochondria for bioenergetics and biosynthesis. MSCs cultured on the NSQ50 surface for 5 days, however, showed increased mitochondrial activity as illustrated by significant up-regulation of fumarate and orthophosphate which are produced by mitochondrial OxPhos and specifically orthophosphate is involved in the final step of OxPhos for ATP generation. These data indicates the shifting of bioenergetics in MSCs from anaerobic glycolysis to aerobic glycolysis. Such a shift has been proposed as necessity for stem cell switching to lineage specific differentiation, as OxPhos is highly efficient way for energy release to support stem cell differentiation (Chen et al., 2008; Cho et al., 2006; Lonergan et al., 2006).

Previous studies have demonstrated that undifferentiated stem cells contain high levels of unsaturated fatty acids (Yanes et al., 2010). These unsaturated structures are characterized as highly reactive metabolites to respond to oxidative conditions (redox plasticity), and thus whose levels decrease upon differentiation. MSCs cultured on the NSQ50 surface not only exhibit bioenergetic shift but also demonstrated significant decrease in unsaturated fatty acids after 3 days of culture. The down-regulation of unsaturated fatty acids on the surface indicates these metabolites are involved in the regulation of redox status and activation of oxidative pathways in mitochondria which regulate the balance between stem cell self-renewal and differentiation change on activation to osteogenesis (Smith et al., 2000). Stem cells maintain self-renewal under a reduced state, whereas they promote differentiation under oxidative state (Ezashi et al., 2005; Tsatmali et al., 2005). Thus, these data suggest MSCs on the NSQ50 surface initiate differentiation after 3 days and, again, this is consistent with the the establishment of signalling molecules promoting MSCs differentiation at the same time period in previous chapters.

The involvement of metabolites, specifically unsaturated fatty acids in MSC differentiation on the NSQ50 surface presented interesting questions about how these metabolites contribute to MSC osteogenic lineage specific commitment and differentiation. Signalling pathway analysis demonstrated that eicosanoids derived from polyunsaturated fatty acids directly link to PPAR $\gamma$  and serve as ligands to the nuclear receptor (Tontonoz et al., 1994b). Thus, the significant flux down-regulation of polyunsaturated fatty acids which was observed in MSCs on the NSQ50 surface after 3 days cell culture could perhaps inactivate PPAR $\gamma$  expression and subsequently inhibit adipocyte commitment. Considering the fact that adipocytes and osteoblasts share the same precursor in MSCs, the inhibition of adipocyte commitment would simultaneously enhance osteogenic differentiation of MSCs.

The roles of BMP2 signalling for osteogenesis of MSCs on the NSQ50 surface have been established in chapter 4. Recent study demonstrates that biomaterials which elicit high extracellular Ca<sup>2+</sup> concentration enhance BMP2 expression by the regulation of type L voltage-gated Ca<sup>2+</sup> channels (Barradas et al., 2012). Previous studies have established the roles of fatty acids for Ca<sup>2+</sup> signalling by regulation of type L voltage-gated Ca<sup>2+</sup> channels (Shimada and Somlyo, 1992; Xiao et al., 1997). Significant increases in long chain saturated fatty acids which possess the capacity of regulation on type L voltage-gated Ca<sup>2+</sup> channels, such as lauric acid were not observed in MSCs on the NSQ50 surface. However, unsaturated fatty acids, such as oleic acid, arachidonic acid, linolenic acid and linoleic acid were significantly down-regulated in MSCs on the surface and thus could contribute to Ca<sup>2+</sup> signalling. Thus, it is rational to propose that the down-regulation of unsaturated fatty acids could enhance Ca<sup>2+</sup> signalling and subsequently help induce BMP2 expression to impact the osteogenic commitment of MSCs on the NSQ50 surface.

#### **5.4.2 Conclusion**

Metabolomics is a valuable approach providing insights on stem cell fate commitment and other functions. Early time point investigation of metabolism of MSCs on the NSQ50 nanotopography that induced osteogenesis of MSCs

revealed metabolites changed and implied potential roles for metabolites in MSC osteogenic lineage specific commitment and differentiation.

Bioenergetics of MSC appears to shift to mitochondrial OxPhos for highly efficient ATP generation to meet the requirement of differentiating. This shifting results in the down-regulation of unsaturated fatty acids which play multiple regulatory roles for MSCs osteogenic fate determination and differentiation, and these observations are in line with the results of signalling molecules promoting MSCs osteogenic differentiation on the NSQ50 surface obtained in previous chapters.

## **Chapter 6. Conclusions and future work**

## Summary

The major conclusions identified in this project are described in this chapter, including the functional coupling of gene expression with MSC osteogenic differentiation on the NSQ50 surface, and molecular regulatory events underlying the nanotopography induced osteogenesis of MSCs. Conclusions are also drawn for the systematic features of MSCs investigated as a result of the original metabolomics data and the possible functional coupling of metabolites and signalling molecules in the regulation of osteogenesis of MSCs on the NSQ50 surface. Possible directions of enquiry for future work are also described.

## 6.1 Conclusions

Non-invasive nanotopographical features provide a valuable tool which has been used to investigate the molecular mechanisms regulating MSC fate determination and lineage specific differentiation. The NSQ50 nanotopography has been characterized for osteogenic phenotype induction of MSCs, providing a promising instrument to functionally activate MSCs osteogenic lineage specific differentiation. The functional biology of MSCs on the osteoinductive NSQ50 surface was investigated for three purposes: Firstly, to characterize functional relationship of the gene expression with the osteogenic differentiation process of MSCs on the surface, secondly to dissect the molecular regulatory events guiding MSC response to the surface, and finally to gain the insight of metabolism of MSCs on the surface with potential links to molecular signalling considered.

### 6.1.1 Functional coupling of gene expression and osteogenic differentiation

Genes involved in stem cell osteogenic differentiation can be categorised into two groups: genes encoding transcription factors and genes encoding osteogenic markers. Transcription factor genes such as C-MYC, RUNX2 and OSX, and osteogenic marker genes including ALP, OPN and OCN were selected for the study, whose temporal sequence expression would reflect the different stages of

MSCs osteogenic differentiation on the NSQ50 surface. This work was guided by the seminal work of Lian and Stein (Lian and Stein, 1992).

### **6.1.2 Transcriptional control of MSC osteogenic differentiation**

MSC self-renewal requires C-MYC expression, and expression of RUNX2 and OSX control MSCs osteogenic lineage specific differentiation. The results of temporal sequence expression of these transcription factors in MSC on the NSQ50 surface revealed that the significant down-regulation of C-MYC correlated with significant up-regulation of RUNX2 when MSCs cultured on NSQ50 surface for 5 days. These data suggest that MSCs switching the stemness to osteogenic lineage specific occurred at 5 days of culture on the surface. Significant up-regulation of OSX followed RUNX2 expression and occurred at 11 and 13 days cell culture, suggesting the OSX was required to complete the differentiation of osteoblast precursors to mature and functional osteoblasts. This ties in well with observations in the literature (Sinha and Zhou, 2013).

Mature osteoblasts are marked by high levels of expression of osteogenic marker genes such as ALP, OPN and OCN which were observed in MSCs on the NSQ50 surface after three weeks cell culture and followed by the matrix minerals produced by mature osteoblasts after 28 days cell culture on the surface. Further analysis by measuring expression of the transcription factors MSX2 and DLX5 which are mediated in RUNX2-independent of OSX expression (Liu et al., 2007b; Matsubara et al., 2008) suggested that OSX modulation was reliant on RUNX2 in MSCs on the NSQ50 surface.

### **6.1.3 BMP2 signalling and osteogenesis of MSCs on the NSQ50 surface**

BMP2 signalling was identified as the earliest molecular signal to induce RUNX2 and subsequent OPN expression. BMP2 and its receptor BMPR1A were significantly up-regulated after 3 days of culture on the surface. The results of down-regulation of RUNX2 by applying the BMP2 antagonist noggin which interacts with BMPR1A and inhibits BMP2 signalling (Gazzerro and Canalis, 2006)

indicated that the RUNX2 was regulated by BMP2 signalling. Furthermore, the inhibition of BMP2 signalling by noggin resulted in the down-regulation of OPN, suggesting the osteogenic differentiation of MSCs on the NSQ50 surface was stimulated by BMP2 signalling via RUNX2.

The regulatory effects of BMP2 signalling on the NSQ50 surface induced osteogenesis of the MSCs was also demonstrated in the regulation of miR-23b which is predicted to target RUNX2 by TargetScan. MiR-23b was significantly down-regulated when RUNX2 was induced in MSCs on the surface. However, inhibiting BMP2 signalling by addition of noggin resulted in the recovery of miR-23b and the down-regulation of RUNX2, indicating miR-23b targeting of RUNX2 was regulated by BMP2 signalling.

#### **6.1.4 Implicating integrin $\alpha\beta 5$ in osteogenesis of MSCs on the NSQ50 surface**

Integrin  $\alpha\beta 5$  was found up-regulated after 5 days of culture on the NSQ50 surface. However, inhibition of  $\beta 5$  by applying an antagonising anti- $\beta 5$  antibody in the culture medium resulted in almost unchanged expression of RUNX2. Further analysis indicated integrin  $\beta 3$  was up-regulated while  $\beta 5$  was inhibited suggesting that cells switched to using the alternative VN receptor (Hynes et al., 2002). Functionalizing the NSQ50 surface with the ligand of  $\alpha\beta 5$ , VN by immobilization resulted in up-regulation of RUNX2, suggesting that integrins are involved in the regulation of osteogenic differentiation of MSCs on the NSQ50 surface.

##### **6.1.5.1 Synergic effects of the interplay of BMP2 and integrin $\alpha\beta 5$ on osteogenesis of MSCs on the NSQ50 surface**

Integrin  $\alpha\beta 5$  was found to be regulated by BMP2 signalling on the NSQ50 surface. Expression of integrin  $\alpha\beta 5$  was suppressed by inhibiting BMP2 signalling, and subsequently resulted in down-regulation of vinculin. Further analysis of the relation of BMP2 signalling to integrin  $\alpha\beta 5$  expression demonstrated that BMPR1A co-localized to  $\alpha\beta 5$ . VN immobilisation further enhanced activation of

$\alpha$ v $\beta$ 5 and BMPR1A co-expression. The interplay of BMP2 signalling and integrin  $\alpha$ v $\beta$ 5 resulted in enhanced stimulation of RUNX2 in MSCs on NSQ50.

### **6.1.6 Metabolism of MSCs on the NSQ50 surface**

Stem cell fate commitment and lineage specific differentiation is a systematic biological process. Metabolomics data obtained from MSCs cultured on the NSQ50 surface at early stages of culture indicated that nanotopography induced MSC osteogenic differentiation was not only regulated by genetic modulation of MSCs but also synchronized by metabolism of the cells, and that was controlled by potential links between gene expression, signalling pathways and metabolic status of the cells (Katada et al., 2012).

Metabolic data indicated that the bioenergetics of MSCs on the surface shifted balance from anaerobic to aerobic processes after 3 days of cell culture and resulted in activation of mitochondrial OxPhos (Chen et al., 2008). This was illustrated by reduction of the glycolytic flux of D-glucose without increase in the output of glycolysis, but instead, increases in fumarate and orthophosphate were noted which are the products of OxPhos were significantly increased after 3 days of culture on the surface (Cho et al., 2006; Lonergan et al., 2006).

The metabolic data provided by growth of MSCs on the surface also demonstrated that unsaturated fatty acids, which are highly reactive metabolites and that respond to oxidative conditions (Yanes et al., 2010), were significantly decreased after 3 days of cell culture. This reduction indicated MSCs on the NSQ50 surface switched stem state to differentiation, as stem cells maintain self-renewal under a reduced state, and promote differentiation under oxidative state (Ezashi et al., 2005; Tzatzmali et al., 2005).

The reduction of unsaturated fatty acids on the surface also suggested possible links of metabolism with PPARG and BMP2 signalling pathways. Unsaturated fatty acids such as 9(S)-HODE act as ligands for PPARG (Tontonoz et al., 1994b). 9(S)-HODE was observed to be significantly down-regulation in MSCs on the NSQ50 surface after 3 days of cell culture, indicating the inhibition of adipocyte

commitment of the MSCs. Furthermore, unsaturated fatty acids such as oleic acid, arachidonic acid, linolenic acid and linoleic acid negatively regulate  $\text{Ca}^{2+}$  signalling that can enhance BMP2 expression (Barradas et al., 2012; Shimada and Somlyo, 1992; Xiao et al., 1997). Thus, the reduction of unsaturated fatty acids in MSCs on the NSQ50 surface may contribute to osteogenic lineage-specific commitment and differentiation in two ways: inhibition of MSC adipocyte commitment resulting in simultaneous osteogenic commitment of MSC; and up-regulation of  $\text{Ca}^{2+}$  signalling resulting in increased expression of BMP2.

## 6.2 Future work

Many aspects of the work in this thesis would be interesting to extend and could provide further insights into the interpretation of nanotopographical cues on MSC fate determination and lineage-specific differentiation.

NSQ50 induced MSC endogenous BMP2 expression would be interesting to explore further by quantifying the amount of BMP2 secreted by the cells. This would enable us to quantitatively estimate the rate of BMP2 generated by the cells on the surface and provide useful information for further osteogenic nanotopography designing and clinical application. RhBMP2 has been applied in clinical administration. Thus, if nanotopography can induce MSCs to secrete BMP2 at the level of clinic requirement, it would increase its usefulness for bone graft generation *in vitro*, but also for *in situ* bone repair *in vivo*. This is particularly important as clinical use of soluble BMP2 at the high doses required for effect has been implicated in serious respiratory, neurological, and inflammatory complications and these led the FDA to issue a Public Health Notification of life threatening complications associated with this clinical gold standard for bone repair (Lo et al., 2012; Vo et al., 2012; Woo, 2012).

The BMP2 signalling inducing RUNX2 via BMP2-SMAD1/5 and/or BMP2-miR-23b pathways and subsequently stimulates osteogenesis of MSCs on the NSQ50 surface has been established in this thesis. It would be interesting to distinguish the contributions of BMP2-SMADs and BMP2-miR-23b pathways to RUNX2

induction, and this could be achieved by manipulating the expression of either SMAD1/5 or miR-23b. Furthermore, identification of pathways through which BMP2 signalling regulates miR-23b would also be interesting work in the context of molecular mechanisms of MSCs fate determination and differentiation.

MiRNAs targeting osteogenic transcription factors, as investigated in this thesis, could also be extended. It would be interesting to investigate miRNA profiling for genome wide miRNA expression during different MSCs osteogenesis stages on the NSQ50 surface. This would enable us to identify more miRNAs which are involved in the regulation of MSC biological functions at different stages, and could be achieved by the high-throughput approaches as miRNA-array (Thomson et al., 2007) and miRNA-seq (Luo, 2012). This would also enable a wider comparison at genome level of the miRNA similarities and differences between undifferentiated MSCs and osteoblasts derived from MSCs, after induction by different methods (i.e., chemical induction (Li et al., 2014a), stiffness induction (Engler et al., 2006), confinement induction (McBeath et al., 2004), and nanotopography induction (Kilian et al., 2010)), and thus, provide unique miRNA signature for the insights into the regulatory mechanisms of nanotopographical cues.

Metabolism of MSCs on the NSQ50 surface investigated in this thesis could also extend in future. It would be interesting to directly measure enzymatic reactions in MSCs on the NSQ50 surface. For example, lactate production assay could allow the glycolytic flux to be assessed, and catalase which is antioxidant to reduce ROS in MSC could be measured by activity assay (Li et al., 2014b). Mitochondrial activity of MSCs could also be assessed by measuring mitochondrial mass or the relative mitochondrial DNA copy numbers. These would specifically show the bioenergetic features of MSCs on the NSQ50 surface and validate the data obtained by LC-MS. It would also be interesting to investigate the changes of MSC cellular metabolites influencing the epigenome. This would enable us to link metabolism with gene expression and signalling pathways of the MSCs on the NSQ50 surface and provide a comprehensive view of nanotopography action on MSC fate determination and differentiation.

## References

- Aarden, E.M., Burger, E.H., and Nijweide, P.J. (1994). Function of osteocytes in bone. *J Cell Biochem* 55, 287-299.
- Acampora, D., Merlo, G.R., Paleari, L., Zerega, B., Postiglione, M.P., Mantero, S., Bober, E., Barbieri, O., Simeone, A., and Levi, G. (1999). Craniofacial, vestibular and bone defects in mice lacking the Distal-less-related gene *Dlx5*. *Development* 126, 3795-3809.
- Ai, M., Holmen, S.L., Van Hul, W., Williams, B.O., and Warman, M.L. (2005). Reduced affinity to and inhibition by DKK1 form a common mechanism by which high bone mass-associated missense mutations in *LRP5* affect canonical Wnt signaling. *Mol Cell Biol* 25, 4946-4955.
- Aizawa, T., Kokubun, S., Kawamata, T., Tanaka, Y., and Roach, H.I. (1999). c-Myc protein in the rabbit growth plate. Changes in immunolocalisation with age and possible roles from proliferation to apoptosis. *J Bone Joint Surg Br* 81, 921-925.
- Ambros, V. (2004). The functions of animal microRNAs. *Nature* 431, 350-355.
- Arikawa, E., Sun, Y., Wang, J., Zhou, Q., Ning, B., Dial, S.L., Guo, L., and Yang, J. (2008). Cross-platform comparison of SYBR Green real-time PCR with TaqMan PCR, microarrays and other gene expression measurement technologies evaluated in the MicroArray Quality Control (MAQC) study. *BMC Genomics* 9, 328.
- Arinzeh, T.L., Peter, S.J., Archambault, M.P., van den Bos, C., Gordon, S., Kraus, K., Smith, A., and Kadiyala, S. (2003). Allogeneic mesenchymal stem cells regenerate bone in a critical-sized canine segmental defect. *J Bone Joint Surg Am* 85-A, 1927-1935.
- Ariotti, N., Liang, H., Xu, Y., Zhang, Y., Yonekubo, Y., Inder, K., Du, G., Parton, R.G., Hancock, J.F., and Plowman, S.J. (2010). Epidermal growth factor receptor activation remodels the plasma membrane lipid environment to induce nanocluster formation. *Mol Cell Biol* 30, 3795-3804.
- Arnaout, M.A., Mahalingam, B., and Xiong, J.P. (2005). Integrin structure, allostery, and bidirectional signaling. *Annu Rev Cell Dev Biol* 21, 381-410.
- Arnold, M., Cavalcanti-Adam, E.A., Glass, R., Blummel, J., Eck, W., Kanteleiner, M., Kessler, H., and Spatz, J.P. (2004). Activation of integrin function by nanopatterned adhesive interfaces. *Chemphyschem* 5, 383-388.
- Aronson, J. (1997). Limb-lengthening, skeletal reconstruction, and bone transport with the Ilizarov method. *J Bone Joint Surg Am* 79, 1243-1258.
- Arora, K., and Warrior, R. (2001). A new Smurf in the village. *Dev Cell* 1, 441-442.
- Artico, M., Ferrante, L., Pastore, F.S., Ramundo, E.O., Cantarelli, D., Scopelliti, D., and Iannetti, G. (2003). Bone autografting of the calvaria and craniofacial skeleton: historical background, surgical results in a series of 15 patients, and review of the literature. *Surg Neurol* 60, 71-79.
- Arvidson, K., Abdallah, B.M., Applegate, L.A., Baldini, N., Cenni, E., Gomez-Barrena, E., Granchi, D., Kassem, M., Konttinen, Y.T., Mustafa, K., *et al.* (2011). Bone regeneration and stem cells. *J Cell Mol Med* 15, 718-746.

- Arya, M., Shergill, I.S., Williamson, M., Gommersall, L., Arya, N., and Patel, H.R. (2005). Basic principles of real-time quantitative PCR. *Expert Rev Mol Diagn* 5, 209-219.
- Audige, L., Griffin, D., Bhandari, M., Kellam, J., and Ruedi, T.P. (2005). Path analysis of factors for delayed healing and nonunion in 416 operatively treated tibial shaft fractures. *Clin Orthop Relat Res* 438, 221-232.
- Baksh, D., Song, L., and Tuan, R.S. (2004). Adult mesenchymal stem cells: characterization, differentiation, and application in cell and gene therapy. *J Cell Mol Med* 8, 301-316.
- Bandyopadhyay, A., Tsuji, K., Cox, K., Harfe, B.D., Rosen, V., and Tabin, C.J. (2006). Genetic analysis of the roles of BMP2, BMP4, and BMP7 in limb patterning and skeletogenesis. *PLoS Genet* 2, e216.
- Barbuto, R., and Mitchell, J. (2013). Regulation of the osterix (Osx, Sp7) promoter by osterix and its inhibition by parathyroid hormone. *J Mol Endocrinol* 51, 99-108.
- Barradas, A.M., Fernandes, H.A., Groen, N., Chai, Y.C., Schrooten, J., van de Peppel, J., van Leeuwen, J.P., van Blitterswijk, C.A., and de Boer, J. (2012). A calcium-induced signaling cascade leading to osteogenic differentiation of human bone marrow-derived mesenchymal stromal cells. *Biomaterials* 33, 3205-3215.
- Barradas, A.M., Yuan, H., van Blitterswijk, C.A., and Habibovic, P. (2011). Osteoinductive biomaterials: current knowledge of properties, experimental models and biological mechanisms. *Eur Cell Mater* 21, 407-429; discussion 429.
- Bartholomew, A., Sturgeon, C., Siatskas, M., Ferrer, K., McIntosh, K., Patil, S., Hardy, W., Devine, S., Ucker, D., Deans, R., *et al.* (2002). Mesenchymal stem cells suppress lymphocyte proliferation in vitro and prolong skin graft survival in vivo. *Exp Hematol* 30, 42-48.
- Baumann, K. (2013). Stem cells: A metabolic switch. *Nat Rev Mol Cell Biol* 14, 64-65.
- Bautista, D.S., Xuan, J.W., Hota, C., Chambers, A.F., and Harris, J.F. (1994). Inhibition of Arg-Gly-Asp (RGD)-mediated cell adhesion to osteopontin by a monoclonal antibody against osteopontin. *J Biol Chem* 269, 23280-23285.
- Benayahu, D., Fried, A., Efraty, M., Robey, P.G., and Wientroub, S. (1995). Bone marrow interface: preferential attachment of an osteoblastic marrow stromal cell line. *J Cell Biochem* 59, 151-160.
- Bennett, C.N., Longo, K.A., Wright, W.S., Suva, L.J., Lane, T.F., Hankenson, K.D., and MacDougald, O.A. (2005). Regulation of osteoblastogenesis and bone mass by Wnt10b. *Proc Natl Acad Sci U S A* 102, 3324-3329.
- Bettinger, C.J., Zhang, Z., Gerecht, S., Borenstein, J.T., and Langer, R. (2008). Enhancement of In Vitro Capillary Tube Formation by Substrate Nanotopography. *Adv Mater* 20, 99-103.
- Bianco, P., Riminucci, M., Gronthos, S., and Robey, P.G. (2001). Bone marrow stromal stem cells: nature, biology, and potential applications. *Stem Cells* 19, 180-192.
- Biggs, M.J., Richards, R.G., Gadegaard, N., Wilkinson, C.D., Oreffo, R.O., and Dalby, M.J. (2009). The use of nanoscale topography to modulate the dynamics of adhesion formation in primary osteoblasts and ERK/MAPK signalling in STRO-1+ enriched skeletal stem cells. *Biomaterials* 30, 5094-5103.

- Biggs, M.J., Richards, R.G., McFarlane, S., Wilkinson, C.D., Oreffo, R.O., and Dalby, M.J. (2008). Adhesion formation of primary human osteoblasts and the functional response of mesenchymal stem cells to 330nm deep microgrooves. *J R Soc Interface* 5, 1231-1242.
- Boiani, M., and Scholer, H.R. (2005). Regulatory networks in embryo-derived pluripotent stem cells. *Nat Rev Mol Cell Biol* 6, 872-884.
- Boskey, A.L. (1998). Biomineralization: conflicts, challenges, and opportunities. *J Cell Biochem Suppl* 30-31, 83-91.
- Boutin, P. (1972). [Total arthroplasty of the hip by fritted aluminum prosthesis. Experimental study and 1st clinical applications]. *Rev Chir Orthop Reparatrice Appar Mot* 58, 229-246.
- Boyden, L.M., Mao, J., Belsky, J., Mitzner, L., Farhi, A., Mitnick, M.A., Wu, D., Insogna, K., and Lifton, R.P. (2002). High bone density due to a mutation in LDL-receptor-related protein 5. *N Engl J Med* 346, 1513-1521.
- Boyer, L.A., Plath, K., Zeitlinger, J., Brambrink, T., Medeiros, L.A., Lee, T.I., Levine, S.S., Wernig, M., Tajonar, A., Ray, M.K., *et al.* (2006). Polycomb complexes repress developmental regulators in murine embryonic stem cells. *Nature* 441, 349-353.
- Boyle, W.J., Simonet, W.S., and Lacey, D.L. (2003). Osteoclast differentiation and activation. *Nature* 423, 337-342.
- Brandi, M.L. (2009). Microarchitecture, the key to bone quality. *Rheumatology (Oxford)* 48 Suppl 4, iv3-8.
- Brodsky, B., and Persikov, A.V. (2005). Molecular structure of the collagen triple helix. *Adv Protein Chem* 70, 301-339.
- Bruder, S.P., Jaiswal, N., and Haynesworth, S.E. (1997). Growth kinetics, self-renewal, and the osteogenic potential of purified human mesenchymal stem cells during extensive subcultivation and following cryopreservation. *J Cell Biochem* 64, 278-294.
- Bruder, S.P., Kurth, A.A., Shea, M., Hayes, W.C., Jaiswal, N., and Kadiyala, S. (1998). Bone regeneration by implantation of purified, culture-expanded human mesenchymal stem cells. *J Orthop Res* 16, 155-162.
- Buchet, R., Pikula, S., Magne, D., and Mebarek, S. (2013). Isolation and characteristics of matrix vesicles. *Methods Mol Biol* 1053, 115-124.
- Butler, D.L., Goldstein, S.A., and Guilak, F. (2000). Functional tissue engineering: the role of biomechanics. *J Biomech Eng* 122, 570-575.
- Buttery, L.D., Bourne, S., Xynos, J.D., Wood, H., Hughes, F.J., Hughes, S.P., Episkopou, V., and Polak, J.M. (2001). Differentiation of osteoblasts and in vitro bone formation from murine embryonic stem cells. *Tissue Eng* 7, 89-99.
- Cai, L., Sutter, B.M., Li, B., and Tu, B.P. (2011). Acetyl-CoA induces cell growth and proliferation by promoting the acetylation of histones at growth genes. *Mol Cell* 42, 426-437.
- Calderwood, D.A. (2004). Integrin activation. *J Cell Sci* 117, 657-666.
- Calderwood, D.A., Shattil, S.J., and Ginsberg, M.H. (2000). Integrins and actin filaments: reciprocal regulation of cell adhesion and signaling. *J Biol Chem* 275, 22607-22610.

- Campbell, I.D. (2008). Studies of focal adhesion assembly. *Biochem Soc Trans* 36, 263-266.
- Cassidy, J.W., Roberts, J.N., Smith, C.A., Robertson, M., White, K., Biggs, M.J., Oreffo, R.O., and Dalby, M.J. (2014). Osteogenic lineage restriction by osteoprogenitors cultured on nanometric grooved surfaces: the role of focal adhesion maturation. *Acta Biomater* 10, 651-660.
- Cavalcanti-Adam, E.A., Micoulet, A., Blummel, J., Auernheimer, J., Kessler, H., and Spatz, J.P. (2006). Lateral spacing of integrin ligands influences cell spreading and focal adhesion assembly. *Eur J Cell Biol* 85, 219-224.
- Cavalcanti-Adam, E.A., Volberg, T., Micoulet, A., Kessler, H., Geiger, B., and Spatz, J.P. (2007). Cell spreading and focal adhesion dynamics are regulated by spacing of integrin ligands. *Biophys J* 92, 2964-2974.
- Chen, C.T., Shih, Y.R., Kuo, T.K., Lee, O.K., and Wei, Y.H. (2008). Coordinated changes of mitochondrial biogenesis and antioxidant enzymes during osteogenic differentiation of human mesenchymal stem cells. *Stem Cells* 26, 960-968.
- Chen, J.F., Mandel, E.M., Thomson, J.M., Wu, Q., Callis, T.E., Hammond, S.M., Conlon, F.L., and Wang, D.Z. (2006). The role of microRNA-1 and microRNA-133 in skeletal muscle proliferation and differentiation. *Nat Genet* 38, 228-233.
- Chen, X., Li, X., Wang, W., and Lufkin, T. (1996). Dlx5 and Dlx6: an evolutionary conserved pair of murine homeobox genes expressed in the embryonic skeleton. *Ann N Y Acad Sci* 785, 38-47.
- Cheng, S.L., Shao, J.S., Charlton-Kachigian, N., Loewy, A.P., and Towler, D.A. (2003). MSX2 promotes osteogenesis and suppresses adipogenic differentiation of multipotent mesenchymal progenitors. *J Biol Chem* 278, 45969-45977.
- Cho, Y.M., Kwon, S., Pak, Y.K., Seol, H.W., Choi, Y.M., Park do, J., Park, K.S., and Lee, H.K. (2006). Dynamic changes in mitochondrial biogenesis and antioxidant enzymes during the spontaneous differentiation of human embryonic stem cells. *Biochem Biophys Res Commun* 348, 1472-1478.
- Choi, C.H., Hagvall, S.H., Wu, B.M., Dunn, J.C., Beygui, R.E., and CJ, C.J.K. (2007). Cell interaction with three-dimensional sharp-tip nanotopography. *Biomaterials* 28, 1672-1679.
- Choi, K.Y., Kim, H.J., Lee, M.H., Kwon, T.G., Nah, H.D., Furuichi, T., Komori, T., Nam, S.H., Kim, Y.J., and Ryoo, H.M. (2005). Runx2 regulates FGF2-induced Bmp2 expression during cranial bone development. *Dev Dyn* 233, 115-121.
- Christel, P., Meunier, A., Dorlot, J.M., Crolet, J.M., Witvoet, J., Sedel, L., and Boutin, P. (1988). Biomechanical compatibility and design of ceramic implants for orthopedic surgery. *Ann N Y Acad Sci* 523, 234-256.
- Chrzanowska-Wodnicka, M., and Burridge, K. (1996). Rho-stimulated contractility drives the formation of stress fibers and focal adhesions. *J Cell Biol* 133, 1403-1415.
- Chung, S., Dzeja, P.P., Faustino, R.S., Perez-Terzic, C., Behfar, A., and Terzic, A. (2007). Mitochondrial oxidative metabolism is required for the cardiac differentiation of stem cells. *Nat Clin Pract Cardiovasc Med* 4 *Suppl* 1, S60-67.

- Ciccione, W.J., 2nd, Motz, C., Bentley, C., and Tasto, J.P. (2001). Bioabsorbable implants in orthopaedics: new developments and clinical applications. *J Am Acad Orthop Surg* 9, 280-288.
- Clegg, R.M. (1992). Fluorescence resonance energy transfer and nucleic acids. *Methods Enzymol* 211, 353-388.
- Cohen, M.M., Jr. (2006). The new bone biology: pathologic, molecular, and clinical correlates. *Am J Med Genet A* 140, 2646-2706.
- Compton, S.J., and Jones, C.G. (1985). Mechanism of dye response and interference in the Bradford protein assay. *Anal Biochem* 151, 369-374.
- Creek, D.J., Jankevics, A., Breitling, R., Watson, D.G., Barrett, M.P., and Burgess, K.E. (2011). Toward global metabolomics analysis with hydrophilic interaction liquid chromatography-mass spectrometry: improved metabolite identification by retention time prediction. *Anal Chem* 83, 8703-8710.
- Creek, D.J., Jankevics, A., Burgess, K.E., Breitling, R., and Barrett, M.P. (2012). IDEOM: an Excel interface for analysis of LC-MS-based metabolomics data. *Bioinformatics* 28, 1048-1049.
- Crisostomo, P.R., Wang, M., Wairiuko, G.M., Morrell, E.D., Terrell, A.M., Seshadri, P., Nam, U.H., and Meldrum, D.R. (2006). High passage number of stem cells adversely affects stem cell activation and myocardial protection. *Shock* 26, 575-580.
- Crisp, M., Liu, Q., Roux, K., Rattner, J.B., Shanahan, C., Burke, B., Stahl, P.D., and Hodzic, D. (2006). Coupling of the nucleus and cytoplasm: role of the LINC complex. *J Cell Biol* 172, 41-53.
- Curtis, A.S., and Varde, M. (1964). Control of Cell Behavior: Topological Factors. *J Natl Cancer Inst* 33, 15-26.
- Dalby, M.J., Biggs, M.J., Gadegaard, N., Kalna, G., Wilkinson, C.D., and Curtis, A.S. (2007a). Nanotopographical stimulation of mechanotransduction and changes in interphase centromere positioning. *J Cell Biochem* 100, 326-338.
- Dalby, M.J., Gadegaard, N., Curtis, A.S., and Oreffo, R.O. (2007b). Nanotopographical control of human osteoprogenitor differentiation. *Curr Stem Cell Res Ther* 2, 129-138.
- Dalby, M.J., Gadegaard, N., Herzyk, P., Sutherland, D., Agheli, H., Wilkinson, C.D., and Curtis, A.S. (2007c). Nanomechanotransduction and interphase nuclear organization influence on genomic control. *J Cell Biochem* 102, 1234-1244.
- Dalby, M.J., Gadegaard, N., and Oreffo, R.O. (2014). Harnessing nanotopography and integrin-matrix interactions to influence stem cell fate. *Nat Mater* 13, 558-569.
- Dalby, M.J., Gadegaard, N., Tare, R., Andar, A., Riehle, M.O., Herzyk, P., Wilkinson, C.D., and Oreffo, R.O. (2007d). The control of human mesenchymal cell differentiation using nanoscale symmetry and disorder. *Nat Mater* 6, 997-1003.
- Dalby, M.J., McCloy, D., Robertson, M., Agheli, H., Sutherland, D., Affrossman, S., and Oreffo, R.O. (2006a). Osteoprogenitor response to semi-ordered and random nanotopographies. *Biomaterials* 27, 2980-2987.

- Dalby, M.J., McCloy, D., Robertson, M., Wilkinson, C.D., and Oreffo, R.O. (2006b). Osteoprogenitor response to defined topographies with nanoscale depths. *Biomaterials* **27**, 1306-1315.
- Dalby, M.J., Riehle, M.O., Johnstone, H.J., Affrossman, S., and Curtis, A.S. (2003). Nonadhesive nanotopography: fibroblast response to poly(n-butyl methacrylate)-poly(styrene) demixed surface features. *J Biomed Mater Res A* **67**, 1025-1032.
- Das, A., and Botchwey, E. (2011). Evaluation of angiogenesis and osteogenesis. *Tissue Eng Part B Rev* **17**, 403-414.
- de Baat, P., Heijboer, M.P., and de Baat, C. (2005). [Development, physiology, and cell activity of bone]. *Ned Tijdschr Tandheelkd* **112**, 258-263.
- de Jong, D.S., Steegenga, W.T., Hendriks, J.M., van Zoelen, E.J., Olijve, W., and Dechering, K.J. (2004). Regulation of Notch signaling genes during BMP2-induced differentiation of osteoblast precursor cells. *Biochem Biophys Res Commun* **320**, 100-107.
- DeBerardinis, R.J., Lum, J.J., Hatzivassiliou, G., and Thompson, C.B. (2008). The biology of cancer: metabolic reprogramming fuels cell growth and proliferation. *Cell Metab* **7**, 11-20.
- Deng, Z.L., Sharff, K.A., Tang, N., Song, W.X., Luo, J., Luo, X., Chen, J., Bennett, E., Reid, R., Manning, D., *et al.* (2008). Regulation of osteogenic differentiation during skeletal development. *Front Biosci* **13**, 2001-2021.
- Denhardt, D.T., Giachelli, C.M., and Rittling, S.R. (2001). Role of osteopontin in cellular signaling and toxicant injury. *Annu Rev Pharmacol Toxicol* **41**, 723-749.
- Depew, M.J., Liu, J.K., Long, J.E., Presley, R., Meneses, J.J., Pedersen, R.A., and Rubenstein, J.L. (1999). Dlx5 regulates regional development of the branchial arches and sensory capsules. *Development* **126**, 3831-3846.
- Dinopoulos, H., Dimitriou, R., and Giannoudis, P.V. (2012). Bone graft substitutes: What are the options? *Surgeon* **10**, 230-239.
- Dominici, M., Le Blanc, K., Mueller, I., Slaper-Cortenbach, I., Marini, F., Krause, D., Deans, R., Keating, A., Prockop, D., and Horwitz, E. (2006). Minimal criteria for defining multipotent mesenchymal stromal cells. The International Society for Cellular Therapy position statement. *Cytotherapy* **8**, 315-317.
- Drosse, I., Volkmer, E., Capanna, R., De Biase, P., Mutschler, W., and Schieker, M. (2008). Tissue engineering for bone defect healing: an update on a multi-component approach. *Injury* **39 Suppl 2**, S9-20.
- Ducheyne, P., and Healy, K.E. (1988). The effect of plasma-sprayed calcium phosphate ceramic coatings on the metal ion release from porous titanium and cobalt-chromium alloys. *J Biomed Mater Res* **22**, 1137-1163.
- Ducheyne, P., Radin, S., Heughebaert, M., and Heughebaert, J.C. (1990). Calcium phosphate ceramic coatings on porous titanium: effect of structure and composition on electrophoretic deposition, vacuum sintering and in vitro dissolution. *Biomaterials* **11**, 244-254.

- Ducy, P., Desbois, C., Boyce, B., Pinero, G., Story, B., Dunstan, C., Smith, E., Bonadio, J., Goldstein, S., Gundberg, C., *et al.* (1996). Increased bone formation in osteocalcin-deficient mice. *Nature* 382, 448-452.
- Ducy, P., Zhang, R., Geoffroy, V., Ridall, A.L., and Karsenty, G. (1997). *Osf2/Cbfa1*: a transcriptional activator of osteoblast differentiation. *Cell* 89, 747-754.
- Engler, A.J., Sen, S., Sweeney, H.L., and Discher, D.E. (2006). Matrix elasticity directs stem cell lineage specification. *Cell* 126, 677-689.
- Evans, E.A., and Calderwood, D.A. (2007). Forces and bond dynamics in cell adhesion. *Science* 316, 1148-1153.
- Ezashi, T., Das, P., and Roberts, R.M. (2005). Low O<sub>2</sub> tensions and the prevention of differentiation of hES cells. *Proc Natl Acad Sci U S A* 102, 4783-4788.
- Ferre, F. (1992). Quantitative or semi-quantitative PCR: reality versus myth. *PCR Methods Appl* 2, 1-9.
- Fisher, J., and Dowson, D. (1991). Tribology of total artificial joints. *Proc Inst Mech Eng H* 205, 73-79.
- Flemming, R.G., Murphy, C.J., Abrams, G.A., Goodman, S.L., and Nealey, P.F. (1999). Effects of synthetic micro- and nano-structured surfaces on cell behavior. *Biomaterials* 20, 573-588.
- Friedenstein, A.J., Deriglasova, U.F., Kulagina, N.N., Panasuk, A.F., Rudakowa, S.F., Luria, E.A., and Ruadkow, I.A. (1974). Precursors for fibroblasts in different populations of hematopoietic cells as detected by the in vitro colony assay method. *Exp Hematol* 2, 83-92.
- Friedenstein, A.J., Petrakova, K.V., Kurolesova, A.I., and Frolova, G.P. (1968). Heterotopic of bone marrow. Analysis of precursor cells for osteogenic and hematopoietic tissues. *Transplantation* 6, 230-247.
- Friedl, P. (2004). Prespecification and plasticity: shifting mechanisms of cell migration. *Curr Opin Cell Biol* 16, 14-23.
- Galindo, M., Pratap, J., Young, D.W., Hovhannisyan, H., Im, H.J., Choi, J.Y., Lian, J.B., Stein, J.L., Stein, G.S., and van Wijnen, A.J. (2005). The bone-specific expression of *Runx2* oscillates during the cell cycle to support a G1-related antiproliferative function in osteoblasts. *J Biol Chem* 280, 20274-20285.
- Gallea, S., Lallemand, F., Atfi, A., Rawadi, G., Ramez, V., Spinella-Jaegle, S., Kawai, S., Faucheu, C., Huet, L., Baron, R., *et al.* (2001). Activation of mitogen-activated protein kinase cascades is involved in regulation of bone morphogenetic protein-2-induced osteoblast differentiation in pluripotent C2C12 cells. *Bone* 28, 491-498.
- Gaur, T., Lengner, C.J., Hovhannisyan, H., Bhat, R.A., Bodine, P.V., Komm, B.S., Javed, A., van Wijnen, A.J., Stein, J.L., Stein, G.S., *et al.* (2005). Canonical WNT signaling promotes osteogenesis by directly stimulating *Runx2* gene expression. *J Biol Chem* 280, 33132-33140.
- Gautschi, O.P., Frey, S.P., and Zellweger, R. (2007). Bone morphogenetic proteins in clinical applications. *ANZ J Surg* 77, 626-631.

- Gazzerro, E., and Canalis, E. (2006). Bone morphogenetic proteins and their antagonists. *Rev Endocr Metab Disord* 7, 51-65.
- Geiger, B., Spatz, J.P., and Bershadsky, A.D. (2009). Environmental sensing through focal adhesions. *Nat Rev Mol Cell Biol* 10, 21-33.
- Giachelli, C.M. (2001). Ectopic calcification: new concepts in cellular regulation. *Z Kardiol* 90 Suppl 3, 31-37.
- Giannoudis, P.V., Dinopoulos, H., and Tsiridis, E. (2005). Bone substitutes: an update. *Injury* 36 Suppl 3, S20-27.
- Giulietti, A., Overbergh, L., Valckx, D., Decallonne, B., Bouillon, R., and Mathieu, C. (2001). An overview of real-time quantitative PCR: applications to quantify cytokine gene expression. *Methods* 25, 386-401.
- Goessler, U.R., Bugert, P., Bieback, K., Stern-Straeter, J., Bran, G., Hormann, K., and Riedel, F. (2008). Integrin expression in stem cells from bone marrow and adipose tissue during chondrogenic differentiation. *Int J Mol Med* 21, 271-279.
- Gong, Y., Slee, R.B., Fukai, N., Rawadi, G., Roman-Roman, S., Reginato, A.M., Wang, H., Cundy, T., Glorieux, F.H., Lev, D., *et al.* (2001). LDL receptor-related protein 5 (LRP5) affects bone accrual and eye development. *Cell* 107, 513-523.
- Gradl, D., Kuhl, M., and Wedlich, D. (1999). The Wnt/Wg signal transducer beta-catenin controls fibronectin expression. *Mol Cell Biol* 19, 5576-5587.
- Greenblatt, M.B., Shim, J.H., Zou, W., Sitara, D., Schweitzer, M., Hu, D., Lotinun, S., Sano, Y., Baron, R., Park, J.M., *et al.* (2010). The p38 MAPK pathway is essential for skeletogenesis and bone homeostasis in mice. *J Clin Invest* 120, 2457-2473.
- Greenwood, J.A., and Murphy-Ullrich, J.E. (1998). Signaling of de-adhesion in cellular regulation and motility. *Microsc Res Tech* 43, 420-432.
- Gruenloh, W., Kambal, A., Sondergaard, C., McGee, J., Nacey, C., Kalomoiris, S., Pepper, K., Olson, S., Fierro, F., and Nolte, J.A. (2011). Characterization and in vivo testing of mesenchymal stem cells derived from human embryonic stem cells. *Tissue Eng Part A* 17, 1517-1525.
- Guarino, V., Causa, F., and Ambrosio, L. (2007). Bioactive scaffolds for bone and ligament tissue. *Expert Rev Med Devices* 4, 405-418.
- Guicheux, J., Lemonnier, J., Ghayor, C., Suzuki, A., Palmer, G., and Caverzasio, J. (2003). Activation of p38 mitogen-activated protein kinase and c-Jun-NH2-terminal kinase by BMP-2 and their implication in the stimulation of osteoblastic cell differentiation. *J Bone Miner Res* 18, 2060-2068.
- Habibovic, P., and de Groot, K. (2007). Osteoinductive biomaterials--properties and relevance in bone repair. *J Tissue Eng Regen Med* 1, 25-32.
- Haque, F., Lloyd, D.J., Smallwood, D.T., Dent, C.L., Shanahan, C.M., Fry, A.M., Trembath, R.C., and Shackleton, S. (2006). SUN1 interacts with nuclear lamin A and cytoplasmic nesprins to provide a physical connection between the nuclear lamina and the cytoskeleton. *Mol Cell Biol* 26, 3738-3751.

- Harada, S., and Rodan, G.A. (2003). Control of osteoblast function and regulation of bone mass. *Nature* 423, 349-355.
- Hardouin, P., Anselme, K., Flautre, B., Bianchi, F., Bascouleguet, G., and Bouxin, B. (2000). Tissue engineering and skeletal diseases. *Joint Bone Spine* 67, 419-424.
- Harrison, R.G. (1911). On the Stereotropism of Embryonic Cells. *Science* 34, 279-281.
- Hartung, A., Bitton-Worms, K., Rechtman, M.M., Wenzel, V., Boergermann, J.H., Hassel, S., Henis, Y.I., and Knaus, P. (2006). Different routes of bone morphogenic protein (BMP) receptor endocytosis influence BMP signaling. *Mol Cell Biol* 26, 7791-7805.
- Hassan, M.Q., Gordon, J.A., Beloti, M.M., Croce, C.M., van Wijnen, A.J., Stein, J.L., Stein, G.S., and Lian, J.B. (2010). A network connecting Runx2, SATB2, and the miR-23a~27a~24-2 cluster regulates the osteoblast differentiation program. *Proc Natl Acad Sci U S A* 107, 19879-19884.
- Hassan, M.Q., Javed, A., Morasso, M.I., Karlin, J., Montecino, M., van Wijnen, A.J., Stein, G.S., Stein, J.L., and Lian, J.B. (2004). Dlx3 transcriptional regulation of osteoblast differentiation: temporal recruitment of Msx2, Dlx3, and Dlx5 homeodomain proteins to chromatin of the osteocalcin gene. *Mol Cell Biol* 24, 9248-9261.
- Hay, E., Faucheu, C., Suc-Royer, I., Touitou, R., Stiot, V., Vayssiere, B., Baron, R., Roman-Roman, S., and Rawadi, G. (2005). Interaction between LRP5 and Frat1 mediates the activation of the Wnt canonical pathway. *J Biol Chem* 280, 13616-13623.
- Hayashi, Y., Haimovich, B., Reszka, A., Boettiger, D., and Horwitz, A. (1990). Expression and function of chicken integrin beta 1 subunit and its cytoplasmic domain mutants in mouse NIH 3T3 cells. *J Cell Biol* 110, 175-184.
- Heath, C.A. (2000). Cells for tissue engineering. *Trends Biotechnol* 18, 17-19.
- Hench, L.L. (1980). Biomaterials. *Science* 208, 826-831.
- Hench, L.L., and Polak, J.M. (2002). Third-generation biomedical materials. *Science* 295, 1014-1017.
- Henriksen, K., Karsdal, M.A., and Martin, T.J. (2014). Osteoclast-derived coupling factors in bone remodeling. *Calcif Tissue Int* 94, 88-97.
- Henriksen, K., Neutzsky-Wulff, A.V., Bonewald, L.F., and Karsdal, M.A. (2009). Local communication on and within bone controls bone remodeling. *Bone* 44, 1026-1033.
- Hoffman, L.M., and Carpenter, M.K. (2005). Characterization and culture of human embryonic stem cells. *Nat Biotechnol* 23, 699-708.
- Hoffmann, A., Preobrazhenska, O., Wodarczyk, C., Medler, Y., Winkel, A., Shahab, S., Huylebroeck, D., Gross, G., and Verschueren, K. (2005). Transforming growth factor-beta-activated kinase-1 (TAK1), a MAP3K, interacts with Smad proteins and interferes with osteogenesis in murine mesenchymal progenitors. *J Biol Chem* 280, 27271-27283.
- Holleville, N., Mateos, S., Bontoux, M., Bollerot, K., and Monsoro-Burq, A.H. (2007). Dlx5 drives Runx2 expression and osteogenic differentiation in developing cranial suture mesenchyme. *Dev Biol* 304, 860-874.
- Hollister, S.J., and Murphy, W.L. (2011). Scaffold translation: barriers between concept and clinic. *Tissue Eng Part B Rev* 17, 459-474.

- Hu, R., Li, H., Liu, W., Yang, L., Tan, Y.F., and Luo, X.H. (2010). Targeting miRNAs in osteoblast differentiation and bone formation. *Expert Opin Ther Targets* 14, 1109-1120.
- Hu, S., Chen, J., Fabry, B., Numaguchi, Y., Gouldstone, A., Ingber, D.E., Fredberg, J.J., Butler, J.P., and Wang, N. (2003). Intracellular stress tomography reveals stress focusing and structural anisotropy in cytoskeleton of living cells. *Am J Physiol Cell Physiol* 285, C1082-1090.
- Hu, S., Eberhard, L., Chen, J., Love, J.C., Butler, J.P., Fredberg, J.J., Whitesides, G.M., and Wang, N. (2004). Mechanical anisotropy of adherent cells probed by a three-dimensional magnetic twisting device. *Am J Physiol Cell Physiol* 287, C1184-1191.
- Huang, J., Zhao, L., Xing, L., and Chen, D. (2010a). MicroRNA-204 regulates Runx2 protein expression and mesenchymal progenitor cell differentiation. *Stem Cells* 28, 357-364.
- Huang, Z., Nelson, E.R., Smith, R.L., and Goodman, S.B. (2007). The sequential expression profiles of growth factors from osteoprogenitors [correction of osteroprogenitors] to osteoblasts in vitro. *Tissue Eng* 13, 2311-2320.
- Huang, Z., Ren, P.G., Ma, T., Smith, R.L., and Goodman, S.B. (2010b). Modulating osteogenesis of mesenchymal stem cells by modifying growth factor availability. *Cytokine* 51, 305-310.
- Hudalla, G.A., Kouris, N.A., Koepsel, J.T., Ogle, B.M., and Murphy, W.L. (2011). Harnessing endogenous growth factor activity modulates stem cell behavior. *Integr Biol (Camb)* 3, 832-842.
- Humphries, J.D., Byron, A., and Humphries, M.J. (2006). Integrin ligands at a glance. *Journal of Cell Science* 119, 3901-3903.
- Hwang, Y.S., Polak, J.M., and Mantalaris, A. (2008). In vitro direct osteogenesis of murine embryonic stem cells without embryoid body formation. *Stem Cells Dev* 17, 963-970.
- Hynes, R.O. (2002). Integrins: bidirectional, allosteric signaling machines. *Cell* 110, 673-687.
- Hynes, R.O., Lively, J.C., McCarty, J.H., Taverna, D., Francis, S.E., Hodivala-Dilke, K., and Xiao, Q. (2002). The diverse roles of integrins and their ligands in angiogenesis. *Cold Spring Harb Symp Quant Biol* 67, 143-153.
- Ichida, F., Nishimura, R., Hata, K., Matsubara, T., Ikeda, F., Hisada, K., Yatani, H., Cao, X., Komori, T., Yamaguchi, A., *et al.* (2004). Reciprocal roles of MSX2 in regulation of osteoblast and adipocyte differentiation. *J Biol Chem* 279, 34015-34022.
- Ikebe, C., and Suzuki, K. (2014). Mesenchymal stem cells for regenerative therapy: optimization of cell preparation protocols. *Biomed Res Int* 2014, 951512.
- Illich, D.J., Demir, N., Stojkovic, M., Scheer, M., Rothamel, D., Neugebauer, J., Hescheler, J., and Zoller, J.E. (2011). Concise review: induced pluripotent stem cells and lineage reprogramming: prospects for bone regeneration. *Stem Cells* 29, 555-563.
- Impellitteri, N.A., Toepke, M.W., Lan Levengood, S.K., and Murphy, W.L. (2012). Specific VEGF sequestering and release using peptide-functionalized hydrogel microspheres. *Biomaterials* 33, 3475-3484.

- Ingber, D.E. (2003). Tensegrity II. How structural networks influence cellular information processing networks. *J Cell Sci* *116*, 1397-1408.
- Ingber, D.E. (2006). Cellular mechanotransduction: putting all the pieces together again. *FASEB J* *20*, 811-827.
- Ishaug-Riley, S.L., Crane, G.M., Gurlek, A., Miller, M.J., Yasko, A.W., Yaszemski, M.J., and Mikos, A.G. (1997). Ectopic bone formation by marrow stromal osteoblast transplantation using poly(DL-lactic-co-glycolic acid) foams implanted into the rat mesentery. *J Biomed Mater Res* *36*, 1-8.
- Itoh, T., Nozawa, Y., and Akao, Y. (2009). MicroRNA-141 and -200a are involved in bone morphogenetic protein-2-induced mouse pre-osteoblast differentiation by targeting distal-less homeobox 5. *J Biol Chem* *284*, 19272-19279.
- Ivaska, J., and Heino, J. (2010). Interplay between cell adhesion and growth factor receptors: from the plasma membrane to the endosomes. *Cell Tissue Res* *339*, 111-120.
- Jackson, A., Vayssiere, B., Garcia, T., Newell, W., Baron, R., Roman-Roman, S., and Rawadi, G. (2005). Gene array analysis of Wnt-regulated genes in C3H10T1/2 cells. *Bone* *36*, 585-598.
- Jadlowiec, J.A., Celil, A.B., and Hollinger, J.O. (2003). Bone tissue engineering: recent advances and promising therapeutic agents. *Expert Opin Biol Ther* *3*, 409-423.
- Janson, I.A., Kong, Y.P., and Putnam, A.J. (2014). Nanotopographic substrates of poly (methyl methacrylate) do not strongly influence the osteogenic phenotype of mesenchymal stem cells in vitro. *PLoS One* *9*, e90719.
- Javed, A., Afzal, F., Bae, J.S., Gutierrez, S., Zaidi, K., Pratap, J., van Wijnen, A.J., Stein, J.L., Stein, G.S., and Lian, J.B. (2009). Specific residues of RUNX2 are obligatory for formation of BMP2-induced RUNX2-SMAD complex to promote osteoblast differentiation. *Cells Tissues Organs* *189*, 133-137.
- Jin, G.Z., Kim, T.H., Kim, J.H., Won, J.E., Yoo, S.Y., Choi, S.J., Hyun, J.K., and Kim, H.W. (2013). Bone tissue engineering of induced pluripotent stem cells cultured with macrochanneled polymer scaffold. *J Biomed Mater Res A* *101*, 1283-1291.
- Jones, A.C., Arns, C.H., Hutmacher, D.W., Milthorpe, B.K., Sheppard, A.P., and Knackstedt, M.A. (2009). The correlation of pore morphology, interconnectivity and physical properties of 3D ceramic scaffolds with bone ingrowth. *Biomaterials* *30*, 1440-1451.
- Kanchanawong, P., Shtengel, G., Pasapera, A.M., Ramko, E.B., Davidson, M.W., Hess, H.F., and Waterman, C.M. (2010). Nanoscale architecture of integrin-based cell adhesions. *Nature* *468*, 580-584.
- Kao, C.L., Tai, L.K., Chiou, S.H., Chen, Y.J., Lee, K.H., Chou, S.J., Chang, Y.L., Chang, C.M., Chen, S.J., Ku, H.H., *et al.* (2010). Resveratrol promotes osteogenic differentiation and protects against dexamethasone damage in murine induced pluripotent stem cells. *Stem Cells Dev* *19*, 247-258.
- Kaps, C., Hoffmann, A., Zilberman, Y., Pelled, G., Haupl, T., Sittinger, M., Burmester, G., Gazit, D., and Gross, G. (2004). Distinct roles of BMP receptors Type IA and IB in osteo-/chondrogenic differentiation in mesenchymal progenitors (C3H10T1/2). *Biofactors* *20*, 71-84.

- Kapustin, A.N., and Shanahan, C.M. (2011). Osteocalcin: a novel vascular metabolic and osteoinductive factor? *Arterioscler Thromb Vasc Biol* *31*, 2169-2171.
- Karp, J.M., Ferreira, L.S., Khademhosseini, A., Kwon, A.H., Yeh, J., and Langer, R.S. (2006). Cultivation of human embryonic stem cells without the embryoid body step enhances osteogenesis in vitro. *Stem Cells* *24*, 835-843.
- Katada, S., Imhof, A., and Sassone-Corsi, P. (2012). Connecting threads: epigenetics and metabolism. *Cell* *148*, 24-28.
- Kilian, K.A., Bugarija, B., Lahn, B.T., and Mrksich, M. (2010). Geometric cues for directing the differentiation of mesenchymal stem cells. *Proc Natl Acad Sci U S A* *107*, 4872-4877.
- Kim, B.S., Kang, K.S., and Kang, S.K. (2010). Soluble factors from ASCs effectively direct control of chondrogenic fate. *Cell Prolif* *43*, 249-261.
- Kim, E.C., Kim, T.H., Jung, J.H., Hong, S.O., and Lee, D.W. (2014). Enhanced osteogenic differentiation of MC3T3-E1 on rhBMP-2-immobilized titanium via click reaction. *Carbohydr Polym* *103*, 170-178.
- Kim, J., and Ma, T. (2013). Autocrine fibroblast growth factor 2-mediated interactions between human mesenchymal stem cells and the extracellular matrix under varying oxygen tension. *J Cell Biochem* *114*, 716-727.
- Kim, S.S., Park, M.S., Gwak, S.J., Choi, C.Y., and Kim, B.S. (2006a). Accelerated bonelike apatite growth on porous polymer/ceramic composite scaffolds in vitro. *Tissue Eng* *12*, 2997-3006.
- Kim, V.N. (2005). MicroRNA biogenesis: coordinated cropping and dicing. *Nat Rev Mol Cell Biol* *6*, 376-385.
- Kim, Y.J., Kim, H.N., Park, E.K., Lee, B.H., Ryoo, H.M., Kim, S.Y., Kim, I.S., Stein, J.L., Lian, J.B., Stein, G.S., *et al.* (2006b). The bone-related Zn finger transcription factor Osterix promotes proliferation of mesenchymal cells. *Gene* *366*, 145-151.
- Kirkham, J., Firth, A., Vernals, D., Boden, N., Robinson, C., Shore, R.C., Brookes, S.J., and Aggeli, A. (2007). Self-assembling peptide scaffolds promote enamel remineralization. *J Dent Res* *86*, 426-430.
- Kliwer, S.A., Sundseth, S.S., Jones, S.A., Brown, P.J., Wisely, G.B., Koble, C.S., Devchand, P., Wahli, W., Willson, T.M., Lenhard, J.M., *et al.* (1997). Fatty acids and eicosanoids regulate gene expression through direct interactions with peroxisome proliferator-activated receptors alpha and gamma. *Proc Natl Acad Sci U S A* *94*, 4318-4323.
- Kobayashi, S., Takahashi, H.E., Ito, A., Saito, N., Nawata, M., Horiuchi, H., Ohta, H., Iorio, R., Yamamoto, N., and Takaoka, K. (2003). Trabecular minimodeling in human iliac bone. *Bone* *32*, 163-169.
- Koenig, B.B., Cook, J.S., Wolsing, D.H., Ting, J., Tiesman, J.P., Correa, P.E., Olson, C.A., Pecquet, A.L., Ventura, F., Grant, R.A., *et al.* (1994). Characterization and cloning of a receptor for BMP-2 and BMP-4 from NIH 3T3 cells. *Mol Cell Biol* *14*, 5961-5974.
- Kokubo, T., Miyaji, F. & Kim, H. M. (1996). Spontaneous formation of bonelike apatite on chemically treated titanium metals. *J Am Ceram Soc* *79*, , 1127-1129.

- Komori, T., Yagi, H., Nomura, S., Yamaguchi, A., Sasaki, K., Deguchi, K., Shimizu, Y., Bronson, R.T., Gao, Y.H., Inada, M., *et al.* (1997). Targeted disruption of *Cbfa1* results in a complete lack of bone formation owing to maturational arrest of osteoblasts. *Cell* **89**, 755-764.
- Kua, H.Y., Liu, H., Leong, W.F., Li, L., Jia, D., Ma, G., Hu, Y., Wang, X., Chau, J.F., Chen, Y.G., *et al.* (2012). c-Abl promotes osteoblast expansion by differentially regulating canonical and non-canonical BMP pathways and p16INK4a expression. *Nat Cell Biol* **14**, 727-737.
- Kulangara, K., Yang, Y., Yang, J., and Leong, K.W. (2012). Nanotopography as modulator of human mesenchymal stem cell function. *Biomaterials* **33**, 4998-5003.
- Kulkarni, N.H., Onyia, J.E., Zeng, Q., Tian, X., Liu, M., Halladay, D.L., Frolik, C.A., Engler, T., Wei, T., Kriauciunas, A., *et al.* (2006). Orally bioavailable GSK-3alpha/beta dual inhibitor increases markers of cellular differentiation in vitro and bone mass in vivo. *J Bone Miner Res* **21**, 910-920.
- Kuniyasu, H. (2008). The Roles of Dietary PPARgamma Ligands for Metastasis in Colorectal Cancer. *PPAR Res* **2008**, 529720.
- Kurata, H., Guillot, P.V., Chan, J., and Fisk, N.M. (2007). Osterix induces osteogenic gene expression but not differentiation in primary human fetal mesenchymal stem cells. *Tissue Eng* **13**, 1513-1523.
- Kuznetsov, S.A., Cherman, N., and Robey, P.G. (2011). In vivo bone formation by progeny of human embryonic stem cells. *Stem Cells Dev* **20**, 269-287.
- Kuznetsov, S.A., Mankani, M.H., Gronthos, S., Satomura, K., Bianco, P., and Robey, P.G. (2001). Circulating skeletal stem cells. *J Cell Biol* **153**, 1133-1140.
- Kvansakul, M., Adams, J.C., and Hohenester, E. (2004). Structure of a thrombospondin C-terminal fragment reveals a novel calcium core in the type 3 repeats. *EMBO J* **23**, 1223-1233.
- Kyle, S., Aggeli, A., Ingham, E., and McPherson, M.J. (2010). Recombinant self-assembling peptides as biomaterials for tissue engineering. *Biomaterials* **31**, 9395-9405.
- Lai, C.F., and Cheng, S.L. (2002). Signal transductions induced by bone morphogenetic protein-2 and transforming growth factor-beta in normal human osteoblastic cells. *J Biol Chem* **277**, 15514-15522.
- Lai, C.F., and Cheng, S.L. (2005). Alphasbeta integrins play an essential role in BMP-2 induction of osteoblast differentiation. *J Bone Miner Res* **20**, 330-340.
- Lanctot, C., Cheutin, T., Cremer, M., Cavalli, G., and Cremer, T. (2007). Dynamic genome architecture in the nuclear space: regulation of gene expression in three dimensions. *Nat Rev Genet* **8**, 104-115.
- Landis, W.J. (1995). The strength of a calcified tissue depends in part on the molecular structure and organization of its constituent mineral crystals in their organic matrix. *Bone* **16**, 533-544.
- Larionov, A., Krause, A., and Miller, W. (2005). A standard curve based method for relative real time PCR data processing. *BMC Bioinformatics* **6**, 62.

- Le Saux, G., Magenau, A., Bocking, T., Gaus, K., and Gooding, J.J. (2011). The relative importance of topography and RGD ligand density for endothelial cell adhesion. *PLoS One* 6, e21869.
- Lee, K.S., Kim, H.J., Li, Q.L., Chi, X.Z., Ueta, C., Komori, T., Wozney, J.M., Kim, E.G., Choi, J.Y., Ryoo, H.M., *et al.* (2000). Runx2 is a common target of transforming growth factor beta1 and bone morphogenetic protein 2, and cooperation between Runx2 and Smad5 induces osteoblast-specific gene expression in the pluripotent mesenchymal precursor cell line C2C12. *Mol Cell Biol* 20, 8783-8792.
- Lee, K.Y., and Mooney, D.J. (2001). Hydrogels for tissue engineering. *Chem Rev* 101, 1869-1879.
- Lee, M.H., Kwon, T.G., Park, H.S., Wozney, J.M., and Ryoo, H.M. (2003). BMP-2-induced Osterix expression is mediated by Dlx5 but is independent of Runx2. *Biochem Biophys Res Commun* 309, 689-694.
- Levy, L., Wei, Y., Labalette, C., Wu, Y., Renard, C.A., Buendia, M.A., and Neuveut, C. (2004). Acetylation of beta-catenin by p300 regulates beta-catenin-Tcf4 interaction. *Mol Cell Biol* 24, 3404-3414.
- Lewis, G. (1997). Polyethylene wear in total hip and knee arthroplasties. *J Biomed Mater Res* 38, 55-75.
- Li, T., Li, H., Fan, J., Zhao, R.C., and Weng, X. (2014a). MicroRNA Expression Profile of Dexamethasone-Induced Human Bone Marrow-Derived Mesenchymal Stem Cells During Osteogenic Differentiation. *J Cell Biochem* 115, 1683-1691.
- Li, Y., Yan, M., Yang, J., Raman, I., Du, Y., Min, S., Fang, X., Mohan, C., and Li, Q.Z. (2014b). Glutathione S-transferase Mu 2-transduced mesenchymal stem cells ameliorated anti-glomerular basement membrane antibody-induced glomerulonephritis by inhibiting oxidation and inflammation. *Stem Cell Res Ther* 5, 19.
- Li, Z., Hassan, M.Q., Jafferji, M., Aqeilan, R.I., Garzon, R., Croce, C.M., van Wijnen, A.J., Stein, J.L., Stein, G.S., and Lian, J.B. (2009). Biological functions of miR-29b contribute to positive regulation of osteoblast differentiation. *J Biol Chem* 284, 15676-15684.
- Li, Z., Hassan, M.Q., Volinia, S., van Wijnen, A.J., Stein, J.L., Croce, C.M., Lian, J.B., and Stein, G.S. (2008). A microRNA signature for a BMP2-induced osteoblast lineage commitment program. *Proc Natl Acad Sci U S A* 105, 13906-13911.
- Lian, J.B., and Stein, G.S. (1992). Concepts of osteoblast growth and differentiation: basis for modulation of bone cell development and tissue formation. *Crit Rev Oral Biol Med* 3, 269-305.
- Lian, J.B., Stein, G.S., Javed, A., van Wijnen, A.J., Stein, J.L., Montecino, M., Hassan, M.Q., Gaur, T., Lengner, C.J., and Young, D.W. (2006). Networks and hubs for the transcriptional control of osteoblastogenesis. *Rev Endocr Metab Disord* 7, 1-16.
- Little, R.D., Recker, R.R., and Johnson, M.L. (2002). High bone density due to a mutation in LDL-receptor-related protein 5. *N Engl J Med* 347, 943-944; author reply 943-944.
- Little, S.C., and Mullins, M.C. (2009). Bone morphogenetic protein heterodimers assemble heteromeric type I receptor complexes to pattern the dorsoventral axis. *Nat Cell Biol* 11, 637-643.

- Liu, T., Gao, Y., Sakamoto, K., Minamizato, T., Furukawa, K., Tsukazaki, T., Shibata, Y., Bessho, K., Komori, T., and Yamaguchi, A. (2007a). BMP-2 promotes differentiation of osteoblasts and chondroblasts in Runx2-deficient cell lines. *J Cell Physiol* 211, 728-735.
- Liu, W., Toyosawa, S., Furuichi, T., Kanatani, N., Yoshida, C., Liu, Y., Himeno, M., Narai, S., Yamaguchi, A., and Komori, T. (2001). Overexpression of Cbfa1 in osteoblasts inhibits osteoblast maturation and causes osteopenia with multiple fractures. *J Cell Biol* 155, 157-166.
- Liu, Z., Lavine, K.J., Hung, I.H., and Ornitz, D.M. (2007b). FGF18 is required for early chondrocyte proliferation, hypertrophy and vascular invasion of the growth plate. *Dev Biol* 302, 80-91.
- Lo, K.W., Ulery, B.D., Ashe, K.M., and Laurencin, C.T. (2012). Studies of bone morphogenetic protein-based surgical repair. *Adv Drug Deliv Rev* 64, 1277-1291.
- Locasale, J.W., and Cantley, L.C. (2011). Metabolic flux and the regulation of mammalian cell growth. *Cell Metab* 14, 443-451.
- Lonergan, T., Brenner, C., and Bavister, B. (2006). Differentiation-related changes in mitochondrial properties as indicators of stem cell competence. *J Cell Physiol* 208, 149-153.
- Long, M., and Rack, H.J. (1998). Titanium alloys in total joint replacement--a materials science perspective. *Biomaterials* 19, 1621-1639.
- Lu, M., Lin, S.C., Huang, Y., Kang, Y.J., Rich, R., Lo, Y.C., Myszka, D., Han, J., and Wu, H. (2007). XIAP induces NF-kappaB activation via the BIR1/TAB1 interaction and BIR1 dimerization. *Mol Cell* 26, 689-702.
- Luo, S. (2012). MicroRNA expression analysis using the Illumina microRNA-Seq Platform. *Methods Mol Biol* 822, 183-188.
- Luzi, E., Marini, F., Sala, S.C., Tognarini, I., Galli, G., and Brandi, M.L. (2008). Osteogenic differentiation of human adipose tissue-derived stem cells is modulated by the miR-26a targeting of the SMAD1 transcription factor. *J Bone Miner Res* 23, 287-295.
- Lynch, M.P., Capparelli, C., Stein, J.L., Stein, G.S., and Lian, J.B. (1998). Apoptosis during bone-like tissue development in vitro. *J Cell Biochem* 68, 31-49.
- M, L.I., Eriksen, E.F., and Bunger, C. (1996). Bone morphogenetic protein-2 but not bone morphogenetic protein-4 and -6 stimulates chemotactic migration of human osteoblasts, human marrow osteoblasts, and U2-OS cells. *Bone* 18, 53-57.
- Manganelli, G., Fico, A., Masullo, U., Pizzolongo, F., Cimmino, A., and Filosa, S. (2012). Modulation of the pentose phosphate pathway induces endodermal differentiation in embryonic stem cells. *PLoS One* 7, e29321.
- Maniotis, A.J., Chen, C.S., and Ingber, D.E. (1997). Demonstration of mechanical connections between integrins, cytoskeletal filaments, and nucleoplasm that stabilize nuclear structure. *Proc Natl Acad Sci U S A* 94, 849-854.
- Manolagas, S.C. (2000). Birth and death of bone cells: basic regulatory mechanisms and implications for the pathogenesis and treatment of osteoporosis. *Endocr Rev* 21, 115-137.

- Mardis, E.R. (2008). The impact of next-generation sequencing technology on genetics. *Trends Genet* 24, 133-141.
- Marotti, G. (1996). The structure of bone tissues and the cellular control of their deposition. *Ital J Anat Embryol* 101, 25-79.
- Matsubara, T., Kida, K., Yamaguchi, A., Hata, K., Ichida, F., Meguro, H., Aburatani, H., Nishimura, R., and Yoneda, T. (2008). BMP2 regulates Osterix through Msx2 and Runx2 during osteoblast differentiation. *J Biol Chem* 283, 29119-29125.
- Mavis, B., Demirtas, T.T., Gumusderelioglu, M., Gunduz, G., and Colak, U. (2009). Synthesis, characterization and osteoblastic activity of polycaprolactone nanofibers coated with biomimetic calcium phosphate. *Acta Biomater* 5, 3098-3111.
- McBeath, R., Pirone, D.M., Nelson, C.M., Bhadriraju, K., and Chen, C.S. (2004). Cell shape, cytoskeletal tension, and RhoA regulate stem cell lineage commitment. *Dev Cell* 6, 483-495.
- McBride, H.M., Neuspiel, M., and Wasiak, S. (2006). Mitochondria: more than just a powerhouse. *Curr Biol* 16, R551-560.
- McMurray, R.J., Gadegaard, N., Tsimbouri, P.M., Burgess, K.V., McNamara, L.E., Tare, R., Murawski, K., Kingham, E., Oreffo, R.O., and Dalby, M.J. (2011). Nanoscale surfaces for the long-term maintenance of mesenchymal stem cell phenotype and multipotency. *Nat Mater* 10, 637-644.
- McNamara, L.E., Sjostrom, T., Seunarine, K., Meek, R.D., Su, B., and Dalby, M.J. (2014). Investigation of the limits of nanoscale filopodial interactions. *J Tissue Eng* 5, 2041731414536177.
- Mendes, S.C., Bezemer, J., Claase, M.B., Grijpma, D.W., Bellia, G., Degli-Innocenti, F., Reis, R.L., de Groot, K., van Blitterswijk, C.A., and de Bruijn, J.D. (2003). Evaluation of two biodegradable polymeric systems as substrates for bone tissue engineering. *Tissue Eng* 9 Suppl 1, S91-101.
- Middleton, J.C., and Tipton, A.J. (2000). Synthetic biodegradable polymers as orthopedic devices. *Biomaterials* 21, 2335-2346.
- Misawa, H., Kobayashi, N., Soto-Gutierrez, A., Chen, Y., Yoshida, A., Rivas-Carrillo, J.D., Navarro-Alvarez, N., Tanaka, K., Miki, A., Takei, J., *et al.* (2006). PuraMatrix facilitates bone regeneration in bone defects of calvaria in mice. *Cell Transplant* 15, 903-910.
- Miyazono, K., Maeda, S., and Imamura, T. (2005). BMP receptor signaling: transcriptional targets, regulation of signals, and signaling cross-talk. *Cytokine Growth Factor Rev* 16, 251-263.
- Mizuno, Y., Tokuzawa, Y., Ninomiya, Y., Yagi, K., Yatsuka-Kanesaki, Y., Suda, T., Fukuda, T., Katagiri, T., Kondoh, Y., Amemiya, T., *et al.* (2009). miR-210 promotes osteoblastic differentiation through inhibition of AcvR1b. *FEBS Lett* 583, 2263-2268.
- Mizuno, Y., Yagi, K., Tokuzawa, Y., Kanesaki-Yatsuka, Y., Suda, T., Katagiri, T., Fukuda, T., Maruyama, M., Okuda, A., Amemiya, T., *et al.* (2008). miR-125b inhibits osteoblastic differentiation by down-regulation of cell proliferation. *Biochem Biophys Res Commun* 368, 267-272.

- Monis, P.T., Giglio, S., and Saint, C.P. (2005). Comparison of SYTO9 and SYBR Green I for real-time polymerase chain reaction and investigation of the effect of dye concentration on amplification and DNA melting curve analysis. *Anal Biochem* *340*, 24-34.
- Moon, R.T., Kohn, A.D., De Ferrari, G.V., and Kaykas, A. (2004). WNT and beta-catenin signalling: diseases and therapies. *Nat Rev Genet* *5*, 691-701.
- Murugan, R., and Ramakrishna, S. (2006). Nano-featured scaffolds for tissue engineering: a review of spinning methodologies. *Tissue Eng* *12*, 435-447.
- Na, K., Kim, S., Woo, D.G., Sun, B.K., Yang, H.N., Chung, H.M., and Park, K.H. (2007). Synergistic effect of TGFbeta-3 on chondrogenic differentiation of rabbit chondrocytes in thermo-reversible hydrogel constructs blended with hyaluronic acid by in vivo test. *J Biotechnol* *128*, 412-422.
- Na, S., Collin, O., Chowdhury, F., Tay, B., Ouyang, M., Wang, Y., and Wang, N. (2008). Rapid signal transduction in living cells is a unique feature of mechanotransduction. *Proc Natl Acad Sci U S A* *105*, 6626-6631.
- Naganawa, T., Xiao, L., Coffin, J.D., Doetschman, T., Sabbieti, M.G., Agas, D., and Hurley, M.M. (2008). Reduced expression and function of bone morphogenetic protein-2 in bones of Fgf2 null mice. *J Cell Biochem* *103*, 1975-1988.
- Nakashima, A., Katagiri, T., and Tamura, M. (2005). Cross-talk between Wnt and bone morphogenetic protein 2 (BMP-2) signaling in differentiation pathway of C2C12 myoblasts. *J Biol Chem* *280*, 37660-37668.
- Nakashima, K., and de Crombrughe, B. (2003). Transcriptional mechanisms in osteoblast differentiation and bone formation. *Trends Genet* *19*, 458-466.
- Nakashima, K., Zhou, X., Kunkel, G., Zhang, Z., Deng, J.M., Behringer, R.R., and de Crombrughe, B. (2002). The novel zinc finger-containing transcription factor osterix is required for osteoblast differentiation and bone formation. *Cell* *108*, 17-29.
- Navarro, E., Serrano-Heras, G., Castano, M.J., and Solera, J. (2015). Real-time PCR detection chemistry. *Clin Chim Acta* *439*, 231-250.
- Neuss, S., Denecke, B., Gan, L., Lin, Q., Bovi, M., Apel, C., Woltje, M., Dhanasingh, A., Salber, J., Knuchel, R., *et al.* (2011). Transcriptome analysis of MSC and MSC-derived osteoblasts on Resomer(R) LT706 and PCL: impact of biomaterial substrate on osteogenic differentiation. *PLoS One* *6*, e23195.
- Newberry, E.P., Latifi, T., and Towler, D.A. (1998). Reciprocal regulation of osteocalcin transcription by the homeodomain proteins Msx2 and Dlx5. *Biochemistry* *37*, 16360-16368.
- Nissinen, L., Pirila, L., and Heino, J. (1997). Bone morphogenetic protein-2 is a regulator of cell adhesion. *Exp Cell Res* *230*, 377-385.
- Nobta, M., Tsukazaki, T., Shibata, Y., Xin, C., Moriishi, T., Sakano, S., Shindo, H., and Yamaguchi, A. (2005). Critical regulation of bone morphogenetic protein-induced osteoblastic differentiation by Delta1/Jagged1-activated Notch1 signaling. *J Biol Chem* *280*, 15842-15848.

- Noel, D., Gazit, D., Bouquet, C., Apparailly, F., Bony, C., Plence, P., Millet, V., Turgeman, G., Perricaudet, M., Sany, J., *et al.* (2004). Short-term BMP-2 expression is sufficient for in vivo osteochondral differentiation of mesenchymal stem cells. *Stem Cells* 22, 74-85.
- Nohe, A., Hassel, S., Ehrlich, M., Neubauer, F., Sebald, W., Henis, Y.I., and Knaus, P. (2002). The mode of bone morphogenetic protein (BMP) receptor oligomerization determines different BMP-2 signaling pathways. *J Biol Chem* 277, 5330-5338.
- Nohe, A., Keating, E., Knaus, P., and Petersen, N.O. (2004). Signal transduction of bone morphogenetic protein receptors. *Cell Signal* 16, 291-299.
- Novikova, L.N., Novikov, L.N., and Kellerth, J.O. (2003). Biopolymers and biodegradable smart implants for tissue regeneration after spinal cord injury. *Curr Opin Neurol* 16, 711-715.
- Ohtsuki, C., Iida, H., Hayakawa, S., and Osaka, A. (1997). Bioactivity of titanium treated with hydrogen peroxide solutions containing metal chlorides. *J Biomed Mater Res* 35, 39-47.
- Orimo, H. (2010). The mechanism of mineralization and the role of alkaline phosphatase in health and disease. *J Nippon Med Sch* 77, 4-12.
- Oryan, A., Alidadi, S., Moshiri, A., and Maffulli, N. (2014). Bone regenerative medicine: classic options, novel strategies, and future directions. *J Orthop Surg Res* 9, 18.
- Otto, F., Thornell, A.P., Crompton, T., Denzel, A., Gilmour, K.C., Rosewell, I.R., Stamp, G.W., Beddington, R.S., Mundlos, S., Olsen, B.R., *et al.* (1997). *Cbfa1*, a candidate gene for cleidocranial dysplasia syndrome, is essential for osteoblast differentiation and bone development. *Cell* 89, 765-771.
- Owen, M., and Friedenstein, A.J. (1988). Stromal stem cells: marrow-derived osteogenic precursors. *Ciba Found Symp* 136, 42-60.
- P, M., S, H., R, M., M, G., and W, S.K. (2011). Adult mesenchymal stem cells and cell surface characterization - a systematic review of the literature. *Open Orthop J* 5, 253-260.
- Panopoulos, A.D., Yanes, O., Ruiz, S., Kida, Y.S., Diep, D., Tautenhahn, R., Herrerias, A., Batchelder, E.M., Plongthongkum, N., Lutz, M., *et al.* (2012). The metabolome of induced pluripotent stem cells reveals metabolic changes occurring in somatic cell reprogramming. *Cell Res* 22, 168-177.
- Parfitt, A.M. (1994). Osteonal and hemi-osteonal remodeling: the spatial and temporal framework for signal traffic in adult human bone. *J Cell Biochem* 55, 273-286.
- Parfitt, A.M., Mundy, G.R., Roodman, G.D., Hughes, D.E., and Boyce, B.F. (1996). A new model for the regulation of bone resorption, with particular reference to the effects of bisphosphonates. *J Bone Miner Res* 11, 150-159.
- Park, J., Bauer, S., von der Mark, K., and Schmuki, P. (2007). Nanosize and vitality: TiO<sub>2</sub> nanotube diameter directs cell fate. *Nano Lett* 7, 1686-1691.
- Park, S.B., Seo, K.W., So, A.Y., Seo, M.S., Yu, K.R., Kang, S.K., and Kang, K.S. (2012). SOX2 has a crucial role in the lineage determination and proliferation of mesenchymal stem cells through Dickkopf-1 and c-MYC. *Cell Death Differ* 19, 534-545.

- Pattappa, G., Heywood, H.K., de Bruijn, J.D., and Lee, D.A. (2011). The metabolism of human mesenchymal stem cells during proliferation and differentiation. *J Cell Physiol* 226, 2562-2570.
- Pattappa, G., Thorpe, S.D., Jegard, N.C., Heywood, H.K., de Bruijn, J.D., and Lee, D.A. (2013). Continuous and uninterrupted oxygen tension influences the colony formation and oxidative metabolism of human mesenchymal stem cells. *Tissue Eng Part C Methods* 19, 68-79.
- Pedraza, C.E., Nikolcheva, L.G., Kaartinen, M.T., Barralet, J.E., and McKee, M.D. (2008). Osteopontin functions as an opsonin and facilitates phagocytosis by macrophages of hydroxyapatite-coated microspheres: implications for bone wound healing. *Bone* 43, 708-716.
- Phimphilai, M., Zhao, Z., Boules, H., Roca, H., and Franceschi, R.T. (2006). BMP signaling is required for RUNX2-dependent induction of the osteoblast phenotype. *J Bone Miner Res* 21, 637-646.
- Place, E.S., Evans, N.D., and Stevens, M.M. (2009). Complexity in biomaterials for tissue engineering. *Nat Mater* 8, 457-470.
- Platt, J.L. (1996). The immunological barriers to xenotransplantation. *Crit Rev Immunol* 16, 331-358.
- Pollick, S., Shors, E.C., Holmes, R.E., and Kraut, R.A. (1995). Bone formation and implant degradation of coralline porous ceramics placed in bone and ectopic sites. *J Oral Maxillofac Surg* 53, 915-922; discussion 922-913.
- Ponte, A.L., Marais, E., Gallay, N., Langonne, A., Delorme, B., Herault, O., Charbord, P., and Domenech, J. (2007). The in vitro migration capacity of human bone marrow mesenchymal stem cells: comparison of chemokine and growth factor chemotactic activities. *Stem Cells* 25, 1737-1745.
- Popat, K.C., Chatvanichkul, K.I., Barnes, G.L., Latempa, T.J., Jr., Grimes, C.A., and Desai, T.A. (2007). Osteogenic differentiation of marrow stromal cells cultured on nanoporous alumina surfaces. *J Biomed Mater Res A* 80, 955-964.
- Porter, J.R., Henson, A., Ryan, S., and Popat, K.C. (2009). Biocompatibility and mesenchymal stem cell response to poly(epsilon-caprolactone) nanowire surfaces for orthopedic tissue engineering. *Tissue Eng Part A* 15, 2547-2559.
- Pratap, J., Javed, A., Languino, L.R., van Wijnen, A.J., Stein, J.L., Stein, G.S., and Lian, J.B. (2005). The Runx2 osteogenic transcription factor regulates matrix metalloproteinase 9 in bone metastatic cancer cells and controls cell invasion. *Mol Cell Biol* 25, 8581-8591.
- Prigione, A., Fauler, B., Lurz, R., Lehrach, H., and Adjaye, J. (2010). The senescence-related mitochondrial/oxidative stress pathway is repressed in human induced pluripotent stem cells. *Stem Cells* 28, 721-733.
- Quarto, R., Mastrogiacomo, M., Cancedda, R., Kutepov, S.M., Mukhachev, V., Lavroukov, A., Kon, E., and Marcacci, M. (2001). Repair of large bone defects with the use of autologous bone marrow stromal cells. *N Engl J Med* 344, 385-386.

- Raaijmakers, M.H., van Emst, L., de Witte, T., Mensink, E., and Raymakers, R.A. (2002). Quantitative assessment of gene expression in highly purified hematopoietic cells using real-time reverse transcriptase polymerase chain reaction. *Exp Hematol* 30, 481-487.
- Ramm Sander, P., Hau, P., Koch, S., Schutze, K., Bogdahn, U., Kalbitzer, H.R., and Aigner, L. (2013). Stem cell metabolic and spectroscopic profiling. *Trends Biotechnol* 31, 204-213.
- Riedy, M.C., Timm, E.A., Jr., and Stewart, C.C. (1995). Quantitative RT-PCR for measuring gene expression. *Biotechniques* 18, 70-74, 76.
- Ringrose, L., and Paro, R. (2007). Polycomb/Trithorax response elements and epigenetic memory of cell identity. *Development* 134, 223-232.
- Ripamonti, U. (1991). The induction of bone in osteogenic composites of bone matrix and porous hydroxyapatite replicas: an experimental study on the baboon (*Papio ursinus*). *J Oral Maxillofac Surg* 49, 817-830.
- Ririe, K.M., Rasmussen, R.P., and Wittwer, C.T. (1997). Product differentiation by analysis of DNA melting curves during the polymerase chain reaction. *Anal Biochem* 245, 154-160.
- Robledo, R.F., Rajan, L., Li, X., and Lufkin, T. (2002). The *Dlx5* and *Dlx6* homeobox genes are essential for craniofacial, axial, and appendicular skeletal development. *Genes Dev* 16, 1089-1101.
- Rodrigues, C.V., Serricella, P., Linhares, A.B., Guerdes, R.M., Borojevic, R., Rossi, M.A., Duarte, M.E., and Farina, M. (2003). Characterization of a bovine collagen-hydroxyapatite composite scaffold for bone tissue engineering. *Biomaterials* 24, 4987-4997.
- Roodman, G.D. (1996). Advances in bone biology: the osteoclast. *Endocr Rev* 17, 308-332.
- Rose, F.R., and Oreffo, R.O. (2002). Bone tissue engineering: hope vs hype. *Biochem Biophys Res Commun* 292, 1-7.
- Rosen, V. (2011). Harnessing the parathyroid hormone, Wnt, and bone morphogenetic protein signaling cascades for successful bone tissue engineering. *Tissue Eng Part B Rev* 17, 475-479.
- Ross, F.P., and Teitelbaum, S.L. (2005).  $\alpha$  and  $\beta$  and macrophage colony-stimulating factor: partners in osteoclast biology. *Immunol Rev* 208, 88-105.
- Rubin, C.T., and Lanyon, L.E. (1987). Kappa Delta Award paper. Osteoregulatory nature of mechanical stimuli: function as a determinant for adaptive remodeling in bone. *J Orthop Res* 5, 300-310.
- Ryoo, H.M., Hoffmann, H.M., Beumer, T., Frenkel, B., Towler, D.A., Stein, G.S., Stein, J.L., van Wijnen, A.J., and Lian, J.B. (1997). Stage-specific expression of *Dlx-5* during osteoblast differentiation: involvement in regulation of osteocalcin gene expression. *Mol Endocrinol* 11, 1681-1694.
- Sachlos, E., and Czernuszka, J.T. (2003). Making tissue engineering scaffolds work. Review: the application of solid freeform fabrication technology to the production of tissue engineering scaffolds. *Eur Cell Mater* 5, 29-39; discussion 39-40.
- Satokata, I., Ma, L., Ohshima, H., Bei, M., Woo, I., Nishizawa, K., Maeda, T., Takano, Y., Uchiyama, M., Heaney, S., *et al.* (2000). *Msx2* deficiency in mice causes pleiotropic defects in bone growth and ectodermal organ formation. *Nat Genet* 24, 391-395.

- Sawada, R., Ito, T., and Tsuchiya, T. (2006). Changes in expression of genes related to cell proliferation in human mesenchymal stem cells during in vitro culture in comparison with cancer cells. *J Artif Organs* *9*, 179-184.
- Scheltema, R.A., Jankevics, A., Jansen, R.C., Swertz, M.A., and Breitling, R. (2011). PeakML/mzMatch: a file format, Java library, R library, and tool-chain for mass spectrometry data analysis. *Anal Chem* *83*, 2786-2793.
- Schepers, E., de Clercq, M., Ducheyne, P., and Kempeneers, R. (1991). Bioactive glass particulate material as a filler for bone lesions. *J Oral Rehabil* *18*, 439-452.
- Schulze, A., and Downward, J. (2000). Analysis of gene expression by microarrays: cell biologist's gold mine or minefield? *J Cell Sci* *113 Pt 23*, 4151-4156.
- Schwartzman, M., Palma, M., Sable, J., Abramson, J., Hu, X., Sheetz, M.P., and Wind, S.J. (2011). Nanolithographic control of the spatial organization of cellular adhesion receptors at the single-molecule level. *Nano Lett* *11*, 1306-1312.
- Semino, C.E. (2008). Self-assembling peptides: from bio-inspired materials to bone regeneration. *J Dent Res* *87*, 606-616.
- Serra, J., Gonzalez, P., Chiussi, S., Leo'n, B. & Pe'rez-Amor, M (2001). Processing of bioglass coatings by excimer laser ablation. *Key Eng Mater*, 635-638.
- Shah, A.K., Lazatin, J., Sinha, R.K., Lennox, T., Hickok, N.J., and Tuan, R.S. (1999). Mechanism of BMP-2 stimulated adhesion of osteoblastic cells to titanium alloy. *Biol Cell* *91*, 131-142.
- Shattil, S.J., and Newman, P.J. (2004). Integrins: dynamic scaffolds for adhesion and signaling in platelets. *Blood* *104*, 1606-1615.
- Shi, K., Lu, J., Zhao, Y., Wang, L., Li, J., Qi, B., Li, H., and Ma, C. (2013). MicroRNA-214 suppresses osteogenic differentiation of C2C12 myoblast cells by targeting Osterix. *Bone* *55*, 487-494.
- Shi, S., and Gronthos, S. (2003). Perivascular niche of postnatal mesenchymal stem cells in human bone marrow and dental pulp. *J Bone Miner Res* *18*, 696-704.
- Shim, J.H., Greenblatt, M.B., Xie, M., Schneider, M.D., Zou, W., Zhai, B., Gygi, S., and Glimcher, L.H. (2009). TAK1 is an essential regulator of BMP signalling in cartilage. *EMBO J* *28*, 2028-2041.
- Shimada, T., and Somlyo, A.P. (1992). Modulation of voltage-dependent Ca channel current by arachidonic acid and other long-chain fatty acids in rabbit intestinal smooth muscle. *J Gen Physiol* *100*, 27-44.
- Shirakabe, K., Terasawa, K., Miyama, K., Shibuya, H., and Nishida, E. (2001). Regulation of the activity of the transcription factor Runx2 by two homeobox proteins, Msx2 and Dlx5. *Genes Cells* *6*, 851-856.
- Shyh-Chang, N., Daley, G.Q., and Cantley, L.C. (2013a). Stem cell metabolism in tissue development and aging. *Development* *140*, 2535-2547.
- Shyh-Chang, N., Locasale, J.W., Lyssiotis, C.A., Zheng, Y., Teo, R.Y., Ratanasirintraoort, S., Zhang, J., Onder, T., Unternaehrer, J.J., Zhu, H., *et al.* (2013b). Influence of threonine metabolism on S-adenosylmethionine and histone methylation. *Science* *339*, 222-226.

- Shyh-Chang, N., Zheng, Y., Locasale, J.W., and Cantley, L.C. (2011). Human pluripotent stem cells decouple respiration from energy production. *EMBO J* 30, 4851-4852.
- Singh, A.M., and Dalton, S. (2009). The cell cycle and Myc intersect with mechanisms that regulate pluripotency and reprogramming. *Cell Stem Cell* 5, 141-149.
- Sinha, K.M., and Zhou, X. (2013). Genetic and molecular control of osterix in skeletal formation. *J Cell Biochem* 114, 975-984.
- Sjostrom, T., Dalby, M.J., Hart, A., Tare, R., Oreffo, R.O., and Su, B. (2009). Fabrication of pillar-like titania nanostructures on titanium and their interactions with human skeletal stem cells. *Acta Biomater* 5, 1433-1441.
- Slaughter, B.V., Khurshid, S.S., Fisher, O.Z., Khademhosseini, A., and Peppas, N.A. (2009). Hydrogels in regenerative medicine. *Adv Mater* 21, 3307-3329.
- Smith, C.A., Want, E.J., O'Maille, G., Abagyan, R., and Siuzdak, G. (2006). XCMS: processing mass spectrometry data for metabolite profiling using nonlinear peak alignment, matching, and identification. *Anal Chem* 78, 779-787.
- Smith, J., Ladi, E., Mayer-Proschel, M., and Noble, M. (2000). Redox state is a central modulator of the balance between self-renewal and differentiation in a dividing glial precursor cell. *Proc Natl Acad Sci U S A* 97, 10032-10037.
- Smith, W.L. (1989). The eicosanoids and their biochemical mechanisms of action. *Biochem J* 259, 315-324.
- Song, L., Webb, N.E., Song, Y., and Tuan, R.S. (2006). Identification and functional analysis of candidate genes regulating mesenchymal stem cell self-renewal and multipotency. *Stem Cells* 24, 1707-1718.
- Stenderup, K., Justesen, J., Clausen, C., and Kassem, M. (2003). Aging is associated with decreased maximal life span and accelerated senescence of bone marrow stromal cells. *Bone* 33, 919-926.
- Stevens, M.M., and George, J.H. (2005). Exploring and engineering the cell surface interface. *Science* 310, 1135-1138.
- Streit, S., Michalski, C.W., Erkan, M., Kleeff, J., and Friess, H. (2009). Northern blot analysis for detection and quantification of RNA in pancreatic cancer cells and tissues. *Nat Protoc* 4, 37-43.
- Sun, W., Julie Li, Y.S., Huang, H.D., Shyy, J.Y., and Chien, S. (2010). microRNA: a master regulator of cellular processes for bioengineering systems. *Annu Rev Biomed Eng* 12, 1-27.
- Sung, H.J., Meredith, C., Johnson, C., and Galis, Z.S. (2004). The effect of scaffold degradation rate on three-dimensional cell growth and angiogenesis. *Biomaterials* 25, 5735-5742.
- Tai, G., Polak, J.M., Bishop, A.E., Christodoulou, I., and Buttery, L.D. (2004). Differentiation of osteoblasts from murine embryonic stem cells by overexpression of the transcriptional factor osterix. *Tissue Eng* 10, 1456-1466.
- Taichman, R.S. (2005). Blood and bone: two tissues whose fates are intertwined to create the hematopoietic stem-cell niche. *Blood* 105, 2631-2639.

- Takada, I., Kouzmenko, A.P., and Kato, S. (2009). Molecular switching of osteoblastogenesis versus adipogenesis: implications for targeted therapies. *Expert Opin Ther Targets* *13*, 593-603.
- Takahashi, K., Okita, K., Nakagawa, M., and Yamanaka, S. (2007a). Induction of pluripotent stem cells from fibroblast cultures. *Nat Protoc* *2*, 3081-3089.
- Takahashi, K., Tanabe, K., Ohnuki, M., Narita, M., Ichisaka, T., Tomoda, K., and Yamanaka, S. (2007b). Induction of pluripotent stem cells from adult human fibroblasts by defined factors. *Cell* *131*, 861-872.
- Takeda, S., Bonnamy, J.P., Owen, M.J., Ducky, P., and Karsenty, G. (2001). Continuous expression of Cbfa1 in nonhypertrophic chondrocytes uncovers its ability to induce hypertrophic chondrocyte differentiation and partially rescues Cbfa1-deficient mice. *Genes Dev* *15*, 467-481.
- Tashiro, K., Inamura, M., Kawabata, K., Sakurai, F., Yamanishi, K., Hayakawa, T., and Mizuguchi, H. (2009). Efficient adipocyte and osteoblast differentiation from mouse induced pluripotent stem cells by adenoviral transduction. *Stem Cells* *27*, 1802-1811.
- Tataria, M., Perryman, S.V., and Sylvester, K.G. (2006). Stem cells: tissue regeneration and cancer. *Semin Pediatr Surg* *15*, 284-292.
- Tavassoli, M., and Crosby, W.H. (1968). Transplantation of marrow to extramedullary sites. *Science* *161*, 54-56.
- Tezuka, K., Yasuda, M., Watanabe, N., Morimura, N., Kuroda, K., Miyatani, S., and Hozumi, N. (2002). Stimulation of osteoblastic cell differentiation by Notch. *J Bone Miner Res* *17*, 231-239.
- Thomas, D.M., Johnson, S.A., Sims, N.A., Trivett, M.K., Slavin, J.L., Rubin, B.P., Waring, P., McArthur, G.A., Walkley, C.R., Holloway, A.J., *et al.* (2004). Terminal osteoblast differentiation, mediated by runx2 and p27KIP1, is disrupted in osteosarcoma. *J Cell Biol* *167*, 925-934.
- Thomson, J.M., Parker, J.S., and Hammond, S.M. (2007). Microarray analysis of miRNA gene expression. *Methods Enzymol* *427*, 107-122.
- Tian, X.F., Heng, B.C., Ge, Z., Lu, K., Rufaihah, A.J., Fan, V.T., Yeo, J.F., and Cao, T. (2008). Comparison of osteogenesis of human embryonic stem cells within 2D and 3D culture systems. *Scand J Clin Lab Invest* *68*, 58-67.
- Tontonoz, P., Hu, E., Graves, R.A., Budavari, A.I., and Spiegelman, B.M. (1994a). mPPAR gamma 2: tissue-specific regulator of an adipocyte enhancer. *Genes Dev* *8*, 1224-1234.
- Tontonoz, P., Hu, E., and Spiegelman, B.M. (1994b). Stimulation of adipogenesis in fibroblasts by PPAR gamma 2, a lipid-activated transcription factor. *Cell* *79*, 1147-1156.
- Tormala, P. (1992). Biodegradable self-reinforced composite materials; manufacturing structure and mechanical properties. *Clin Mater* *10*, 29-34.
- Tormos, K.V., Anso, E., Hamanaka, R.B., Eisenbart, J., Joseph, J., Kalyanaraman, B., and Chandel, N.S. (2011). Mitochondrial complex III ROS regulate adipocyte differentiation. *Cell Metab* *14*, 537-544.

- Tsatmali, M., Walcott, E.C., and Crossin, K.L. (2005). Newborn neurons acquire high levels of reactive oxygen species and increased mitochondrial proteins upon differentiation from progenitors. *Brain Res* 1040, 137-150.
- Tsimbouri, P.M., McMurray, R.J., Burgess, K.V., Alakpa, E.V., Reynolds, P.M., Murawski, K., Kingham, E., Oreffo, R.O., Gadegaard, N., and Dalby, M.J. (2012). Using nanotopography and metabolomics to identify biochemical effectors of multipotency. *ACS Nano* 6, 10239-10249.
- Tsimbouri, P.M., Murawski, K., Hamilton, G., Herzyk, P., Oreffo, R.O., Gadegaard, N., and Dalby, M.J. (2013). A genomics approach in determining nanotopographical effects on MSC phenotype. *Biomaterials* 34, 2177-2184.
- Tsuji, K., Bandyopadhyay, A., Harfe, B.D., Cox, K., Kakar, S., Gerstenfeld, L., Einhorn, T., Tabin, C.J., and Rosen, V. (2006). BMP2 activity, although dispensable for bone formation, is required for the initiation of fracture healing. *Nat Genet* 38, 1424-1429.
- Tsutsumi, S., Shimazu, A., Miyazaki, K., Pan, H., Koike, C., Yoshida, E., Takagishi, K., and Kato, Y. (2001). Retention of multilineage differentiation potential of mesenchymal cells during proliferation in response to FGF. *Biochem Biophys Res Commun* 288, 413-419.
- Tu, Q., Valverde, P., and Chen, J. (2006). Osterix enhances proliferation and osteogenic potential of bone marrow stromal cells. *Biochem Biophys Res Commun* 341, 1257-1265.
- Tuma, R.S., Beaudet, M.P., Jin, X., Jones, L.J., Cheung, C.Y., Yue, S., and Singer, V.L. (1999). Characterization of SYBR Gold nucleic acid gel stain: a dye optimized for use with 300-nm ultraviolet transilluminators. *Anal Biochem* 268, 278-288.
- Vacanti, C.A. (2006). The history of tissue engineering. *J Cell Mol Med* 10, 569-576.
- Vander Heiden, M.G., Cantley, L.C., and Thompson, C.B. (2009). Understanding the Warburg effect: the metabolic requirements of cell proliferation. *Science* 324, 1029-1033.
- Varum, S., Rodrigues, A.S., Moura, M.B., Momcilovic, O., Easley, C.A.t., Ramalho-Santos, J., Van Houten, B., and Schatten, G. (2011). Energy metabolism in human pluripotent stem cells and their differentiated counterparts. *PLoS One* 6, e20914.
- Vasenius, J., Helevirta, P., Kuisma, H., Rokkanen, P., and Tormala, P. (1994). Absorbable self-reinforced polyglycolide (SR-PGA) screws for the fixation of fractures and osteotomies: strength and strength retention in vitro and in vivo. *Clin Mater* 17, 119-123.
- Viguet-Carrin, S., Garnero, P., and Delmas, P.D. (2006). The role of collagen in bone strength. *Osteoporos Int* 17, 319-336.
- Vo, T.N., Kasper, F.K., and Mikos, A.G. (2012). Strategies for controlled delivery of growth factors and cells for bone regeneration. *Adv Drug Deliv Rev* 64, 1292-1309.
- Wahl, D.A., and Czernuszka, J.T. (2006). Collagen-hydroxyapatite composites for hard tissue repair. *Eur Cell Mater* 11, 43-56.
- Wan, C., Shao, J., Gilbert, S.R., Riddle, R.C., Long, F., Johnson, R.S., Schipani, E., and Clemens, T.L. (2010). Role of HIF-1 $\alpha$  in skeletal development. *Ann N Y Acad Sci* 1192, 322-326.

- Wang, N., Tytell, J.D., and Ingber, D.E. (2009). Mechanotransduction at a distance: mechanically coupling the extracellular matrix with the nucleus. *Nat Rev Mol Cell Biol* 10, 75-82.
- Wang, W., Chen, K., and Xu, C. (2006). DNA quantification using EvaGreen and a real-time PCR instrument. *Anal Biochem* 356, 303-305.
- Wang, Y., Wan, C., Deng, L., Liu, X., Cao, X., Gilbert, S.R., Bouxsein, M.L., Faugere, M.C., Guldberg, R.E., Gerstenfeld, L.C., *et al.* (2007). The hypoxia-inducible factor alpha pathway couples angiogenesis to osteogenesis during skeletal development. *J Clin Invest* 117, 1616-1626.
- Weiss, P., and Garber, B. (1952). Shape and Movement of Mesenchyme Cells as Functions of the Physical Structure of the Medium: Contributions to a Quantitative Morphology. *Proc Natl Acad Sci U S A* 38, 264-280.
- Wellen, K.E., Hatzivassiliou, G., Sachdeva, U.M., Bui, T.V., Cross, J.R., and Thompson, C.B. (2009). ATP-citrate lyase links cellular metabolism to histone acetylation. *Science* 324, 1076-1080.
- Westendorf, J.J., Kahler, R.A., and Schroeder, T.M. (2004). Wnt signaling in osteoblasts and bone diseases. *Gene* 341, 19-39.
- Westendorf, J.J., Zaidi, S.K., Cascino, J.E., Kahler, R., van Wijnen, A.J., Lian, J.B., Yoshida, M., Stein, G.S., and Li, X. (2002). Runx2 (Cbfa1, AML-3) interacts with histone deacetylase 6 and represses the p21(CIP1/WAF1) promoter. *Mol Cell Biol* 22, 7982-7992.
- Wheeler, D.L., Campbell, A.A., Graff, G.L., and Miller, G.J. (1997). Histological and biomechanical evaluation of calcium phosphate coatings applied through surface-induced mineralization to porous titanium implants. *J Biomed Mater Res* 34, 539-543.
- Whyte, M.P. (1994). Hypophosphatasia and the role of alkaline phosphatase in skeletal mineralization. *Endocr Rev* 15, 439-461.
- Williams, D.F. (1999). *The Williams dictionary of biomaterials* (Liverpool, Liverpool University Press).
- Williams, D.F. (2009). On the nature of biomaterials. *Biomaterials* 30, 5897-5909.
- Wilson, S.R., Peters, C., Saftig, P., and Bromme, D. (2009). Cathepsin K activity-dependent regulation of osteoclast actin ring formation and bone resorption. *J Biol Chem* 284, 2584-2592.
- Wittwer, C.T., Herrmann, M.G., Moss, A.A., and Rasmussen, R.P. (1997). Continuous fluorescence monitoring of rapid cycle DNA amplification. *Biotechniques* 22, 130-131, 134-138.
- Wong, M.L., and Medrano, J.F. (2005). Real-time PCR for mRNA quantitation. *Biotechniques* 39, 75-85.
- Woo, E.J. (2012). Recombinant human bone morphogenetic protein-2: adverse events reported to the Manufacturer and User Facility Device Experience database. *Spine J* 12, 894-899.
- Wood, M.A., Bagnaninchi, P., and Dalby, M.J. (2008). The beta integrins and cytoskeletal nanoimprinting. *Exp Cell Res* 314, 927-935.

- Xiao, Y.F., Gomez, A.M., Morgan, J.P., Lederer, W.J., and Leaf, A. (1997). Suppression of voltage-gated L-type Ca<sup>2+</sup> currents by polyunsaturated fatty acids in adult and neonatal rat ventricular myocytes. *Proc Natl Acad Sci U S A* *94*, 4182-4187.
- Yajima, A., Inaba, M., Tominaga, Y., and Ito, A. (2008). Bone formation by minimodeling is more active than remodeling after parathyroidectomy. *Kidney Int* *74*, 775-781.
- Yamasaki, H., and Sakai, H. (1992). Osteogenic response to porous hydroxyapatite ceramics under the skin of dogs. *Biomaterials* *13*, 308-312.
- Yanes, O., Clark, J., Wong, D.M., Patti, G.J., Sanchez-Ruiz, A., Benton, H.P., Trauger, S.A., Despons, C., Ding, S., and Siuzdak, G. (2010). Metabolic oxidation regulates embryonic stem cell differentiation. *Nat Chem Biol* *6*, 411-417.
- Yim, E.K., Reano, R.M., Pang, S.W., Yee, A.F., Chen, C.S., and Leong, K.W. (2005). Nanopattern-induced changes in morphology and motility of smooth muscle cells. *Biomaterials* *26*, 5405-5413.
- Yu, J.S., Tsai, H.C., Wu, C.C., Weng, L.P., Li, H.P., Chung, P.J., and Chang, Y.S. (2002). Induction of inducible nitric oxide synthase by Epstein-Barr virus B95-8-derived LMP1 in Balb/3T3 cells promotes stress-induced cell death and impairs LMP1-mediated transformation. *Oncogene* *21*, 8047-8061.
- Yuan, H., Fernandes, H., Habibovic, P., de Boer, J., Barradas, A.M., Walsh, W.R., van Blitterswijk, C.A., and De Bruijn, J.D. (2011). 'Smart' biomaterials and osteoinductivity. *Nat Rev Rheumatol* *7*, c1; author reply c2.
- Yuan, H., Yang, Z., Li, Y., Zhang, X., De Bruijn, J.D., and De Groot, K. (1998). Osteoinduction by calcium phosphate biomaterials. *J Mater Sci Mater Med* *9*, 723-726.
- Zaragosi, L.E., Ailhaud, G., and Dani, C. (2006). Autocrine fibroblast growth factor 2 signaling is critical for self-renewal of human multipotent adipose-derived stem cells. *Stem Cells* *24*, 2412-2419.
- Zayzafoon, M. (2006). Calcium/calmodulin signaling controls osteoblast growth and differentiation. *J Cell Biochem* *97*, 56-70.
- Zhang, C. (2010). Transcriptional regulation of bone formation by the osteoblast-specific transcription factor *Osx*. *J Orthop Surg Res* *5*, 37.
- Zhang, J., Khvorostov, I., Hong, J.S., Oktay, Y., Vergnes, L., Nuebel, E., Wahjudi, P.N., Setoguchi, K., Wang, G., Do, A., *et al.* (2011). UCP2 regulates energy metabolism and differentiation potential of human pluripotent stem cells. *EMBO J* *30*, 4860-4873.
- Zheng, H., Guo, Z., Ma, Q., Jia, H., and Dang, G. (2004). *Cbfa1/osf2* transduced bone marrow stromal cells facilitate bone formation in vitro and in vivo. *Calcif Tissue Int* *74*, 194-203.
- Ziegler, W.H., Liddington, R.C., and Critchley, D.R. (2006). The structure and regulation of vinculin. *Trends Cell Biol* *16*, 453-460.
- Zuk, P.A., Zhu, M., Ashjian, P., De Ugarte, D.A., Huang, J.I., Mizuno, H., Alfonso, Z.C., Fraser, J.K., Benhaim, P., and Hedrick, M.H. (2002). Human adipose tissue is a source of multipotent stem cells. *Mol Biol Cell* *13*, 4279-4295.

